

https://dspace.org/

Histo-morphological Perturbations in the Testes of Diabetic Sprague Dawley Rat Following Atripla® And Alcohol Co-administration

Owembabazi, Elna

2023-08

University of the Witwatersrand, Johannesburg

https://hdl.handle.net/10539/45020

Owembabazi, Elna. (2023). Histo-morphological Perturbations in the Testes of Diabetic Sprague Dawley Rat Following Atripla® And Alcohol Co-administration. [PhD thesis, University of the Witwatersrand, Johannesburg]. WIReDSpace. https://hdl.handle.net/10539/45020

Downloaded from a DSpace repository. https://dspace.org/

Histo-morphological Perturbations in the Testes of Diabetic Sprague Dawley Rat Following Atripla® and Alcohol Co-administration

By

Elna Owembabazi

Student number: 2278202

This thesis is submitted in the fulfilment of the requirements for the degree of Doctor of Philosophy in Anatomical Sciences

Faculty of Health Sciences, University of the Witwatersrand, Johannesburg, South Africa.

Supervisor

Prof. Ejikeme Felix Mbajiorgu (Ph.D.)

Co-Supervisor

Dr. Pilani Nkomozepi (Ph.D.)

August 2023

DECLARATION

I, Elna Owembabazi declare that this PhD thesis is my original work, submitted for a Doctor of Philosophy degree in Anatomical Sciences, Faculty of Health Sciences, University of the Witwatersrand, Johannesburg, South Africa, and has never been submitted before in any other form for any degree or in another university.



Elna Owembabazi

30th August 2023

DEDICATION

I fondly dedicate this work to my late Grandpa Mr. Peter Sabiti and Grandma Mrs. Zerida Ntontori. Am forever grateful for their selfless love, profound advice, and great guidance that imparted confidence in me to always go after what I want.

ACKNOWLEDGEMENTS

All my praises and gratitude are forever due to the Almighty GOD for endlessly blessing me.

I would like to appreciate Prof. Ejikeme Felix Mbajiorgu and Dr. Pilani Nkomozepi for agreeing to supervisor me and their relentless support, constructive criticism, guidance, and patience throughout this study program. Also, I want to thank Dr. Tanya Calvey for her invaluable input and support towards my successful enrolment and completion of my Ph.D.

Sincere thanks go to my colleagues Jaclyn Asouzu Johnson, Idemudia Eguavoen, and Vaughan Perry for their collaborative work and immense appreciation goes to Hasiena Ali for readily availing her assistance with the laboratory experiments.

I would like to extend appreciation to my former supervisors; undergraduate project, Dr. Andrew Baguma; MSc. project, Dr. Ninsiima Herbert Izo and Prof. Mario Edgar Fernandez Diaz, under their guidance I learned and developed a passion for academia and research.

Am very grateful for the amazing Twine family and my wholesome friends for keeping me grounded and motivated during my study program.

Special appreciation goes to the chairman board of trustees Kampala International University, Dr. Al Hajji Hassan Basajjabalaba for the financial support throughout my academic journey.

PUBLICATIONS

1. Elna Owembabazi, Pilani Nkomozepi, Tanya Calvey, & Ejikeme Felix Mbajiorgu (2023). Co-administration of Alcohol and Combination Antiretroviral Therapy (cART) in Male Sprague Dawley Rats: A Study on Testicular Morphology, Oxidative, and Cytokines Perturbations. *Anatomy & Cell Biology:* 56(2):236-251. https://doi.org/10.5115/acb.22.229.

2. Elna Owembabazi, Pilani Nkomozepi, & Ejikeme Felix Mbajiorgu (2023). Androgen Receptor (AR) Depletion Underlies the Reproductive Dysfunctions in Male Rats Exposed to Alcohol and Combination Antiretroviral Therapy (cART). *Andrologia*, vol. 2023, Article ID 2966391, 12 pages, 2023. https://doi.org/10.1155/2023/2966391.

3. Elna Owembabazi, Pilani Nkomozepi, & Ejikeme Felix Mbajiorgu (2023). Impact of Concurrent Exposure of Diabetic male Sprague Dawley rats to Alcohol and Combination Antiretroviral Therapy (cART) on reproductive capacity. *Applied Sciences:*13(8), 5096. https://doi.org/10.3390/app13085096.

4. Elna Owembabazi, Pilani Nkomozepi, & Ejikeme Felix Mbajiorgu (2023). Potential Role of Inducible nitric oxide Synthase (iNOS) Activity in Testicular Dysfunction Following Co-administration of Alcohol and Combination Antiretroviral Therapy (cART) in Diabetic Rats: An Immunohistochemistry Study. *Toxicological Research:* 2023. https://doi.org/10.1007/s43188-023-00200-5.

ABSTRACT

A decline in male fertility is increasingly becoming a major concern in this millennium. However, the associated effects of diabetes, alcohol abuse, and cART use and their interaction which are clinically important in male reproductive health have not received proper attention. Each of these conditions (diabetes, alcohol abuse, and cART use) has been shown to negatively impact the male reproductive system. Moreover, diabetes, alcohol abuse, and cART are intricately connected and thus can and occur simultaneously in an individual, a scenario that might provoke severe reproductive dysfunctions. Therefore, this study investigated the impact of diabetes, alcohol abuse, cART use, and their combinations on testicular histomorphometry, reproductive hormone profile, oxidative and inflammatory markers, germ cell proliferation and apoptosis, and androgen receptor expression.

A total of forty-eight HIV naive rats (48) were divided into two main groups, non-diabetic and diabetic groups, which were further subdivided into four subgroups consisting of six rats each. The non-diabetic groups (1-4); Group 1; Control, Group 2: Alcohol treated (A), Group 3: combination antiretroviral therapy treated (cART), and Group 4: alcohol plus cART treated (A+cART). The diabetic groups (5-8); Group 5: diabetic only (DM), Group 6: diabetic treated with alcohol (DM+A), Group 7: diabetic treated with cART (DM+cART), and Group 8: diabetic treated with both alcohol and cART (DM+A+cART). The rats were fed normal rat chow and terminated after 90 days of treatment. Blood was drawn through a cardiac puncture into plain vacutainers, thereafter, animals were perfused with 0.1M phosphate buffer, and the testes harvested, weighed, and then fixed in 10% neutral buffered formalin for histology and immunohistochemistry analysis.

During the experimental period, hyperglycemia, low glucose tolerance, and polydipsia were observed in the diabetic groups (5-8) only. Though, a general decrease in testis weight, volume, and size was found in all treated groups compared to the control group, a significant ($p<0.05$) decrease was detected in the DM+A group only. With exception of the DM+A+cART group, the epithelial area fraction, epithelial height, and tubule area and diameter reduced significantly in all treated groups. The luminal area fraction and luminal diameter which significantly reduced in cART, DM, and DM+cART groups, were increased in A+cART. Further, connective tissue and interstitial area fractions increased significantly in all treated groups. The spermatogonia increased significantly in A, cART, DM, and DM+A+cART groups relative to control group, but reduced significantly in DM+A. However, spermatocytes, round spermatids, and elongated spermatids decreased significantly in all treated groups, with exception of spermatocytes of the alcohol group. All treated groups showed a decrease in the number of

Sertoli cells relative to the control but a significant decrease was only found in the DM+A group, but all treated groups had significantly decreased Leydig cell diameter and volume. Johnsen's testicular score was significantly reduced in A, A+cART, DM, and DM+A treated groups. Additionally, varying severity of seminiferous tubules (ST) lesions such as shrinkage of ST, lifting of epithelium, widened intercellular space, karyolysis, epithelial sloughing, ST atrophy, multinucleated giant cells, and germinal epithelium derangement were observed in the treated animal groups. Further, the thickness ST basement membrane increased significantly in cART, DM, and DM+cART groups but testis capsule thickness increased significantly in A+cART, DM+A, and DM+A+cART groups. The testicular interstitial connective tissue fibers viz. collagen, reticulin, and elastin reduced significantly in all treated groups, except for the reticulin which was non-significantly decreased in the alcohol (A) group. Furthermore, luteinizing hormone was significantly elevated in A and A+cART groups but significantly reduced in the DM+A+cART group. However, follicle-stimulating hormone increased significantly in all treated groups, with exception of DM+cART group. Testosterone levels were significantly reduced in DM, DM+A, and DM+A+cART groups, but no significant difference ($p>0.05$) was found in the inhibin B level in all treated groups compared to the control. In addition, the intensity and number of Sertoli and Leydig cells expressing androgen receptor were significantly reduced in all treated groups, except for the number of Sertoli cells expressing androgen receptor in the alcohol group. Expression of inflammatory markers (IL-1β, TNF-α, and IL-6) was upregulated in all treated groups, with exception of IL-1β of the A+cART group and TNF-α of cART and A+cART groups. The markers for oxidative stress (iNOS, MDA, and 8-OHDG) and apoptosis (caspase 3) were upregulated in all treated groups, with exception of MDA in the alcohol group. Though, the number of germ cells expressing proliferation marker Ki-67 was significantly reduced in all treated groups, the staining intensity was significantly increased compared to the control group.

The results show that diabetes, alcohol abuse, cART, and their combinations have deleterious effects on the testicular histoarchitecture and function, which are suggested to result from the upregulation of oxidants and cytokines and androgen receptor depletion. The results further suggest that the interaction arising from a co-presence of cART and alcohol in diabetic condition could mildly diminish their independent effects due to their common cytochrome P450 metabolic pathway. This study yielded invaluable data on the contribution of cART-alcohol-diabetes interaction on the male reproductive functioning/dysfunction and hopefully will help clinicians in managing reproductive challenges in patients of this category.

TABLE OF CONTENTS

Contents

DECLARATION ii
DEDICATION iii
ACKNOWLEDGEMENTS iv
PUBLICATIONS v
ABSTRACT vi
TABLE OF CONTENTS viii
LIST OF FIGURES xii
LIST OF TABLES xiii
LIST OF SYMBOLS, ABBREVIATIONS, AND ACRONYMS xiv
THESIS CHAPTER OUTLINE xvi
CHAPTER 1: INTRODUCTION 1
1.1 Background 1
1.2 Study rationale 4
1.3 Hypothesis of the study 5
1.4 Aim and objectives 5
1.4.1 Aim 5
1.3.2 Objectives 5
CHAPTER 2: LITERATURE REVIEW 6
2.1 Male reproductive system 6
2.2 Embryology of the testis 6
2.3 Anatomy of the testis 6
2.3.1 Gross anatomy of testis 7
2.3.2 Microanatomy of testis 8
2.4 Leydig cell and steroidogenesis 9
2.4.1 Leydig cell structure and function 9
2.4.2 Steroidogenesis process 11
2.5 Sertoli cell and blood-testis-barrier (BTB) 13
2.5.1 Sertoli cell structure and function 13
2.5.2 The structure and function of blood-testis-barrier (BTB) 14
2.6 Spermatogenesis and the spermatogenic cycle and wave 16
2.6.1 Spermatogenesis 16
2.6.2 Spermatogenic cycle and wave 18
2.7 Male hypothalamic pituitary gonadal (HPG) axis 21
2.8 Male infertility and its treatment 23

2.8.1 Male infertility 23
2.8.2 Male infertility treatment 26
2.9 Apoptosis in the testis 27
2.9.1 Male germ cell apoptosis 27
2.9.2 Testicular somatic cell apoptosis 28
2.10 Testis-immune axis and inflammation 28
2.10.1 Testis-immune axis 28
2.10.2 Testis inflammation 30
2.11 Impact of oxidative stress on testicular function 31
2.12 Influence of alcohol on male reproductive function 33
2.12.1 Alcohol use and its toxicity 33
2.12.2 Alcohol-linked reproductive impairments 37
2.13 HIV/AIDS and cART associated reproductive dysfunctions 39
2.13.1 HIV/AIDs epidemiology 39
2.13.2 Antiretroviral (ARV) drugs and Combination antiretroviral therapy (cART) 41
2.13.3 Reproductive dysfunctions associated HIV/AIDS and cART 46
2.14 Diabetes and male reproduction 47
2.14.1 Types of diabetes 47
2.14.2 Prevalence and trends of diabetes 48
2.14.3 Testicular glucose metabolism 51
2.14.4 Diabetes-related male infertility 52
2.15 Impact of diabetes, alcohol, and cART interaction on the male reproductive system 53
CHAPTER 3: MATERIALS AND METHODS 55
3.1 Chemical and reagents 55
3.2 Ethical clearance 55
3.3 Animals 55
3.4 Type 2 diabetes mellitus induction and tests 55
3.5 cART (Atripla) and alcohol treatment preparation 56
3.6 Experimental design 56
3.5 Animal terminal procedures 58
3.5.1 Testis weight and size 59
3.5.2 Testis volume 59
3.5.3 Gonadosomatic index (GSI) 59
3.6 Reproductive hormone immunoassay 59
3.7 Histology and histomorphometry 60
3.7.1 Haematoxylin and Eosin (H&E) staining protocol for basic histology 61
3.7.2 Periodic acid Schiff (PAS) staining protocol for basement membrane 61
3.7.3 Masson's Trichrome staining protocol for collagen 61

3.7.4 Gordon and Sweet's silver impregnation staining protocol for reticulin 62
3.7.5 Gomori's Aldehyde Fuchsin staining protocol for elastin 62
3.8 Testicular component area fractions 62
3.9 Seminiferous tubule morphometry 63
3.10 Germinal epithelium cell quantification 63
3.11 Leydig cell morphometry 63
3.12 Histopathological evaluation 63
3.12.1 Johnsen's testicular score 63
3.12.2 Histological changes 64
3.13 Measurement of seminiferous tubule basement membrane (STBM) 64
3.14 Evaluation of testicular capsule thickness 64
3.15 Connective tissue fibers quantification 65
3.16 Immunohistochemistry technique 65
3.17 Data analysis 66
BRIDGING NOTE 67
CHAPTER 4: FIRST MANUSCRIPT 68
CHAPTER 5: SECOND MANUSCRIPT 90
CHAPTER 6: THIRD MANUSCRIPT 109
CHAPTER 7: FOURTH MANUSCRIPT 138
CHAPTER 8: GENERAL DISCUSSION, CONCLUSION, AND RECOMMENDATIONS 156
8.1 Preamble 156
8.1.1 The effect of diabetes, alcohol, cART, and their combinations on testicular morphometry 157
8.1.2 The effect of diabetes, alcohol, cART, and their combinations on spermatogenic germ cells 158
8.1.3 The effect of diabetes, alcohol, cART, and their combinations on testicular somatic cells 158
8.1.4 The effect of diabetes, alcohol, cART, and their combinations on testis histology 159
8.1.5 The effect of diabetes, alcohol, cART, and their combinations on testicular connective tissue 159
8.1.6 The effect of diabetes, alcohol, cART, and their combinations on reproductive hormones 160
8.1.7 The effect of diabetes, alcohol, cART, and their combinations on the expression of testicular androgen receptor 160
8.1.8 The effect of diabetes, alcohol, cART, and their combinations on the expression of oxidative stress markers in the testis 161
8.1.9 The effect of diabetes, alcohol, cART, and their combinations on testicular cytokines 162
8.1.10 The effect of diabetes, alcohol, cART, and their combinations on germ cell apoptosis 162
8.1.11 The effect of diabetes, alcohol, cART, and their combinations on the testicular expression of proliferation marker, Ki-67 163

8.2 Conclusion 163
8.3 Recommendations and further study 164
REFERENCE LIST 165
APPENDIX 206
Ethics clearance certificate 206
Sample size calculation 207
Treatment preparation and dosage calculation 207
Published article 209
Manuscript submission confirmation 225
Turnitin report 227

LIST OF FIGURES

Figure 2.1: An illustration of the gross anatomy of testis and associated structures. 8
Figure 2.2: Rat testis cross section showing testicular parenchyma microanatomy, H&E stain. 9
Figure 2.3: Schematic illustration of Leydig cell testosterone biosynthesis from cholesterol. 13
Figure 2.4: Schematic drawing of blood-testicular barrier (BTB) structure. 16
Figure 2.5: Illustration of spermatogenesis phases. 18
Figure 2.6: Spermatogenic cell associations at different stages (I–XII) of germinal epithelium in mouse testis, PAS stain. 20
Figure 2.7: An illustration of a spermatogenic wave showing different stages of germinal epithelium along a seminiferous tubule. 21
Figure 2.8: Schematic representation of HPG axis showing feedback mechanism. 23
Figure 2.9: The percentage of alcohol consumers (current and former) and lifetime abstainers in the populace aged ≥15 globally and in the different WHO regions. 34
Figure 2.10: Average consumed alcohol per capita (APC) (in liters of absolute alcohol) in the populace aged ≥15 in different countries. 35
Figure 3.1: Experimental design illustration 58

LIST OF TABLES

Table 2.1:Definitions of a standard drink in different countries and the guidelines for low-risk alcohol consumption 36
Table 2.2: Global HIV data 40
Table 2.3: List of Federal Drug Agency (FDA) approved ARV drugs 42
Table 2.4: List of HIV treatment regimen (cART) approved by the Federal Drug Agency (FDA) 45
Table 2.5:Diabetes global prevalence trends, projection, and 2021 deaths 49
Table 2.6: Diabetes prevalence trends and projection of the most affected countries in Africa 50
Table 3.1: Modified Johnsen scoring criteria 64
Table 3.2: Antibody dilutions used 66

LIST OF SYMBOLS, ABBREVIATIONS, AND ACRONYMS

α	Alpha
β	Beta
%	Percentage
℃	Degrees Celsius
g	Gram
kg	Kilogram
L	Litre
M	Molar
mg	Milligram
mL	Millilitre
mmol	Millimoles
pg	Picogram
µg	Microgram
µL	Microlitre
µm	Micrometre
µmol	Micromole
&	And
e.g.	For example
i.e.	That is
Viz.	Namely
8-OHDG	8-hydroxydeoxyguanosine
A	Alcohol
A+cART	Alcohol and combination antiretroviral therapy.
AIDS	Acquired immunodeficiency syndrome
ANOVA	Analysis of variance
APC	Alcohol per capita
AR	Androgen receptor
ARV	Antiretroviral
BTB	Blood-testis-barrier
cART	Combination antiretroviral therapy
DM	Diabetes
DM+A	Diabetes and alcohol
DM+A+cART	Diabetes and alcohol and combination antiretroviral therapy

DM+cART	Diabetes and combination antiretroviral therapy
ELISA	Enzyme-linked immunosorbent assay
FBG	Fasting blood glucose
FSH	Follicle-stimulating hormone
GnRH	Gonadotropin-releasing hormone
GSI	Gonadosomatic index
H&E	Hematoxylin and eosin
HH	Hypogonadotrophin hypogonadism
HIV	Human immunodeficiency virus
HPG	Hypothalamic-pituitary-gonadal
IL-1β	Interleukin-1beta
IL-6	Interleukin-6
INHB	Inhibin B
iNOS	Inducible nitric oxide synthase
LH	Luteinizing hormone
MDA	Malondialdehyde
NCDs	Non-communicable diseases
NNRTIs	Non-nucleoside reverse transcriptase inhibitors
NO	Nitric oxide
NRTIs	Nucleoside reverse transcriptase inhibitors
OS	Oxidative stress
PAS	Periodic acid Schiff
PBS	Phosphate-buffered saline
PEP	Post-exposure prophylaxis
PLWHA	People living with HIV/AIDS
PrEP	Pre-exposure prophylaxis
ROS	Reactive oxygen species
SEM	Standard error of the mean
ST	Seminiferous tubules
STBM	Seminiferous tubule basement membrane
STZ	Streptozotocin
TNF-α	Tumor necrosis factor-alpha
TT	Testosterone
WHO	World Health Organisation

THESIS CHAPTER OUTLINE

This thesis is organised into eight chapters as follows:

Chapter one, a general introduction section that details the study background, rationale, aim, and objectives.

Chapter two, presents the overall literature review that concisely detail information on male reproductive system, infertility, and common associated pathological mechanism and diabetes, alcohol, and combination antiretroviral therapy (cART), their interaction, and associated male reproductive dysfunctions.

Chapter three, a general methodology section describing the materials, experimental design, and laboratory techniques used in the study.

Chapters 4-7, consists of the results section presented in form of manuscripts that focused on parameters evaluated to delineate the impact of the treatment interactions on male reproductive system. These chapters are listed below as follows:

Chapter four, published article in Anatomy & Cell Biology journal (see appendix): Elna Owembabazi, Pilani Nkomozepi, Tanya Calvey, Ejikeme Felix Mbajiorgu. Co-administration of Alcohol and Combination Antiretroviral Therapy (cART) in Male Sprague Dawley Rats: A Study on Testicular Morphology, Oxidative, and Cytokines Perturbations. Anat Cell Biol. 2023 (doi: 10.5115/acb.22.229).

Chapter five, a manuscript under final review process in Andrologia journal titled: Androgen Receptor (AR) Depletion Underlies the Reproductive Dysfunctions in Male Rats Exposed to Alcohol and Combination Antiretroviral Therapy (cART).

Chapter six, a manuscript under review in Applied Sciences journal titled: Impact of Concurrent Exposure of Diabetic male Sprague Dawley rats to Alcohol and Combination Antiretroviral Therapy (cART) on reproductive capacity: Evaluation of Testicular Histomorphology, Hormonal Profile, and Androgen Receptor Expression.

Chapter seven, a manuscript under review in Toxicological Research journal titled: Potential Role of Inducible nitric oxide Synthase (iNOS) Activity in Testicular Dysfunction Following Co-administration of Alcohol and Combination Antiretroviral Therapy (cART) in Diabetic Rats: An Immunohistochemistry Study.

Chapter eight, a general thesis discussion, conclusion and recommendations based on key findings from this study.

CHAPTER 1: INTRODUCTION

1.1 Background

Decline in male fertility and the high prevalence of non-communicable diseases (NCDs) are increasingly becoming a global health concern (Agarwal et al., 2021; Mattli et al., 2019). Increased prevalence of NCDs such as diabetes, hypertension, cardiovascular diseases, and cancer has been associated with the rise in male infertility incidence (Khawcharoenporn and Sha, 2016; Mann, Shiff, et al., 2020). Additionally, modern life is mainly characterized by limited physical activity and consumption of high-calorie processed foods (Jamison and Mosley, 1991), which have been implicated in the development of NCDs, and consequently worsening the global disease burden (Ding et al., 2016). Other lifestyle choices like alcohol abuse, cigarette smoking, and illicit drug use have also significantly contributed to the increase in NCDs (Kelly et al., 2014; Nojilana et al., 2016). In South Africa, the predominance of high carbohydrate staple food (Steyn et al., 2012), obesity (Pheiffer et al., 2018), and excessive alcohol consumption (Coetzee et al., 2019) have contributed to the rise in diabetes incidence. The prevalence of diabetes in South Africa is the second highest in Africa, following an over two-fold increase since 2017 from 5.4% to the current 11.3% (IDF, 2021).

Diabetes is a group of chronic metabolic disorders characterized by persistent hyperglycemia linked to insulin resistance and/or insufficient secretion (Blair, 2016). It is linked to complications in carbohydrate, fat, and protein metabolism and has suddenly emerged as a significant public health concern (American Diabetes Association, 2014). Moreover, diabetes is associated with impairments in numerous body systems viz. vascular diseases, retinopathy, nephropathy, dementia, and grave reproductive dysfunctions in both men and women (Singh et al., 2014; Asmat et al., 2016). Recently, diabetes prevalence is increasing not only among the adult but also in children and young adults of reproductive age (Condorelli et al., 2018; Forouhi and Wareham, 2019), which necessitates greater attention in research to further delineate and possibly mitigate the associated organ pathology and negative health outcomes.

Associated with the increasing incidence of diabetes is the increased prevalence of alcohol consumption in young adults of reproductive age (Newton et al., 2013; Kann et al., 2014), which predisposes the affected individuals to a disease-drug interaction (i.e. diabetes-alcohol interaction). Alcohol is incidentally, the most socially accepted recreational substance worldwide (Trangenstein et al., 2018). However, excessive alcohol consumption is reckoned

as a leading cause of male sexual dysfunction and subfertility (Condorelli et al., 2015; Kolesnikova et al., 2015; Nishi et al., 2018). The contribution of alcohol to male reproductive dysfunction is further complicated by the risky behaviours associated with alcohol influence (Scott-Sheldon et al., 2016), such as high indulgence in unprotected sex and multiple sexual partners implicated in increase of human immunodeficiency virus (HIV) infection spread (Kumar et al., 2015) and consequent enrolment into the combination antiretroviral therapy (cART) program. This leads to HIV-alcohol-diabetes comorbidity condition which is a prevalent health scenario in the society. Apart from South Africa being one of the countries with a high incidence of diabetes (Pheiffer et al., 2018) and high HIV prevalence with the biggest cART program globally (Lippman et al., 2019), it is also facing a high prevalence of alcohol abuse. A recent national survey reported that 33.1 % of the South African population consumes alcohol regularly (Vellios et al., 2018), moreover, South Africa's alcohol per capita (APC) consumption average (11.5 liters) is almost double the global average (6.4 liters).

Furthermore, previous studies have documented that alcohol consumption causes early onset and deterioration of diabetes (Pourentezari et al., 2016; Long et al., 2018) and cART (Braithwaite and Bryant, 2010; Kumar et al., 2012) adverse effects. Alcohol has been reported to deteriorate glucose regulation and insulin resistance in diabetic conditions (Kim and Kim, 2012; Engler et al., 2013), and subsequently accentuating diabetes-induced organ complications (Pourentezari et al., 2016; Long et al., 2018) and as well hinders adherence to cART (Michel et al., 2010; Schneider et al., 2016; Shubber et al., 2016). Further, alcohol has been shown to dose-dependently aggravate HIV progression and reduced cART efficacy (Chander et al., 2006; Braithwaite et al., 2007; Mondal et al., 2019).

Atripla®, a fixed dose cART drug approved by the Food and Drug Administration (FDA) as a first-line medication for human immunodeficiency virus/acquired immunodeficiency syndrome (HIV/AIDS) is commonly used in South Africa (Mocroft et al., 2014). It is a combination of nucleoside reverse transcriptase inhibitors (NRTIs) (tenofovir disoproxil fumarate and emtricitabine), and a non-nucleoside reverse transcriptase inhibitor (NNRTI) (efavirenz) (Jungmann et al., 2019). The advent of cART has improved the prognosis of HIV infection through a reduction in viral replication and has led to improved quality of life of people living with HIV/AIDS (PLWHA) (UNAIDS, 2016; Oyeyipo et al., 2018). Additionally, cART is further used as a preventative measure both as pre-and post-exposure prophylaxis (PrPEP), taken by seronegative individuals with a high risk of HIV exposure (UNAIDS, 2016).

These include prostitutes (sex workers), medical professionals with accidental needle pricks and seronegative-seropositive spouses and/or partners who need to take cART on precautionary basis. Though, there has been improved life expectancy amongst PLWHAs, nevertheless, cART has been associated with multiple organ toxicities (Kanmaz and Lee, 2000) such as reproductive (Azu, 2012), cardiovascular (Diouf et al., 2012), metabolic (Srinivasa and Grinspoon, 2014), and hepato-renal (Akang et al., 2020). A cohort study found an increase of more than four-fold in diabetes incidence in PLWHA on cART (Brown et al., 2005). Further, both HIV infection and cART regimen have been observed to induce diabetes (Kalra et al., 2011; Lin et al., 2018). Equally, heavy alcohol consumption is associated with increased diabetes incidence (Kim and Kim, 2012; Wake, 2021). Previously, Howard et al. (2004) found that diabetes incidence increased by up to 43% in persons that consumed more than 3 drinks per day. Since, HIV-positive individuals on cART may be predisposed to development of diabetes and these individuals also consume alcohol regularly which also subject them to onset of diabetes, a scenario of cART-alcohol-diabetes interaction therefore exist in one individual. Amongst others, the reproductive health implications of this may be huge.

Incidentally, diabetes, alcohol, and cART have each been individually reported to cause impairments in the male reproductive system, including; hypogonadism, sexual dysfunction, subfertility, and infertility (Mallidis et al., 2011; Dissanayake et al., 2019). Clinical and experimental diabetes is documented to cause a decrease in testis weight, tubular diameter, and epithelial height, hypothalamic-pituitary-gonadal (HPG) axis dysfunction, diminished sperm vitality, increased fragmented sperm DNA, ejaculatory disorders, and decreased sexual arousal (Gandhi and Dagur, 2016; Condorelli et al., 2018; Long et al., 2018; Ray and Pramanik, 2020). Clinical and experimental studies have demonstrated hypogonadism, testicular atrophy, decreased number of spermatogenic cells, reduced libido, erectile disorder, and poor sperm quality following alcohol consumption (Rachdaoui and Sarkar, 2013; Dosumu et al., 2014; Oremosu and Akang, 2015; Finelli et al., 2022). Experimental and clinical use of cART have been associated with derangement of testis structure, necrosis of germinal epithelium, increased interstitial infiltrate, reproductive hormone imbalance, reduction of ejaculate volume and sperm motility, diminished DNA integrity (Kushnir and Lewis, 2011; Azu et al., 2014; Ogedengbe et al., 2016; Savasi et al., 2018).

Most testicular and spermatozoa dysfunctions are associated with high reactive oxygen species (ROS) (Agarwal et al., 2018; Dutta et al., 2021). Unfortunately, diabetes, alcohol, and cART are known to stimulate increased ROS accumulation (Das and Vasudevan, 2007; Blake and Trounce, 2014; Ikekpeazu et al., 2019). Subsequently, ROS evoke oxidative stress (OS) and inflammatory cytokine release (Nna et al., 2019; Dutta et al., 2021). Although the individual impacts of diabetes, alcohol, and cART on the male reproductive system have been studied separately, these morbidities presently occur in an individual simultaneously. Nonetheless, their combinatorial role in male reproductive dysfunctions and subfertility/infertility which is tremendously increasing globally is still not fully understood. Hence, the possible toxicities that could arise due to the concurrent presence of diabetes, alcohol, and cART in the body on testicular histo-morphology and the possible underlying mechanisms were evaluated. The impact of alcohol intake and cART use in diabetic condition on the testicular histoarchitecture, reproductive hormone levels, oxidative stress, proinflammatory cytokines, apoptosis, germ cell proliferation, and androgen receptor expression were assessed in the current study.

1.2 Study rationale

A high incidence of diabetes (Condorelli et al., 2018), alcohol abuse (World Health Organisation, 2011), and cART use (Khawcharoenporn and Sha, 2016) has been reported in males of reproductive age. Unfortunately, each of these conditions has been shown to adversely impact the male reproductive system (Azu, 2012; Condorelli et al., 2018; Finelli et al., 2022). Additionally, diabetes, alcohol abuse, and cART use are intricately connected and can occur in an individual simultaneously. For instance, alcohol is a recognized risk factor for diabetes (Rehm, 2011; Goecke and Baumeister, 2021), and is linked to an increase in transmission of HIV (Watson et al., 2014; Kumar et al., 2015; Schneider et al., 2016; Scott-Sheldon et al., 2016), thus is indirectly linked to rising cART use (Watson et al., 2014). Equally, an increase in alcohol use in individuals living with HIV including those on cART has also been documented (McCance-Katz et al., 2013; Mondal et al., 2019). Incidentally, both HIV infection and cART have been implicated in diabetes induction (Avari and Devendra, 2017; Bam et al., 2020). Consequently, a multimorbidity of diabetes, alcohol, and cART poses severe reproductive challenges amongst other adverse complications. However, there is no scientific literature available about the impact of a multimorbidity of these three conditions which are prevalent in males of reproductive age on male fertility. Therefore, this study investigated the impacts of concomitant use of alcohol and cART in a diabetic condition on the male reproductive system. The findings of this study serve as a basis for further experimental and

clinical research and highlights male reproductive dysfunctions that could emerge in diabetic people living with HIV/AIDS (PLWHA) and on cART, who consume alcohol regularly.

1.3 Hypothesis of the study

The interactive effects of alcohol and cART in diabetic condition will cause alterations in the testicular histoarchitecture and reproductive hormones which disrupts the spermatogenesis process, subsequently leading to male reproductive dysfunctions.

1.4 Aim and objectives

1.4.1 Aim

To determine changes in testicular histomorphology, immunohistochemical, and hormonal perturbations associated with alcohol and combination antiretroviral drug therapy (cART) co-administration in diabetic rats.

1.3.2 Objectives

To investigate the interactive effects of alcohol and cART in diabetes on the:

- blood reproductive hormone profile (luteinizing hormone (LH), follicle-stimulating hormone (FSH), testosterone (TT), and inhibin B (INB)) using enzyme-linked immunosorbent assay (ELISA).
- testis morphometry and histology using hematoxylin and eosin (H&E) staining technique.
- seminiferous tubule basement membrane (STBM) and testis capsule thickness using periodic acid Schiff (PAS) and Masson's trichrome stain respectively.
- testicular connective tissue components (collagen, reticular, and elastic fibers) using Masson's trichrome, Gordon and Sweet's silver impregnation, and Gomori's Aldehyde Fuchsin stains respectively.
- testis oxidative stress biomarker viz. inducible nitric oxide synthase (iNOS), malondialdehyde (MDA), and 8-hydroxydeoxyguanosine (8-OHDG) using immunohistochemistry technique.
- inflammatory cytokines viz. interleukin-1beta (IL-1β), interleukin-6 (IL-6), and tumor necrosis factor-alpha (TNF-α) using immunohistochemistry technique.
- germ cell apoptosis (caspase-3) and proliferation (Ki-67) using immunohistochemistry technique.
- testicular androgen receptor (AR) expression using immunohistochemistry technique.

CHAPTER 2: LITERATURE REVIEW

2.1 Male reproductive system

The primary function of the male reproductive system is the production of haploid male gametes (Ravindranath et al., 2003; Lara et al., 2018) and their delivery to the female reproductive tract via the penile urethral meatus during copulation (Basu, 2011; Singh, 2014). It consists of the male gonad, the testis and accessory sex glands and structures (seminal vesicles, prostate, and bulbourethral glands), genital tracts (efferent ductules, epididymis, vas deferens, ejaculatory duct, and urethra), scrotum, and a penis (Young et al., 1967, 2013). While the testis is responsible for spermatozoa formation, the genital ducts and accessory glands produce secretions that provide nutrients to spermatozoa, and together with the spermatozoa form the semen (Basu, 2011; Junqueira and Carneiro, 2005). In addition, testes also synthesize male androgens, mainly testosterone which is essential for the development and maintenance of male secondary sexual characteristics and general male physiology (Gilbert and Barresi, 2017; Ravindranath et al., 2003; Victor et al., 2022). Additionally, functioning of male reproductive system is tightly regulated by endocrine hormones of the hypothalamic-pituitary-gonadal (HPG) axis (Ramaswamy and Weinbauer, 2014; Clavijo and Hsiao, 2018).

2.2 Embryology of the testis

Embryonically, testes develop in the posterior lumbar region of abdominal cavity and then descend into the scrotum with layer of peritoneum (tunica vaginalis), nerves, lymphatics, and blood vessels (Junqueira and Carneiro, 2005; Young et al., 2013). In humans, testes descend prenatally through an inguinal ring, reaching the scrotum during the 33rd week of development (Sadler, 2012; Singh, 2014). On the contrary, the testis in rats descends postnatally, reaching the scrotal sac between 4-6 weeks of development (Harnaen et al., 2007), and when the rats are not breeding the testes move up through the open inguinal canal to the abdominal cavity (Hutson et al., 2013) which could be termed a period of breeding inactivity.

2.3 Anatomy of the testis

Testis, the male gonad, is a primary reproductive organ (Ravindranath et al., 2003; Basu, 2011), responsible for spermatogenesis and testosterone synthesis (Lara et al., 2018; Acharyya, 2021). Mammalian testis are paired and each testis is suspended by the spermatic cord into the scrotal sac compartment (Ravindranath et al., 2003; Titi-Lartey and Khan, 2022), which lies exterior to the abdominal cavity (Palleti, 2008; Singh, 2014; Victor et al., 2022). The testes are separated

from each other by a scrotal septum. The temperature in the scrotal sac is slightly lower than the body temperature, thus providing the vital condition for efficient spermatozoa production (Skandhan and Rajahariprasad, 2007; Hutson et al., 2013; Hamilton et al., 2016).

2.3.1 Gross anatomy of testis

Testes of mammals are ovoid-shaped organs that lie obliquely in the scrotum, with the upper pole tilted anterolaterally and the lower pole posteromedially (Palleti, 2008; Singh, 2014; Victor et al., 2022). Male species that engage polygynous mating patterns and are territorial have smaller testis compared to the monogamous males which possess bigger testes (Heske and Ostfeld, 1990). The testis is covered by three membranes; an outer investing layer of peritoneum, the tunica vaginalis; followed by tunica albuginea, a fibrous capsule that gives rise to septa that divides the testis into lobules; and an innermost tunica vasculosa, containing a capillary network and fine connective tissue that covers the septa of lobules (Junqueira and Carneiro, 2005; Young et al., 2013) (Fig. 2.1). Further, blood is supplied by testicular arteries, that arise from abdominal aorta just below the origin of renal arteries and descend retroperitoneally. The arteries pass through the inguinal canal and join the spermatic cord to reach the testis. The blood is drained by a venous plexus (pampiniform) that converge to form the testicular vein. The right testicular vein drains into the inferior vena cava, and the left vein joins the left renal vein. Testicular lymphatics ascend in the spermatic cord alongside the blood vessels and drain into para-aortic lymph nodes at the 1st lumbar level. The testis is innervated by sympathetic nerves originating from the T10 spinal segment that pass through the lesser splanchnic nerve and synapse at the celiac ganglia. Then the postganglionic fibers follow the testicular artery course to reach the testis. Equally, sensory fibers travel through the sympathetic pathway, passing the sensory information via the dorsal root ganglion of T10 spinal nerve. In addition, sensory innervation to the tunica vaginalis of testis is via the genital branch of the genitofemoral nerve of the lumbar plexus (Junqueira and Carneiro, 2005; Young et al., 2013).

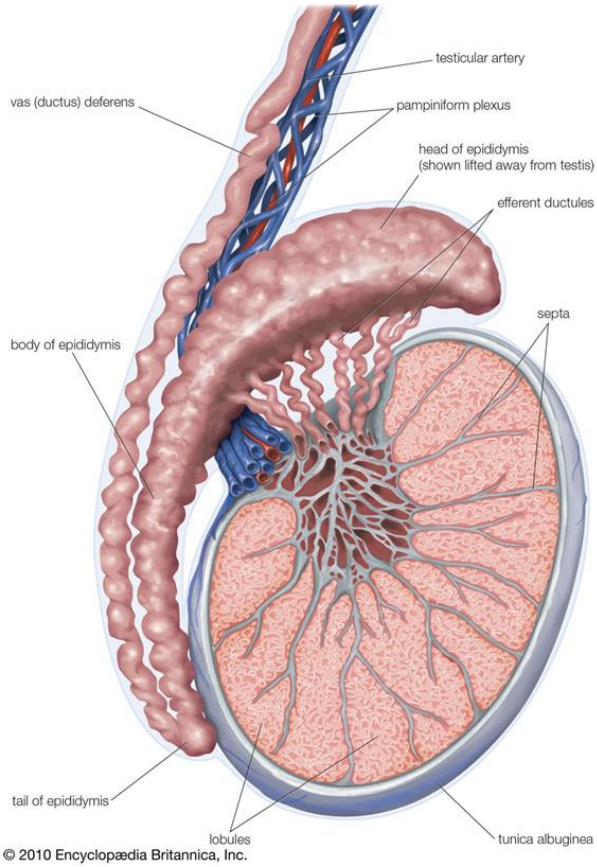


Figure 2.1: An illustration of the gross anatomy of testis and associated structures.
Source: https://www.britannica.com/science/ductus-deferens

2.3.2 Microanatomy of testis

Testicular tissue consists of two major components, the tubular and intertubular which perform the spermatogenesis and steroidogenesis processes respectively (Ravindranath et al., 2003; Deshmukh et al., 2013). The tubular component is composed of seminiferous tubules, which are long tortuous loops that form straight tubules (tubuli recti) at both ends. Tubuli recti converge at the mediastinum to join the rete testis, which in turn deliver the spermatozoa and testicular fluid into epididymis via ductuli efferentes (Ravindranath et al., 2003; Deshmukh et al., 2013). Furthermore, the seminiferous tubule consists of a tunica propria, seminiferous epithelium, and a lumen (Gofur, Khan, Karim, and Islam, 1970; Ravindranath et al., 2003; Lara et al., 2018). Tunica propria is made up of a discontinuous layer of large elongated peritubular cells, the myoid cells (Gofur et al., 1970; Chen et al., 2014), and the basement membrane where the seminiferous epithelium rests (Siu and Cheng, 2004; Losinno et al., 2012).

The seminiferous epithelium contains spermatogenic and Sertoli cells, the spermatogenic cells are stacked up in concentric layers, with early spermatogenic cells (spermatogonia and early spermatocytes) situated close to the basement membrane and maturing spermatogenic cells (zygotene spermatocytes to spermatids) lie adjacent to the lumen (Ravindranath et al., 2003; Deshmukh et al., 2013) (Fig. 2.2). The Sertoli cells give support and nourish germ cells (Petersen and Söder, 2006; França et al., 2016), further, junctions formed by between adjacent Sertoli cells create a blood-testis barrier (BTB) which divides the seminiferous epithelium into a basal and adluminal compartment (Yan Cheng and Mruk, 2012). Conversely testicular intertubular component also referred to as the interstitium lies between the tubules (Hadley, 2007; Deshmukh et al., 2013) and consists of connective tissue (collagen, reticulin, and elastin), arterioles, capillaries, venules, lymph vessels, and nerves (Young et al., 2013; Falade et al., 2017). Leydig cells, fibroblasts, and macrophages are also embedded in the interstitium (Ravindranath et al., 2003; Seevagan et al., 2019).

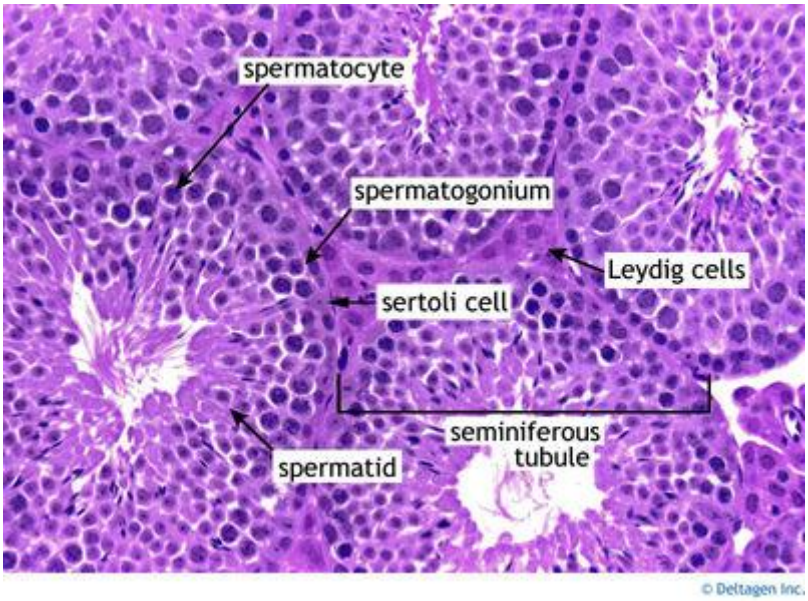


Figure 2.2: Rat testis cross section showing testicular parenchyma microanatomy, H&E stain. Source: http://histology-world.com/photoalbum//displayimage.php?pos=-1161

2.4 Leydig cell and steroidogenesis

2.4.1 Leydig cell structure and function

Leydig cells are polyhedral somatic cells found in the testis interstitial that synthesize androgens via steroidogenesis (Hooker, 1970; Ge et al., 2006; Martin, 2016). Their nucleus is oval and centrally located, peripherally one to three nucleoli are present (Hooker, 1970;

Aladamat and Tadi, 2022). The cytoplasm has abundant smooth endoplasmic reticulum (SER), lipid droplets, and mitochondria (Martin, 2016). These features are necessary for steroid synthesis function of Leydig cells (Aladamat and Tadi, 2022). The steroidogenesis process is regulated by the hypothalamic-pituitary-gonadal (HPG) axis, particularly the luteinizing hormone (LH) secreted by the pituitary gland (Ivell et al., 2014; Coss, 2018). Noteworthy, the Leydig cell steroidogenic capacity is suggested to be determined by the amount of cytoplasmic smooth endoplasmic reticulum and mitochondria rather than the number and size of the cell themselves (Clavijo & Hsiao, 2018; Wang et al., 2017; Zirkin & Papadopoulos, 2018).

Male androgens (testosterone (TT), dihydrotestosterone (DHT), and androstenedione are essential for testis development, successful spermatogenesis, blood-testis barrier integrity, brain masculinization, development and maintenance of male secondary sexual characteristics and behaviours, and general wellbeing (O'Donnell et al., 2001; Smith and Walker, 2014; Victor et al., 2022). However, germ cells do not express androgen receptors (AR), thus the impact of androgen on the germ cell progression is transduced via the Sertoli cells that possess AR (Petersen and Söder, 2006; Smith and Walker, 2014; O'Hara and Smith, 2015). Accordingly, efficient Leydig cell function is very important for male fertility preservation (O'Hara and Smith, 2015; Zirkin and Papadopoulos, 2018; Heinrich and DeFalco, 2020). Notably, following initiation of gonadal differentiation by the fetal Sertoli cell anti-Mullerian hormone, androgen production by Leydig cells commences and continues for life (Petersen and Söder, 2006; Zirkin and Papadopoulos, 2018; Aladamat and Tadi, 2022). The appearance of androgen during embryonic development stimulates the formation of male urogenital organs (Sadler, 2012; Singh, 2014; Titi-Lartey and Khan, 2020).

In mammalian species, fetal and adult Leydig cells exist, and their morphology and steroidogenic capacity vary at different stages (Griswold and Behringer, 2009; Martin, 2016). Fetal Leydig cells synthesize androstenedione, an intermediate compound of testosterone and insulin-like 3 (INSL3) that regulates the development and descent of testis from the abdomen to scrotal sac (Martin, 2016; Zirkin and Papadopoulos, 2018). The fetal Sertoli cells are necessary for completing androgen synthesis (Shima and Morohashi, 2017; O'Donnell et al., 2022), they express 17b-hydroxysteroid dehydrogenase 3 (HSD17B3) for converting androstenedione into testosterone (Griswold and Behringer, 2009; Lara et al., 2018). In addition, fetal Sertoli cell enzyme 5α reductase converts some testosterone into

dihydrotestosterone (DHT) (Griswold and Behringer, 2009; Martin, 2016). Testosterone and DHT induce mesonephric Wolffian duct development into male internal (epididymis, vas deferens, seminal vesicles, and ejaculatory ducts) and external (prostate, penis, and scrotum) genitals respectively (Sadler, 2012; Singh, 2014; Titi-Lartey and Khan, 2020).

Conversely, during puberty, adult Leydig cells develop from peritubular interstitial progenitor cells (Shima and Morohashi, 2017; Titi-Lartey and Khan, 2020). The adult Leydig cells express HSD17B3 which enables them to complete androgen production independent of Sertoli cells (Martin, 2016; Lara et al., 2018). Simultaneously, HSD17B3 is silenced in Sertoli cells and adult Leydig cells synthesize androgens exclusively (Griswold and Behringer, 2009; Lara et al., 2018). However, Leydig cell mitotic and apoptotic activities cease after puberty (SAEZ et al., 1989; Martin, 2016) and Leydig cell androgen production capacity declines with age (Harman et al., 2001; Wang et al., 2017).

2.4.2 Steroidogenesis process

Leydig cell steroidogenesis is a complex multistep process for biosynthesis of androgens (testosterone) from cholesterol (Miller and Auchus, 2011; Wang et al., 2017; Andric and Kostic, 2019) (Fig. 2.3). Fundamentally, the steroidogenesis process is regulated by the hypothalamic-pituitary axis hormones (Ivell et al., 2014; Coss, 2018; Andric and Kostic, 2019). Steroid biosynthesis is initiated by luteinizing hormone (LH) released by the pituitary gland in response to gonadotropin-releasing hormone (GnRH) from the hypothalamus binding to the LH receptor (LHR) on Leydig cell (Miller and Auchus, 2011; Ho et al., 2017; Wang et al., 2017). In response to LH, Leydig cell synthesizes cyclic adenosine 3',5'-monophosphate (cAMP) from adenosine triphosphate (ATP) (Haider, 2007; Zirkin and Papadopoulos, 2018; Andric and Kostic, 2019). Sequentially, cAMP stimulates the translocation of cholesterol from cytoplasm source to outer mitochondrial membrane (Miller and Auchus, 2011; Wang et al., 2017).

Then, steroidogenic acute regulatory protein (StAR) mediates cholesterol transfer (Haider, 2007; Papadopoulos and Miller, 2012; Zirkin and Papadopoulos, 2018). The mitochondria inner membrane matrix has the enzyme P450 side-chain cleavage (P450scc) encoded by the Cytochrome P450 Family 11 Subfamily A1 (CYP11A1) gene that catalyzes the transformation

of cholesterol into pregnenolone (Papadopoulos and Miller, 2012; Zirkin and Papadopoulos, 2018; Andric and Kostic, 2019). Eventually, pregnenolone is transported to the SER and is serially converted into testosterone by SER steroidogenic enzymes (Cytochrome P450 Family 17 Subfamily A1 (CYP17A1), 3β-hydroxysteroid dehydrogenase (3β-HSD), and 17β-HSD) (Haider, 2007; Papadopoulos and Miller, 2012; Zirkin and Papadopoulos, 2018). Notably, defects in steroidogenic regulatory proteins interfere with androgen production, leading to diminished Leydig cell biosynthetic capacity (Miller and Auchus, 2011; Wang et al., 2017).

Furthermore, macrophages coexist with Leydig cells in testicular interstitium (Hooker, 1970; Ravindranath et al., 2003; Martin, 2016) and the interaction between the two cell types is indirectly involved in increasing Leydig cell androgen production (Goluža et al., 2014; Heinrich and DeFalco, 2020). In vitro studies have demonstrated an increase in testosterone synthesis when macrophages were added to the Leydig cell culture (Yee and Hutson, 1985; Goluža et al., 2014; Martin, 2016; Heinrich and DeFalco, 2020). Furthermore, Sertoli cell secretions in response to follicle-stimulating hormone (FSH) stimulation influence Leydig cell steroidogenesis (Martin, 2016; Neves et al., 2017). The luteinizing hormone releasing hormone-like peptide and inhibin released by Sertoli cells have both stimulatory and inhibitory impacts on androgen production accordingly (Sharpe et al., 1981; Martin, 2016).

Consequently, interference in the Leydig cell steroidogenesis process leads to primary hypogonadism, a condition characterized by reduced testosterone levels (Beattie et al., 2015; Zirkin & Papadopoulos, 2018). Hypogonadism is a major contributing factor to male infertility and is linked to the decline in male physic via muscle and bone mass wasting (Ho et al., 2017; Tywanek et al., 2021). Additionally, low testosterone is a risk factor for neurocognitive disorders (Pike et al., 2006; Yeap, 2014). Earlier studies showed that HPG axis dysfunctions that occur during menopause/andropause are associated with brain degenerative changes and aging (Atwood et al., 2005; Meethal and Atwood, 2005; Blair et al., 2015). Recently, testosterone has been identified to play a part in the severe acute respiratory syndrome coronavirus 2 (SARS-CoV-2) infection (COVID-19) clinical severity (Hussain et al., 2020; Dutta and Sengupta, 2021). The accumulating evidence showing involvement of testosterone in several vital physiological processes and clinical pathogenesis demonstrates the importance of well-regulated steroidogenesis in the maintenance of male fecundity and wellbeing (Martin, 2016; Lotti et al., 2021).

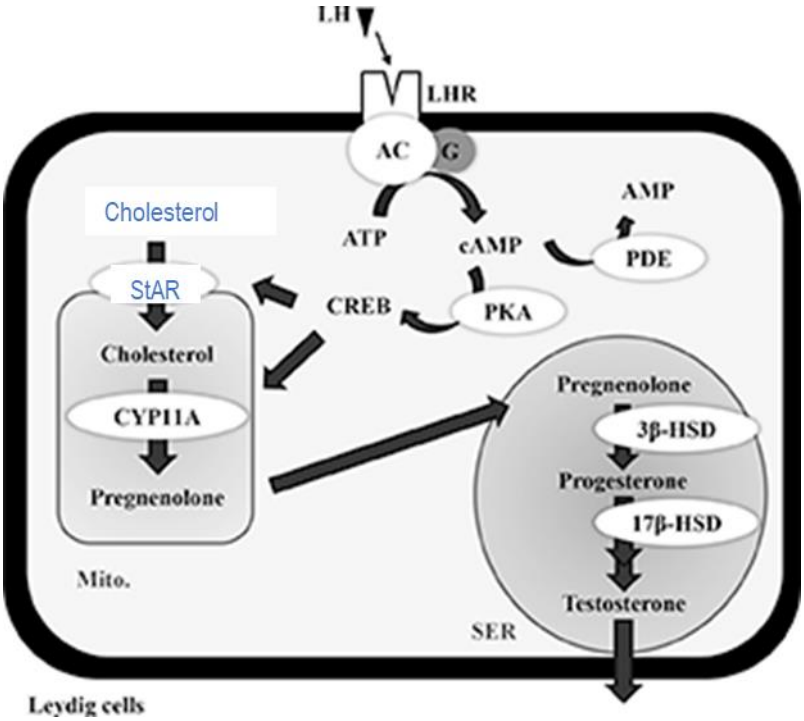


Figure 2.3: Schematic illustration of Leydig cell testosterone biosynthesis from cholesterol. Source: Ho et al., 2017

2.5 Sertoli cell and blood-testis-barrier (BTB)

2.5.1 Sertoli cell structure and function

Sertoli cells have one of the most complex cell structure in the body (Hess and França, 2004; França et al., 2016; Shah et al., 2021). They are irregular broad columnar cells that extend from the basement membrane to adluminal compartment of seminiferous epithelium (Hess and França, 2005; Hess and Vogl, 2015). Sertoli cells have an extensive cytoskeleton consisting of microfilaments, intermediate filaments, and microtubules (Nakai and Hess, 1994; Hess and França, 2004; Hess and Vogl, 2015) that support the cells' asymmetric dynamic shape (Mruk and Cheng, 2004; França et al., 2016). Remarkably, fetal Sertoli cells express the SRY gene which is responsible for the formation of testis determining factor in the primitive gonad (Griswold, 1998; Petersen and Söder, 2006; Singh, 2014). Thus, appearance of fetal Sertoli cells marks and initiates the development of male gonads (testis) (Petersen and Söder, 2006; Sadler, 2012; Singh, 2014). The anti-Müllerian hormone secreted exclusively by fetal Sertoli cells causes degeneration of the paramesonephric ducts to inhibit formation of female genital ducts (Griswold, 1998; Petersen and Söder, 2006; Singh, 2014; Titi-Lartey and Khan, 2020). Sertoli cells proliferate extensively during prenatal and neonatal periods, followed by several years of dormancy (Petersen & Söder, 2006; Sharpe, McKinnell, Kivlin, & Fisher, 2003;

Tarulli, Stanton, Lerchl, & Meachem, 2006). After which, a peak proliferation occurs in response to a sudden male hormone increase at the onset of puberty and then the cells start differentiating into the mature Sertoli cell form (Sharpe et al., 2003; O'Donnell et al., 2022) and subsequently the proliferation ceases after puberty (Petersen and Söder, 2006; Tarulli et al., 2012; França et al., 2016).

Each Sertoli cell nurses a clone of differentiating germ cells, the number of Sertoli cells determines the testis size and spermatozoa quantity (Petersen and Söder, 2006; Rebourcet et al., 2017; Oduwole et al., 2018). The several Sertoli cell functions include germ cell nourishment, germinal epithelium structural support, phagocytosis of spermatid residual bodies and apoptotic spermatogenic cells, secretion of seminiferous fluid, and creation of an immune privilege microenvironment (Griswold, 1995; Petersen and Söder, 2006; Kaur et al., 2014; Lara et al., 2018). Furthermore, Sertoli cells are essential in the maintenance of seminiferous epithelium structural integrity (Mruk and Cheng, 2004; Domke et al., 2014; Lara et al., 2018). They form the blood-testis-barrier (BTB) via their specialized Sertoli to Sertoli cell tight, adhering, and gap junctions (Mruk and Cheng, 2004; Yan Cheng and Mruk, 2012; Shah et al., 2021).

2.5.2 The structure and function of blood-testis-barrier (BTB)

The BTB of seminiferous tubule is amongst the tightest mammalian blood tissue barriers (Cheng et al., 2011; Islam et al., 2017). It differs from other blood tissue barriers (blood-brain and blood-retina/ocular) that are formed by tight junctions between microvascular endothelial cells (Mruk and Cheng, 2015; Islam et al., 2017). In addition to the tight junction, BTB consists of desmosomes, adhering (basal ectoplasmic specializations), and gap junctions between Sertoli cells adjacent to the basement membrane of the seminiferous tubule (Domke et al., 2014; Miller and Cherrington, 2018). The BTB divides seminiferous epithelium into two compartments (Yan Cheng and Mruk, 2012): a basal compartment that lies exterior to the BTB and an apical compartment that lies interior to the BTB (Wong and Cheng, 2005; Domke et al., 2014; Islam et al., 2017) (Fig. 2.4). Conversely, spermatogonia renewal and proliferation and germ cell progression from type B spermatogonia to preleptotene spermatocyte take place in the basal compartment (Wong and Cheng, 2005; Yan Cheng and Mruk, 2012) after which the BTB under goes a dynamic period involving restructuring of its complex junctions to allow migration of preleptotene spermatocytes from the basal to the apical compartment (Cheng and Mruk, 2009; Su et al., 2011; Miller and Cherrington, 2018). Thus, the rest of the steps of

spermatogenesis cell progression i.e., from zygotene spermatocytes to mature spermatozoa occur in a specialized immune-privileged microenvironment after crossing the BTB (Su et al., 2011; Mruk and Cheng, 2015). Studies have shown that adhesion protein complexes, actin regulatory proteins, cytokines (transforming growth factor-3, tumor necrosis factor-α, and interleukin-1), and androgens (testosterone) are regulators of BTB cyclic dynamics (Lui and Cheng, 2007; Wen et al., 2018).

Furthermore, immunological barrier integrity must be maintained during the BTB restructuring period to prevent formation of antibodies against spermatogenesis germ cells (post the preleptotene spermatocyte stage) (Yan Cheng and Mruk, 2012; Chen et al., 2018), autoantigen that leads to autoimmune disease and consequently male infertility (Li et al., 2012; Islam et al., 2017). The immunological barrier interruption as preleptotene spermatocytes transit the BTB is avoided by establishing a new BTB behind the degenerating old BTB integral membrane proteins (Yan Cheng and Mruk, 2012; Islam et al., 2017; Chen et al., 2018). Impairment of the BTB complex structure and function has been implicated in cadmium, bisphenol A induced testicular toxicity, and consequent dysfunctions (Cheng et al., 2011; Yan Cheng and Mruk, 2012)

Further, the complex BTB structure and its tight regulation hinder drug delivery to the germinal epithelium (Diamantopoulos and Kortsaris, 2010) and development of effective reversible male contraception options (Yan Cheng and Mruk, 2012). Notably, Sertoli cells mediate spermatogonial stem cells (SSCs) self-renewal, differentiation, and apoptosis (Hai et al., 2014). Therefore, Sertoli cells are potential targets for delivering treatment for impaired/disturbances of spermatogenesis and germ cell tumors (França et al., 2016; Korivi and Pagliaro, 2022). In addition, Sertoli cell biological characteristics provide innovative approaches for efficient male infertility gene therapy and potential male contraceptive targets (Dufour et al., 2004; Hai et al., 2014).

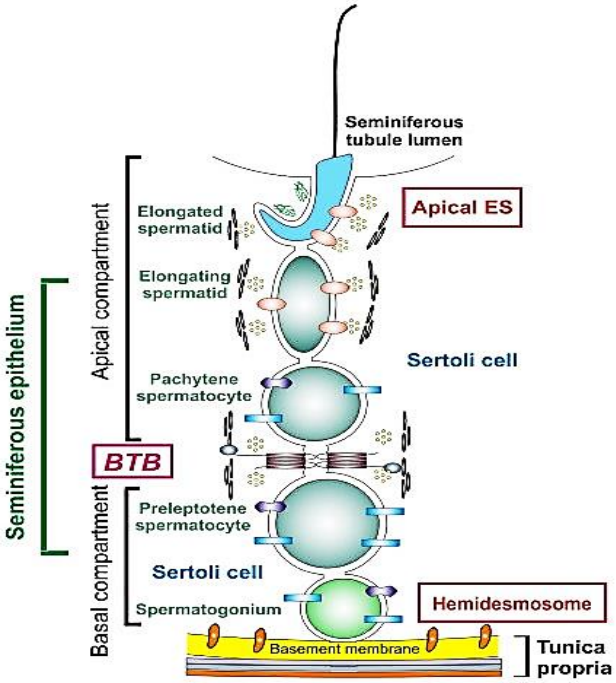


Figure 2.4: Schematic drawing of blood-testicular barrier (BTB) structure

Source: Yan Cheng & Mruk, 2012

2.6 Spermatogenesis and the spermatogenic cycle and wave

2.6.1 Spermatogenesis

Spermatogenesis is a process in which diploid spermatogonia stem cells form haploid spermatozoa male gamete (Singh, 2014; Griswold, 2016). It occurs in testicular seminiferous tubules, commencing at puberty, and lasts a lifetime (Sadler, 2012; Gilbert and Barresi, 2017; Lara et al., 2018). The process of spermatogenesis involves both mitotic and meiotic cell divisions and can be divided into five phases: proliferative, differentiation, meiotic, spermiogenesis, and spermiation (Young et al., 1967, 2013) (Fig. 2.5).

I. During the proliferative phase, a pool of cells emerges from the spermatogonia stem cell population to form type A spermatogonia which are relatively small cells located close to the basal lamina. Type A spermatogonia divide mitotically to produce a population of dark and light type A spermatogonia. The dark type A spermatogonia are reserved for the next cycle. The light type A spermatogonia cells undergo several mitotic divisions to form a cellular clone.

II. In the differentiation phase, the light type A spermatogonia during their successive mitotic division differentiate into type B spermatogonia, progenitor cells committed to sperm formation. Type B spermatogonia are the biggest cells amongst the

spermatogenic lineage cells, they divide mitotically forming preleptotene primary spermatocytes.

III. The Meiotic phase comprises two successive divisions, meiosis I and II. The primary spermatocytes enter meiosis I division, undergoing prolonged prophase followed by a rapid first meiosis completion. They form two haploid secondary spermatocytes. Secondary spermatocyte goes through meiosis II division quickly and forms two round spermatids each. The round spermatids have a dark-stained rounded nucleus and are smaller compared to the spermatocyte, and they lie adjacent to the seminiferous tubule lumen.

IV. Spermiogenesis is the stage where the round spermatids undergo extensive morphological remodelling to form elongated spermatids, which are further transformed into highly specialized cells, the spermatozoa. It entails; the formation of a nuclear acrosomal cap, nucleus condensation, tail (flagellum) formation, and shedding off most of the cytoplasm. The resulting spermatozoa consist of a head, neck, and long flagellum.

V. Spermiation is the final step in spermatogenesis during which spermatozoa are released into seminiferous lumen. Spermatozoa then propel in testicular fluid medium to the rete testis and continue in a peristaltic movement to the epididymis.

During the mitotic division of type A spermatogonia, the daughter cells are separate, however, after forming the type B spermatogonium, the successive daughter cells remain connected via cytoplasmic bridges (Young et al., 1967; Sadler, 2012; Singh, 2014). After completion of spermatogenesis, the extra cytoplasm and cytoplasmic bridges are shed off as residual bodies, freeing up the spermatids (Young et al., 2013; Gilbert and Barresi, 2017). Additionally, spermatogenesis does not proceed simultaneously in the different portions of the seminiferous tubule, this asynchrony leads to the presence of germ cells at different stages of within the seminiferous tubule at any point, which is termed the cycle of seminiferous germinal epithelium (Griswold, 2016; Lara et al., 2018).

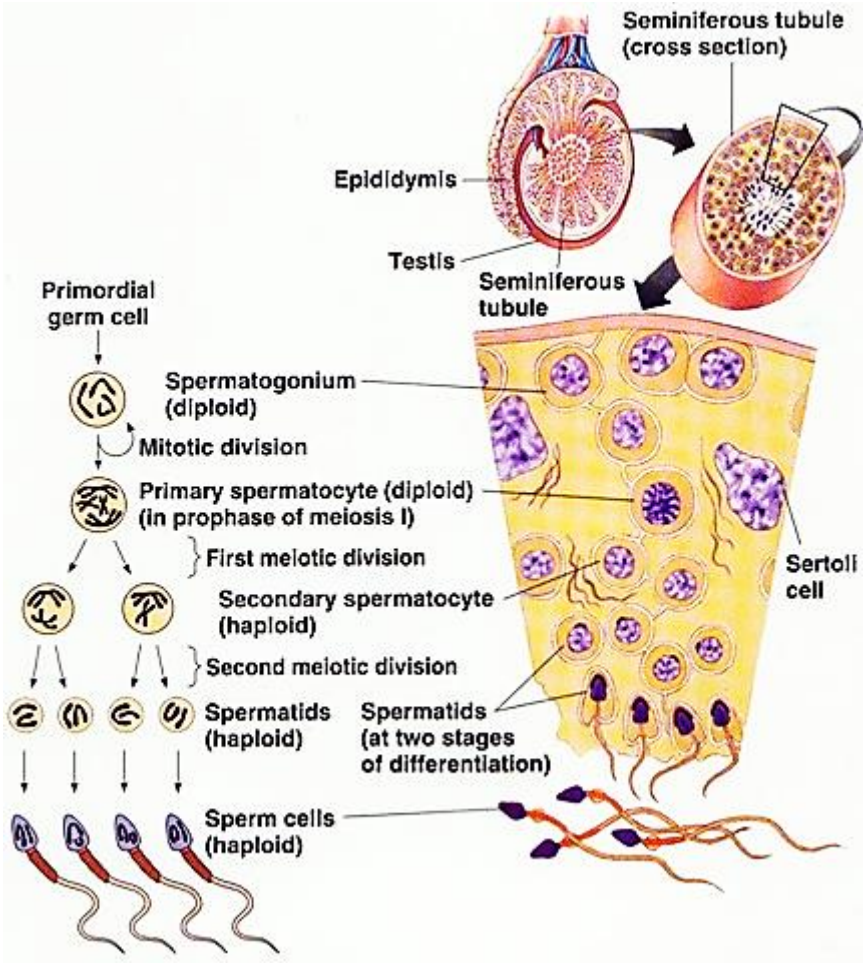


Figure 2.5: Illustration of spermatogenesis phases

Source:https://www.majordifferences.com/2013/06/difference-between-spermatogenesis-and.html

2.6.2 Spermatogenic cycle and wave

2.6.2.1 Spermatogenic cycle

The time a germ cell takes to differentiate from spermatogonia into a mature/elongated spermatid is known as the **spermatogenic cycle** (Leblond & Clermont, 1952; Nakata, Sonomura, & Iseki, 2017). A cycle consists of different germ cell progression steps in the germinal epithelium vertical axis, with each step lasting for a specific duration (Meistrich and Hess, 2013; Lara et al., 2018). Since spermatogenesis is a continuous process, cells at different progression steps coexist at a specific time in the cycle and thus cellular associations are constant (M. D. Griswold, 2016; Leblond & Clermont, 1952). A seminiferous tubule cross-section shows an epithelium consisting of Sertoli and different spermatogenic cells, the layers of spermatogenic cells are organized concentrically according to their progression level. The

spermatogonia and early spermatocytes consecutively lie adjacent to the basement membrane and successive layers of cells from leptotene spermatocytes to spermatids lie adjacent to the lumen (Lara et al., 2018). Distinctive stages of the germinal epithelium cycle have been categorized using several methods (Meistrich and Hess, 2013; Lara et al., 2018) such as spermatid acrosomal, tubular morphology, a combination of spermatid acrosomal and tubular morphology, and protein immunolocalization (Griswold, 2016; Nakata et al., 2017).

Using the spermatid acrosomal method, (Leblond & Clermont, 1952) categorized the associations of spermatogenic cells into 14 stages in rats, 12 stages in mice, and 6 stages in humans (Lara et al., 2018). In this classical method, periodic acid-Schiff's reaction (PAS) was used to detect the changes in spermatid acrosomic system (Leblond & Clermont, 1952) (Hess and De Franca, 2008). Briefly, the general features that indicate germinal epithelium stages are as follows (Fig. 2.6). For **stage I,** young spermatids heads are far from the basement membrane, they have a smaller nucleus compared to the successive stages and a globular like cytoplasm. For **stage II-V,** an acrosomal system forms around the spermatid nucleus, and the spermatid heads congregate into distinct bundles that migrate in the direction of the Sertoli cell nucleus, which are located basally. For s**tage VI,** acrosomal system is sufficiently grown and spreads covering the nucleus like a small cap, and the elongated spermatids bundles start moving towards the lumen. For s**tages VII-VIII,** the elongated spermatid heads lie adjacent to the lumen and their tails form whirls in the center of the lumen. Additionally, two spermatid generations are present in **stages I-VIII**, the newly formed round spermatids, and the mature elongated spermatids. Further, one generation of spermatids that are transitioning from round to elongated is present in stages **IX-XIV**. For s**tage IX,** the spermatid nuclei begin to flatten and elongate, and residual bodies are gradually resorbed into the Sertoli cell cytoplasm. For **stage X-XIII,** the spermatids have an elongated nucleus and a globular cytoplasm and start forming bundles between the older spermatocytes that are directed towards the Sertoli cell nucleus. For **stage XIV,** the spermatid nuclei begin to contract longitudinally, the spermatids are no longer clustered in bundles, and their globular cytoplasms are seen in the lumen (LEBLOND and CLERMONT, 1952). However, the stages of germinal epithelium can be divided into three groups viz. early: stages I-V, middle: stages VI-VIII; and late: stages IX-XII for research studies (Hess and De Franca, 2008).

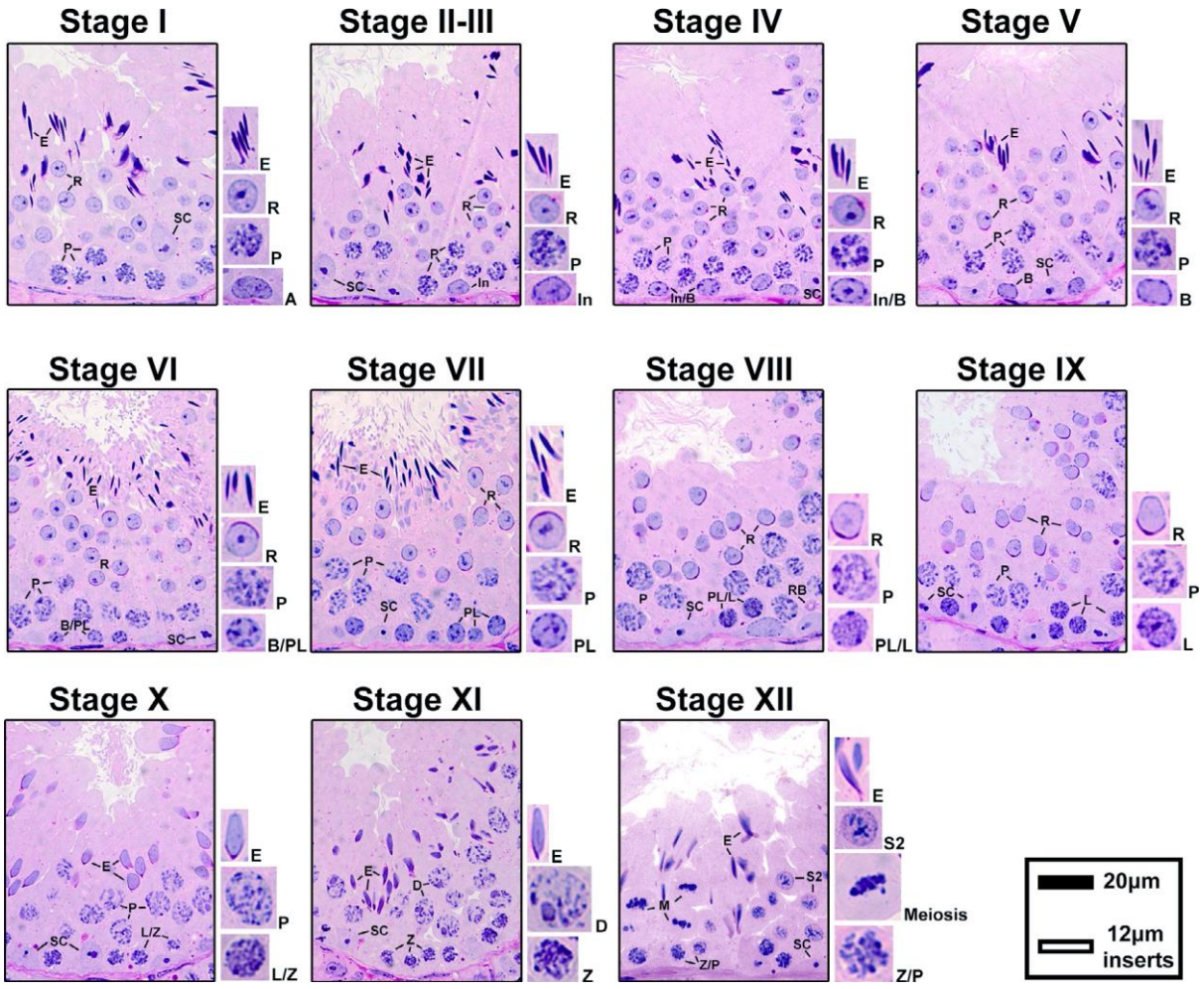


Figure 2.6: Spermatogenic cell associations at different stages (I–XII) of germinal epithelium in mouse testis, PAS stain.

Key: SC, Sertoli cells; A, type A spermatogonia; In, intermediate spermatogonia; B, type B spermatogonia; Pl, preleptotene spermatocyte; L, leptotene spermatocyte; Z, zygotene spermatocyte; P, pachytene spermatocyte; D, diplotene spermatocyte; S2, secondary spermatocyte; R, round spermatid; and E, elongated spermatid. Source: Lara et al., 2018

2.6.2.2 Spermatogenic cycle and wave

On the other hand, a series of different stages of the spermatogenic cycle are present along the seminiferous tubule longitudinal axis (length), referred to as the **spermatogenic wave** (Perey et al., 1961; Hogarth and Griswold, 2010; Nakata et al., 2017) (Fig. 2.7). The stages are arranged in descending order in most of the segments along the tubule length i.e., from the rete testis to the distal tubular portion (Hogarth and Griswold, 2010; Lara et al., 2018). Fewer segments have an ascending stage number arrangement (Perey et al., 1961; Nakata et al., 2017).

The spermatogenic wave and the arrangement of the stages are essential for producing spermatozoa consistently and for efficiency in its propulsion to the rete testis (Perey et al., 1961; Griswold, 2016; Lara et al., 2018).

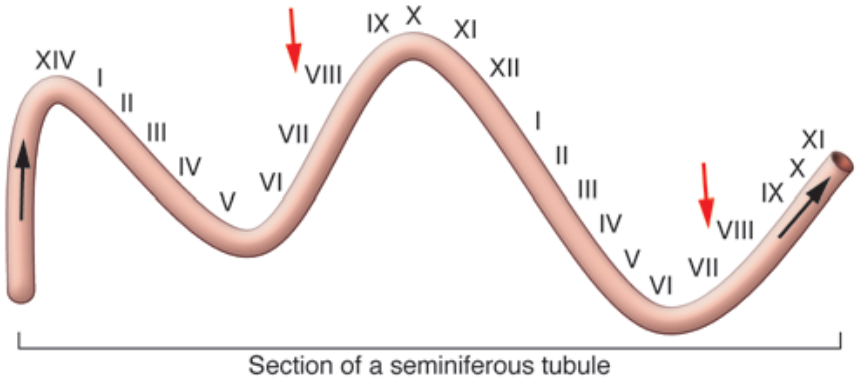


Figure 2.7: An illustration of a spermatogenic wave showing different stages of germinal epithelium along a seminiferous tubule.
Points of meiotic initiation are indicated by red arrows and the black arrows show the direction of the wave. Source: Hogarth and Griswold, 2010

2.7 Male hypothalamic pituitary gonadal (HPG) axis

The HPG axis consists of; hypothalamus, anterior portion of pituitary gland, and testis (gonad) in males (Bennett, 2010; Clavijo and Hsiao, 2018). It is responsible for the endocrine control of testicular function (Ramaswamy and Weinbauer, 2014; Corradi et al., 2016). Normal androgen (testosterone) and sperm production require an impeccable coordinated HPG axis action (Corradi et al., 2016; Clavijo and Hsiao, 2018; Coss, 2018). Gonadotrophin-releasing hormone (GnRH) is secreted episodically in the hypothalamus (Plant, 2015; Corradi et al., 2016), and flows through the hypophyseal portal blood pathway to anterior pituitary (Plant, 2015; Clavijo and Hsiao, 2018), stimulating the secretion of gonadotropins, follicle-stimulating (FSH) and luteinizing hormone (LH) (Ivell et al., 2014; Coss, 2018).

The gonadotropins (LH and FSH) are released into the general blood circulation for transportation to the testis where they regulate the somatic testicular cell function, Leydig and Sertoli cell respectively (Marques et al., 2000; Corradi et al., 2016; Coss, 2018). The LH binds to LH receptor (LHR) on Leydig cell to stimulate steroidogenesis of androgens (testosterone) (Ivell et al., 2014; Gurung and Jialal, 2019; Shah et al., 2021) while FSH independently or

together with testosterone stimulates Sertoli cell function including spermatogenesis regulation (Ramaswamy and Weinbauer, 2014; Coss, 2018) and biosynthesis of inhibin, transferrin, and seminiferous fluid (Petersen and Söder, 2006; Barbotin et al., 2019). Actions of the HPG axis are controlled via a negative feedback mechanism (Corradi et al., 2016; Coss, 2018), whereby testosterone and inhibin stimulate or inhibit secretion of GnRH, LH, and FSH by the hypothalamus and anterior pituitary respectively (Marques et al., 2000; Ivell et al., 2014; Clavijo and Hsiao, 2018) (Fig. 2.8).

Further, congenital or acquired disorders that impair the function of HPG axis at different levels lead to an imbalance in reproductive hormones, a condition termed hypogonadism (Kim, 2015; Foyouzi, 2019; Barber et al., 2021). Hypogonadism could be primary or central; primary hypogonadism, also referred to as testicular hypogonadism, is majorly due to impairment of testicular steroidogenesis process (Fraietta et al., 2013; Clavijo and Hsiao, 2018), and is characterized by increased levels of LH and FSH and a reduction in testosterone levels (Salonia et al., 2019). Central hypogonadism, also known as hypo-gonadotrophin hypogonadism (HH), results from defects in either the pituitary or hypothalamic and is referred to as secondary and tertiary hypogonadism respectively (Kim, 2015; Clavijo and Hsiao, 2018; Barber et al., 2021). The HH can be differentiated from primary/testicular hypogonadism by the low testosterone levels displayed along with reduced or normal LH and FSH levels (Rey et al., 2013; Corradi et al., 2016). However, a mixed primary and central hypogonadism is generally observed in older males (Dandona and Rosenberg, 2010; Rey et al., 2013) and has been suggested to result from decreased receptor sensitivity for GnRH, LH, and FSH (Surampudi et al., 2012; Salonia et al., 2019).

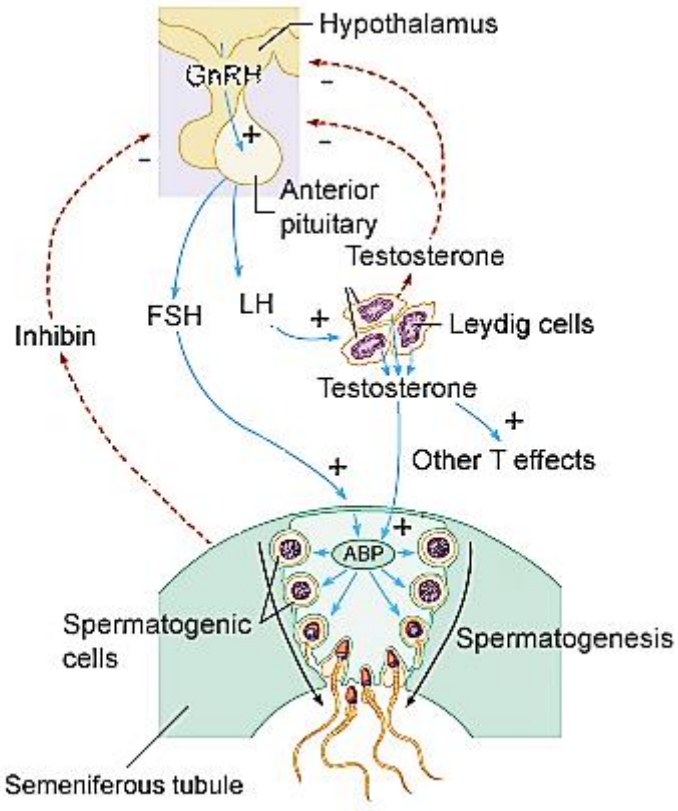


Figure 2.8: Schematic representation of HPG axis showing feedback mechanism.
Source: https://www2.nau.edu/~gaud/bio301/content/hpg.htm

2.8 Male infertility and its treatment

2.8.1 Male infertility

Reports indicate that disturbances of the hypothalamic-pituitary-gonadal (HPG) axis may lead to male reproductive insufficiency and infertility amongst other causes (Clavijo and Hsiao, 2018; Sengupta et al., 2022). There has been an increase in the global trend of male infertility since 1990, with sub-Saharan Africa highly affected (Inhorn and Patrizio, 2014; Agarwal et al., 2021). World health organization (WHO) defines infertility as a failure of a reproductive-age non-contracepting couple to achieve a pregnancy after one year of frequent vaginal unprotected sexual intercourse (Kocyigit, 2015). Infertility affects 15% (48.5 million) couples worldwide (Agarwal et al., 2015; Sun et al., 2019). Whilst male infertility, an inability to make a fertile female conceive contributes to 50% of couple infertility recorded (Kocyigit, 2015; Agarwal et al., 2021). A global survey reported an annual increase of 0·291% in male infertility (Sun et al., 2019). Compelling evidence shows that various factors can impair male fertility, these include physiological factors such as weight and age, lifestyle factors (diet, exercising, and

substance abuse including alcohol use), environmental factors (toxins and radiation), psychological factors (trauma, anxiety, and stress), and pathological factors (bacterial and viral infections, inflammatory diseases, and metabolic disorders, autoimmune diseases, and neoplasms) (Dutta et al., 2021).

Male infertility is broadly classified into coital and azoospermia infertility (Hamada et al., 2013; Naz and Kamal, 2017), occurring due to reversible or irreversible reproductive insufficiency conditions (Jungwirth et al., 2012; Raheem et al., 2019). Azoospermia infertility, a sperm-devoid ejaculate, can occur due to either spermatogenesis impairment (Hamada et al., 2013; Raheem et al., 2019) or genital duct obstruction (Jungwirth et al., 2012; Naz and Kamal, 2017). However, in coital infertility, both spermatogenesis and genital ducts are normal (Raheem and Ralph, 2011; Raheem et al., 2019), but ejaculation is affected due to sexual dysfunction (Jungwirth et al., 2012; Naz and Kamal, 2017). Further, male infertility decreases the individual's quality of life and is categorized as a form of health impairment in males (Ventimiglia et al., 2016; Agarwal et al., 2021), especially when infertility is accompanied by hypogonadism and/or sexual dysfunction (Lotti and Maggi, 2018; Pillai and McEleny, 2021). Aetiologies for male infertility include acquired and congenital disorders (Ventimiglia et al., 2016; Pillai and McEleny, 2021), however, 50% of the infertility cases are idiopathic (Jungwirth et al., 2012; Dimitriadis et al., 2017). These affect fertility at different levels and can be classified into pre-testicular, testicular, and post-testicular factors (Naz and Kamal, 2017; Pillai and McEleny, 2021).

Pre-testicular aetiologies consist majorly the hypogonadotrophin hypogonadism (HH), an endocrine disorder in the hypothalamic-pituitary part of HPG axis (Krausz, 2011; Fraietta et al., 2013; Salonia et al., 2019) and coital disorders, including erectile dysfunction, retrograde ejaculation, and anejaculation (Raheem and Ralph, 2011; Naz and Kamal, 2017). Additionally, HH is also referred to as central or secondary hypogonadism could be a result of congenital or acquired factors (Bianco and Kaiser, 2009; Pienkowski et al., 2011; Foyouzi, 2019). Congenital HH is characterized by a delayed onset or completion of puberty (Fraietta et al., 2013; Kim, 2015; Salonia et al., 2019), in which all reproductive hormone levels are inadequate due to a defect in gonadotropin-releasing hormone (GnRH) (Bianco and Kaiser, 2009; Lotti and Maggi, 2018). The identified gene defects involved in congenital HH include the Kallmann syndrome genes (KAL-1, KAL-2 (FGFR1), PROK2/PROK2R, FGF8) and the idiopathic HH genes (GnRH1/GNRHR, KiSS1/GPR54 IHH, TAC3/TAC3R) (Krausz, 2011; Kim, 2015; Foyouzi,

2019). Acquired HH mostly appears in adulthood and presents mild symptoms such as a decrease in seminal fluid volume and reduced libido (Krausz, 2011; Naz and Kamal, 2017). There are several causes of acquired HH, including tumors (pituitary and brain), head injury, brain radiotherapy, infections (fungal, sarcoidosis, hemochromatosis), autoimmune hypophysitis, some chronic diseases, certain medications, alcohol, illicit drug abuse, and nutritional deficiencies (Fraietta et al., 2013; Sansone et al., 2018; Salonia et al., 2019).

Testicular aetiologies of male infertility primarily affect the testicular structure and function, causing steroidogenesis or/and spermatogenesis disorders (Krausz, 2011; Ventimiglia et al., 2016; Pillai and McEleny, 2021). The several acquired causes of testicular dysfunction include testicular torsion, cryptorchidism, testicular trauma, varicocele, mumps orchitis, chemo- and radiotherapy, medication (endocrine disruptors, antiandrogens, and opioids), alcohol abuse, testicular cancer, systemic diseases (live cirrhosis, renal failure), and sexually transmitted diseases (STDs) (Krausz, 2011; Naz and Kamal, 2017; Agarwal et al., 2021). Also, chromosomal abnormalities such as Klinefelter, Swyer's, and Turner's syndromes, generally characterized by gonadal dysgenesis results in testicular impairments that manifest as infertility (Pienkowski et al., 2011; Foyouzi, 2019).

Post-testicular aetiologies are mostly related to obstructions in the genital ducts that conduct sperm from the testis till it is delivered into the female vaginal canal via the external urethral orifice (Hamada et al., 2013; Naz and Kamal, 2017). These include epididymal obstruction, congenital bilateral absence of the vas deferens, ejaculatory duct obstruction, hypospadias, genital tract infections (GTI), inflammatory diseases of accessory glands (prostatitis), and post urinary bladder neck and transurethral resection of prostate (TURP) surgeries (Krausz, 2011; Sansone et al., 2018). Additionally, a high incidence of testis cancer and carcinoma *in situ* (CIS) has been reported in sub-fertile and infertile men (Dieckmann and Pichlmeier, 2004; McLachlan et al., 2007). Eisenberg and colleagues reported a 2.9-fold increased risk for testicular cancer in patients with azoospermia (Eisenberg et al., 2013) while a 2.6-fold increased risk of prostate cancer was reported in men with male factor infertility (Walsh et al., 2009). Additionally, a study in Denmark found CIS in testis biopsies of 13 men out of the 543 men (2.4%) with fertility challenges (McLachlan et al., 2007).

2.8.2 Male infertility treatment

There is a big gap in the management of infertility with no available treatment options for most underlying causes of male infertility (Tournaye, 2000; Inhorn and Patrizio, 2014; Agarwal et al., 2021). Except for some cases of central hypogonadism and post-testicular impairments, there is no established treatment for most male infertility issues (Krausz, 2011; Mulholland et al., 2011; Pillai and McEleny, 2021). Assisted reproduction techniques (ART) such as (intrauterine insemination (IUI), in vitro fertilization (IVF), and intracytoplasmic sperm injection (ICSI) are the primary procedures for infertile men seeking to have biological children (Bernie et al., 2013; Inhorn and Patrizio, 2014).

The ART services are not only inaccessible in most places but also very expensive (Inhorn and Patrizio, 2014). In addition, there is a low success rate of pregnancies, thus, multiple attempts are required (Mulholland et al., 2011; Inhorn and Patrizio, 2014; Gnessi et al., 2018). Moreover, it has a high risk of transmitting the known and un-known genetic defects linked to infertility (Agarwal et al., 2021; Krausz, 2011; Martins, Majzoub, and Agawal, 2019). Increased incidence of congenital anomalies has been reported in babies fathered by men who underwent ART because of infertility (Semião-Francisco et al., 2010; Pillai and McEleny, 2021). Due to the high failure rate, and to improve the success rate of ART preventable factors such as restraining alcohol intake should be enforced and ART services denied to those who do not adhere (Inhorn and Patrizio, 2014; Agarwal et al., 2021). Also, genetic screening and counselling should be conducted to prevent transferring of genetic anomalies to the conceptus (Tournaye, 2000; Krausz, 2011; Agarwal et al., 2021).

Unfortunately, reproductive hormonal tests are not sensitive to the various forms of spermatogenesis impairment and thus do not give insight about successful viable sperm retrieval for ART (McLachlan et al., 2007; Semião-Francisco et al., 2010; Bernie et al., 2013). Details regarding ART are obtained from an extensive sperm and testicular assessment (Tournaye, 2000; Gnessi et al., 2018; Akerman et al., 2020), which can be applied in selecting the most appropriate technique (IUI, IVF, ICSI) (Tournaye, 2000; Bernie et al., 2013; Inhorn and Patrizio, 2014), and determination of sperm retrieval method (percutaneous epididymal or testicular Sperm Aspiration and microsurgical epididymal or testicular sperm extraction) to use (McLachlan et al., 2007; Semião-Francisco et al., 2010; Leung et al., 2014).

Hormone treatment, especially testosterone replacement therapy is increasingly becoming popular (Bhatia et al., 2015; Zirkin and Papadopoulos, 2018). Hormone supplementation is beneficial for young and older men with hypogonadism (Modelska-Ziolkiewicz, 2009; Dołan et al., 2015; Neves et al., 2017). In general, bioavailability of testosterone decreases with age due to a gradual decline in Leydig cell testosterone synthesis and elevation of sex hormone binding globulin (SHBG) (Bassil et al., 2009; Surampudi et al., 2012). Low testosterone (hypogonadism) can be due to impairment in the hypothalamus or anterior pituitary gland, resulting in inadequate LH levels (hypogonadotropic hypogonadism) (Corradi et al., 2016). However, hypogonadism commonly results from deficiencies in Leydig cell steroidogenesis (testicular hypogonadism) (Beattie et al., 2015; Neves et al., 2017). LH or human chorionic gonadotropin (HCG) hormone is administered in hypogonadotropic hypogonadism males to improve testosterone production (Zirkin and Papadopoulos, 2018), while males with testicular hypogonadism are treated with exogenous testosterone to elevate blood testosterone levels (Beattie et al., 2015). Testosterone replacement therapy is documented to increase blood testosterone levels and produce improvement in sexual function, mood, body physic, and general welfare in both young and aging males (Surampudi et al., 2012; Bhatia et al., 2015; Zirkin and Papadopoulos, 2018).

2.9 Apoptosis in the testis

Apoptosis is a well-orchestrated process of cell death involving a sequence of biochemical events that occur either in the intrinsic or extrinsic signalling pathway (El-Mehi and Faried, 2019; Lossi, 2022). In the testis, apoptosis is a constant process that is essential for maintenance of normal sperm production (El-Mehi & Faried, 2019; Shaha, Tripathi, & Mishra, 2010).

2.9.1 Male germ cell apoptosis

A limited number of germ cells is supported by Sertoli cells at a time (Print and Loveland, 2000), thus, a programmed cell death (apoptosis) is required to limit spermatogonia cell density during the proliferation phase (Hai et al., 2014; Murphy and Richburg, 2014). Apoptosis is also involved in monitoring sperm quality and DNA integrity through elimination of germ cells with chromosomal damage during meiosis (Murphy and Richburg, 2014; Lara et al., 2018). An intricate balance between germ cell proliferation and apoptosis is maintained (Print and Loveland, 2000; Hai et al., 2014), this is regulated by signalling from paracrine hormones such as Desert Hedgehog (Dhh), stem cell factor (SCF), and leukemia inhibitory factor (LIF) and

endocrine hormones including gonadotrophins (LH and FSH) and androgens (testosterone and DHT) (Print and Loveland, 2000; Sharma et al., 2015). However, several testicular disorders such as testicular infection, inflammation, environmental toxins, and genetic disorders augment apoptosis causing hypospermatogenesis (Shaha et al., 2010; El-Mehi and Faried, 2019). Apoptosis induced by testicular impairments can be mediated through activation of mitochondrial outer membrane permeabilization by BCL-2-family pro-apoptotic proteins (intrinsic) (Lara et al., 2018), or Fas-ligand cell membrane death receptor (extrinsic) (Aitken et al., 2011), or both apoptotic pathways leading to activation of caspases that execute cell demise (Sharma and Agarwal, 2013; El-Mehi and Faried, 2019).

2.9.2 Testicular somatic cell apoptosis

Reports indicate that testicular somatic cells (Leydig and Sertoli cells) are more resistant to apoptosis compared to germ cells (Wangikar et al., 2011; Murphy and Richburg, 2014) and are involved in reversal of testis impairments following treatment of the disorder or discontinuation of the causative toxicant (Wangikar et al., 2011; Yuko Ito and Otsuki, 2013). This observation has been attributed to the ability of Leydig and Sertoli cells to degrade their own damaged cellular organelles in a precise coordinated process of autophagy (Wangikar et al., 2011; Zhu, Yin, et al., 2019), in addition, Sertoli cells express high levels of anti-apoptotic markers (Bcl-w and Bcl-xL) (Yan et al., 2000; Yuko Ito and Otsuki, 2013). Though the number of Sertoli cells is may not be usually affected by some toxicants or disease conditions (Pajarinen and Karhunen, 1994; Yuko Ito and Otsuki, 2013), disruptions in its ultrastructure, particularly the cytoskeleton are relatively common (Mruk and Cheng, 2004; Trindade et al., 2013).

2.10 Testis-immune axis and inflammation

2.10.1 Testis-immune axis

Some mammalian tissues including the brain, eye, testis, and pregnant uterus exhibit a unique immunological ability (Simpson, 2006), and thus the survival of allo- and xeno-grafts is longer in these tissues (Zhao et al., 2014). Further, a more distinct immune status has been demonstrated in the testis, which tolerates both allo- and auto-antigens without producing substantial immune reactions (Fijak & Meinhardt, 2006; Kaur et al., 2021). In addition, the Sertoli cells play an immune-protective role (Fijak and Meinhardt, 2006; Li et al., 2012), that enhanced survival of graft when co-transplanted with Sertoli cells (Suarez-Pinzon et al., 2000; Zhao et al., 2014).

Cytokines are cell signalling molecules typically secreted by hematopoietic linage immune cells such as lymphocytes, macrophages, and mast cells, their basic function is regulation of cell's immune response, inflammation, and hematopoietic cell differentiation (Lewko and Oldham, 2009; Sivangala and Sumanlatha, 2015). However, cytokine production in the non-immune cell including endothelial cells, epithelial cells, adipocytes, and testicular cells has been documented (Coppack, 2001; Syriou et al., 2018; Roan et al., 2019). Testicular cytokines play a regulatory function in steroidogenesis and spermatogenesis processes (de Oliveira, Cerri, and Sasso-Cerri, 2021), as well as normal testis development (Loveland et al., 2017). Compelling evidence from previous studies shows that several pro-inflammatory/inflammatory and anti-inflammatory cytokines are produced by testicular cells (Leydig cells, macrophages, myoid cells, Sertoli cells, and germ cells) under normal conditions (Hedger and Meinhardt, 2003; Loveland et al., 2017; de Oliveira et al., 2021). The documented cytokines in normal testis so far include:

a) stem cell factor (SCF), a pro-inflammatory cytokine is produced in the Sertoli cells during testicular development, it plays a role in primordial germ cells migration, adhesion, proliferation, and survival (Mauduit et al., 1999; Qin et al., 2017).
b) the transforming growth factor-ß (TGF ß) cytokine family is an example of anti-inflammatory cytokines, it is expressed in the developing and prepubertal testis by the germ cells, Sertoli cells, myoid cells, Leydig cells, and TGF ß is involved in the regulation of development of these cells (Avallet et al., 1994; Cupp & Skinner, 2001; Petersen & Söder, 2006).
c) tumour necrosis factor (TNF-α) is a pro-inflammatory cytokine present in pachytene spermatocytes, round spermatids, and activated interstitial macrophages, TNF-α is involved in regulating germ cell survival (Moore and Hutson, 1994; Hedger and Meinhardt, 2003; de Oliveira et al., 2021).
d) interleukin-1 (IL-1), a pro-inflammatory cytokine has two isoforms in the normal testis IL-1α and IL-1ß. The IL-1α is expressed by Sertoli cells, pachytene spermatocytes, and round spermatids (SÖDER et al., 1991; Haugen et al., 1994), while IL-1ß is expressed in Leydig cells and macrophages (Cudicini et al., 1997; Gow et al., 2001), but both IL-1 isoforms are essential in Leydig cell steroidogenesis, Sertoli cell protein production, and germ cells proliferation and differentiation (Petersen and Söder, 2006).

e) interleukin-6 (IL-6), a pro-inflammatory cytokine is found in Sertoli cells, and it stimulates Sertoli cell protein secretion (Cudicini et al., 1997; Hedger and Meinhardt, 2003).
f) Fas ligand (FasL) is a pro-inflammatory cytokine that is expressed on the Sertoli cell surface, it is involved in maintenance of germ cell integrity via removal of damaged germ cells (French et al., 1996; Francavilla et al., 2000).
g) macrophage migration inhibitory factor (MIF) is a pro-inflammatory cytokine. In the testis, it is localized in the Leydig cells rather than the macrophages, and MIF regulates peritubular cell and Sertoli cell secretory functions (Meinhardt et al., 1996; Loveland et al., 2017).
h) leukaemia inhibitor factor (LIF) is a pro-inflammatory cytokine, peritubular cells are a main source of LIF in the testis (Piquet-Pellorce, Dorval-Coiffec, Pham, and Jégou, 2000). During testis development, LIF works together with SCF to promote primordial germ cell survival, and in post-pubertal testis is involved in spermatogenesis regulation (Hedger and Meinhardt, 2003; de Oliveira et al., 2021).

2.10.2 Testis inflammation

The existence of cytokines in the testis does not make it resistant to inflammation, but the same cytokines produced in normal testis once upregulated induce inflammation (Zhao et al., 2014; Syriou et al., 2018). Inflammation is the body's physiological response to harmful stimuli such as injury, infection, and toxins (Hedger and Meinhardt, 2003; Somade et al., 2019). The testis is particularly susceptible to inflammation, simply because the non-immune testicular cells are potent cytokines producers, thus a rapid elevation in cytokine level is evoked in a presence of harmful stimuli (Hedger and Meinhardt, 2003; Loveland et al., 2017). Consequently, local and systemic infectious and non-infectious diseases that cause testicular inflammation have been implicated in male reproductive dysfunctions (Loveland et al., 2017). The most common testicular inflammatory conditions such as testicular torsion, varicocele, and orchitis are associated with deterioration of spermatogenesis (Dutta et al., 2021). One mechanism suggested to be involved in inflammatory-associated testicular dysfunction is disruption of the Leydig cell steroidogenesis process which leads to production of inadequate androgen (testosterone) levels, subsequently causing spermatogenesis dysregulation (Hales, 2002; Leisegang and Henkel, 2018).

Furthermore, IL-6, a pro-inflammatory cytokine is vital in testicular immunopathology (Loveland et al., 2017), a study by Pérez et al., (2012) demonstrated that upregulation of IL-6 disrupts the blood-testis barrier. This results in a compromised immune privilege milieu that can lead to autoimmunity and subsequently cause infertility (Hedger and Meinhardt, 2003; Loveland et al., 2017). Additionally, Morales-Montor et al., 2001 found that upregulation of IL-6 was associated with feminization of male mice infected with Taenia crassiceps, which resulted from elevated conversion of androgens to estrogens by aromatase. However, in IL-6 knock-out male mice infected with Taenia crassiceps, the aromatase activity was inhibited, which prevented the mice from becoming feminised (Morales-Montor et al., 2001). Accordingly, cytokines upregulation disrupts the spermatogenesis and steroidogenesis processes and are a hallmark of testicular dysfunction (Hedger and Meinhardt, 2003; Loveland et al., 2017). Hence, disturbance of the delicate testicular immune homeostasis can eventually lead to infertility (Zhao et al., 2014; Gong and Han, 2021). Additionally, previous studies have shown that inflammation induces oxidative stress in the testis (Dutta et al., 2021). Cytokine upregulation has been shown to accelerate reactive oxygen species (ROS) formation, and elevation of ROS leads to oxidative stress (Azenabor et al., 2015; Loveland et al., 2017; Dutta et al., 2021). However, oxidative stress is a potent mediator of inflammation, thus the two pathophysiological mechanisms are interlinked (Azenabor et al., 2015; Dutta et al., 2021). Meanwhile, testicular inflammation and oxidative stress are the most predominant underlying causes of male reproductive dysfunctions, more so the two can occur simultaneously (Turner and Lysiak, 2008; Dutta et al., 2021).

2.11 Impact of oxidative stress on testicular function

Unstable forms of oxygen known as free radicals are generated during normal mitochondrial oxidative phosphorylation (Auten and Davis, 2009; Duluc et al., 2014). Free radicals have one or more unpaired electrons in the outer atomic orbit and are thus readily reactive (Kohen and Nyska, 2002; Davies, 2003). Once an electron is added to the dioxygen (O_2) free radical, a primary reactive oxygen species (ROS) superoxide anion radical ($O_2^{-\cdot}$) is produced (Kohen and Nyska, 2002; Pryor et al., 2006; Aprioku, 2013). Via a series of reactions $O_2^{-\cdot}$ is transformed into hydroxyl radical ($\cdot OH$), peroxyl radical ($ROO^{\cdot}$), or hydrogen peroxide (H_2O_2) secondary ROS (Kohen and Nyska, 2002; Turner and Lysiak, 2008). In addition, a group of ROS including peroxynitrite ($ONOO_2$), nitroxyl anion, nitrogen dioxide ($\cdot NO_2$), and peroxynitrous acid is produced from nitric oxide (NO) (Davies, 2003; Pryor et al., 2006). NO is a free radical

generated by the nitric oxide synthase (NOS) from amino acid L-arginine (Kolasa et al., 2009; Aprioku, 2013; Yu et al., 2017). The three NOS isoforms are endothelial NOS (eNOS or NOS3), inducible NOS (iNOS or NOS2), and neuronal NOS (nNOS or NOS1) (Turner and Lysiak, 2008). Further, eNOS and nNOS are calcium-dependent NOS that produce NO in very small quantities (Zamora et al., 2000; Kolasa et al., 2009). However, iNOS is calcium-independent, it produces larger quantities of NO and has been reported to play a role in testicular dysfunction (O'Bryan et al., 2000; Köksal et al., 2003; Kolasa et al., 2009).

Unharmful levels of ROS are maintained in the cell by the continuous scavenging actions of several antioxidants such as superoxide dismutase (SOD), catalase (CAT), glutathione peroxidase (GPX), glutathione reductase (GR), and glutathione-S-transferase (GST) (D'Autréaux and Toledano, 2007; Asadi et al., 2017). In addition, melatonin, cytochrome C, and dietary factors (zinc, vitamin C (ascorbic acid), vitamin E (α-tocopherol), and selenium) have shown antioxidant properties (Aitken and Roman, 2008; Auten and Davis, 2009; Kurutas, 2016). The antioxidants via a chain of reaction convert ROS into oxygen and water (D'Autréaux and Toledano, 2007; Aprioku, 2013).

Conversely, ROS participates in the modulation of cell signaling and maintenance of homeostasis during normal cellular processes (D'Autréaux and Toledano, 2007; Turner and Lysiak, 2008; Wu et al., 2020). However, an imbalance between ROS formation and their removal by the antioxidant system leads to a grave cellular consequence termed oxidative stress (Duluc et al., 2014; Kurutas, 2016; Ikekpeazu et al., 2019). ROS stimulate membrane lipid peroxidation that produces unsaturated reactive aldehyde, malondialdehyde (MDA) (Zhu et al., 2019) and they cause DNA damage by inducing DNA oxidation to form 8-hydroxydeoxyguanosine (8-OHdG) (Zubkova and Robaire, 2006; Sharma and Agarwal, 2013). Also, upregulation of iNOS by oxidative stress evokes increased NO formation (Ishikawa et al., 2005; Aprioku, 2013), perpetuating ROS production and eventually exacerbation of oxidative stress cell damages (Nna et al., 2019).

The testis is vulnerable to oxidative stress (Owyong and Ramasamy, 2018; Nna et al., 2019; Zhu et al., 2019; Dutta et al., 2021), because of the high mitochondrial oxygen consumption to support the inherent cell division during the process of spermatogenesis (Aitken and Roman, 2008; Asadi et al., 2017). Additionally, the testicular tissue contains relatively high amounts of unsaturated fatty acids that can easily be oxidized to form MDA (Guerriero et al., 2014; Zhu et

al., 2019). Furthermore, as the germ cells advance in the spermatogenic process, most of their cytoplasm is shed off to form the condensed, elongated spermatid, thus antioxidant concentration to neutralize oxidants is reduced (Adaramoye et al., 2013; Owyong and Ramasamy, 2018). However, due to the weak nature of the testicular artery (Asadi et al., 2017), the testis is poorly vascularized causing low oxygen tension and intense competition for vital elements (Aitken and Roman, 2008; Asadi et al., 2017) which renders the testis venerable. Previous studies have suggested that low oxygen tension is a mechanism to limit formation of ROS in large amounts (Tremellen, 2012).

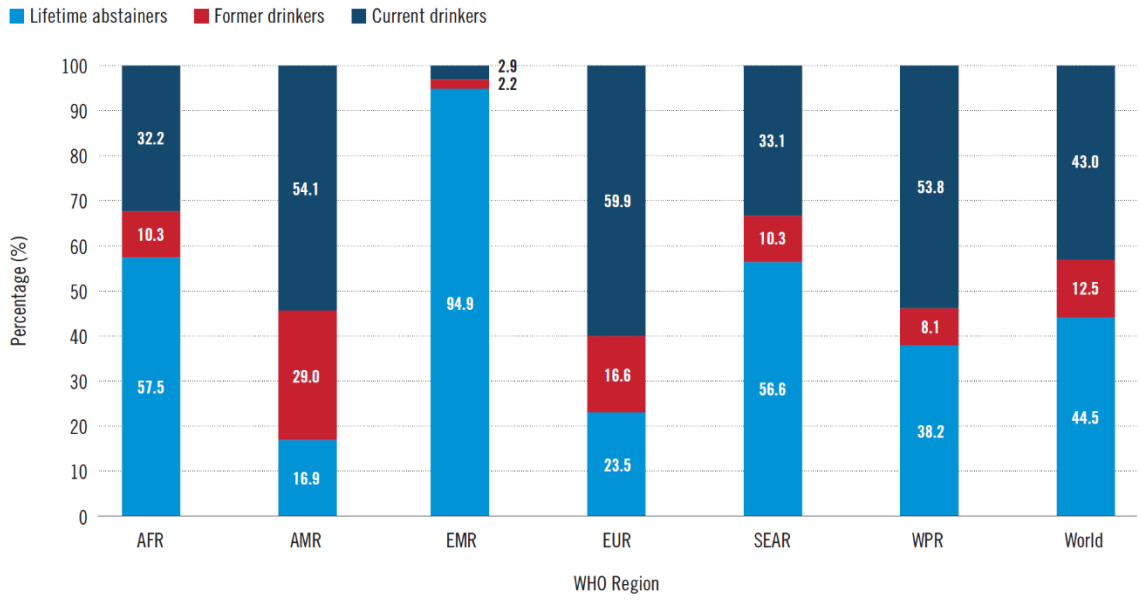
Oxidative stress is a common feature occurring in many conditions associated with male reproductive system dysfunctions (Hamilton et al., 2016; Asadi et al., 2017), ranging from testicular disorders, chronic diseases, long-term medications, toxicant exposure, and aging, to lifestyle choices such as illicit drug and alcohol abuse (Aitken and Roman, 2008; Wu et al., 2020). Multiple studies have demonstrated a reduction in antioxidant markers (SOD, CAT, and GPX) and an increase in oxidative markers (8-OHdG and iNOS) in animals with induced testicular damage (Asadi et al., 2017; Borg et al., 2020). Compelling evidence show that ROS in low concentrations is essential for successful spermiogenesis process, particularly spermatozoa capacitation and sperm-oocyte fusion (Oremosu and Akang, 2015; Dutta et al., 2021), slight increases have grave consequences (Hamilton et al., 2016; Zhu et al., 2019). Oxidative stress triggers initiation of inflammation and apoptotic activity in testicular tissue (Asadi et al., 2017; Owyong and Ramasamy, 2018), which in turn, results in alterations in spermatogenesis and steroidogenesis processes (Zhu et al., 2019).

2.12 Influence of alcohol on male reproductive function

2.12.1 Alcohol use and its toxicity

Alcohol is the most common and widely consumed recreational substance (Trangenstein et al., 2018) and its consumption is relatively acceptable in most communities (Hammer et al., 2018). Globally, 43% of the population aged ≥ 15 are alcohol consumers, and the percentage of male alcohol consumers (53.6%) almost doubles that of females (32.3%) (World Health Organisation, 2011) (İlhan and Yapar, 2020) (Fig. 2.9). According to the 2018 WHO global alcohol and health report, the average consumed alcohol per capita (APC) has increased from 5.7 liters of absolute alcohol in 2000 to 6.4 liters in 2016. The prevalence of alcohol consumption in South African population aged ≥15 years is 33.1%, slightly less than half of

the males (47.7%), and about a fifth of female populations 20.2% in South Africa are current alcohol consumers (Marx et al., 2021). Moreover, 43.0% of the consumers are binge drinkers, reported to consume ≥5 standard drinks in a single drinking occasion. Binge drinking is consumption of alcohol that typically increases the blood alcohol concentration (BAC) to ≥ 0.08 g/dL (National Institute on Alcohol Abuse and Alcoholism, 2004). Prevalence of binge drinking is also highest in males (48%) compared to females (32%) (Vellios and van Walbeek, 2018). A south African national survey reported that the proportion of alcohol consumers increased by more than 6% since 2008 from 26.9% to 33.1% currently and binge drinking slightly increased from 41% in 2008 to 43% (Marx et al., 2021). Furthermore, the South African APC of 11.5 liters of absolute alcohol is among the highest levels of alcohol consumption worldwide (Fig. 2.10), it is almost twice the global APC average (6.4 liters). The APC in South Africa is projected to increase to 12.1 liters in 2025 (Vellios and van Walbeek, 2018).



AFR: African, AMR: Americas, EMR: Eastern Mediterranean, EUR: European, SEAR South-East Asia, WPR: Western Pacific

Figure 2.9: The percentage of alcohol consumers (current and former) and lifetime abstainers in the populace aged ≥15 globally and in the different WHO regions.

Source: WHO, 2018

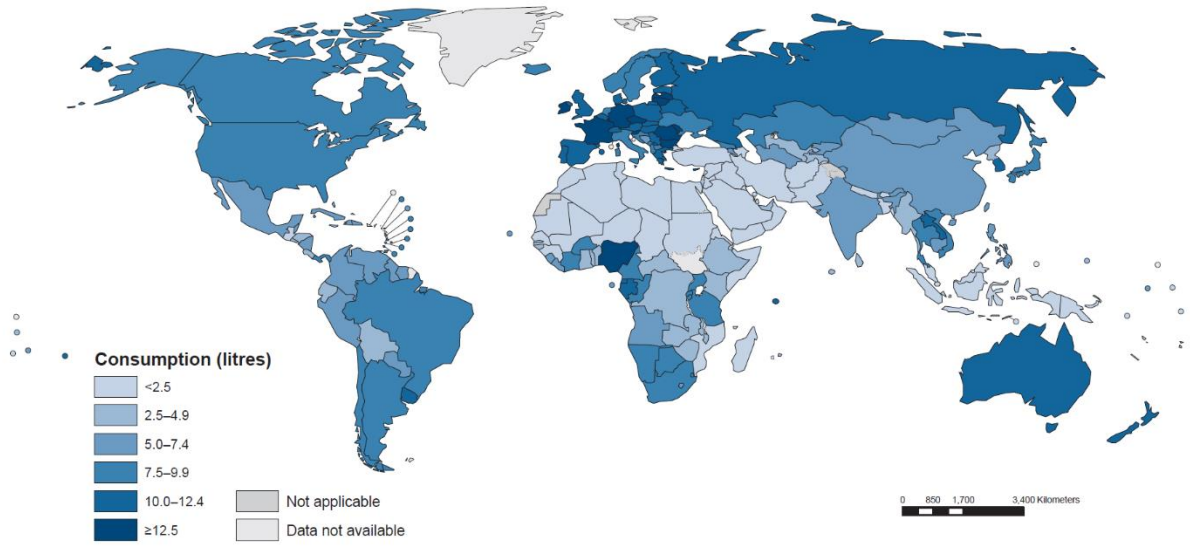


Figure 2.10: Average consumed alcohol per capita (APC) (in liters of absolute alcohol) in the populace aged ≥15 in different countries.

Source: WHO, 2018

The term standard drink is commonly used when referring to alcoholic drinks and is defined as a drink that contains a fixed amount of absolute alcohol (Trangenstein et al., 2018). However, the volume of a standard drink varies in different types of beer, wines, and spirits (Vellios and van Walbeek, 2018). Accordingly, the amount of absolute alcohol making up a standard drink also vary in different countries; 8 g in United Kingdom, 10 g in Australia, and 14 g in United States (Kalinowski and Humphreys, 2016) (Table 2.1). Internationally, alcohol consumption is classified for men and women respectively as heavy when ≥ 14 and ≥ 7 standard drinks or ≥ 100 g and ≥ 60 g of absolute alcohol are consumed per week (National Institute on Alcohol Abuse and Alcoholism, 2004). Then, binge drinking is when ≥ 5 and ≥ 4 standard drinks or ≥ 60 g and ≥ 40 g of absolute alcohol are consumed per occasion (National Institute on Alcohol Abuse and Alcoholism, 2004).

Table 2.1:Definitions of a standard drink in different countries and the guidelines for low-risk alcohol consumption

Country	Standard drink (g)	Guidelines			
		Women		Men	
		(g)/day	(g)/week	(g)/day	(g)/week
Australia [15]	10	20	–	20	–
Austria [10]	20	16	112	24	168
Bosnia and Herzegovina [27]	10	10	–	20	–
Bulgaria[a]	13	–	–	–	–
Canada [16]	~13.6	~27	~136	~40.7	~204
Chile [23]	14	42	98	56	196
China[a]	10	–	–	50	100
Croatia[a]	10	10	–	20	–
Denmark [17]	12	–	84	–	168
Estonia[a]	10	20	–	40	–
Fiji [18]	10	20	100	30	150
France [19]	10	20	140	30	210
Germany [24]	12	12	–	24	–
Grenada [6]	~14	~14	–	~14	–
Iceland [7]	8	–	112	–	168
India [28,45]	10	10	–	20	–
Ireland [31]	10	–	110	–	170
Italy [43]	12	20	–	36	–
Japan [8]	–	20	–	40	–
Latvia [44]	12	12–16	96	24	156
Luxembourg [14]	12.8	12.8	–	25.6	–
Malta[a]	8–10	–	112–140	–	168–210
Malaysia[a]	10	–	–	–	–
Mexico [9]	14	14	126	28	168
New Zealand [20,25]	10	20	100	30	150
Philippines [42]	14	14	–	28	–
Poland [21]	10	20	140	40	280
Portugal[a]	10–12	10–24	–	10–24	–
Singapore [37]	10	10	–	20	–
Slovenia[a]	10	10	–	20	–
South Africa [11]	~11–12	24	–	24	–
Spain [39]	10	–	110	–	170
Sweden [30]	10	10	–	20	–
Switzerland [13]	10–12	20–24	–	30–36	–
United Kingdom [22]	8	16–24	–	24–32	–
United States [12,46]	14	42	98	56	196
Vietnam [38]	10	20	140	40	280

[a]Guidelines obtained through personal communication with those listed in the Acknowledgements section.

Source: Kalinowski & Humphreys, 2016

Markedly, alcohol intoxication (drunkenness) is associated with both the consumed and the drinking pattern. These two factors are also related to alcohol's toxic effects (Rehm, 2011; Patrick et al., 2016). Moreover, most of the disorders linked to alcohol use have a dose dependant pattern (Rehm et al., 2009; Patel et al., 2016). Accordingly, heavy alcohol consumption and binge drinking are important risk factors for deteriorating socioeconomic

state and many health challenges (CDC, 2015), contributing to a great increase in the public health disease burden and injury-associated disabilities (Bardach et al., 2019; İlhan and Yapar, 2020).

In South Africa, alcohol consumption is more prevalent and is ranked the fifth cause of death (Forouzanfar et al., 2016) and is as well linked to other leading causes of death in the country such as motor accidents, domestic violence, and sexually transmitted infections (Trangenstein et al., 2018). Since alcohol can permeate almost all body organs (Rachdaoui and Sarkar, 2017), it interferes with normal cellular physiology and results in multiple system dysfunction including the body's vital systems such as nervous, cardiovascular, endocrine, and reproductive systems (Rehm, 2011; Rachdaoui and Sarkar, 2017; Finelli et al., 2022). Globally, a high percentage (26.5%) of the young adult population of reproductive age consume alcohol, males form the larger portion (World Health Organisation, 2011). The future impact on the reproductive health of this high alcohol consumption by the reproductive-age males of the present generation, coupled with cART therapy and diabetes is unknown and requires attention. Therefore, the present study will contribute towards unveiling hidden male reproductive health challenges (often overlooked) that inevitably manifest later in life.

2.12.2 Alcohol-linked reproductive impairments

The two main testicular functions, steroidogenesis, and spermatogenesis are adversely affected by alcohol (Duca et al., 2019). Animal and human studies have reported several male reproduction dysfunctions associated with alcohol intake including hypogonadism, testicular atrophy, germ cell loss, and sexual dysfunction (erectile disorder and reduced libido) (Rachdaoui and Sarkar, 2013; Oremosu and Akang, 2015; Finelli et al., 2022). Both central (hypothalamic-pituitary) and testicular (primary) hypogonadism has been demonstrated by previous studies (Rachdaoui and Sarkar, 2017; Duca et al., 2019). Impact of alcohol on the hypothalamus and pituitary hormones has mostly been reported following acute alcohol ingestion (Emanuele and Emanuele, 1998; Frias et al., 2002; Duca et al., 2019). Gianoulakis, (1990) studied the effect of acute ethanol administration on the HPG axis and found a rise in the release of ß-endorphin-like peptides from the hypothalamus which interfered with gonadotropin-releasing hormone (GnRH) secretion, in turn negatively impacted gonadotropins (LH and FSH) synthesis, and ultimately leads to a reduction in testosterone production. A direct impact of alcohol on the pituitary has also been reported in animal models (Emanuele

and Emanuele, 1998; Rachdaoui and Sarkar, 2017), as well as downregulation of LH gene expression has been reported following alcohol administration (Duca et al., 2019).

Further, alcohol and its major metabolite, acetaldehyde are well-established toxicants of Leydig cells that reduce the Leydig cell‘s steroidogenic capacity (Emanuele and Emanuele, 1998; Rachdaoui and Sarkar, 2017). Alcohol and acetaldehyde cause inhibition of enzymes involved in testosterone formation i.e., 3ß-hydroxysteroid dehydrogenase (3ßHSD) and 17-ketosteroid reductase (17KSR) (Cicero et al., 1980; Muthusami and Chinnaswamy, 2005). Enzymes 3ß HSD and 17KSR catalyze the conversion of pregnenolone to progesterone and from androstenedione to testosterone, respectively (Muthusami and Chinnaswamy, 2005; Wang et al., 2017). Also, alcohol is associated with an increase in ROS formation which is known to downregulate steroidogenic acute regulatory protein (StAR) expression (Jana et al., 2010; Duca et al., 2019) while StAR mediates the only rate-limiting step in the steroidogenesis process, the transfer of cholesterol from the outer to the inner mitochondrial membrane (Aghazadeh et al., 2015; Wang et al., 2017)

Additionally, elevation in androgen metabolism stimulated by alcohol contributes to a reduction in testosterone levels (Gordon et al., 1979; Rachdaoui and Sarkar, 2017; Mayer et al., 2018). Alcohol stimulates aromatase, an enzyme that catalyzes the conversion of testosterone and androstenedione into estradiol and estrone (Gordon et al., 1979; Purohit, 2000; Rachdaoui and Sarkar, 2013). The aromatization of these steroids is suggested to lead to gynecomastia commonly observed in male alcoholic individuals (Purohit, 2000; Duca et al., 2019). Furthermore, testicular tissue damage and germinal epithelium cell loss are induced through activation of apoptosis by alcohol (Yuko Ito and Otsuki, 2013), and in vitro and in vivo studies have shown an up regulation of apoptotic markers Fas-L, p53, Bcl-2, and caspase-3 in the testis cells following alcohol exposure (Zhu et al., 2000; Jana et al., 2010; Giannessi et al., 2015).

In addition, nutritional deficiencies, particularly protein malnutrition and low micronutrients such as dietary antioxidants (zinc and vitamins) are commonly observed in people who consume alcohol regularly (Halsted and Medici, 2012), contributing to ROS accumulation (oxidative stress) which is deleterious to the testicular tissue (Condorelli et al., 2015). However, the testicular damage caused by alcohol can be reversible (Vicari et al., 2002; Condorelli et al., 2015), both clinical and animal studies have found that withdrawing from alcohol can lead to

a restoration of normal testicular function (Agarwal et al., 2021; Dosumu, Osinubi, & Duru, 2014; Guthauser et al., 2014).

On the other hand, the risky sexual activity associated with alcohol intoxication contributes to an increase in the spread of HIV infection (Kumar et al., 2015; Schneider et al., 2016; Scott-Sheldon et al., 2016) and the consequent use of cART. Additionally, many HIV patients on cART therapy continue to consume alcohol regularly for euphoric purposes (McCance-Katz et al., 2013; Mondal et al., 2019). The prevalence of alcohol abuse in people living with HIV/AIDS (PLWHA) is reported to be more than twofold higher compared to that of the general populace (Necho et al., 2020). This points to both drugs being concomitantly present in the body, a scenario that may lead to serious adverse health challenges that will complicate the clinical management of PLWHA. Previous studies have observed a hindrance of adherence to cART in alcohol consumers (Schneider et al., 2016; Shubber et al., 2016). Further, clinical studies have reported an association of alcohol consumption with reduced viral suppression dose-dependently (Chander et al., 2006; Braithwaite et al., 2007), augmentation of cART adverse effects (Braithwaite and Bryant, 2010; Kumar et al., 2012), and diminished life expectancy (Braithwaite and Bryant, 2010; Kumar et al., 2012; Schneider et al., 2012). A study by Braithwaite et al., (2007) reported a decrease of 1 - 3.3 years in the life expectancy of PLWHA on cART that consume alcohol regularly.

2.13 HIV/AIDS and cART associated reproductive dysfunctions

2.13.1 HIV/AIDs epidemiology

The epidemic of HIV infection and its associated acquired immunodeficiency syndrome (AIDS) has been the largest worldwide challenge since its outbreak in the 1980s, and more than 40 million deaths due to HIV/AIDs have been recorded to date (UNAIDS, 2019). HIV is spread via contact with the blood and body fluids of an infected person such as having unprotected sex, blood transfusions, hypodermic needle pricks, and from mother to child during pregnancy, delivery, or breastfeeding (WHO, 2021). HIV/AIDs epidemic has added a great disease and economic burden on countries globally (Beigbeder, 2018; UNAIDS, 2022). About 0.8% (38.4 million) of the adult populace (≥15 years) are currently living with HIV/AIDs (WHO, 2021) (Table 2.2). The number of new infections has decreased since the peak of the HIV/AIDs epidemic in 1996, however, in sub-Saharan Africa, the prevalence of HIV/AIDs is still very high (UNAIDS, 2019) and is one of biggest health challenge threatening the survival of millions

of people in the region (Bulstra et al., 2020; WHO, 2021). The number of people currently living with HIV/AIDs in sub-Saharan Africa accounts for 54.6% (20.6 million) of the global prevalence (UNAIDS, 2019). Particularly, the Southern Africa region has the highest HIV/AIDs incidence in the world. Countries within the region that are highly affected include Zimbabwe, Botswana, Swaziland, Namibia, Lesotho, Zambia, Malawi, Mozambique, and South Africa. The HIV/AIDs prevalence in each of these countries is ≥ 20% of the adult population (15 years or older) (UNAIDS, 2019; Bulstra et al., 2020).

Table 2.2: Global HIV data

	2000	2005	2010	2020	2021
People living with HIV	26.0 million [22.9 million–29.7 million]	28.5 million [25.1 million–32.5 million]	30.8 million [27.2 million–35.2 million]	37.8 million [33.3 million–43.1 million]	38.4 million [33.9 million–43.8 million]
New HIV infections (total)	2.9 million [2.2 million–3.9 million]	2.5 million [1.9million–3.3 million]	2.2 million [1.7 million–2.9 million]	1.5 million [1.2 million–2.0 million]	1.5 million [1.1 million–2.2 million]
New HIV infections (aged 15+ years)	2.4 million [1.8 million–3.2 million]	2.0 million [1. 5 million–2. 7 million]	1.9 million [1.4 million–2.5 million]	1.4 million [1.0 million–1.8 million]	1.3 million [990 000–1.8 million]
New HIV infections (aged 0–14 years)	520 000 [350 000–770 000]	470 000 [320 000–700 000]	320 000 [220 000–480 000]	170 000 [110 000–250 000]	160 000 [110 000–230 000]
AIDS-related deaths	1.7 million [1.3 million–2.2 million]	2.0 million [1.6 million–2.6 million]	1.4 million [1.1 million–1.8 million]	690 000 [540 000–900 000]	650 000 [510 000–860 000]
People accessing antiretroviral therapy	560 000	2.0 million	7.8 million	27.2 million	28.7 million
HIV resources available*	US$ 5.1 billion	US$ 9.3 billion	US$ 16.7 billion	US$ 21.6 billion	US$ 21.4 billion

Source: UNAIDS global HIV statistics fact sheet (UNAIDS, 2019)

2.13.2 Antiretroviral (ARV) drugs and Combination antiretroviral therapy (cART)

2.13.2.1 Antiretroviral (ARV) drugs

The ARV drugs were developed to treat infections caused by retroviruses, primarily HIV (Verma, Singh, Bansal, and Singh, 2013). They have played a vital role in HIV/AIDS management, drastically improving prognosis, and reducing mortality due to HIV/AIDS (Kemnic and Gulick, 2019). The seven different classes of ARV drugs (Table 2.3) are Nucleoside reverse transcriptase inhibitors (NRTIs), Non-nucleoside reverse transcriptase inhibitors (NNRTIs), Protease inhibitors (PIs), Fusion inhibitors (FIs), chemokine receptor antagonists (CCR5A), Integrase strand transfer inhibitors (INSTIs), and Post-attachment inhibitors (PAIs) (UNAIDS, 2016).

Table 2.3: List of Federal Drug Agency (FDA) approved ARV drugs

Drug Class	Generic Name (Other names and acronyms)	Brand Name	FDA Approval Date
Nucleoside Reverse Transcriptase Inhibitors (NRTIs)			
NRTIs block reverse transcriptase, an enzyme HIV needs to make copies of itself.	abacavir (abacavir sulfate, ABC)	Ziagen	December 17, 1998
	emtricitabine (FTC)	Emtriva	July 2, 2003
	lamivudine (3TC)	Epivir	November 17, 1995
	tenofovir disoproxil fumarate (tenofovir DF, TDF)	Viread	October 26, 2001
	zidovudine (azidothymidine, AZT, ZDV)	Retrovir	March 19, 1987
Non-Nucleoside Reverse Transcriptase Inhibitors (NNRTIs)			
NNRTIs bind to and later alter reverse transcriptase, an enzyme HIV needs to make copies of itself.	doravirine (DOR)	Pifeltro	August 30, 2018
	efavirenz (EFV)	Sustiva	September 17, 1998
	etravirine (ETR)	Intelence	January 18, 2008
	nevirapine (extended release nevirapine, NVP)	Viramune	June 21, 1996
		Viramune XR	March 25, 2011
	rilpivirine (rilpivirine hydrochloride, RPV)	Edurant	May 20, 2011
Protease Inhibitors (PIs)			
PIs block HIV protease, an enzyme HIV needs to make copies of itself.	atazanavir (atazanavir sulfate, ATV)	Reyataz	June 20, 2003
	darunavir (darunavir ethanolate, DRV)	Prezista	June 23, 2006
	fosamprenavir (fosamprenavir calcium, FOS-APV, FPV)	Lexiva	October 20, 2003
	ritonavir (RTV)	Norvir	March 1, 1996
	tipranavir (TPV)	Aptivus	June 22, 2005
Fusion Inhibitors			
Fusion inhibitors block HIV from entering the CD4 T lymphocyte (CD4 cells) of the immune system.	enfuvirtide (T-20)	Fuzeon	March 13, 2003
CCR5 Antagonists			
CCR5 antagonists block CCR5 coreceptors on the surface of certain immune cells that HIV needs to enter the cells.	maraviroc (MVC)	Selzentry	August 6, 2007
Integrase Strand Transfer Inhibitor (INSTIs)			
Integrase inhibitors block HIV integrase, an enzyme HIV needs to make copies of itself.	cabotegravir (cabotegravir sodium, CAB)	Vocabria	January 22, 2021
	dolutegravir (dolutegravir sodium, DTG)	Tivicay	August 12, 2013
		Tivicay PD	June 12, 2020
	raltegravir (raltegravir potassium, RAL)	Isentress	October 12, 2007
		Isentress HD	May 26, 2017
Attachment Inhibitors			
Attachment inhibitors bind to the gp120 protein on the outer surface of HIV, preventing HIV from entering CD4 cells.	fostemsavir (fostemsavir tromethamine, FTR)	Rukobia	July 2, 2020
Post-Attachment Inhibitors			
Post-attachment inhibitors block CD4 receptors on the surface of certain immune cells that HIV needs to enter the cells.	ibalizumab-uiyk (Hu5A8, IBA, Ibalizumab, TMB-355, TNX-355)	Trogarzo	March 6, 2018

Source: https://hivinfo.nih.gov/understanding-hiv/fact-sheets/fda-approved-hiv-medicines

2.13.2.2 Combination antiretroviral therapy (cART)

For effective suppression of HIV replication, ARV drugs are used in combination as recommended by the world health organization (WHO, 2013). Combination antiretroviral therapy (cART) also referred to as highly active antiretroviral therapy (HAART) are long-term treatment regimen for HIV/AIDs (UNAIDS, 2016). They consist of three or more ARV drugs from at least two classes to target the virus at different stages of the developmental cycle (Kemnic and Gulick, 2019). Examples of Federal Drug Agency (FDA) approved cART are listed in table 2.4. A combination of ARV drugs consisting of two NRTIs and one NNRTI or PI is recommended as the first-line cART for adults living with HIV/AIDs (UNAIDS, 2016). Atripla® is amongst the common cART drug used as the first-line treatment for human immunodeficiency virus/acquired immunodeficiency syndrome (HIV/AIDS) in South Africa (Mocroft et al., 2014). It is a single cART tablet consisting of 600mg Efavirenz, 300mg Tenofovir disproxil fumarate, and 200mg Emtricitabine (Frampton and Croom, 2006). Efavirenz (EFV) is a NNRTI, while Tenofovir disoproxil fumarate (TDF) and emtricitabine (FTC) are NRTIs (Jungmann et al., 2019).

Further, cART is popularly used as a strategy for HIV prevention in form of pre- (PrEP) and post-exposure prophylaxis (PEP), and a combination of TDF and FTC has been approved to be used in PrEP and PEP (Centers for Disease Control and Prevention, 2019). PrEP is utilized by HIV-negative individuals at high risk of being exposed to HIV such as sex workers or injection drug users (WHO, 2019), PEP is administered after exposure to HIV through sex with HIV positive person or when a healthcare provider pricked by a needle which has been used on HIV positive person (UNAIDS, 2016) (i.e. HIV contaminated needle). In addition, aviremic HIV-positive individuals with a serodiscordant or seronegative partner who wish to have biological children (particularly those that cannot afford the cost of assisted reproduction) or unprotected sexual intercourse have an option of the negative partner taking PrEP or PEP to prevent HIV contraction (Centers for Disease Control and Prevention, 2019). In general, the advent of cART has improved HIV/AIDs prognosis through effective reduction of viral load and opportunistic infections, and thus significantly improved the quality of life and expectancy of people living with HIV/AIDs (PLWHA) (UNAIDS, 2016).

Essentially, the global expansion of access to cART has transformed HIV/AIDs from a life-threatening disease to a manageable chronic condition (ONUSIDA, 2017). However, cART

use is not without side effects or toxicity. Both short- and long-term toxic effects on multiple body organs have been reported (Shirasaka, 2010; Azu, 2012; Ogedengbe et al., 2016). The commonly reported clinical adverse effects are lipodystrophy, neuropathy, pancreatitis, myositis, cardiovascular disorders, hepatic steatosis, insulin resistance, and hypogonadism (Kanmaz & Lee, 2000; Khan et al., 2014). Due to increased HIV/AIDs prevalence in the reproductive age group of the population (Kushnir and Lewis, 2011; Akang et al., 2019), hypogonadism related to cART is of great concern because of the fertility issues that accompany it (Akhigbe, Hamed, and Odetayo, 2021). Below is the representative of approved HIV/AIDs treatment regimens available worldwide.

Table 2.4: List of HIV treatment regimen (cART) approved by the Federal Drug Agency (FDA)

Combination HIV Medicines		
Generic Name (Other names and acronyms)	**Brand Name**	**FDA Approval Date**
abacavir, dolutegravir, and lamivudine (abacavir sulfate / dolutegravir sodium / lamivudine, ABC / DTG / 3TC)	Triumeq	August 22, 2014
	Triumeq PD	March 30, 2022
abacavir, lamivudine, and zidovudine (abacavir sulfate / lamivudine / zidovudine, ABC / 3TC / ZDV)	Trizivir	November 14, 2000
atazanavir and cobicistat (atazanavir sulfate / cobicistat, ATV / COBI)	Evotaz	January 29, 2015
bictegravir, emtricitabine, and tenofovir alafenamide (bictegravir sodium / emtricitabine / tenofovir alafenamide fumarate, BIC / FTC / TAF)	Biktarvy	February 7, 2018
cabotegravir and rilpivirine (CAB and RPV, CAB plus RPV, Cabenuva kit, cabotegravir extended-release injectable suspension and rilpivirine extended-release injectable suspension)	Cabenuva	January 22, 2021
darunavir and cobicistat (darunavir ethanolate / cobicistat, DRV / COBI)	Prezcobix	January 29, 2015
darunavir, cobicistat, emtricitabine, and tenofovir alafenamide (darunavir ethanolate/cobicistat/emtricitabine/ tenofovir AF, darunavir ethanolate/cobicistat/emtricitabine/tenofovir alafenamide, darunavir/cobicistat /emtricitabine /tenofovir AF, darunavir/cobicistat/emtricitabine/tenofovir alafenamide fumarate, DRV/COBI/FTC/TAF)	Symtuza	July 17, 2018
dolutegravir and lamivudine (dolutegravir sodium / lamivudine, DTG / 3TC)	Dovato	April 8, 2019
dolutegravir and rilpivirine (dolutegravir sodium / rilpivirine hydrochloride, DTG / RPV)	Juluca	November 21, 2017
doravirine, lamivudine, and tenofovir disoproxil fumarate (doravirine / lamivudine / TDF, doravirine / lamivudine / tenofovir DF, DOR / 3TC / TDF)	Delstrigo	August 30, 2018
efavirenz, emtricitabine, and tenofovir disoproxil fumarate (efavirenz/emtricitabine/tenofovir DF, EFV/FTC/TDF)	Atripla	July 12, 2006
efavirenz, lamivudine, and tenofovir disoproxil fumarate (EFV / 3TC / TDF)	Symfi	March 22, 2018
efavirenz, lamivudine, and tenofovir disoproxil fumarate (EFV / 3TC / TDF)	Symfi Lo	February 5, 2018
elvitegravir, cobicistat, emtricitabine, and tenofovir alafenamide (elvitegravir / cobicistat / emtricitabine / tenofovir alafenamide fumarate, EVG / COBI / FTC / TAF)	Genvoya	November 5, 2015
elvitegravir, cobicistat, emtricitabine, and tenofovir disoproxil fumarate (QUAD, EVG/COBI/FTC/TDF)	Stribild	August 27, 2012
emtricitabine, rilpivirine, and tenofovir alafenamide (emtricitabine / rilpivirine / tenofovir AF, emtricitabine / rilpivirine / tenofovir alafenamide fumarate, emtricitabine / rilpivirine hydrochloride / tenofovir AF, emtricitabine / rilpivirine hydrochloride / tenofovir alafenamide, emtricitabine / rilpivirine hydrochloride / tenofovir alafenamide fumarate, FTC / RPV / TAF)	Odefsey	March 1, 2016
emtricitabine, rilpivirine, and tenofovir disoproxil fumarate (emtricitabine / rilpivirine hydrochloride / tenofovir disoproxil fumarate, emtricitabine / rilpivirine / tenofovir, FTC / RPV / TDF)	Complera	August 10, 2011
emtricitabine and tenofovir alafenamide (emtricitabine / tenofovir AF, emtricitabine / tenofovir alafenamide fumarate, FTC/TAF)	Descovy	April 4, 2016
emtricitabine and tenofovir disoproxil fumarate (emtricitabine / tenofovir DF, FTC / TDF)	Truvada	August 2, 2004
lamivudine and tenofovir disoproxil fumarate (3TC / TDF)	Cimduo	February 28, 2018
lamivudine and zidovudine (3TC / ZDV)	Combivir	September 27,1997
lopinavir and ritonavir (ritonavir-boosted lopinavir, LPV/r, LPV / RTV)	Kaletra	September 15,2000

Source: https://hivinfo.nih.gov/understanding-hiv/fact-sheets/fda-approved-hiv-medicines

2.13.3 Reproductive dysfunctions associated HIV/AIDS and cART

The postulated mechanisms of several cART-induced toxicities are mitochondrial damage and oxidative stress (Kanmaz and Lee, 2000; Savasi et al., 2018). Multiple studies have consistently demonstrated an increase in ROS formation during cART use (Azu, 2012; Tripathi et al., 2020) causing an oxidant-antioxidant imbalance that leads to cellular oxidative stress (Savasi et al., 2018). Further, lipid peroxidation stimulated by oxidative stress is particularly detrimental to spermatozoa because of the high content of unsaturated fatty acid in their membrane (Asadi et al., 2017; Oyeyipo et al., 2018).

Mitochondrial toxicity resulting in cellular respiratory dysfunction and decreased mitochondrial energy generation is a prominent burden of cART, particularly the NRTIs (Pavili et al., 2010; Savasi et al., 2018). In vivo and in vitro experiments have demonstrated that NRTIs cause deletions of mitochondrial DNA (mtDNA) via inhibition of mtDNA polymerase enzyme (Gardner, Hall, Chinnery, and Payne, 2014). Exposure to zidovudine (AZT), an example of NRTIs was found to negatively affect the number of mtDNA copies in the placenta, heart, and skeletal muscles of monkey fetuses (Divi et al., 2007; Kushnir and Lewis, 2011). Also, previous studies have shown that mitochondria damage is associated with dysregulation of spermatozoa metabolism (Kehl et al., 2011; Leeuwen et al., 2008), leading to sperm morphology and motility impairments (Azu et al., 2014; Savasi et al., 2018).

Furthermore, during steroidogenesis, pregnenolone a precursor for testosterone is formed from cholesterol in the Leydig cell mitochondria (Aghazadeh et al., 2015). Thus, deletion or damage of mitochondria would interfere with testosterone production (Wang et al., 2017). Several animal and human studies have reported that cART significantly reduces plasma levels of gonadotropins and androgens, hypogonadism (Kushnir and Lewis, 2011; Rochira et al., 2011; Awodele et al., 2018). Some researchers have suggested that the testicular deleterious effects of cART are mediated via hypogonadism (Akhigbe et al., 2021; Azu et al., 2014). Furthermore, PIs have been implicated in apoptosis inhibition, apoptosis is necessary for the regulation of germ cell numbers and removal of cells with damaged chromosomes. Therefore, inhibition of apoptosis can result in production of poor sperm quality.

Research studies have shown that both HIV infection and cART can impair male reproductive function, causing histopathological changes in the testes and sperm morphology that eventually lead to male reproductive dysfunctions (Barboza et al., 2004). In an autopsy study, the testis of more than 95% of individuals who died of AIDS showed testicular atrophy, thickened basement membrane, hypo-spermatogenesis, and increased interstitial infiltrate (Da Silva et al., 1990). Recent studies demonstrated deleterious effects of cART on the testicular tissue and sperm parameters including a reduction of seminiferous tubules diameter (Azu et al., 2014), diminished sperm count, quality, and motility (Ajayi and Akhigbe, 2020), and increased abnormal spermatozoa and DNA fragmentation (Savasi et al., 2018). Additionally, research has shown a high incidence of diabetes in PLWHA (Diouf et al., 2012; Avari and Devendra, 2017), which has been attributed to the long-term use of cART (Kalra et al., 2011; Olasile et al., 2018). Previous studies have reported glucose intolerance, hyperglycemia, dyslipidemia, and lipodystrophy in PLWHA who have taken NRTIs (stavudine, zidovudine, and didanosine) and PI (indinavir, lopinavir, and ritonavir) for a longer period (> 12 months) (Hardy et al., 2001; Larson et al., 2006; Kalra et al., 2011). These cART-associated metabolism disorders contribute to the development of insulin resistance, which leads to diabetes onset (Diouf et al., 2012; Srinivasa and Grinspoon, 2014). Conversely, the concurrence of cART and diabetes has debilitating effects on several organs (Mastan et al., 2009; Avari and Devendra, 2017).

2.14 Diabetes and male reproduction

2.14.1 Types of diabetes

Diabetes is a group of long-term metabolic disorders with several aetiologies associated with prolonged hyperglycemia and impaired metabolism of proteins, lipids, and carbohydrates (Zaccardi, Webb, Yates, and Davies, 2016). The main established cause of diabetes is defects in the production and action of insulin, insulin is a hormone produced by beta cells of the islets of Langerhans of the pancreas in response to glucose majorly (Blair, 2016). The international diabetes federation (IDF) classifies diabetes into four major types; (a) type 1 diabetes (T1D), characterized by insufficient insulin production because of autoimmune-mediated beta-cell loss; (b) type 2 diabetes (T2D), which is a result of insulin resistance together with a reduction in insulin production; (c) gestational diabetes, that occurs during pregnancy due to glucose metabolism disorder; (d) specific diabetes, this type of diabetes is due to several causes ranging from diseases to chemical insults (Cho et al., 2017; Kaser et al., 2019). Therefore, in addition to genetic and lifestyle, other factors including chronic exposure to drugs (e.g., combined

antiretroviral (cART)) and alcohol consumption are potent predisposing factors of diabetes onset.

2.14.2 Prevalence and trends of diabetes

Diabetes is one of the most predominant public health burdens worldwide, and its incidence is drastically increasing in both developed and developing countries (Saeedi et al., 2019). In 2019, approximately 463 million adults aged 20–79 years were diabetic, the number increased to 537 million in 2021, and is estimated to reach 700 million in 2045 (IDF, 2021) (Table 2.5). Unfortunately, slightly more than half of the diabetic cases are undiagnosed (i.e., 50.1% of people living with diabetes are not aware of it), and the highest number of undiagnosed diabetes cases was found in Africa (Saeedi et al., 2019). Further, in Africa, the highest number of people living with diabetes is in Egypt (8 million), followed by South Africa (4.2 million) (IDF, 2021) (Table 2.6). Diabetes prevalence has increased globally by about 62% since 2009 and its incidence is higher in men, 9.6% than in women, 9.0% (Saeedi et al., 2019). Additionally, a rapid increase in the incidence of diabetes in persons aged less than 40 years has been reported (Lascar et al., 2018). This is particularly of great concern since the affected persons are subjected to a longer period of hyperglycaemic exposure, and thus at high risk of developing more severe diabetes complications (Condorelli et al., 2018).

Table 2.5:Diabetes global prevalence trends, projection, and 2021 deaths

Regions/ Diabetes parameters	2000	2011	2021	2030	2045	Death in 2021
Africa	2.5 million	14.7 million	24 million	33.4 million	55.2 million	416,000
North America and the Caribbean	21.4 million	37.7 million	51 million	57 million	63 million	931,000
The Middle East and North Africa	17 million	32.6 million	73 million	95 million	135.7 million	796,000
South and Central America	8.5 million	25.1 million	32 million	40 million	49 million	410,000
South-East Asia	34.8 million	71.4 million	90 million	113.3 million	151.5 million	747,000
Western Pacific	44 million	131.9 million	206 million	238.3 million	260.2 million	2.3 million
Europe	22.4 million	52.7 million	61 million	67 million	69 million	1.1 million

Source: Source: International Diabetes Federation Diabetes Atlas 10th edition (IDF, 2021)

Table 2.6: Diabetes prevalence trends and projection of the most affected countries in Africa

Country/Year	2011/people	2021/people	2030/people	2045/people
Algeria	1.4 million	2 million	2.5 million	3.4 million
Democratic Republic of Congo	730,000	1.9 million	2.7 million	4.8 million
Egypt	7.3 million	> 8 million	13.7 million	19.9 million
Ethiopia	1.3 million	1.9 million	2.7 million	4.7 million
Morocco	1.2 million	2.3 million	2.8 million	3.5 million
Nigeria	3 million	3.6 million	4.9 million	7.9 million
South Africa	1.9 million	4.2 million	5.4 million	7.4 million
Sudan	1.6 million	3.5 million	4.7 million	7.4 million
Uganda	307,000	716,000	1 million	1.9 million
Tanzania	472,000	2.9 million	4.2 million	7.3 million

Source: International Diabetes Federation Diabetes Atlas 10th edition (IDF, 2021)

Hyperglycaemia describes a state of uncontrollable high blood glucose concentration, exceeding the normal value (mean fasting blood glucose, 5.6 - 6.9 mmol/l) (Zaccardi et al., 2016). It is diagnosed using the fasting blood glucose test levels (FBG) or oral glucose tolerance test (OGT). Hyperglycaemia is implicated by values that are consistently above 7 mmol/l for FBG or for OGT, 11 mmol/l two hours following an oral intake of 75 g glucose (WHO/IDF Consultation, 2006). Chronic hyperglycemia leads to development of multiple diabetic complications through augmentation of reactive oxygen species (ROS) production (Volpe, Villar-Delfino, Anjos, and Nogueira-Machado, 2018) Consequently, causing damage and dysfunctions of several organs such as the kidneys, eyes, heart, nerves, blood vessels, and gonads (Asmat et al., 2016; Omolaoye Temidayo and Du Plessis Stefan, 2018). Further, studies have reported the involvement of hyperglycemia in metabolic pathways that lead to cytokine production, inflammation, advanced glycation end products (AGEs) formation, and cell death (LaRocca et al., 2016; Maresch et al., 2018; Volpe et al., 2018).

2.14.3 Testicular glucose metabolism

Glucose metabolism is vital in the maintenance of basic cell activity and functions. In the testis, glucose metabolism plays a regulatory role in steroidogenesis, spermatogenesis, spermatozoa motility, and fertilization capability (Ding et al., 2015). Due to the blood-testis-barrier (BTB), blood-to-germ transportation of glucose and its metabolic intermediates from the basal to apical epithelial compartment is highly controlled (Alves et al., 2013; Riera et al., 2009). Testicular cells express metabolic features such as glucose transporters (Glut1, Glut2, Glut3, Glut4, and GLUT8) and insulin family growth factors (insulin (I), insulin-like growth factors 1 (IGF1) and 2 (IGF2), insulin receptors (INSR), and type-I insulin-like growth factor receptor (INS1R) which are involved in regulating nucleotide uptake and secretion of lactate, pyruvate, and transferrin by Sertoli cells (Riera et al., 2009; Maresch et al., 2018). The lactate produced by the Sertoli cells from glucose is the primary source of energy for germ cells for successful spermatogenesis (Mateus et al., 2018; Dimakopoulou et al., 2019).

Additionally, hypothalamic-pituitary-gonadal (HPG) axis hormones (GnRH, LH, FSH, and TT) also participate in the regulation of glucose transport in the testis (Alves et al., 2013; Maresch et al., 2018). Since glucose metabolism in the testis is unique and tightly controlled, dysregulations occurring in diabetic conditions can lead to alternations in the cellular function and subsequently impair the spermatogenesis and steroidogenesis processes. Moreover,

oxidative stress, dyslipidemia, and inflammation which are common complications of diabetes have been implicated in dysfunctions of the male reproductive system (Agbaje et al., 2007; Ding et al., 2015; Zubi & Alfarisi, 2021). However, the exact molecular mechanism involved in the impairment of the testicular function process in diabetic condition remains to be established.

2.14.4 Diabetes-related male infertility

The continuous increment in the prevalence of diabetes has been linked to the diminishing fertility factor (Condorelli et al., 2018; Ding et al., 2015). Previously the most prevalent diabetes type, T2D, which accounts for 90% of diabetic cases was commonly known to commence in old age, however, is now increasingly detected in all ages (both young and old) (Temidayo and Stefan, 2018). The onset of diabetes at an early age is of great concern because of the prolonged period of hyperglycemia exposure that consequently causes multiple diabetic complications including disruptions of male reproductive function (Agbaje et al., 2007; HE et al., 2021; Maresch et al., 2018).

Clinical diabetes and animal-induced diabetes studies have shown that both T1D and T2D are detrimental to the male reproductive system (Condorelli et al., 2018; HE et al., 2021). For instance, diabetes is suggested to impact epigenetic modification (DNA methylation, histone modifications, and noncoding RNAs) during gonadal development and spermatogenesis processes, leading to epigenetic defects that are inheritable to the next generation(s) (Pinney and Simmons, 2012; Ding et al., 2015; Donkin and Barrès, 2018). Accordingly, prenatal exposure to hyperglycemia has been shown to cause postpubertal testicular impairments such as relatively small testis size, low seminal fluid levels, and poor sperm quality in male offspring (Jelodar et al., 2009; Arendt et al., 2018; Türk et al., 2018).

Diabetics can alter male reproductive functioning at different levels i.e., pre-testicular, testicular, and post-testicular, resulting in subfertility or infertility (Condorelli et al., 2018).
(i) Pretesticular, several studies have reported reproductive hormone dysregulation in diabetic condition (Pitteloud et al., 2005; Schoeller et al., 2012; Shaikh et al., 2016).
(ii) Testicular, hyperglycemia, and ROS in diabetic condition have been shown to negatively affect testicular function (Maresch et al., 2018). Several studies have reported a reduction in seminiferous tubule diameter, Leydig cell number, germ cell population, and sperm quality and

an increase in DNA fragmentation (Agbaje et al., 2007; Navarro-Casado et al., 2010; Ray and Pramanik, 2020).

(iii) Post-testicular, alternations beyond the testis have been linked to neuropathy (Gandhi and Dagur, 2016; Ray and Pramanik, 2020), a common diabetes complication that is suggested to be involved in the onset of sexual dysfunctions such as diminished sexual arousal, erectile dysfunction, and ejaculatory disorders (Gandhi and Dagur, 2016; HE et al., 2021). Furthermore, diabetes-induced inflammation in the male genital tract and accessory glands could impair sperm transportation and alter seminal fluid parameters including leukocytospermia (Condorelli et al., 2014; Calogero et al., 2017).

2.15 Impact of diabetes, alcohol, and cART interaction on the male reproductive system

A soaring number of males with diabetes (Condorelli et al., 2018), alcohol abuse (World Health Organisation, 2011), and cART use (Khawcharoenporn and Sha, 2016) have been reported in the reproductive age. This infers that they would experience a longer period of exposure to these conditions, which is worrisome because of the multiple long-term organ dysfunctions associated with diabetes (Volpe et al., 2018), alcohol (Rachdaoui and Sarkar, 2013), and cART (Khan et al., 2014). Previous studies have shown an increase in reactive oxygen species (ROS) formation during diabetes (Blake and Trounce, 2014), alcohol abuse (Das and Vasudevan, 2007), and cART use (Ikekpeazu et al., 2019), ROS subsequently evoke oxidative stress (OS) and inflammation. The two (OS and inflammation) are the common mechanisms involved in induction of diabetes (Volpe et al., 2018), alcohol (Finelli et al., 2022), and cART (Gnanasekaran, 2020) multi-organ complications. Moreover, OS and inflammation are key factors in pathogenesis of reproductive dysfunction (Tremellen, 2012; Maresch et al., 2018). Conversely, each of these conditions (diabetes, alcohol abuse, and cART) has been shown to negatively impact the male reproductive system separately (Azu, 2012; Condorelli et al., 2018; Finelli et al., 2022). Incidentally, diabetes, alcohol abuse, and cART are intricately connected, thus can occur simultaneously in an individual (Kumar et al., 2015; Scott-Sheldon et al., 2016; Avari and Devendra, 2017; Mondal et al., 2019; Goecke and Baumeister, 2021), a scenario that could aggravates testicular ROS production.

Markedly, many of the factors associated with the dysfunction of the male reproductive system including increased ROS (oxidative stress), inflammation, and mitochondria damage are as well associated with adverse effects demonstrated in these conditions, diabetes, alcohol abuse,

and cART (Tremellen, 2012; Maresch et al., 2018; Dutta et al., 2021). Accumulation of ROS in the testis is associated with increased spermatozoa DNA fragmentation (SDF), a well-known contributing factor to male infertility (Robinson et al., 2012; Cho and Agarwal, 2018). Additionally, SDF is linked to a low success rate of ART conception, reduced fertilization chances, poor embryo quality, and an increase in miscarriage and stillbirth incidence (Robinson et al., 2012; Evenson, 2013; Savasi et al., 2018). Furthermore, alcohol has been demonstrated to augment the deleterious effects of diabetes and cART on sperm parameters. Pourentezari and colleagues reported a more significant reduction in sperm count, motility, and viability and an increase in abnormal sperm morphology and mitochondrial DNA deletions in diabetic mice treated with alcohol (Pourentezari et al., 2016). Whilst alcohol was found to exacerbate the increase in the number of immotile and abnormal sperms in rats treated with cART (Ogedengbe et al., 2018), cART has also been shown to aggravate the decrease in sperm count and progressive motility in rats induced with diabetes (Olasile et al., 2018). Since diabetes, alcohol abuse, and cART use are prevalent amongst males of reproductive age and teenagers due to active sexual life, lifestyle of alcohol abuse, and unhealthy dietary habits and yet they have the desire to procreate, it is crucial to investigate the impact of concomitant occurrence of diabetes, alcohol abuse, and cART use on male fertility factor.

CHAPTER 3: MATERIALS AND METHODS

3.1 Chemical and reagents

Streptozotocin (STZ) (S0130) was procured from Sigma-Aldrich Chemical Company (St. Louis, MO, USA) and Atripla, a combination antiretroviral (cART) drug was purchased from Bristol-Myers Squibb and Gilead Sciences (Foster City, CA, USA). The primary antibodies interleukin-1beta (IL-1β) (ab2105), interleukin-6 (IL-6) (ab9324), tumor necrosis factor-alpha (TNF-α) (ab6671), caspase 3 (ab4051), Ki-67 (ab15580), inducible nitric oxide synthase (iNOS) (ab115819), malondialdehyde (MDA) (ab243066), 8-hydroxydeoxyguanosine (8-OHDG) (ab62623), and androgen receptor (ab105225) were procured from Abcam (Cambridge, MA, USA). Biotinylated goat anti-rabbit (BA-1000) and goat anti-mouse (BA-9200) secondary antibodies and Avidin-Biotin Complex kit (ABC) (PK-6100) were procured from Vector Laboratories (Burlingame, CA, USA). Then, ELISA kits for luteinizing hormone (LH) (E-EL-R0026), follicle stimulating hormone (FSH) (E-EL-R0391), testosterone (TT) (E-EL-R0155), and inhibin B (INHB) (E-EL-R1027) were purchased from Elabscience (Houston, Texas, USA).

3.2 Ethical clearance

This study was approved by the University of the Witwatersrand (Wits) Animal Research Ethics committee (AREC) (approval number: 2018/011/58/C) and all experiments were conducted at the Wits Animal Research Facility (WARF) in compliance with the guidelines set forth by AREC.

3.3 Animals

Forty-eight adult male Sprague Dawley rats (10 weeks old), weighing between 330-370 grams were used in the study. Each rat was separately housed in a clean well-ventilated plastic cage with steel lids and dimensions of 430mm in length, 220mm in width, and 200mm in height with pinewood shaving beddings and were maintained at 21-23ºC room temperature, with lighting conditions of 12/12-hour light/dark cycle throughout the experiment.

3.4 Type 2 diabetes mellitus induction and tests

A modified Wilson & Islam, 2012 diabetic model that utilizes a fructose diet and Streptozotocin (STZ) injection to induce peripheral insulin resistance and insulin secretion impairment respectively was used in the current study. The baseline blood glucose level was measured to

establish the absence of pre-existing diabetic conditions before commencing two weeks of a 20% fructose reconstituted rat chow diet (Appendix I). After which, the animals were fasted for 5 hours prior to a single dose of freshly prepared 40mg/kg STZ in 0.05M (pH 4.5) citrate buffer (Appendix II) administered intraperitoneally. Three days (72 hours) after STZ injection, the blood glucose (non-fasting) levels were measured, and rats with glucose levels ≥ 250 mg/dl were considered diabetic. The confirmed diabetic rats were then put on a standard rat chow diet. To confirm that the diabetic state was maintained during the whole experimental period, the blood glucose levels were monitored using an AccuChek Compact glucometer (Roche Diagnostics, Indianapolis, IN) through a needle prick of the tail vein to measure levels of random non-fasting blood glucose weekly, fasting blood glucose preceded by overnight (12-hours fast) bi-weekly, and oral glucose tolerance monthly preceded by overnight fast and periodic blood glucose measurements at 0, 15, 30, 60, 120 minutes.

3.5 cART (Atripla) and alcohol treatment preparation

Atripla, a combination antiretroviral drug consisting of efavirenz 600 mg + emtricitabine 200 mg + tenofovir 245 mg was administered in accordance with extrapolated human equivalent dose of 23.22 mg/kg (Frampton and Croom, 2006) (Appendix). Then, the equivalent animal dose of cART tablet per gram per body weight was calculated and added to gelatine to formulate cubes for daily cART treatments. The gelatine cubes were prepared following Zhang & Zhang, 2011 recipe, however, each gelatine cube content was minimized to a single calorie to ensure that it does not influence the diabetic state (Appendix). Whilst 10% v/v alcohol in drinking water was administered, alcohol was diluted in distilled water in a ratio of 1 to 10 and administered as drinking water daily in the water bottles of alcohol treated animal groups (Dutra Gonçalves et al., 2017).

3.6 Experimental design

To ensure that a feasible number of animals were handled at a time, the experiment was conducted in two phases. The sample size was approved by the ethics committee following the calculation of the sample size using Power analysis for sample size (see Appendix). However, all the 90 animals were not used in the experiment. Rather a total of forty-eight HIV naive rats (48) were divided into two main groups, non-diabetic (24) and diabetic groups (24). These two main groups were further subdivided into four subgroups consisting of six rats each (Fig. 3.1). The non-diabetic groups (consisting of groups1-4); Group 1: Control, received no treatment. Group 2: Alcohol treated (A), received 10% v/v alcohol in drinking water daily. Group 3:

combination antiretroviral therapy treated (cART), received a human equivalent dose of 23mg/kg of cART in gelatine cubes daily. Group 4: alcohol plus cART treated (A+cART), received both alcohol and cART daily.

The diabetic groups (5-8); Group 5: diabetic (DM), diabetes was induced as described above. Group 6: diabetic animals treated with alcohol (DM+A), following diabetes induction, animals received 10% v/v alcohol in drinking water daily. Group 7: diabetic animals treated with cART (DM+cART), following diabetes induction, animals received a human equivalent dose of 23mg/kg of cART daily. Group 8: diabetic animal treated with both alcohol and cART (DM+A+cART).

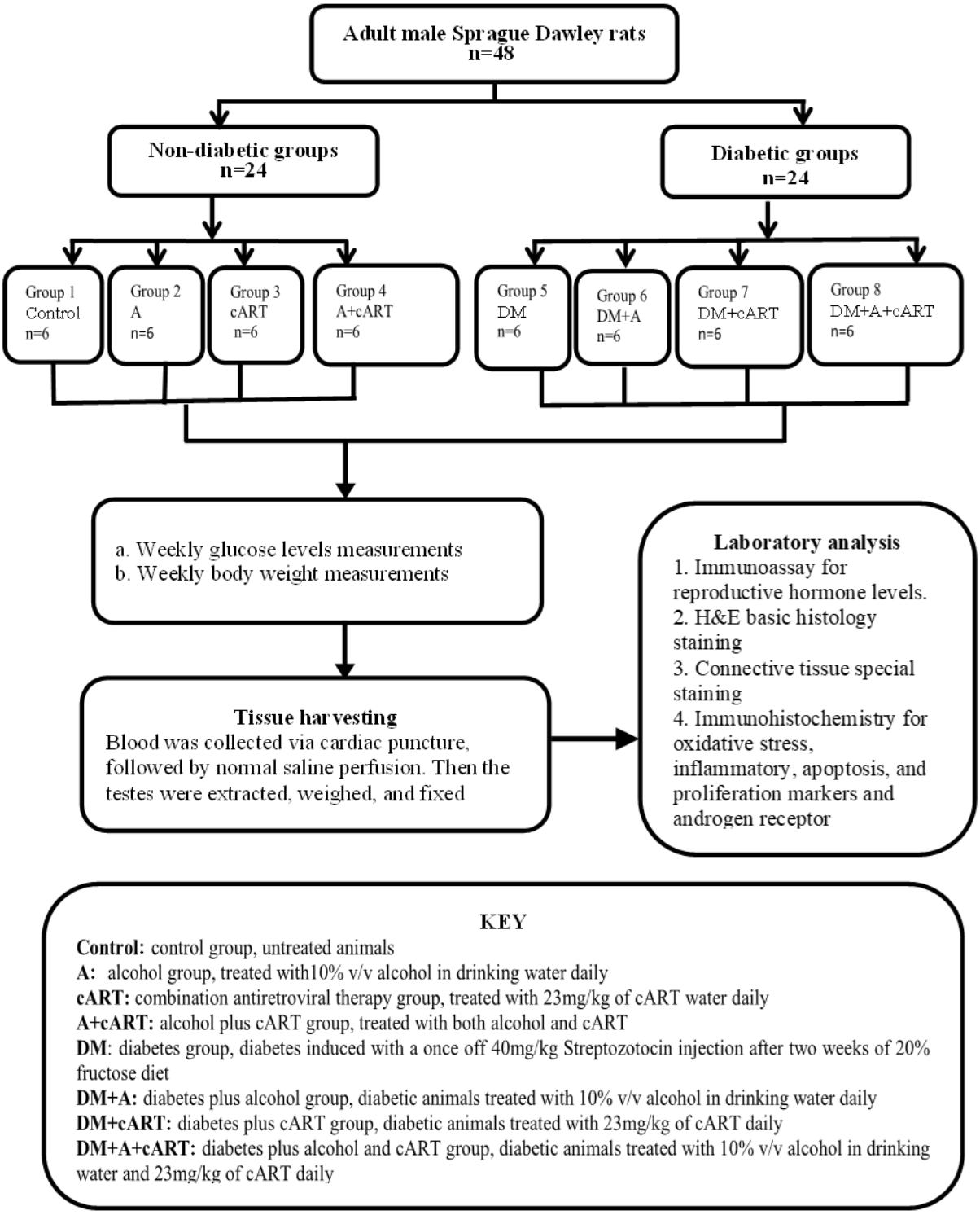


Figure 11: Experimental design illustration

3.5 Animal terminal procedures

After 90 days of treatment, the rats were weighed, anesthetized with 240mg/ml pentobarbitone dose, and terminated. Blood was withdrawn through a cardiac puncture into a plain vacutainer. The rats were perfused with 2 mL/min of 0.1M phosphate buffer (PB) in 0.9% saline, thereafter,

testes were harvested, weighed, and the weight recorded and then fixed in 10% neutral buffered formalin for histology and immunohistochemical analysis. Collected blood samples were left to clot, then centrifuged, and the serum was transferred into a new Eppendorf tube and stored at -80℃ for immunoassays.

3.5.1 Testis weight and size

The testes were weighed using an electronic scale (Kern PCB 200-2 weighing scale) immediately after extraction. The testis length and width were measured using a sliding digital Vernier caliper as described by Parhizkar et al., 2014. The spheroid formula below was then used to determine the testis size.

$$Testis\ size = width^2 \times length \times 0.523\ (mm)$$

3.5.2 Testis volume

Testis volume was determined using the water displacement method (Ansa et al., 2017). The initial volume (Vi) of distilled water in a graduated cylinder was recorded, and then the final volume (Vf) was recorded after adding the testis to the graduated cylinder containing the known amount of water. The volume of the testis (Vt) was calculated as shown below.

$$Vt = Vf - Vi\ (\text{mm}^3)$$

3.5.3 Gonadosomatic index (GSI)

The GSI was calculated using the final body and testis weights using the formula by Olasile et al., 2018:

$$\text{GSI} = \frac{Testis\ weight}{Body\ weight} \times 100\ (\%)$$

3.6 Reproductive hormone immunoassay

Enzyme-linked immunosorbent assay (ELISA) was used to determine serum reproductive hormone levels. For luteinizing (LH), follicle stimulating (FSH), and inhibin B (INHB) a sandwich ELISA technique was conducted, while a competitive ELISA technique was carried out for testosterone (TT) assay. Serum samples and all reagents were allowed to reach room temperature before assay commencement. The wash buffer, standard working solutions, biotinylated detection antibody, and horseradish peroxidase (HRP) conjugate were prepared for the experiment according to the manufacturer's guidelines. Samples were diluted in a threefold, and standards and samples were run in duplicates (side by side on the plate). The assay procedure was conducted as follows: for the sandwich technique, a volume of 100 µL for the standards and samples was carefully added to the bottom of the respective plate wells. The plates were then sealed and incubated for 90 min at 37℃. Thereafter, the solution was decanted

from the wells, and without washing the plate, a 100 µL of the biotinylated detection antibody (BDA) working solution was added to each well. Then, the plate was sealed and incubated for 60 min at 37°C. Whilst in the competitive technique for TT assay, a volume of 50 µL for standards and samples was added to respective plate wells, followed immediately by addition of 50 µL of BDA working solution after which the plate was sealed and incubated for 45 min at 37°C. The next steps were similar for both techniques. After incubation, the solution was removed from the wells and the plate was placed in a microplate washer, where 350 uL of wash buffer was added to each well and allowed to soak for 60 sec per cycle for three cycles of plate washing. Then, 100 µL of HRP conjugate working solution was added to each well, the plate was sealed and incubated at 37°C for 30 min. Afterward, the solution was decanted from the wells, and the wash step carried as mentioned above but for five cycles. Subsequently, 90 µ of substrate reagent was added to each well, and the plate was sealed, wrapped in aluminum foil (to protect it from light), and gently shaken before incubation for 15 min at 37°C. Immediately after incubation, a stop solution was added to each well. The plate was then put on a micro-plate reader set at 450 nm filter to measure the optical densities (OD). The microplate reader was set up according to the user's manual guidelines and preheated for 15 minutes before measuring the optical densities. The average OD values for standards and samples were calculated. Then, the average OD for standard zero was subtracted from the average OD for standards and samples. A standard curve was plotted with the standard concentration and OD values. The average OD values for each sample (y-axis) were used to determine the corresponding concentration of TT, LH, FSH, and INHB from the standard curve (x-axis).

3.7 Histology and histomorphometry

The testes were processed for histology analysis using an automated tissue processor (MicromeSTP 120, Thermo Fisher Scientific, Walldorf, Germany) and embedded in paraffin wax. The testis block for each animal was serially sectioned at 5µm thickness using a Leica rotatory microtome (Leica RM 2125 RTS). The first series of sections were stained with H&E (for morphometry and histology), the second series with periodic acid Schiff (PAS) (for basement membrane), the third series with Masson's Trichrome (for collagen), the fourth series with Gordon and Sweet's silver impregnation (for reticulin), and the fifth series with Gomori's Aldehyde Fuchsin (for elastin) (Cordatos, 2002). Stained sections were examined using the Axioskop 2 plus light microscope (Nikon Eclipse Ci, 104C type). Photomicrographs of stained sections were obtained using a linked computerized Zeiss digital image system, the AxioCam

208 color (Zeiss group, Oberkochen, Germany). Six camera fields were captured per section and 4 sections per animal were observed per group (n=6) (i.e., 144 sections per group) and used for morphometric assessment.

3.7.1 Haematoxylin and Eosin (H&E) staining protocol for basic histology

Four sections per animal in each group were deparaffinized in a series of xylene, then hydrated in a series of decreasing alcohol concentrations, and rinsed in running tap water for 5 minutes. Thereafter, the sections were stained with Mayer's hematoxylin for 10 minutes, followed by rinsing in running tap water for 5 minutes. Then, differentiated in acid alcohol for 2 quick dips and rinsed in running tap water for 5 minutes. Followed by staining with eosin for 2 minutes and rinsing in running tap water for 5 minutes. The sections were then dehydrated in a series of increasing alcohol concentrations and cleared in xylene. Dibutylphthalate Polystyrene Xylene (DPX) was added to the section before putting a coverslip.

Staining results; nuclei: blue stained and cytoplasm: purple stained.

3.7.2 Periodic acid Schiff (PAS) staining protocol for basement membrane

The sections were deparaffinized, hydrated, and rinsed in running tap water for 5 minutes. Sections were oxidized in 1% periodic acid solution for 5 minutes and thereafter rinsed in running tap water for 5 minutes. Then, placed in Schiff reagent for 20 minutes, after which the sections were rinsed in running tap water for 5 minutes and counter-stained in Mayer's hematoxylin for 1 minute. Followed by rinsing in running tap water for 5 minutes, dehydration, clearing, and adding a coverslip with DPX.

Staining results; basement membrane: purple-stained and background: blue-stained.

3.7.3 Masson's Trichrome staining protocol for collagen

The tissue sections were deparaffinized, hydrated, and rinsed in running tap water for 5 minutes. Immerse sections in Celestin blue stain for 5 minutes, rinse in running tap water for 5 minutes and then stain with Mayer's hematoxylin for 5 minutes. Followed by rinsing in running tap water for 5 minutes, staining with acid fuchsin stain for 10 minutes, and rinsing in running tap water for 2 minutes. Thereafter, immersed in freshly prepared 5% phosphomolybdic acid for 10 minutes, drain off excess (do not rinse), and stain with light green for 10 minutes. Followed by rinsing in running tap water for 5 minutes, dehydration, clearing, and adding a coverslip with DPX.

Staining results; collagen: green stained, nuclei: black stained, and erythrocyte blood cells: red stained.

3.7.4 Gordon and Sweet's silver impregnation staining protocol for reticulin

The tissue sections were deparaffinized, hydrated, and rinsed in running tap water for 5 minutes. Sections were oxidized in acidified potassium permanganate for 3 minutes, thereafter, rinsed in running tap water for 5 minutes. Followed by bleaching with 2% oxalic acid for 1 minute, rinsing in running tap water for 5 minutes, and sections were then placed in a mordant, 4% iron alum for 10 minutes. After which the sections were rinsed in running tap water for 5 minutes and placed into an ammoniacal silver solution for 10 seconds. Then, rinsed in running tap water for 2 dips and placed in 10% formalin for 1 minute (reducing step). Sections were rinsed in running tap water for 1 minute and toned in 0.2% gold chloride for 5 minutes. Thereafter, rinsed in running tap water for 5 minutes and placed in 2% sodium thiosulphate for 5 minutes. Followed by rinsing in running tap water for 1 minute, dehydration, clearing, and adding a coverslip with DPX.

Staining results; reticulin: black stained and background: yellow stained.

3.7.5 Gomori's Aldehyde Fuchsin staining protocol for elastin

The sections were deparaffinized, hydrated, and rinsed in running tap water for 5 minutes. Then, sections were immersed in 70% alcohol for 1 minute and after draining were immediately transferred into Aldehyde Fuchsin Solution for 15 minutes. Followed by 3 changes of 95% alcohol, 2 minutes in each, and 2 dips in 70% alcohol. Thereafter, the sections were rinsed in running tap water for 10 minutes. Followed by staining in Mayer's hematoxylin for 10 seconds, rinsing in running tap water for 10 minutes, and immersion in 50% alcohol for 2 dips. The sections were then immersed in Eosin for 2 dips, after which the excess stain was drained off (without rinsing in water). Followed by dehydrating, clearing, and adding a coverslip with DPX.

Staining results; elastin: purple-stained and nuclei: dark blue stained.

3.8 Testicular component area fractions

Testicular component (germinal epithelium, luminal, connective tissue, and interstitial space) area fractions were determined using the Fiji 84-intersection grid. The grid was superimposed on H&E-stained images captured at x100 magnification and the intersecting points for each

component were counted. The average intersecting points for each testicular component were calculated in 24 camera fields for each animal (i.e., 144 fields per group) and each testicular component area fraction was determined using the formula below (Kangawa et al., 2019).

$$\text{Area fraction} = \frac{(area\ per\ point \times average\ number\ of\ intersecting\ points)}{total\ area\ of\ photomicrograph} \times 100\ (\%)$$

3.9 Seminiferous tubule morphometry

Using Fiji software, the seminiferous tubular area (TA), tubular diameter (TD), and epithelium height (EH) were measured in 50 round or nearly round seminiferous tubules for each animal (i.e., 300 tubules per group). The Fiji freehand selection tool was used to trace around the seminiferous tubule to determine the tubular area. The average tubular diameter and epithelial height were calculated using the minor and major axes measurements (Kumar and Nagar, 2014). To exclude longitudinal tubules, an average tubule diameter was considered only if D1/D2 ≥ 0.85, a value of D1/D2 =1.0 representing a perfectly rounded circle (Olasile et al., 2018).

3.10 Germinal epithelium cell quantification

The different germinal epithelium cells: Sertoli, spermatogonia, spermatocytes, round, and elongated spermatids) were counted in 10 rounded seminiferous tubules for each rat (i.e., 60 tubules per group) at x400.

3.11 Leydig cell morphometry

The Leydig cell nuclei diameter was measured on H&E-stained images captured at x400 using Fiji software, 50 nuclei with distinct nucleoli were considered for each rat (i.e., 300 per group). The Leydig cell nuclear volume was obtained using the formula reported previously (Monteiro et al., 2012).

$Leydig\ cell\ nuclear\ volume\ = \frac{4}{3}\pi R^3$(µm^3). Where, Radius (R) = D/2, and π = 3.14.

3.12 Histopathological evaluation

3.12.1 Johnsen's testicular score

Spermatogenesis was classified in 50 seminiferous tubules per animal (i.e., 300 tubules per group) using Johnsen's testicular score technique. Each tubule was assigned a score from 10 to 1. Thereafter the number of tubules for an individual score was multiplied by the score, and then the total for all the scores was divided by 50 (the total number of tubules scored) to obtain

the mean Johnsen's score per group for further analysis (Thanh et al., 2020). The modified Johnsen scoring criteria used is shown in Table 3.1.

Table 3.1: Modified Johnsen scoring criteria

Spermatogenesis level	Johnsen's score
Many spermatozoa in the tubule lumen	10
Many elongated spermatids in the apical region of the epithelium	9
Many elongated spermatids still embedded in the Sertoli cell membrane	8
Few elongated spermatids, many round spermatids	7
No elongated spermatids, few round spermatids	6
No spermatids, many spermatocytes	5
Few spermatocytes	4
Spermatogonia cell only	3
Sertoli cells only	2
No seminiferous epithelial cells	1

3.12.2 Histological changes

Testicular H & E-stained sections were examined for histological changes. The observed changes were then graded in 24 microscopic fields (six fields from each of the four sections) for each animal (i.e., 144 fields per group). The changes in each field were semi-quantitatively categorized into five grades as follows; grade 4 = very severe (change seen in >75% of the field), grade 3 = severe (change seen in >50%<75% of the field), grade 2 = moderate (change seen in >25%<50% of the field), grade 1= mild (change seen in <25% of the field), and grade 0 = none (no change in the field) (Erpek et al., 2007).

3.13 Measurement of seminiferous tubule basement membrane (STBM)

Fiji software was used to measure the thickness of the basement membrane in PAS-stained sections images captured at x400. The thickness of STBM was measured at two points (from the minor and major axis) in 50 randomly selected tubules for each animal (i.e., 300 tubules per group) (Omar, Aly, and Badae, 2017).

3.14 Evaluation of testicular capsule thickness

Using Fiji software, the capsule thickness was measured on Masson's Trichrome stained sections. Photomicrographs of six fields from the free surface of the capsule were captured at x400, and three points were measured on each field (i.e., 18 measurements for each animal, 108 per group) (Aire and Ozegbe, 2007).

3.15 Connective tissue fibers quantification

Testicular connective tissue components viz. collagen, reticulin, and elastin fibers were quantified in the photomicrographs of sections stained with Masson's Trichrome, Gordon and Sweet's silver impregnation, and Gomori's Aldehyde Fuchsin techniques respectively. Collagen, reticulin, and elastin fibers were quantified in the 24 microscopic fields captured at x100 for each animal (i.e., 144 sections per group). The images were segmented using the ilastik pixel classification workflow and then the segments were quantified into numerical data in Fiji.

3.16 Immunohistochemistry technique

The sixth series of testicular tissue sections were mounted onto silane-coated slides for antibody immunolabeling. Antibodies for oxidative stress (inducible nitric oxide synthase (iNOS), malondialdehyde (MDA), and 8-hydroxydeoxyguanosine (8-OHDG)), inflammation (interleukin-1beta (IL-1β), interleukin-6 (IL-6), tumor necrosis factor-alpha (TNF-α), apoptosis (caspase 3), proliferation markers (Ki-67), and androgen receptor (AR) were assessed. Following deparaffinization and hydration, antigen retrieval was conducted by incubating testis sections in citrate buffer overnight in a water bath at 60^{o}C. Then, the endogenous peroxidase was inhibited using 1% hydrogen peroxide in methanol for 20 minutes. After rinsing in phosphate-buffered saline (PBS) for three changes of five minutes each, 5% normal goat serum was added to the sections to block nonspecific antibody binding. This was tapped off after 30 minutes, and the primary antibody was added subsequently (Table 3.2) and left overnight (approximately 16 hours) at 4°C. Thereafter, the sections were rinsed in PBS and incubated with the secondary antibody (Table 3.2) for 30 minutes. Thereafter rinsed in PBS and avidin-biotin complex (ABC) reagent was added for 30 minutes. Subsequently, the sections were rinsed in PBS and incubated with 3, 3'-diaminobenzidine tetrachloride (DAB) for five minutes. Then, DAB was washed off under running tap water for five minutes and the slides were counterstained for one minute in hematoxylin. Followed by rinsing in running tap water, dehydration in a series of alcohol, and coverslipped with Dibutylphthalate Polystyrene Xylene (DPX). For each set of immunohistochemical test, two negative control slides were included; one without the primary and the other without the secondary antibody. The images of immunoreactivity localized to both cell nucleus and cytoplasm (IL-1β, TNF-α, iNOS, and MDA) were captured in 24 microscopic fields at x100 for each animal (i.e., 144 sections per group) and were segmented using the ilastik pixel classification workflow. Fiji was then used

for quantification of the ilastik exported image segments to extract numerical data for statistical analysis. For the antibodies with immunoreactivity localized to cell nuclei (IL-6, caspase 3, 8-OHDG, AR, and Ki-67), the total number of immunolabelled cell nuclei were counted in 20 rounded seminiferous tubules per animal (i.e., 120 tubules for each group).

Table 3.2: Antibody dilutions used

Antibodies	Dilution
Primary antibodies	
anti-iNOS	1:100
anti-MDA	1:200
anti-8-OHDG	1:1000
anti-IL-1β	1:200
anti-IL-6	1:200
anti-TNF-α	1:100
anti-caspase 3	1:200
anti-Ki-67	1:1000
anti-AR	1:100
Secondary antibodies	
goat anti-rabbit	1:1000
goat anti-mouse	1:1000

3.17 Data analysis

The data of the studied parameters were analyzed using GraphPad Prism 6 software and expressed as Mean ± SEM. The data were subjected to the Shapiro-Wilks normality test, parametric data were compared using one-way analysis of variance (ANOVA), followed by Bonferroni's *post hoc* test. Non-parametric data (Johnsen's and histological change scores) was compared using Kruskall Wallis, followed by Dunn's *post hoc* test. A P-value of < 0.05 was deemed statistically significant.

BRIDGING NOTE

Chapters 4 to 7 are presented in manuscripts format. This pattern was chosen to clearly highlight reproductive histopathology of the treatments and therefore the significance and contributions of the study. As such the study was structured into four manuscripts, one published, two at final stages of review and acceptance and one recently submitted.

CHAPTER 4: FIRST MANUSCRIPT

Co-administration of Alcohol and Combination Antiretroviral Therapy (cART) in Male Sprague Dawley Rats: A Study on Testicular Morphology, Oxidative, and Cytokines Perturbations

Published in *Anatomy & Cell Biology:* 56(2):236-251 (https://doi.org/10.5115/acb.22.229).

ABSTRACT

Alcohol consumption alongside combination antiretroviral therapy (cART) has attracted research interest, especially because of increasing male infertility. This study investigated the combined effects of alcohol and cART on testicular morphology, biomarkers of oxidative stress, inflammation, and apoptosis. Rats, weighing 330-370g, were divided into four groups of six animals each; control, alcohol treated (A), cART, and alcohol plus cART treated (A+cART). Following 90 days treatment period, rats were euthanized, testis extracted, and routinely processed for histology and immunohistochemical analysis. Significantly decreased epithelial area fraction, increased luminal and connective tissue area fractions, and reduction of epithelial height and spermatocyte number, were recorded in the treated groups compared to control. Extensive seminiferous epithelial lesions including widened intercellular space, karyolysis, and sloughing of germinal epithelium were recorded in all the treated groups. Furthermore, upregulation of inducible nitric oxide synthase (iNOS) and 8-hydroxydeoxyguanosine (8-OHDG), interleukin-6 (IL-6), and caspase 3 recorded in treated animals, was more significant in A+cART group. Also, the levels of IL-1β, TNF-α were more elevated in A and cART treated groups than in A+cART, while MDA was significantly elevated in cART and A+cART treated groups compared to control group. Altogether, the results indicate testicular toxicity of the treatments. It is concluded that consuming alcohol or cART induces oxidative stress, inflammation, and apoptosis in testes of rats, which lead to testicular structural and functional derangements, which are exacerbated when alcohol and cART are consumed concurrently. The result will invaluably assist clinicians in management of reproductive dysfunctions in male HIV/AIDS-alcoholic patients on cART.

Keywords: Alcohol, cART, Testis, Oxidative stress, and Inflammation

INTRODUCTION

Male infertility incidence is rising steadily worldwide and accounts for more than 50% of infertility cases (Sun et al., 2019; Agarwal et al., 2021). Equally, there is a worldwide increase in human immunodeficiency virus (HIV) infection (Simões et al., 2021) and alcohol abuse (İlhan and Yapar, 2020). For instance, about 33% of South African (SA) population consumes alcohol regularly and the SA's average consumed alcohol per capita (APC) almost doubles the global average APC (Trangenstein et al., 2018; Vellios and van Walbeek, 2018). Equally, the country is burdened with high HIV prevalence and has the biggest combination antiretroviral therapy (cART) program globally (Cornell et al., 2017; Lippman et al., 2019). Currently, cART prophylaxis is encouraged among healthcare workers following accidental needle prick, and amongst prostitutes and individuals after unsafe and casual sex with unknown persons or HIV infected individuals (Mabwe et al., 2017; Simões et al., 2021). While the influence of alcohol on risky sexual activity is associated with an increase in the spread of HIV infection (Kumar et al., 2015; Schneider et al., 2016; Scott-Sheldon et al., 2016) and the consequent use of cART, many HIV patients on cART therapy continue to consume alcohol regularly for euphoric purposes (McCance-Katz et al., 2013; Mondal et al., 2019). Furthermore, alcohol has been associated with reduced viral suppression dose-dependently (Chander et al., 2006; Braithwaite et al., 2007); aggravated HIV progression, and reduced cART efficacy (Mondal et al., 2019).

Alcohol and cART have each been shown to have negative long-term consequences on both male and female reproductive organs and other body systems (Kushnir and Lewis, 2011; Ogedengbe et al., 2018; Duca et al., 2019; Apolikhin and Krasnyak, 2021). Excessive alcohol consumption is reckoned as a leading cause of male impotence and infertility (La Vignera et al., 2013). Several testicular and sexual dysfunctions have been reported in habitual/chronic alcohol consumers (Condorelli et al., 2015; Oremosu and Akang, 2015; Van Heertum and Rossi, 2017). Also, cART has been shown to alter reproductive hormones and sperm parameters (Oyeyipo et al., 2018; Savasi et al., 2019). A reduction in testosterone levels, sperm concentration, and DNA integrity have been implicated in long-term use of cART (Azu, 2012; Savasi et al., 2018). Only two reports in literature have shown adverse effects of alcohol and cART interaction on testicular histology (Ogedengbe, Naidu and Azu, 2018; Ogedengbe et al., 2018). The present study evaluated specifically the impact of this interaction on Sertoli and Leydig cells and immunohistochemical localization of the oxidative stress, inflammatory, and apoptotic markers to further delineate possible physio-biochemical impact of alcohol plus cART treatment on the testis. Currently, increasing HIV infection and male infertility are

reported among reproductive age individuals, with high desire for procreation, and might also be regular alcohol consumers (Ogedengbe, Naidu and Azu, 2018). This implies increased alcohol and cART interaction amongst the age group, making their reproductive health a huge health concern. Against this backdrop, this study evaluated testicular toxicity associated with concurrence of alcohol and cART in the body using HIV-naïve male rat model to mimic conditions of cART regimen.

MATERIALS AND METHODS

Chemicals and reagents

These were procured from different reliable sources. A combination antiretroviral drug (Atripla) consisting of 600mg of Efavirenz, 300mg Tenofovir disproxil Fumurate, and 245mg Emtricitabine was procured from Bristol-Myers Squibb and Gilead Sciences (Foster City, CA, USA). Rabbit polyclonal for primary antibodies interleukin-1beta (IL-1β) (ab2105), tumor necrosis factor-alpha (TNF-α) (ab6671), and caspase 3 (ab4051), rabbit monoclonal for primary antibody inducible nitric oxide synthase (iNOS) (ab115819), and mouse monoclonal for primary antibodies interleukin-6 (IL-6) (ab9324), malondialdehyde (MDA) (ab243066), and 8-hydroxydeoxyguanosine (8-OHDG) (ab62623) were procured from Abcam (Cambridge, MA, USA). Whilst biotinylated goat anti-rabbit (BA-1000) and goat anti-mouse (BA-9200) secondary antibodies, and Avidin-Biotin Complex kit (ABC) (PK-6100) were procured from Vector Laboratories (Burlingame, CA, USA).

Ethical clearance

This study was approved by the Animal Research Ethics committee (AREC) (approval number: 2018/011/58/C) of University of the Witwatersrand (Wits) and all experiments were conducted at the Wits Animal Research Facility (WARF) in compliance with the guidelines set forth by AREC.

Animals

Twenty-four adult male Sprague Dawley rats (10 weeks old), weighing between 330-370 grams were used in the study. Each rat was separately housed under sterile conditions in a plastic cage. Animals were fed on normal rat chow and water *ad libitum* and were maintained at 21-23ºC room temperature, with lighting conditions of 12/12-hour light/dark cycle.

Experimental design

Animals were divided into four groups of six rats each as follows; control group, received no treatment; alcohol group (A), which received 10% v/v alcohol in drinking water daily (Dutra Gonçalves et al., 2017); the combination antiretroviral therapy group (cART), received an extrapolated human equivalent dose of 23.22 mg/kg of cART (consisting of efavirenz 600 mg + emtricitabine 200 mg + tenofovir 245 mg) (Frampton and Croom, 2006) in gelatine cubes daily; and alcohol plus cART group (A+cART), received both alcohol and cART daily at same doses indicated above. After 90 days of treatment, the animals were weighed, anesthetized with 240mg/ml pentobarbitone dose, and sacrificed. The animals were perfused with 2 mL/min of 0.1M phosphate buffer (PB) in 0.9% saline and the testes were harvested, weighed, and the wet weight recorded and thereafter fixed in 10% neutral buffered formalin for histology and further analysis.

Testicular morphometry

Testis weight and volume

The weight of the testes was recorded immediately after their extraction using an electronic scale (Kern PCB 200-2 weighing scale). Testis volume was determined using the Archimedes principle of water displacement in a measuring cylinder (Ansa et al., 2017). The initial volume (Vi) of distilled water in a graduated cylinder was recorded, and then the final volume (Vf) was determined after adding the testis to the graduated cylinder containing the known amount of distilled water. The volume of the testis (Vt) was calculated by subtracting the initial volume from the final volume as shown below.

$$Vt = Vf - Vi \ (\text{mm}^3)$$

Testis size

A sliding digital Vernier caliper was used to measure the width and length of the testes, as described by Parhizkar et al (Parhizkar et al., 2014). Testis size was then calculated using the formula below (Parhizkar et al., 2014).

$$Testis\ size = width^2 \times length \times 0.523\ (mm)$$

Histology and histomorphometry (H&E)

The fixed testes were dehydrated sequentially in 70-100% alcohol grades and embedded in molten paraffin wax and serially sectioned at 5µm thickness. The sections were stained with H&E and examined using the Axioskop 2 plus light microscope (Nikon Eclipse Ci, 104C type). Photomicrographs of testicular tissue sections were obtained using a linked computerized Zeiss

digital image system, the AxioCam 208 color (Zeiss group, Oberkochen, Germany) for morphometric assessment. Six camera fields from 4 sections per animal, from six animals per group (i.e., 144 images per group) were captured and used for morphometry and analysis.

Testicular component area fractions

Testicular component (epithelial, luminal, connective tissue, and interstitial space) area fractions were determined using Fiji 84-intersection grid. The grid was superimposed on H&E-stained images captured at x100 and the intersecting points for each component were counted. The average intersecting points for each testicular component were calculated in 144 microscopic field images per group and each testicular component area fraction was determined using the formula below (Kangawa et al., 2019).

$$\text{Area fraction} = \frac{(area\ per\ point \times average\ number\ of\ intersecting\ points)}{total\ area\ of\ photomicrograph} \times 100\ (\%)$$

Seminiferous tubule morphometry

Seminiferous tubule area (TA), tubule diameter (TD), epithelium height (EH), and luminal diameter (LD) were measured in 50 round or nearly round seminiferous tubules for each animal (i.e., 300 tubules per group) using Fiji software. The seminiferous tubule area was determined by tracing around the seminiferous tubule using the Fiji freehand selection tool. The average tubule diameter and epithelial height were calculated using the minor and major axes measurements (Kumar and Nagar, 2014). To exclude longitudinal tubules, an average tubule diameter was considered only if $D1/D2 \geq 0.85$, a value of $D1/D2 = 1.0$ representing a perfectly rounded circle (Olasile et al., 2018).

Germinal epithelium cell quantification

The number of the different germinal epithelium cells (Sertoli, spermatogonia, spermatocytes, round, and elongated spermatids) were counted in H&E-stained sections at x400. Ten rounded seminiferous tubules (stage VII) (Qiu et al., 2013) for each animal were considered (i.e., 60 tubules per group).

Leydig cell morphometry

Using Fiji software, diameters (D) of fifty Leydig nuclei with distinct nucleoli were measured for each animal on H&E-stained images captured at x400. The nuclear volume (an important

parameter in a variety of cell functions) was determined in accordance with previously reported methods (Monteiro et al., 2012), with the formula below.

$Leydig\ cell\ nuclear\ volume\ = \frac{4}{3}\pi R^3$(μm^3). Where, Radius (R) = D/2, and π = 3.14.

Histopathological evaluation

Johnsen's testicular score

Spermatogenesis was classified in 50 stage II-VII seminiferous tubules per animal (i.e., 300 tubules per group) using Johnsen's testicular score. Each tubule was assigned a score from 10 to 1, accordingly, thereafter the number of tubules for an individual score was multiplied by the score, and then the total for all the scores was divided by 50 (the total number of tubules scored) to obtain the mean Johnsen's score per group for further analysis (Thanh et al., 2020). The modified Johnsen scoring criteria used is shown in Table 4.1.

Table 4.1: Modified Johnsen scoring criteria

Spermatogenesis level	Johnsen's score
Many spermatozoa in the tubule lumen	10
Many elongated spermatids in the apical region of the epithelium	9
Many elongated spermatids still embedded in the Sertoli cell membrane	8
Few elongated spermatids, many round spermatids	7
No elongated spermatids, few round spermatids	6
No spermatids, many spermatocytes	5
Few spermatocytes	4
Spermatogonia cell only	3
Sertoli cells only	2
No seminiferous epithelial cells	1

Histological changes

Testicular H & E-stained sections were examined for the presence of histological changes. Observed changes were graded in 24 microscopic fields (six fields from each of the four sections) for each animal (i.e., 144 fields per group). The changes in each field were semi-quantitatively categorized into five grades as follows; grade 4 = very severe (change seen in >75% of the field), grade 3 = severe (change seen in >50%<75% of the field), grade 2 = moderate (change seen in >25%<50% of the field), grade 1= mild (change seen in <25% of the

field), and grade 0 = none (no change in the field) as previously reported by Erpek et al. (Erpek et al., 2007).

Immunohistochemistry for oxidative stress, inflammation, and apoptosis

Testicular tissue sections were mounted on silane-coated slides for antibody immunolabeling. Assessment of oxidative stress using inducible nitric oxide synthase (iNOS), malondialdehyde (MDA), and 8-hydroxydeoxyguanosine (8-OHDG), inflammation (interleukin-1beta (IL-1β), tumor necrosis factor-alpha (TNF-α), and interleukin-6 (IL-6), and caspase 3 for apoptosis were carried out. The sections were incubated in citrate buffer overnight in a water bath at 60^{o}c for antigen retrieval. Then, the endogenous peroxidase was inhibited using 1% hydrogen peroxide in methanol for 20 minutes. After rinsing in phosphate buffered saline (PBS) for three changes of five minutes each, 5% normal goat serum was added to the sections to block nonspecific antibody binding. This was tapped off after 30 minutes, and the primary antibody was added subsequently (1:100 for anti-TNF-α and anti-iNOS, 1:200 for anti- IL-1β, anti- IL-6, anti-MDA, and anti-caspase 3, and 1:1000 for anti-8-OHDG) and left overnight (approximately 16 hours) at 4°C. Thereafter, the sections were rinsed in PBS and incubated with the secondary antibody (1:1000 biotinylated goat anti-rabbit for the IL-1β, TNF-α, iNOS, and caspase 3 antibodies and 1: 1000 biotinylated goat anti-mouse for IL-6, MDA, and 8-OHDG antibodies) for 30 minutes. Then, after rinsing in PBS, avidin-biotin complex (ABC) reagent was added for 30 minutes. Afterward, the sections were rinsed in PBS and incubated with 3, 3'-diaminobenzidine tetrachloride (DAB) for five minutes. DAB was then washed off under running tap water for five minutes and the slides were dipped in hematoxylin for one minute to counter stain. Followed by rinsing in running tap water to remove excess stain, dehydration of slides in alcohol series, and coverslipped with Dibutylphthalate Polystyrene Xylene (DPX). The images of antibodies with immunoreactivity localized to both cell nucleus and cytoplasm (IL-1β, TNF-α, iNOS, and MDA) were captured in 24 microscopic fields at x100 for each animal (i.e., 144 sections per group) and were segmented using the ilastik pixel classification workflow. Fiji was used for quantification of the ilastik exported image segments to extract numerical data for statistical analysis. Details of image segmentation and quantification are shown in appendix. The percentage area of expression for antibodies was calculated using the formula below.

$$\% \text{ Area of expression} = \frac{immunoreactive\ area}{total\ area\ of\ photomicrograph} x100$$

For the antibodies with immunoreactivity localized to cell nuclei (IL-6, 8-OHDG, and caspase 3), the total number of cell nuclei expressing immunoreactivity were counted in 20 rounded stage VII seminiferous tubules for each animal (i.e., 120 tubules for each group).

Data analysis

GraphPad Prism 6 windows software was used for data analysis. Data were expressed as Mean ± SEM. Group means of parametric data were compared using a one-way analysis of variance (ANOVA), followed by Bonferroni's *post hoc* test. Non-parametric data (Johnsen's and histological change scores) were compared using Kruskall Wallis, followed by Dunn's *post hoc* test. Deeming a P-value of < 0.05 statistically significant.

RESULTS

Testicular morphometry

All treated groups (A, cART, and A+cART) showed a non-significant decrease in testis weights, testis volume, and testis size in comparison with the control (Table 4.2).

Table 4.2: Mean testicular morphometry and component area fractions of testes from rats treated with alcohol, cART, and both.

Animal groups	Control	Alcohol (A)	cART	A+cART
Testis morphometry				
Testis weight (g)	1.91±0.05^{a}	1.78±0.04^{a}	1.85±0.03^{a}	1.78±0.09^{a}
Testis volume (mm^3)	1.88±0.09^{a}	1.83±0.08^{a}	1.83±0.08^{a}	1.67±0.11^{a}
Testis size (mm)	1493±40.52^{a}	1491±24.19^{a}	1378±46.83^{a}	1409±43.89^{a}
Area fractions (AF) (%)				
Epithelial (EAF)	74.25±0.50^{a}	71.43±0.60^{b}	71.82±O.53^{b}	70.59±0.47^{b}
Luminal (LAF)	8.56±0.29^{a}	8.64±0.27^{a}	7.38±0.24^{b}	9.80±0.30^{c}
Connective tissue (CTAF)	11.97±0.31^{a}	13.66±0.35^{b}	15.11±0.32^{c}	15.26±0.33^{c}
Interstitial space (ISAF)	4.93±0.12^{a*}	5.73±0.17^{b}	5.77±0.16^{b}	4.99±0.12^{c*}

For all parameters: Values in the same row with similar superscripts are not significantly different. Whilst values in the same row with different superscripts are significantly different ($p<0.05$) except when the different superscripts are both marked with an asterisk (*). A, alcohol; cART, combination antiretroviral therapy; A+cART, alcohol and combination antiretroviral therapy.

Testicular area fractions

The epithelial area fraction (EAF) of treated groups significantly reduced compared to the control, (A, p=0.0012; cART, p=0.0078; and A+cART, p<0.0001) (Table 4.3). The luminal area fraction (LAF) of cART group decreased significantly compared to control (p=0.0123), A (p=0.0059) and A+cART (p<0.0001), but was significantly increased in A+cART compared to control (p= 0.0141). The connective tissue and interstitial space area fractions (CTAF and ISAF respectively) of all the treated groups (A, cART, and A+cART) were increased compared to the control. The increase was significant in CTAF of all treated groups (A: p=0.0017, cART: p<0.0001, and A+cART: p<0.0001) and in ISAF of A (p=0.0008) and cART (p=0.0003) groups. Furthermore, CTAF of cART and A+cART treated groups was significantly higher when compared with group A (p=0.0110 and p=0.0038 respectively), while ISAF of A+cART group was significantly reduced compared to A (p=0.0025) and cART (p=0.0010) groups (Table 4.3).

Table 4.3: Mean for seminiferous tubule, germinal epithelium cell count, and Leydig cell morphometry of testes from rats treated with alcohol, cART, and both.

Animal groups	Control	Alcohol (A)	cART	(A+cART)
Tubule measurements				
Tubule area, TA (μm^2)	78939±692^{a}	68854±773^{b}	65972±739^{c}	72069±803^{d}
Tubule diameter, TD (µm)	310.2±1.30^{a}	286.5±1.54^{b}	283.0±1.52^{b}	293.2±1.56^{c}
Epithelium height, EH (µm)	97.51±0.62^{a}	93.34±0.71^{b}	92.52±0.72^{b}	89.46±0.78^{c}
Luminal diameter, LD (µm)	97.97±3.54^{a}	105.90±2.67^{a*}	84.95±2.06^{b}	116.9±3.38^{c*}
Epithelium cell count				
Spermatogonia	59.20±0.62^{a}	67.93±1.50^{b}	66.43±1.18^{b*}	61.97±1.33^{a*}
Spermatocytes	88.62±0.80^{a}	86.00±1.00^{a*}	84.33±0.71^{b*}	83.72±0.95^{b*}
Round spermatids	92.30±0.95^{a}	80.41±1.47^{b}	84.25±1.43^{b}	83.79±1.18^{b}
Elongated spermatids	102.9±1.02^{a}	83.20±1.13^{b}	85.93±1.48^{b}	85.75±0.80^{b}
Sertoli	23.61±0.24^{a}	22.56±0.38^{a}	22.75±0.28^{a}	22.54±0.31^{a}
Leydig cell nuclear				
Diameter (µm)	5.85±0.04^{a}	5.37±0.04^{b}	5.48±0.05^{b}	5.42±0.04^{b}
Volume (μm^3)	110.00±2.46^{a}	85.95±2.18^{b}	91.73±2.28^{b}	88.03±2.13^{b}

For all parameters: Values in the same row with similar superscripts are not significantly different. Whilst values in the same row with different superscripts are significantly different (p<0.05) except when the different superscripts are both marked with an asterisk (*). A,

alcohol; cART, combination antiretroviral therapy; A+cART, alcohol and combination antiretroviral therapy.

Seminiferous tubule morphometry

All seminiferous tubule measured parameters (area, diameter, epithelium, and lumen) were decreased in all treated groups compared to control, except for lumen of A+cART treated that increased non-significantly ($P>0.05$) (Table 4.3). Tubule area and diameter significantly decreased ($p<0.0001$) in A, cART, and A+cART treated groups relative to control. The tubule area of cART treated group significantly decreased compared to A treated group ($p=0.0413$). In addition, tubule area and diameter were significantly higher in A+cART than in A ($p = 0.0155$ and 0.0089 respectively) and cART ($p<0.0001$) groups. In comparison with the control group, the epithelial height of groups A, cART, and A+cART decreased significantly ($p = 0.0002$, 0.0001, and 0.0001 respectively) while the luminal diameter of A+cART group increased significantly ($p=0.0013$). However, the luminal diameter of cART group was significantly decreased compared to control ($p=0.0340$), A ($p=0.0004$), and A+cART ($p<0.0001$) treated groups.

Germinal epithelium cell count

The results are as shown in table 4.3. The mean number of spermatogonia increased significantly in A and cART-treated groups ($p<0.0001$and $P<0.0002$ respectively) relative to control but was significantly decreased in A+cART ($p=0.0032$) relative to A group. However, spermatocytes were significantly reduced in cART and A+cART groups compared to control, ($p=0.0043$ and $p=0.0007$ respectively). Both round and elongated spermatids decreased significantly ($p<0.0001$) in all treated groups compared to the control. Furthermore, a non-significant decrease ($p>0.05$) in the number of Sertoli cells was found in all the treated groups (A, cART, and A+cART) compared to control.

Leydig cell

Leydig cell nuclear diameter and volume decreased significantly ($p<0.0001$) in all the treated groups (A, cART, and A+cART) compared to control (Table 4.3).

Histopathological evaluation

Johnsen's testicular score

Johnsen's score was used to profile the progress/status of spermatogenesis in the seminiferous tubules. Compared to the control, a significant reduction in Johnsen's score was recorded in A (p=0.0115) and A+cART groups (p=0.0256) (Table 4.4).

Table 4.4: Median Johnsen's score and histological changes observed and their score range in testes of rats treated with alcohol, cART, and both.

Animal groups	**Control**	**Alcohol (A)**	**cART**	**A+cART**
Johnsen's score	8.81^{a}	8.29^{b*}	8.50^{a*}	8.38^{b*}
Histological changes				
Lifting of epithelium	0.06±0.01^{a}	0.18±0.04^{a}	0.09±0.02^{a}	0.15±0.02^{a}
	(0-1)	(0-2)	(0-1)	(0-2)
Widened intercellular space	0.06±0.02^{a}	0.37±0.14^{a*}	0.29±0.09^{a*}	0.82±0.17^{b*}
	(0-1)	(0-2)	(0-2)	(0-4)
Karyolysis	0.00±0.00^{a}	0.11±0.02^{a}	0.17±0.04^{b}	0.13±0.03^{b}
	(0-0)	(0-1)	(0-1)	(0-1)

For all parameters: Values in the same row with similar superscripts are not significantly different. Whilst values in the same row with different superscripts are significantly different ($p<0.05$) except when the different superscripts are both marked with asterisk (*). A, alcohol; cART, combination antiretroviral therapy; A+cART, alcohol and combination antiretroviral therapy.

Histological changes

The most common histological changes observed were lifting of germinal epithelium, widened intercellular space, and karyolysis (Fig. 4.1) and were different across the groups (Table 4.4). However, the difference in epithelial lifting was not significant across the groups but widened intercellular space was significantly higher in A+cART (p=0.0029) compared to control group. Additionally, karyolysis in cART and A+cART groups was significantly high when compared to the control group (p=0.0081 and 0.0346 respectively). Furthermore, seminiferous tubule shrinkage was observed in all treated groups, with sloughing of germinal epithelium into the lumen recorded in A+cART treated animals.

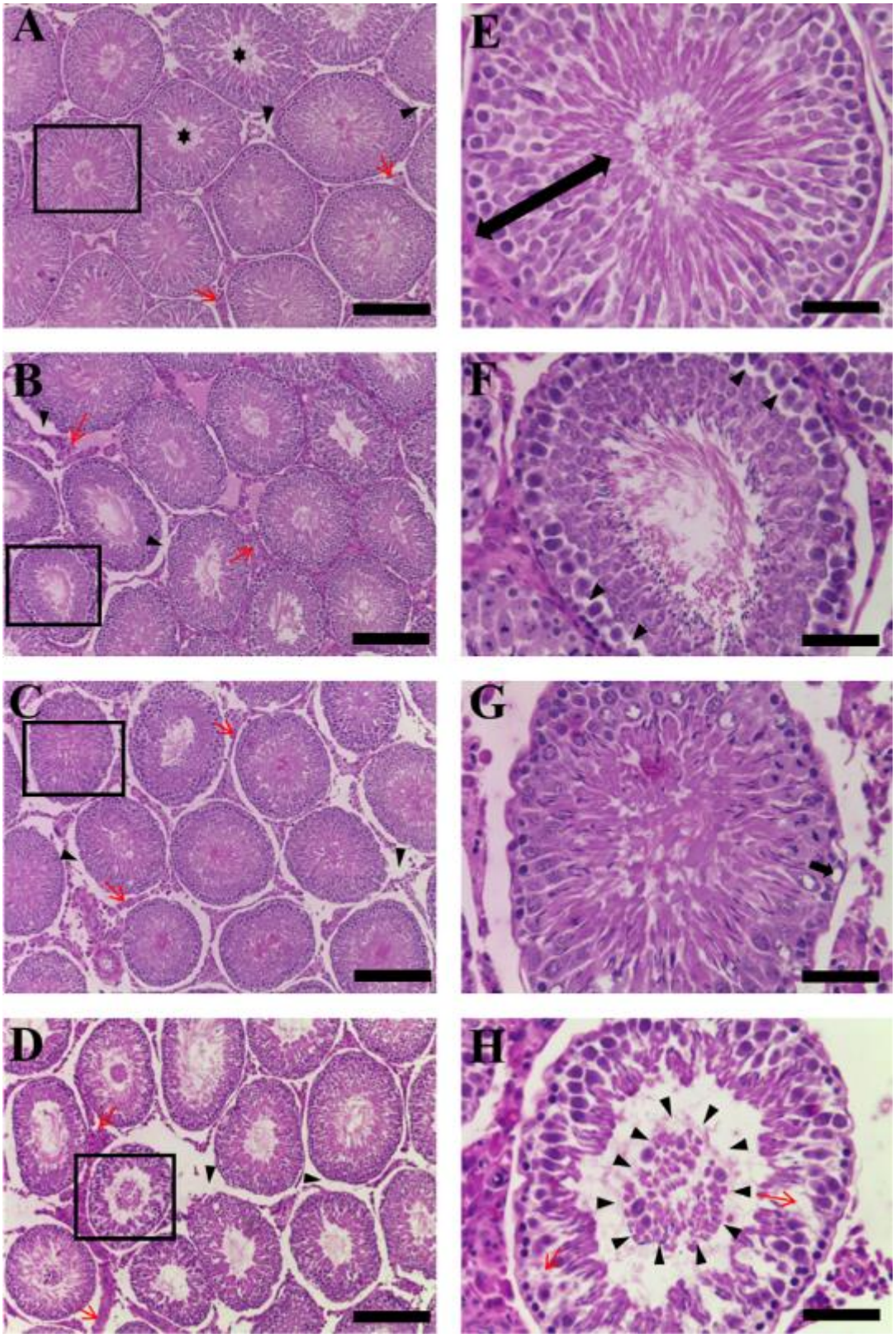


Figure 4.1: Representative photomicrographs of H&E-stained testicular section. Control (image A) shows normal oval-shaped seminiferous tubule with a lumen (asterisks), lying between adjacent tubules is a layer of interstitial (thin arrows) populated with Leydig cells interspersed within the connective tissue, and a thin interstitial space (arrowheads) between the

tubules. Treated groups; alcohol (image B), cART (image C), and A+cART (image D) showed shrinkage of seminiferous tubules and increased interstitial space (arrowheads). Images E, F, G, and H are a magnification of the square area indicated in images A, B, C, and D. Image E, shows the germinal epithelium (double arrow) consisting of discretely arranged series of spermatogenic cells, F shows lifting of epithelium (arrowheads) from the basal cells, G shows karyolysis (thick arrow) of spermatogonia and spermatocytes, and H shows sloughing of epithelium (arrowheads) into the lumen and widened intercellular germ space (thin arrows). The left and right panels are ×100 and ×400 with scale bars of 200μm and 50μm respectively. A, alcohol; cART, combination antiretroviral therapy; A+cART, alcohol and combination antiretroviral therapy.

Immunohistochemistry: oxidative stress, inflammation, and apoptosis

Oxidative stress markers

Oxidative stress markers immunoreactivity (Fig. 4.2) was localized in the cytoplasm and nucleus of macrophages and Leydig cells for both inducible nitric oxide synthase (iNOS) and malondialdehyde (MDA). While 8-hydroxydeoxyguanosine (8-OHDG) immunoreactivity was localized in the spermatogenic cell nuclei and residual bodies. All treated groups (A, cART, and A+cART) demonstrated a significant increase ($p<0.0001$) in expression of iNOS and 8-OHDG relative to the control group (Fig. 4.2). A significant increase of MDA expression was detected in cART and A+cART groups relative to the control group ($p<0.0001$) and in cART and A+cART groups relative to group A ($p<0.0001$ and $p=0.0302$ respectively) (Fig. 4.2).

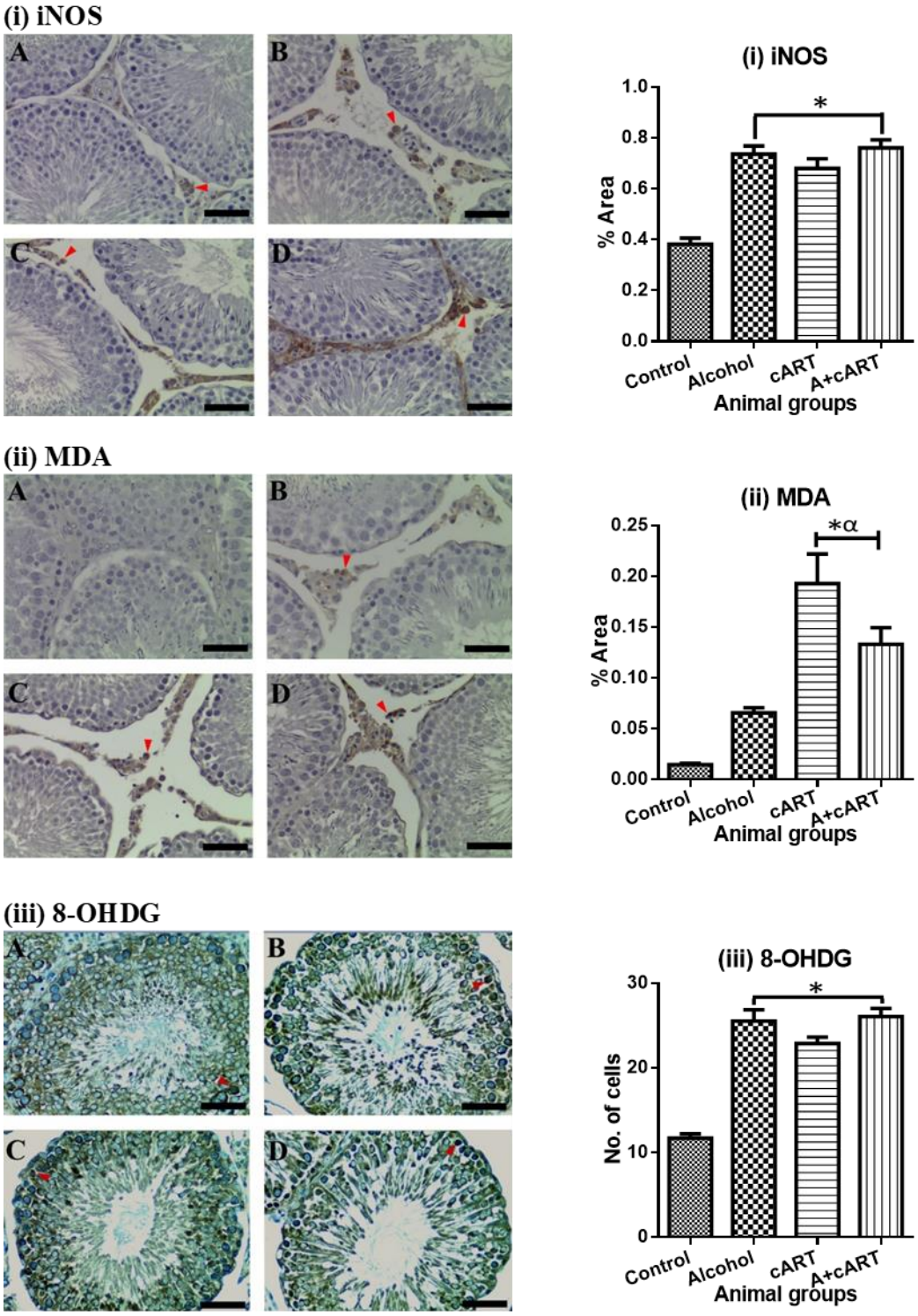


Figure 4.2: Photomicrographs of oxidative stress expression and respective mean of expression graphs. Representative immunoreactivity is indicated with arrowhead. The mean percentage area of expression for iNOS and MDA, and mean number of cells expressing 8-OHDG were reported. Different symbols * and α represent significant differences ($p<0.05$) as analyzed by a Bonferroni's multiple comparison test; '*' significantly increased compared to control and 'α' significantly increased compared to alcohol (A). Magnification, x400; scale

bar, 50μm. Key: Image: A; control group, B; alcohol treated group, C; cART treated group, and D; A+cART treated group. A, alcohol; cART, combination antiretroviral therapy; A+cART, alcohol and combination antiretroviral therapy.

Inflammatory and apoptosis markers

Expressions of interleukin-1beta (IL-1β), tumor necrosis factor-alpha (TNF-α), interleukin-6 (IL-6), and caspase 3 were as presented in figure 4.3. IL-1β expression was significantly elevated ($p<0.0001$) in A and cART treated groups compared to the control. But the expression of IL-1β in cART and A+cART treated groups was significantly decreased relative to A treated group ($p=0.0006$ and $p<0.0001$ respectively) and significantly decreased ($p<0.0001$) in A+cART compared to cART. Although, the expression of TNF-α was increased in all the treated groups against the control, the increase was only significant in A treated animals ($p=0.0001$). Further, the expression TNF-α in A group increased significantly ($p=0.0011$) compared to A+cART treated group. Interleukin-6 (IL-6) was significantly upregulated ($p<0.0001$) in all treated groups (A, cART, and A+cART) compared to the control. Whilst caspase 3 expression significantly increased in A ($p=0.0023$), cART ($p<0.0001$), and A+cART ($p<0.0001$) groups relative to control. Further, caspase 3 expression in A+cART group was significantly higher in comparison to A ($p<0.0001$) and cART ($p=0.0013$) treated groups (Fig. 4.3).

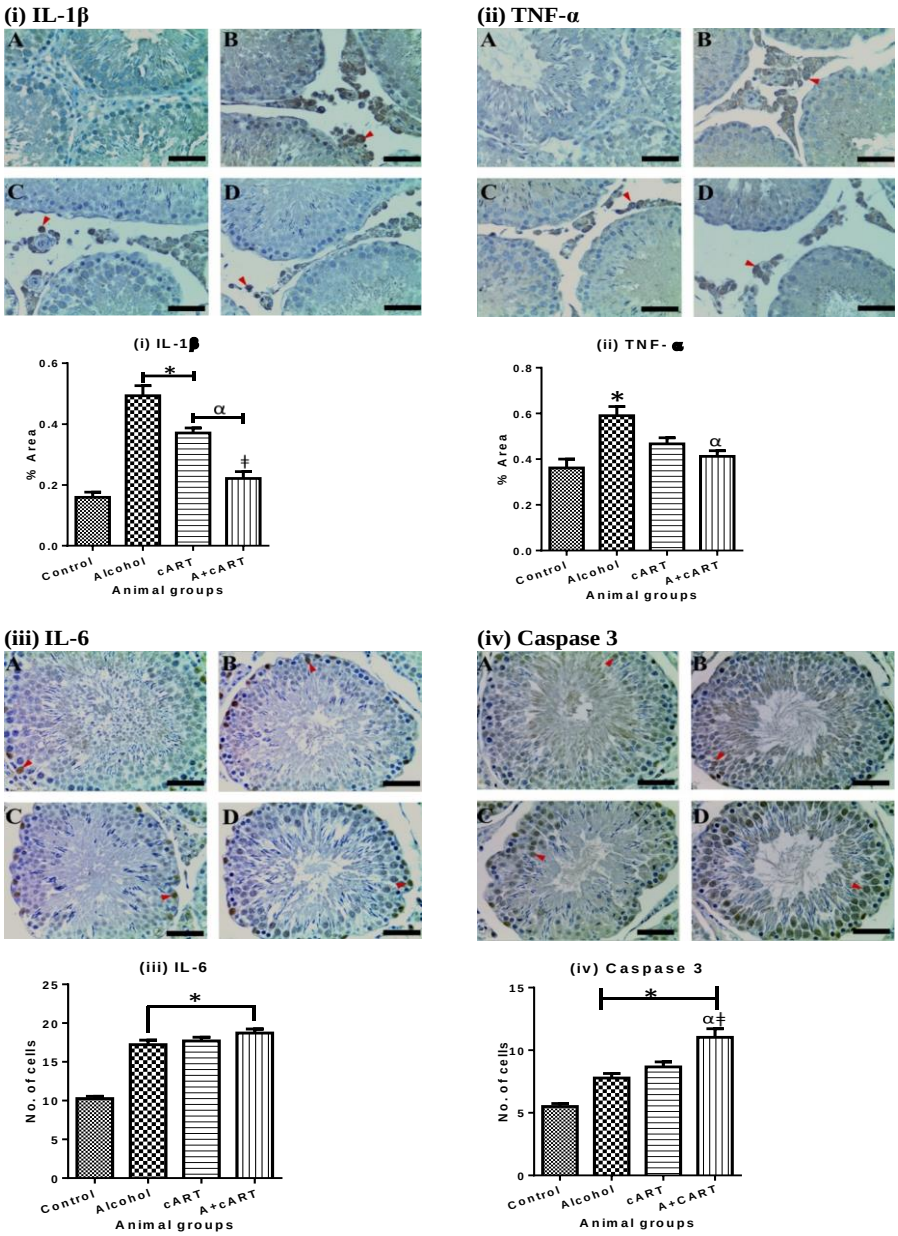


Figure 4.3: Photomicrographs of inflammatory and apoptosis expression and respective mean of expression graphs. Representative immunoreactivity is indicated with arrowhead. The mean percentage area of expression for IL-1β and TNF-α, and the number of cells expressing IL-6 and caspase 3 were reported. Different symbols *, α, and ǂ represent significant differences ($p<0.05$) as analyzed by a Bonferroni's multiple comparison test; '*' significantly increased compared to control, 'α' significantly different compared to alcohol (A), and 'ǂ' significantly different compared to cART. Magnification, x400; scale bar, 50µm. Key: Image: A; control group, B; alcohol treated group, C; cART treated group, and D; A+cART treated group. A, alcohol; cART, combination antiretroviral therapy; A+cART, alcohol and combination antiretroviral therapy.

DISCUSSION

Infertility is a worrisome reproductive health problem in families globally (Agarwal et al., 2021) with a soaring prevalence of male infertility (Sun et al., 2019). The chronic use of combined antiretroviral (cART) blended with alcohol abuse has introduced new variables in male reproductive dysfunctions. Moreover, a high incidence of alcohol use among people living with HIV/AIDS (PLWHA) and on combination antiretroviral therapy (cART) has also been reported (McCance-Katz et al., 2013; Mondal et al., 2019). Markedly, cART and alcohol have individually been reported to negatively impact the male reproductive system (Kushnir and Lewis, 2011; Apolikhin and Krasnyak, 2021) and thus their concomitant use may pose major reproductive dysfunctional challenges, particularly amongst PLWHA that desire to have biological children (Savasi et al., 2019), which is a critical societal necessity.
The result from this study showed non-significant decrease in testicular weight, volume, and size across the treatment groups compared to the control group which is consistent with previous reports (Monteiro et al., 2012; Adaramoye et al., 2015; Ogedengbe et al., 2018; Olasile et al., 2018) and may suggest minimal perturbations of testicular architecture. However, the significantly decreased epithelial area fraction (EAF), and the significantly increased luminal area fraction (LAF) in A+cART treated group point to perturbations of testicular structure and cellular coherency. Furthermore, the significant increases in interstitial space area fraction (ISAF) in A and cART treated groups and non-significant in the A+cART treated group may suggest specific treatment effects and the impact of the A+cART interaction on this parameter. Overall, these changes in the histological component of the testis reflect an alteration of the integrity of testicular morphology, pointing to disruption of the normal testicular paracrine/autocrine factors (such as cytokines) involved in regulation of spermatogenesis and consequently will lead to a decline in spermatogenesis (Azu, 2012; Kangawa et al., 2019).

Furthermore, the increased number of spermatogonia (proliferation of spermatogenesis) observed in testis of the alcohol and cART treated groups, could be an attempt to increase the germ cell pool so as to counteract the diminishing spermatogenesis processes which is in line with a previous clinical study that reported a massive increase in the number of normally differentiated spermatogonia and elevated spermatogonia proliferative activity in a biopsy of patient with non-obstructive azoospermia (Fietz et al., 2020). Additionally, the luminal area fraction (LAF) and diameter (LD) were both slightly increased in the A group but significantly

increased in the A+cART group, suggesting varying degrees of germ cell layer reduction due to different treatments as well as seminiferous tubule shrinkage.

Notably, tubular shrinkage was depicted by the significant reduction in tubular area (TA) and diameter (TD) in testis of treated groups (A, cART, and A+cART), and was consistent with previous findings (Azu, 2012; Dosumu et al., 2014; Ogedengbe et al., 2018). However, LAF and LD were also significantly decreased in the treated groups except in cART group regardless of the diminished EAF, EH, and germinal epithelium cell layers. This could have been due to the prominent seminiferous tubule shrinkage observed in cART treated group which also recorded the greatest reductions in TA and TD. Further, shrunken seminiferous tubules are suggestive of tubule degenerative changes induced by the treatments and subsequently result in germ cell death (Azu et al., 2014). Accordingly, shrinkage of the seminiferous tubules resulted in an increase in interstitial space area fraction (ISAF) in the treated groups compared to the control animals.

Equally, a significant increment in connective tissue area fraction (CTAF) was recorded in the testis of treated animals, suggesting formation of fibrosis in the testis interstitium. Our findings go in line with that of a previous study that reported fibrosis led to increase in thickness of the testicular interstitium in the infertile males (Apa et al., 2002). Testicular fibrosis usually occurs following testis trauma and inflammation amongst others (Yagan, 2000). Fibrosis impairs the integrity of the testicular interstitium and alters the structure and function of the interstitial cells (Leydig, macrophages, and myoid cells), and consequently adversely affects testicular structure and function (Yagan, 2000; Mayerhofer, 2013).

Furthermore, the number of Sertoli cells was not significantly reduced in the treated animals compared to control animals, suggesting that Sertoli cells were less adversely affected. Previous report indicated that Sertoli cells are resistant to apoptosis compared to germ cells (Wangikar et al., 2011), because they contain high levels of anti-apoptotic markers, Bcl-w and Bcl-xL (Yuko Ito and Otsuki, 2013). It has been reported that while the number of Sertoli cells is not usually affected (Pajarinen and Karhunen, 1994; Yuko Ito and Otsuki, 2013), disruptions in its structure are relatively common and can alter the cell's functions, the integrity of the blood-testis barrier (BTB) (Trindade et al., 2013) and consequently lead to dysregulation of spermatogenesis. Though, the present study did not include effects on the Sertoli cell cytoskeleton, previous studies show that its alteration and/or damage leads to sloughing of

germ cells into the lumen and separation of germinal epithelium from the basement membrane (Moffit et al., 2007; Lie et al., 2010; Johnson, 2014), which were both observed in treated animals in the current study.

However, Leydig cell nuclear diameter and volume in testis of treated animals were significantly reduced relative to the control animals and may imply disturbances of Leydig cell function (Jelodar et al., 2009; Trindade et al., 2013; Olasile et al., 2018). The nucleus is the lifeline of the cell, and a previous study showed that quantitative measurements of the nucleus is important in understanding the cell's response to injury and further reported that nuclear volume correlates strongly with cell volume and function (Wu et al., 2022). Leydig cells are present in the testis interstitium, and synthesize androgens via steroidogenesis (Zirkin and Papadopoulos, 2018). Therefore, shrinkage of the nucleus will ultimately affect the Leydig cell's steroidogenic capacity and subsequently lead to disruption of spermatogenesis (Kumari et al., 2011; Neves et al., 2017; Zirkin and Papadopoulos, 2018).

Additionally, in parallel with previous findings (baydilli, 2020; Akhigbe, Hamed and Aremu, 2021), Johnsen's score of the treated groups was reduced compared with the control animal group. Reduction in Johnsen's score is linked to interruption of normal germ cell maturation, germ cell layer loss, and tubule lesions (Salman et al., 2014; Shokoohi et al., 2018). Also, seminiferous tubule germinal epithelium lesions such as lifting of epithelium, widened interstitial space, karyolysis, and sloughed germ cells were more evident in the treated groups compared to control animal group, which supports the reduction in Johnson's score recorded in treated groups. This result confirm testicular toxicity of the treatments (alcohol or/and cART) (Moffit et al., 2007; Duca et al., 2019).

Oxidative stress is a common feature in most male reproductive system dysfunctions (Tremellen, 2012; Sakr and Nooh, 2013; Asadi et al., 2017), occurring as a result of an imbalance between rate of production and clearance of reactive oxygen species (ROS) (Turner and Lysiak, 2008; Wu et al., 2020). High ROS levels have been reported in 30–80% of infertile males (Tremellen, 2012; Wu et al., 2020). Our findings showed upregulation of oxidative stress markers i.e., inducible nitric oxide synthase (iNOS), malondialdehyde (MDA), and 8-hydroxydeoxyguanosine (8-OHDG) in the testis of treated animals. This indicates that alcohol, cART, and their combination induced oxidative stress in the testis. Reports show that iNOS upregulation leads to increased ROS formation (Zhao et al., 2010), ROS have been shown to

induce lipid peroxidation and DNA fragmentation in the testis (Aitken and Roman, 2008; Sharma and Agarwal, 2011; Ikekpeazu et al., 2019). These are the most common consequences of testicular oxidative stress resulting into increased MDA and 8-OHDG formation respectively (Aprioku, 2013; Asadi et al., 2017; Dutta et al., 2021). Previous studies have reported that ROS-induced lipid peroxidation is implicated in male reproductive dysfunction (Tremellen, 2012; Sakr and Nooh, 2013; Asadi et al., 2017), due to substantial amounts of unsaturated fatty acids in the testis tissue (Aitken and Roman, 2008; Guerriero et al., 2014).

Reportedly, elevation of ROS stimulates release of several inflammatory cytokines such as IL-1, TNF-α, and IL-6 mostly via the nuclear factor-kappa beta (NF-kβ) pathway (Aprioku, 2013; Nna et al., 2019; Dutta et al., 2021). In the testis, cytokines are majorly derived from interstitial macrophages, but Leydig and Sertoli cells also secrete cytokines (Kolasa et al., 2009; Coştur et al., 2012; Loveland et al., 2017). Studies show that during testicular injury, activated macrophages, Leydig, and Sertoli cells produce a high concentration of cytokines and iNOS (Kolasa et al., 2009; Coştur et al., 2012; Dutta et al., 2021). In consonance with the above, the elevated levels of pro-inflammatory cytokines observed in the present study may adversely affect the process of spermatogenesis, as reported by previous studies (Hedger and Meinhardt, 2003; Loveland et al., 2017). Somade et al. 2019 found that elevated cytokine levels in testis and kidney of Wistar albino rats, was associated with testiculo-renal toxicosis following acute administration of edible camphor (Somade et al., 2019). Additionally, testicular cytokines have been shown to affect germ cell proliferation, as well as Leydig and Sertoli cells functions and secretions (Loveland et al., 2017). This study findings show that oxidative stress and inflammation are interlinked mechanisms associated with germ cell apoptosis, which might underlie the multidimensional changes observed in testis of animals treated with alcohol or/and cART.

Overall, the study has revealed some important findings in testicular toxicity of the treatments relative to the parameters studied. Interestingly, though the levels of IL-1β and TNF-α, and MDA were elevated in A + cART treated group compared to control animals but comparatively were not as elevated as that of IL-6, iNOS, 8-OHDG, and caspase 3 expression in A+cART treated group. These results suggest possible effect of cytochrome P450 enzyme pathway involved in the metabolism of alcohol and cART (Kumar et al., 2012; Ogedengbe, Naidu and Azu, 2018; Mondal et al., 2019), resulting in reduction of the level of these parameters (IL-1β,

TNF-α, and MDA) in A+cART treated group. Additionally, it may suggest a variation in the effects of different treatment on the studied parameters.

CONCLUSION

Our results show that consumption of alcohol or cART can cause perturbations in the testis morphometric parameters and seminiferous tubule lesions via upregulation of oxidative stress and pro-inflammatory cytokines. In addition, consumption of alcohol and cART concurrently can exacerbate testicular damage. The findings from this study are invaluable for the clinical management of male fertility challenges that could emerge in PLWHA on cART therapy who consume alcohol regularly.

APPENDIX

Image segmentation

Ilastik software (v1.3.3; https://www.ilastik.org) was used for image segmentation. Images were segmented into 3, 3'-diaminobenzidine tetrachloride (DAB) positive area and background (Berg et al., 2019; Chim et al., 2020). A pixel classifier was trained with eight sample images selected from all animal groups (two images per group). The available features i.e., intensity/color, texture, and edge at a sigma of 0.3–10 pixels were included in the classification algorithms. To train the classifier an appropriate brush was used to annotate a few DAB-positive areas (yellow color), and representative areas not stained with DAB were annotated as the background (blue color). To place the annotations precisely, the images were zoomed out. The prediction was inspected after adding each annotation. Then more annotations were added to all training images to refine the classifier and increase its applicability to large training naïve image sets. Once the prediction was of a good standard across the sample images, the trained classifier was applied to image sets, and their simple segmentations were exported for quantification (Fig. A1).

Image quantification

Segmented images were quantified using Fiji software (v1.52e; https://imagej.net/Fiji) into numerical values for statistical analysis (Chim et al., 2020). The ilastik exported image segments were imported into Fiji through the ilastik plugin. Then, the Fiji scale was adjusted according to the magnification of the image. The parameters to measure (area and area fraction) were selected and limited to the threshold. The segments were analyzed using a newly generated macro shown in Figure A2.

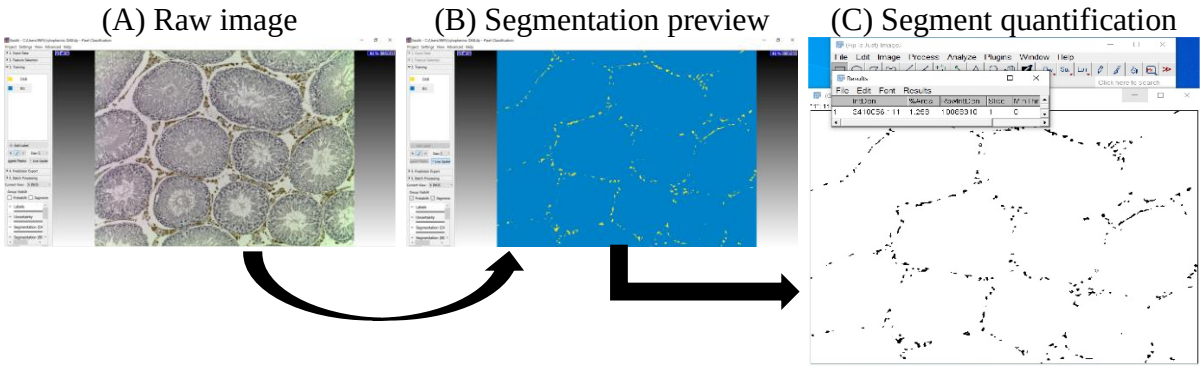


Figure A1: Representative image segmentation and quantification in ilastik and Fiji respectively for antibodies showing positive DAB staining in both cell nucleus and cytoplasm. Panel A shows an immunohistochemically DAB labeled image opened in ilastik, panel B illustrates a preview of the segmentation after adding annotations, and panel C show an ilastik exported image segment opened in Fiji displaying quantified DAB positive area.

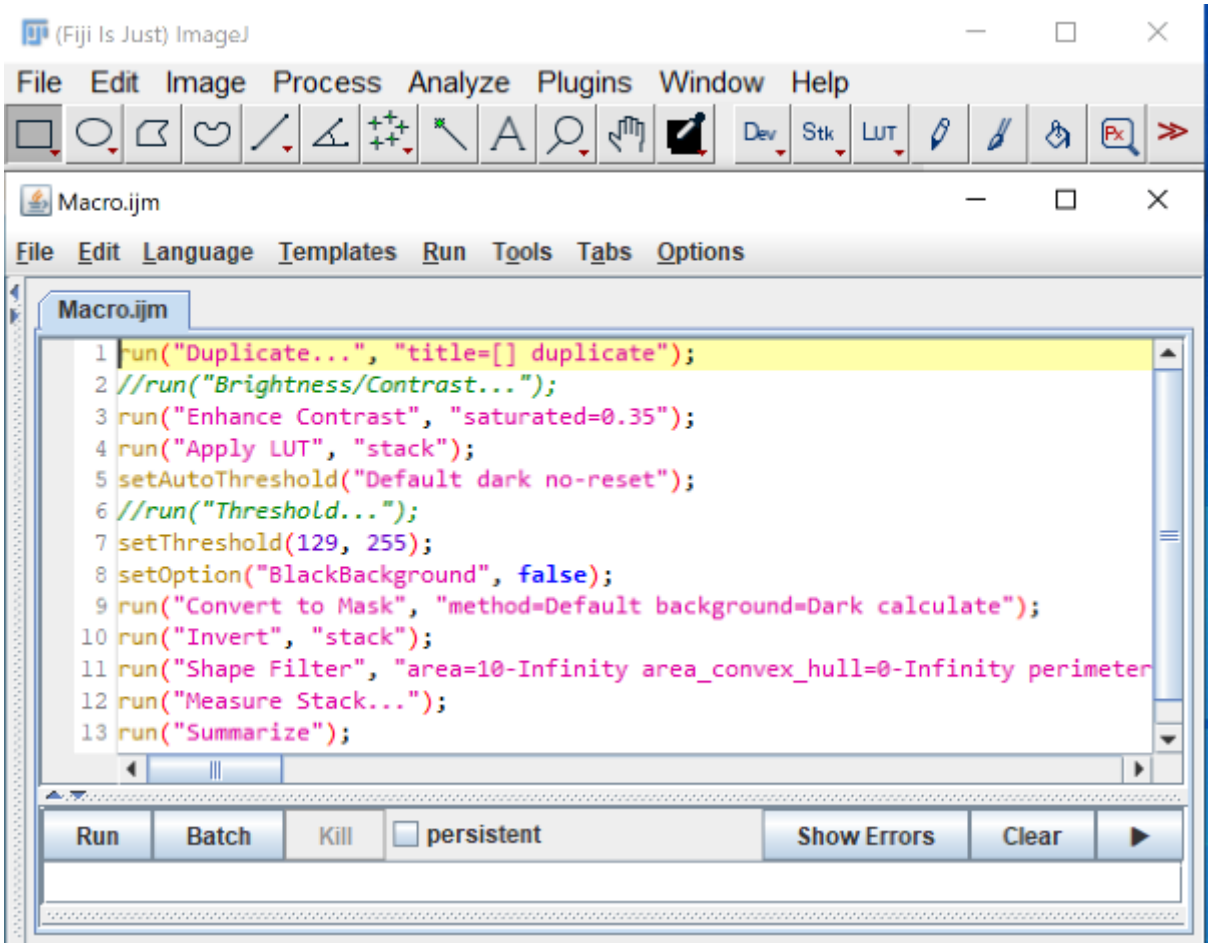


Figure A2: Generated macro showing the steps for quantifying image segments in Fiji.

CHAPTER 5: SECOND MANUSCRIPT

Androgen Receptor (AR) Depletion Underlies the Reproductive Dysfunctions in Male Rats Exposed to Alcohol and Combination Antiretroviral Therapy (cART)

ABSTRACT

The prevalence of alcohol abuse and HIV/AIDS is high in males of reproductive age. Unfortunately, a high incidence of alcohol intake has been reported in HIV/AIDS patients including those on combination antiretroviral therapy (cART). Incidentally, alcohol and cART use have each been implicated in male reproductive dysfunction. Therefore, the interactive effects of alcohol and cART on reproductive hormone levels, testicular connective tissue, and androgen receptor and Ki-67 expression were evaluated in HIV naïve adult male Sprague Dawley rats. Adult male rats were divided into four groups: control, alcohol (A), cART, and A+cART. The rats were terminated after 90 days of treatment. Blood and testis were extracted for the following laboratory analyses/assays; special staining for testicular connective tissue, immunoassay for reproductive hormones, and immunohistochemistry for androgen receptor and Ki-67. Study found significantly ($p<0.05$) increased thickness of seminiferous tubule basement membrane in cART group and testicular capsule in A+cART group. Collagen, reticulin, and elastin fibers decreased significantly in all treated groups, except for reticulin in testis of A group. With exception of luteinizing hormone in cART group, all treated groups had significantly elevated levels of luteinizing and follicle stimulating hormone, but no significant ($p>0.05$) difference was found in their testosterone and inhibin B levels. The number of Sertoli and Leydig cells expressing androgen receptor were significantly reduced in all treated groups, except for A group's number of Sertoli cells expressing androgen receptor. Further, in all treated groups Ki-67 expression significantly reduced relative to control. In this study, with exception of seminiferous tubule basement membrane, all study parameters were greatly altered in A+cART group. We suggest that the exacerbated androgen receptor depletion recorded in A+cART group might have led to the observed severe testicular structural alteration and spermatogenesis derangement.

Keywords: Alcohol, cART, HPG axis, Testis structure, Androgen receptor, and Ki-67.

INTRODUCTION

The high prevalence of combination antiretroviral therapy (cART) use (Khawcharoenporn and Sha, 2016) and alcohol abuse (World Health Organisation, 2011) in males of reproductive age has raised clinical concerns for male infertility. The Sub-Saharan Africa region is the world's epicenter of HIV/AIDs, with a daunting prevalence consistently reported in South Africa (Lippman et al., 2019). About 20% of the adult population is living with HIV in South Africa and thus, the use of cART is common (UNAIDS, 2019). Incidentally, the prevalence of alcohol abuse in people living with HIV/AIDS is alarming (Crane et al., 2017), and is reported to be more than twofold higher compared to that of the general populace (Necho et al., 2020), which points to both drugs being concomitantly present in the body. Moreover, alcohol and cART have each been shown to negatively impact the male reproduction system (Ogedengbe, Naidu and Azu, 2018; Ogedengbe et al., 2018).

Clinical studies have documented hypogonadism and feminization in male chronic alcoholics (Oremosu and Akang, 2015), and in people living with HIV/AIDS on a cART regimen (Wong et al., 2017). The most common encountered manifestations of male hypogonadism include low testosterone levels, gonadal atrophy, gynecomastia, and muscle wasting (Wong et al., 2017; Duca et al., 2019). However, hypogonadism symptoms may not be directly linked to hypothalamic-pituitary-gonadal (HPG) axis impairment, but could also result from disturbances of hormone-receptor interaction and/or partial or complete receptor insensitivity (Corradi et al., 2016). Importantly, testosterone, an androgen synthesized by the Leydig cells is essential for successful spermatozoa production (Bremner et al., 1994; O'Hara and Smith, 2015). The impact of testosterone is mediated via the androgen receptor (Petersen and Söder, 2006; Shah et al., 2021). However, testosterone is also involved in the regulation of androgen receptor expression (Wang et al., 2009; O'Hara and Smith, 2015; Mayer et al., 2018).

In the testis, androgen receptor is expressed in the nuclei of somatic cells viz. Leydig, Sertoli, myoid, and pericyte cells (Bremner et al., 1994; Shan et al., 1997; Basiri et al., 2016) and this receptor has been shown to regulate the structure and functions of these cells (Wang et al., 2009; O'Hara and Smith, 2015; Mayer et al., 2018). Sertoli cells' androgen receptor transduce the action of testosterone on spermatogenesis because germ cells do not express androgen receptor (O'Hara and Smith, 2015; Shah et al., 2021). Additionally, expression of androgen receptor by Sertoli cells is an indicator of the cells' maturity and is essential for formation of an effective blood-testis barrier that creates an immune-privileged microenvironment

necessary for successful spermatogenesis (Petersen and Söder, 2006; Kaur et al., 2014; Shah et al., 2021). Further, the myoid cells' androgen receptor expression is required for retinol processing, an essential factor for initiating spermatogonia differentiation (Mayer et al., 2018; Shah et al., 2021).

Thus, adequate reproductive hormone levels and hormone-receptor interactions are necessary for sufficient germ cell proliferation, differentiation, and maturation (Smith and Walker, 2014) and maintenance of testicular structural integrity (Wang et al., 2009; Mayer et al., 2018). Accordingly, the current study investigated the impact of alcohol and cART co-presence in the body on serum reproductive hormone levels, morphometry of testicular capsule, interstitial connective tissue fibers, and seminiferous tubule basement membrane, and testicular androgen receptors and Ki-67 expressions in male Sprague Dawley rats.

METHODS AND MATERIAL

Chemical and reagents

Atripla, a fixed-dose combination antiretroviral (cART) drug was purchased from Bristol-Myers Squibb and Gilead Sciences (Foster City, CA, USA) and androgen receptor rabbit monoclonal (ab105225) and Ki-67 rabbit polyclonal (ab15580) primary antibodies were purchased from Abcam (Cambridge, MA, USA). The biotinylated goat anti-rabbit (BA-1000) secondary antibody and Avidin-Biotin Complex kit (PK-6100) were purchased from Vector Laboratories (Burlingame, CA, USA). The ELISA kits for luteinizing hormone (LH; E-EL-R0026), follicle stimulating hormone (FSH; E-EL-R0391), testosterone (TT; E-EL-R0155), and inhibin B (E-EL-R1027) were purchased from Elabscience (Houston, Texas, USA).

Ethical clearance

The Animal Research Ethics Committee (AREC) of University of the Witwatersrand (Wits) approved the animal study protocol with approval number 2018/011/58/C. All experiments were carried out at Wits Animal Research Facility in accordance with the guidelines of AREC.

Animals

Twenty-four (24) adult male Sprague Dawley rats (10 weeks old) weighing between 330-370 grams were used. Since treatments were administered in drinking water (alcohol) and in gelatine cubes (cART), the rats were kept individually to ensure that each rat received the appropriate treatment dosage. The rats were housed in clean plastic cages with pinewood

shaving beddings at a room temperature of 21-23ºC, with a 12/12-hour light/dark cycle, and supplied with standard rat chow and water *ad libitum*.

Experimental design

The rats were divided into four groups, each with six rats: control group, which received no treatment; alcohol group (A), which received daily treatment of 10% v/v alcohol in drinking water (Dutra et al., 2017); cART group, received daily treatment of extrapolated human equivalent dose of 23.22mg/kg of cART (consisting of efavirenz 600 mg + emtricitabine 200 mg + tenofovir 245 mg) (Frampton and Croom, 2006) in gelatine cubes daily; and alcohol plus cART group (A+cART), which received both alcohol and cART daily. Rats were treated for 90 days, after which they were weighed, anesthetized with 240mg/ml pentobarbitone, and terminated. Blood was drawn through a cardiac puncture into a plain blood collection tubes. Thereafter, rats were perfused with 2 mL/min of 0.1-M phosphate buffer in 0.9% saline before extracting the testes. The testes were then preserved for subsequent processing in 10% neutral buffered formalin. Collected blood samples were left to clot, then centrifuged, and the serum was transferred into a new Eppendorf tube for storage at -80°C before immunoassay.

Gonadosomatic index

Final body and testis weights were used to calculate the gonadosomatic index, using the formula previously reported by Olasile et al., 2018.

$$\text{Gonadosomatic index} = \frac{Testis\ weight}{Body\ weight} \times 100\ (\%)$$

Immunoassay

Serum levels of reproductive hormones were quantified using enzyme linked immunosorbent assay (ELISA). A sandwich ELISA technique was used for luteinizing (LH), follicle stimulating hormone (FSH), and inhibin B, while a competitive ELISA technique was used for Testosterone (TT) assay. Before commencing the procedure, serum samples and all reagents were allowed to reach room temperature. Then, the wash buffer, standard working solutions, biotinylated detection antibody, and horseradish peroxidase conjugate were prepared for the assay according to the manufacturer's guidelines. A threefold sample dilution was used for the assay and standard and samples were run in duplicates (side by side). The assay procedure was carried out as follows. In the case of sandwich (i.e., LH, FSH, and inhibin B), a volume of 100 µL for the standards and samples was carefully added to the bottom of the respective plate wells. Then, the plates were sealed and incubated at 37°C for 90 min. After that, the solution was decanted from the wells, and without washing the plate, 100 µL of the biotinylated

detection antibody working solution was added to each well. Afterward, the plate was sealed and incubated at 37°C for 60 min. Whereas in the competitive technique for TT assay, a volume of 50 µL for standards and samples was carefully added to the bottom of the respective plate wells, and immediately 50 µL of biotinylated detection antibody working solution was added to each well. Subsequently, the plate was sealed and incubated at 37°C for 45 min. Thereafter, the subsequent steps were similar for both techniques. After incubation, the solution was decanted from the wells before three cycle washing step. The plate was placed in a microplate washer, 350 uL of wash buffer was added to each well and allowed to soak for 60 sec per cycle. Subsequently, 100 µL of horseradish peroxidase conjugate working solution was added to each well, the plate was sealed and incubated at 37°C for 30 min. Then, the solution was decanted from the wells, and the wash step was conducted as above for five cycles. Next, 90µ of substrate reagent was added to each well, the plate was sealed, wrapped in aluminum foil (to protect it from light), and gently shaken before incubation at 37°C for 15 min. Followed by immediate addition of the stop solution to each well of the plate. The plate was put on a micro-plate reader set at 450 nm filter to measure the optical densities (OD). The microplate reader was set up according to the user's manual guidelines and preheated for 15 minutes before measuring the optical densities. The average OD values for standards and samples were calculated. Then, the average OD for standard zero was subtracted from the average OD for standards and samples. A standard curve was plotted with the standard concentration and OD values. The average OD values for each sample (y-axis) were used to determine the corresponding concentration of TT, LH, FSH, and inhibin B from the standard curve (x-axis). The exact concentration was obtained by multiplying the concentration read off the standard curve with the sample dilution factor.

Histo-morphometric analyses

Special histology stains for testicular connective tissue

The fixed testis tissue was dehydrated in a series of 70-100% alcohol grades, embedded in molten paraffin wax, and sections of 5µm thickness were cut. Testicular tissue sections were stained with periodic acid Schiff (PAS) (for basement membrane), Masson's Trichrome (for capsule and collagen), Gordon and Sweet's silver impregnation (for reticulin), and Gomori's Aldehyde Fuchsin (for elastin). Stained testis sections were examined using the Axioskop 2 plus light microscope (Nikon Eclipse Ci, 104C type) and photomicrographs captured with the linked computerized Zeiss digital image system, the AxioCam 208 color (Zeiss group, Oberkochen, Germany) for quantification.

Measurement of seminiferous tubule basement membrane (STBM)

Photomicrographs of PAS-stained sections were captured at x400, and Fiji software was used to measure the thickness of the basement membrane. The thickness of STBM was measured at two points in 50 randomly selected tubules for each rat (i.e., 300 tubules per group) (Omar et al., 2018).

Evaluation of testicular capsule thickness

The capsule thickness was measured on Masson's Trichrome stained sections using Fiji software. Photomicrographs of six fields from the free surface of the capsule were captured at x400, and three points were measured on each field (i.e., 18 measurements for each rat, 108 per group) (Aire and Ozegbe, 2007).

Interstitial connective tissue quantification

Components of testicular connective tissue i.e., collagen, reticulin, and elastin fibers were quantified in photomicrographs of sections stained with Masson's Trichrome, Gordon and Sweet's silver impregnation, and Gomori's Aldehyde Fuchsin techniques respectively. Collagen, reticulin, and elastin fibers were quantified in 24 microscopic fields captured at x100 for each rat (i.e., 144 fields per group).

Image processing for connective tissue quantification

The connective tissue images were segmented using ilastik (v1.3.3; https://www.ilastik.org) and subsequently quantified in Fiji software (v1.52e; https://imagej.net/Fiji). Figure 5.1 illustrates the image processing procedure.

Image segmentation

The image was divided into fibers and background using the Ilastik pixel classification technique (Berg et al., 2019; Chim et al., 2020). Briefly, eight sample photos were used to train pixel classifiers (two images per animal group). The classification algorithms included the available features, such as intensity/color, texture, and edge at a sigma of 0.3–10 pixels. Collagen, reticulin, and elastin were appropriately annotated in a few spots of the image (yellow color) to train the classifier. The background, which represents spaces that are not covered by fibers, was then annotated (blue color) (Fig. 5.1). The predictions were inspected after adding each annotation, the photos were zoomed out to allow more precise placement of annotations. All training photos were then given annotations to improve the classifier and make

it more applicable to huge image sets. Once the prediction was of a good standard across the sample images, the trained classifier was applied to training naïve images and their simple segmentations were exported for quantification.

Image quantification

The ilastik plugin was used to import the produced image segments from ilastik into Fiji so that they could be quantified into numbers for statistical analysis (Fig. 5.1) (Lucero et al., 2016; Chim et al., 2020). The Fiji scale was modified in accordance with the image's magnification. Area, integrated density, and area fraction were chosen as the measurement parameters and were restricted to the threshold. The connective tissue fibers were then quantified in a macro mode (see Appendix). The percentage area occupied by the connective tissue fibers (collagen, reticulin, and elastin) was calculated as follows.

$$\% \text{ Area} = \frac{area\ of\ connective\ fiber}{total\ area\ of\ photomicrograph} x100$$

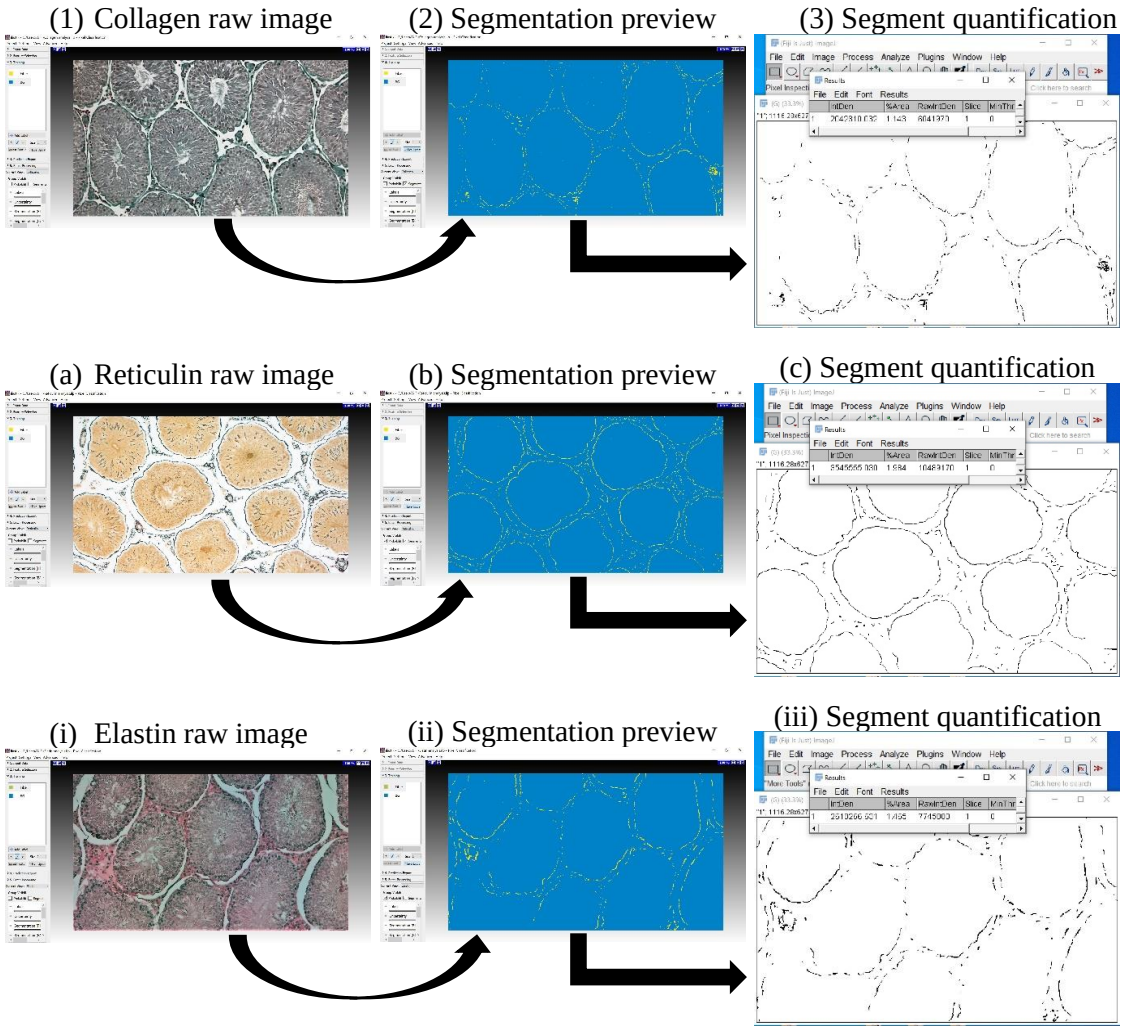


Figure 5.1: Representative connective tissue image segmentation and quantification in ilastik and Fiji respectively. The fibers for collagen, reticulin, and elastin were stained using Masson's Trichrome, Gordon and Sweet's silver impregnation, and Gomori's Aldehyde Fuchsin staining technique respectively. Panels 1, a, and i respectively show raw images of collagen, reticulin, and elastin open in ilastik. Preview of image segmented into fibers and background after adding annotations are demonstrated in panels (2, b, and ii). The respective exported image segments opened in Fiji displaying quantified respective fibers are shown in panels 3, c, and iii.

Immunohistochemistry (IHC) for androgen receptor and Ki-67

Testicular tissue sections of 5μm thickness were mounted onto saline-coated slides and immunolabeled with androgen receptor and Ki-67 antibodies. For antigen retrieval, the sections were treated in citrate buffer pH 6 overnight in a water bath at 60^{o}c. The endogenous peroxidase was then blocked for 20 minutes with 1% hydrogen peroxide in methanol. The sections were then rinsed in phosphate buffered saline (PBS) before being treated with 5% normal goat serum to prevent nonspecific antibody binding. After 30 minutes, the normal goat serum was tapped off, subsequently, the primary antibody was added (1:100 for anti-androgen receptor and 1:1000 for anti-Ki-67) and then left at 4°C overnight (approximately 16 hours). Thereafter, the sections were rinsed in PBS and incubated with a 1:1000 biotinylated goat anti-rabbit secondary antibody for 30 minutes. Then, after rinsing in PBS, avidin-biotin complex reagent was added for 30 minutes. Afterward, the sections were rinsed in PBS and incubated with 3, 3'-diaminobenzidine tetrachloride (DAB) for five minutes. DAB was then washed off under running tap water for five minutes and the slides were immersed in hematoxylin for one minute, followed by five minutes of washing with running tap water and dehydrating in a series of alcohol. Dibutylphthalate Polystyrene Xylene was put on the section along with the coverslip. For each antibody, two control slides were included; one without the primary and the other without the secondary antibody. The number of Leydig cells expressing androgen receptor immunoreactivity was counted in 20 microscopic fields at x400 for each animal (i.e., 120 fields for each group). The number of Sertoli cells expressing androgen receptor immunoreactivity and germ cells expressing Ki-67 immunoreactivity were counted in 20 rounded stages II-VII seminiferous tubules (Bremner et al., 1994) for each animal (i.e., 120 tubules per group).

Data analysis

Data analysis was done using the Windows version of GraphPad Prism 6 and the results are presented as Mean ± SEM. One-way analysis of variance was used to compare the group

means, and the Bonferroni *post hoc* test was performed afterward. A P-value of < 0.05 was deemed statistically significant.

RESULTS

Gonadosomatic index

The study results showed that gonadosomatic index was not significantly different in rats across the treatment groups (Table 5.1).

Table 5.1: Mean gonadosomatic index (GSI) and serum levels of reproductive hormones for rats treated with alcohol, cART, and both.

Animal groups	Control	Alcohol (A)	cART	A+cART
Gonadosomatic index (GSI) (%)	0.37±0.03[a]	0.37±0.02[a]	0.36±0.03[a]	0.38±0.02[a]
Reproductive hormones				
Luteinizing hormone (mIU/mL)	67.23±8.98[a]	109.9±9.76[b]*	82.16±5.38[a]*	112.9±4.03[b]
Follicle stimulating hormone (ng/mL)	69.94±8.80[a]	129±5.26[b]	127.2±16.52[b]	118.2±12.09[b]
Testosterone (ng/mL)	2.83±0.46[a]	2.66±0.49[a]	2.19±0.59[a]	2.14±0.04[a]
Inhibin B (pg/mL)	72.74±6.23[a]	71.78±3.92[a]	74.67±1.69[a]	69.16±4.74[a]

For all parameters: Values in the same row with similar superscripts are not significantly different whilst values in the same row with different superscripts are significantly different ($p<0.05$) except when the different superscripts are both marked with an asterisk (*). A, alcohol; cART, combination antiretroviral therapy; A+cART, alcohol and combination antiretroviral therapy.

Reproductive hormone levels

An increase in serum concentration of luteinizing and follicle stimulating hormones was observed in all treated groups compared to the control (Table 5.1). The luteinizing hormone concentration in A and A+cART groups significantly increased compared to control ($p=0.0072$ and $p=0.0027$ respectively). Further, the luteinizing hormone concentration in A+cART group increased significantly ($p=0.0043$) compared to cART, whilst follicle stimulating hormone significantly increased in all treated (A, cART, and A+cART) groups compared to control, ($p=0.0043$, $p=0.0200$, and $p=0.0266$ respectively). In comparison with the control group, the decrease in serum levels of testosterone and the difference in inhibin B levels of all treated groups were insignificant ($p>0.05$).

Seminiferous tubule basement membrane (STBM) thickness

The basement membrane surrounding the seminiferous tubule was identified as a thin periodic acid Schiff (PAS)-positive staining sheet-like structure with a single layer of flat elongated cells, the myoid cells (Fig. 5.2). Further, positive PAS staining was as well observed in elongated spermatids and some Leydig cells. The testis of rats from the control showed a smooth contoured basement membrane, while the basement membranes of testis from rats treated with alcohol, cART, and A+cART was slightly wavy. The STBM thickness was significantly increased ($p<0.0001$) in cART treated animals compared to control and treated groups A and A+cART (Fig. 5.2). In A and A+cART treated groups, the STBM thickness reduced non-significantly when compared to the control group.

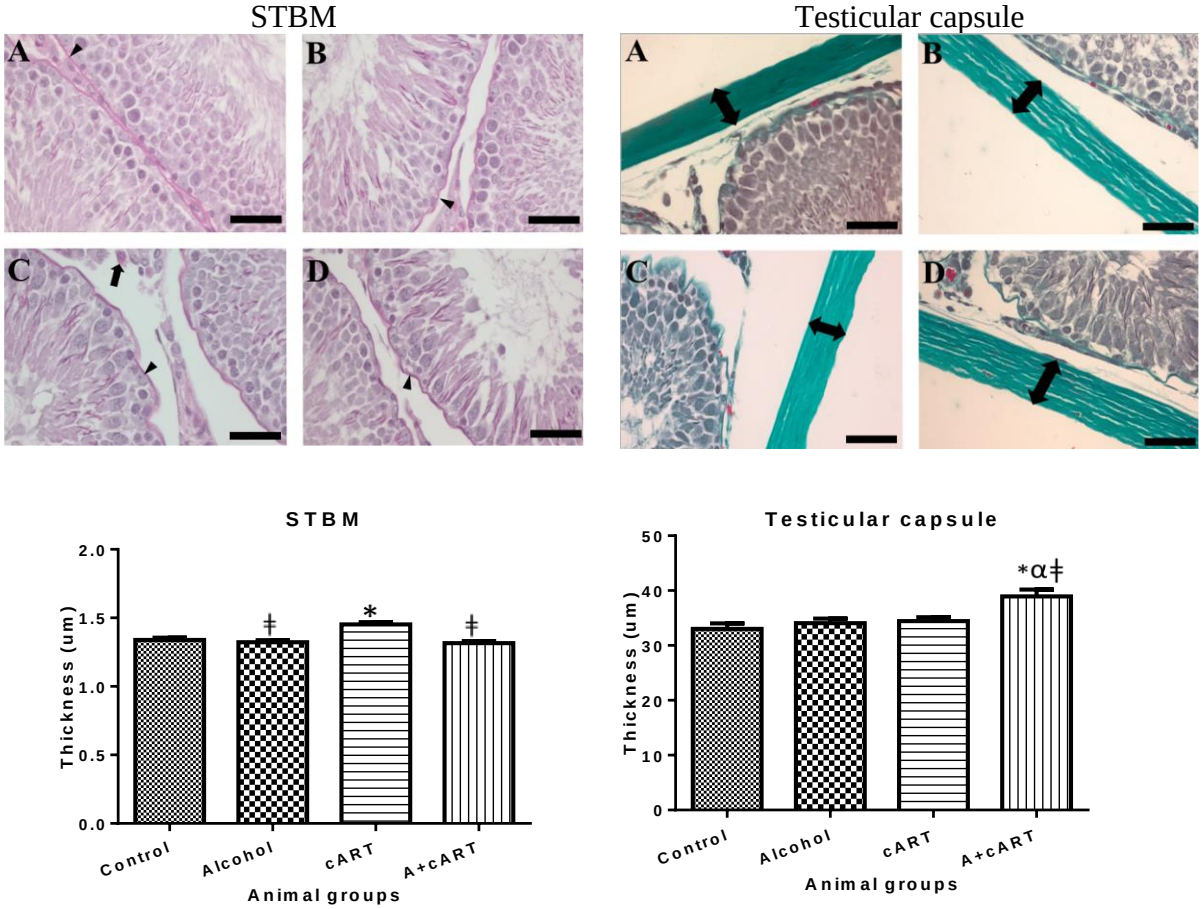


Figure 5.2: Representative seminiferous tubule basement membrane (STBM) (arrowheads) and testicular capsule (double arrows) photomicrographs, PAS and Masson's Trichrome stain respectively. Leydig cell PAS positive (thick arrow) shown in a cART photomicrograph. Graphs show respective mean thickness. Different symbols *, α, and ǂ represent significant differences ($p<0.05$) as analyzed by a Bonferroni's multiple comparison test; '*' significantly increased compared to control, 'α' significantly increased compared to alcohol (A), and 'ǂ' significantly different compared to cART. Magnification, x400; scale bar, 50µm. Key: Image:

A; control group, B; alcohol group, C; cART group, and D; A+cART group. A, alcohol; cART, combination antiretroviral therapy; A+cART, alcohol and combination antiretroviral therapy.

Capsule thickness

The testicular capsule also referred to as the tunica albuginea comprised of majorly collagen fibers braced with a network of myoid cells (Fig. 5.2). Thickness of the capsule was increased across all the treated groups compared to the control, but a significant increase ($p=0.0001$) was only recorded in testis of A+cART treated group. Further, capsule thickness of A+cART treated group was significantly increased compared to alcohol and cART groups, $p=0.0023$ and $p=0.0064$; respectively (Fig. 5.2).

Interstitial connective tissue

The interstitial connective tissue found between seminiferous tubules and surrounding the tubules consisted of collagen, reticulin, and elastin fibers (Fig. 5.3). A general decrease was recorded in connective tissue components of the treated groups relative to control group. Collagen content in treated groups A, cART, and A+cART significantly reduced relative to control, $p=0.0176$, $p<0.0001$, and $p<0.0001$; respectively. Further, collagen in cART group was significantly decreased compared to A ($p<0.0001$) and A+cART ($p=0.0225$). A significant reduction in reticulin fibers was found in cART and A+cART treated groups compared to control ($p=0.0154$ and $p<0.0001$ respectively), whilst reticulin of A+cART group was significantly reduced compared to A ($p<0.0001$) and cART ($p=0.0004$) treated groups. In comparison with the control group, elastin was significantly reduced in all treated groups, (A: $p=0.0144$, cART: $p=0.0338$, and A+cART: $p=0.0010$) (Fig. 5.3).

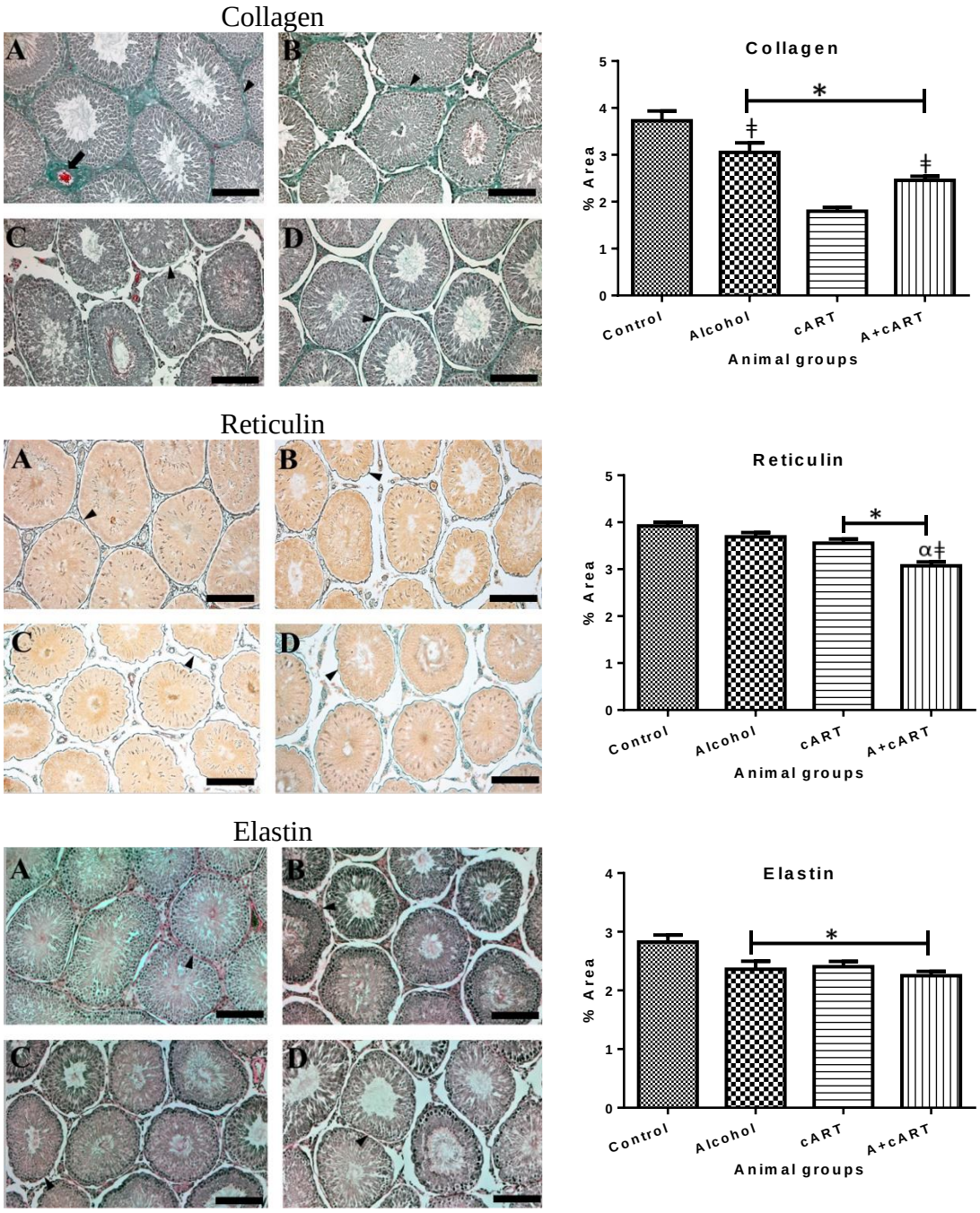


Figure 5.3: Representative collagen, reticulin, and elastin indicated with arrowheads in photomicrographs, Masson's Trichrome, Gordon and Sweet's silver impregnation, and Gomori's Aldehyde Fuchsin stain respectively. A thick arrow indicating a blood vessel is shown in the collagen photomicrograph, panel A. Graphs show respective mean percentage areas. Different symbols *, α, and ǂ represent significant differences ($p<0.05$) as analyzed by a Bonferroni's multiple comparison test; '*' significantly decreased compared to control, 'α' significantly decreased compared to alcohol (A), and 'ǂ' significantly different compared to cART. Magnification, x100; scale bar, 200µm. Key: Image: A; control group, B; alcohol group,

C; cART group, and D; A+cART group. A, alcohol; cART, combination antiretroviral therapy; A+cART, alcohol and combination antiretroviral therapy.

Immunohistochemistry for androgen receptor and germ cell proliferation (Ki-67)

Androgen receptor

In all groups, nuclei of Sertoli, Leydig, pericytes, and myoid cells were positively immunostained with androgen receptor antibody (Fig. 5.4). Noteworthy, germ cells did not show positive immunostaining for androgen receptor either in their cytoplasm or nucleus. The number of Sertoli cells expressing androgen receptor significantly decreased in cART and A+cART treated groups compared to control ($p<0.0001$ for both) and A ($p=0.0025$ and $p<0.0001$; respectively). Further, the number of Sertoli cells expressing androgen receptor in A+cART group decreased significantly compared to cART ($p=0.0195$). But the number of Leydig cells expressing androgen receptor reduced significantly in all treated groups compared to the control, (A: $p=0.0438$, cART: $p<0.0001$, and A+cART: $p<0.0001$). In addition, Leydig cells expressing androgen receptor in cART and A+cART treated groups decreased significantly compared to A ($p=0.0164$ and $p<0.0001$). However, the number of Leydig cells expressing androgen receptor in A+cART was significantly decreased compared to cART ($p=0.0007$) (Fig. 5.4).

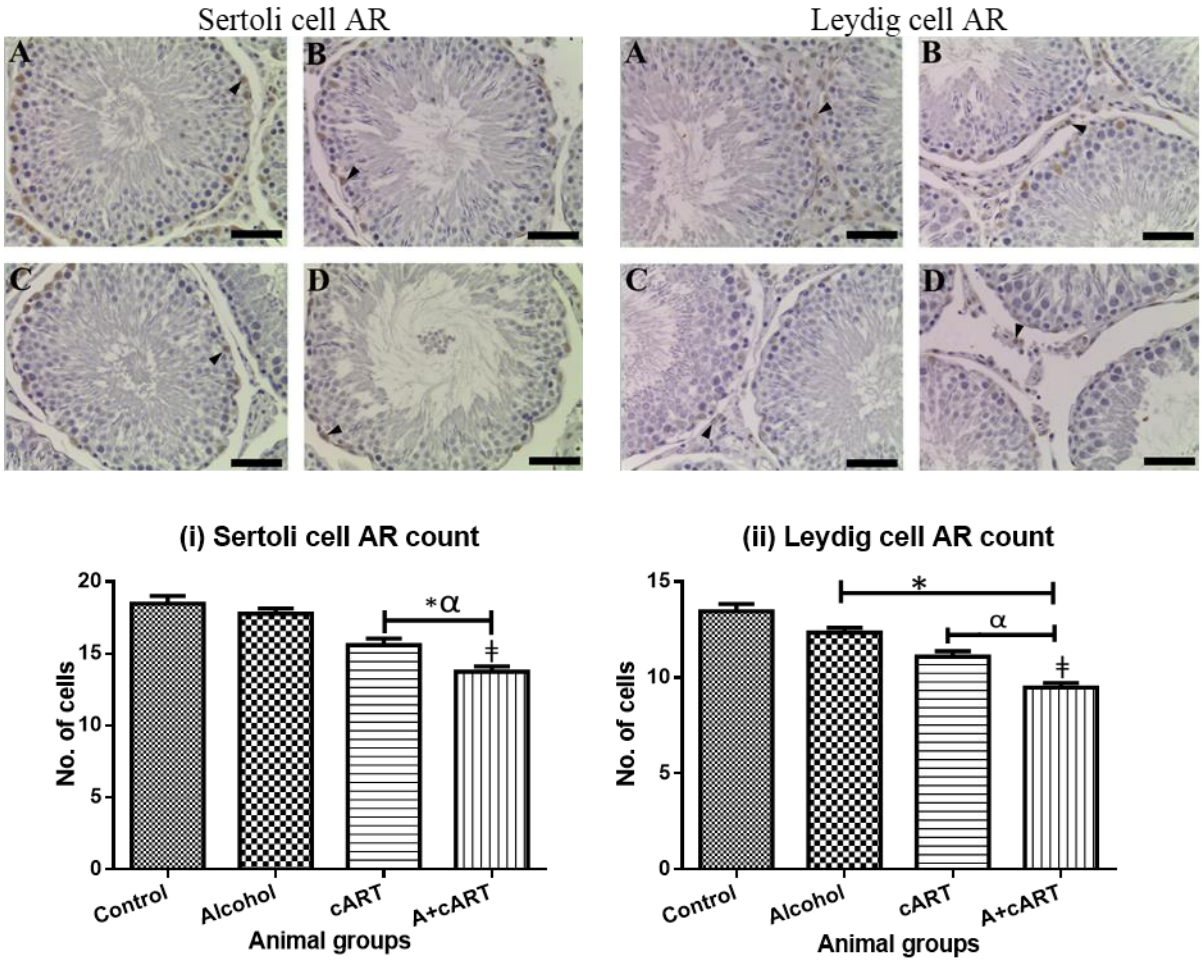


Figure 5.4: Representative photomicrographs showing Sertoli and Leydig cell androgen receptor (AR) immunoreactivity (arrowheads) and respective mean number of immunoreactive cells graphs. Different symbols *, α, and ǂ represent significant differences ($p<0.05$) as analyzed by a Bonferroni's multiple comparison test; '*' significantly decreased compared to control, 'α' significantly decreased compared to alcohol (A), and 'ǂ' significantly decreased compared to cART. Magnification, x400; scale bar, 50μm. Key: Image: A; control group, B; alcohol group, C; cART group, and D; A+cART group. A, alcohol; cART, combination antiretroviral therapy; A+cART, alcohol and combination antiretroviral therapy.

Germ cell proliferation (Ki-67)

Proliferation marker Ki-67 was expressed mainly in spermatocytes and round spermatids across the animal groups. The number of germ cells expressing Ki-67 reduced significantly in all treated groups compared to the control group; A: p=0.0129, cART: p=0.0046, and A+cART: p=0.0002 (Fig. 5.5).

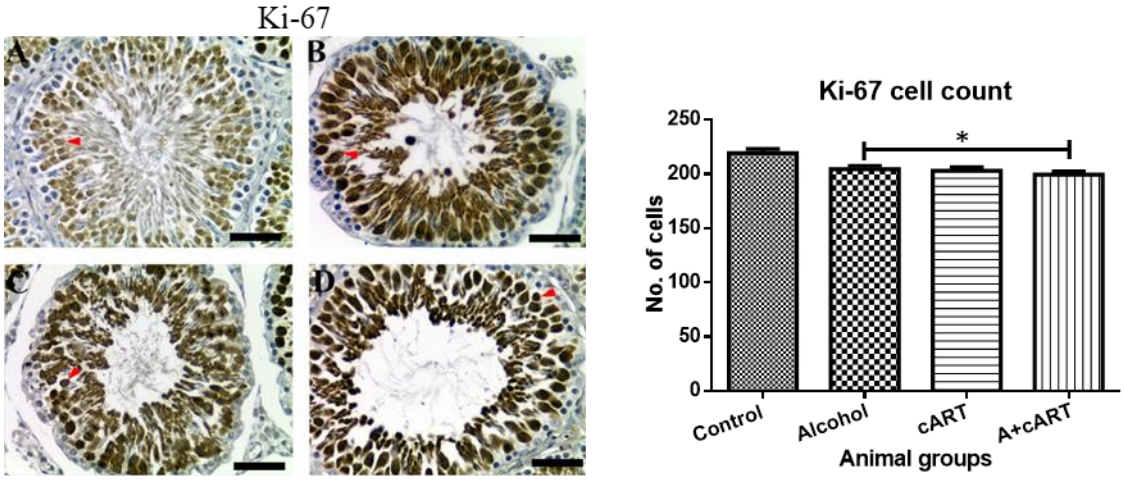


Figure 5.5: Representative photomicrographs showing Ki-67 immunoreactivity (arrowheads) and a graph of the mean number of immunoreactive cells. The symbol * represent significant difference ($p<0.05$) as analyzed by a Bonferroni's multiple comparison test; '*' significantly decreased compared to control. Magnification, x400; scale bar, 50µm. Key: Image: A; control group, B; alcohol group, C; cART group, and D; A+cART group. A, alcohol; cART, combination antiretroviral therapy; A+cART, alcohol and combination antiretroviral therapy.

DISCUSSION

The processes involved in testis development, spermatogenesis, and steroidogenesis are tightly regulated by the hypothalamic-pituitary-gonadal (HPG) axis hormones, i.e. luteinizing hormone (LH), follicle-stimulating hormone (FSH), and testosterone (TT) (Marques et al., 2000; Corradi et al., 2016). These hormones work via respective receptors present in the testicular somatic cells and are controlled through a negative feedback mechanism (Oremosu and Akang, 2015; Clavijo and Hsiao, 2018). The LH and FSH receptors are exclusively present in the Leydig and Sertoli cells respectively (Marques et al., 2000; Gurung and Jialal, 2019), while the TT receptors, also known as the androgen receptors (AR), are expressed by Leydig, Sertoli, myoid, and pericyte cells (Shan et al., 1997; Basiri et al., 2016). Though changes in levels of reproductive hormones have been studied extensively in several male reproductive dysfunctions, investigations about the changes in their respective receptors are scanty. Nevertheless, reproductive hormone receptor resistance, receptor reduction, or both, including changes in reproductive hormone levels are major contributing factors for male reproductive dysfunctions and infertility (Petersen and Söder, 2006; Corradi et al., 2016).

In this study, we observed a significantly elevated LH levels in alcohol and A+cART treated groups and FSH in all treated groups, but no significant changes were detected in levels of TT

and inhibin B relative to control. Similar results of enhanced LH and FSH levels with serious adverse impacts on reproductive male parameters have been reported following alcohol abuse (Muthusami and Chinnaswamy, 2005). Furthermore, decreased or normal TT levels together with elevated gonadotropins (LH and FSH) levels, similar to the present result, are associated with poor sperm quality and azoospermia (Zhao et al., 2020). However, contrary to our findings, a previous report (Oremosu and Akang, 2015) indicated a reduction in LH, FSH, and TT levels in rats treated with alcohol. Discrepancies in reports also exist on the impact of cART on reproductive hormones levels, with some studies showing no significant changes (Ogedengbe et al., 2018), decreased levels (Akhigbe, Hamed and Odetayo, 2021), and increased levels (Collazos et al., 2002; Olojede et al., 2022). In this study, rats treated with cART had significantly increased FSH levels, an insignificant increase in LH and inhibin B levels, but TT level was insignificantly decreased. The conflicting results could be due to the different doses and durations of the treatments, and the different drug component combinations in the case of cART studies.

Notably, normal germ cell development requires a well-balanced interplay between reproductive hormones of the HPG axis, gonadotropins (LH and FSH) and testicular hormones (TT and inhibin B) (Corradi et al., 2016). Consequently, alteration in the negative feedback mechanism signals would lead to hormonal imbalance and subsequently affect the processes and progress of spermatogenesis (Clavijo and Hsiao, 2018). The negative feedback mechanism for gonadotropin releasing hormone (GnRH) and LH production by the hypothalamus and pituitary respectively is modulated by TT (Marques et al., 2000; Corradi et al., 2016). Inhibin B, a gonadal peptide hormone synthesized by Sertoli cells is responsible for the FSH feedback regulation (Petersen and Söder, 2006; Clavijo and Hsiao, 2018). Therefore, the observed significant elevations of LH and FSH with unaltered TT and inhibin B levels in treated rats could have resulted from a disruption in the feedback mechanism, which invariably will lead to dysregulation of spermatogenesis. Additionally, the hormonal imbalance might result from a hormone-receptor resistant state due to a decrease in androgen receptors and/or sensitivity, which is characterized by elevated LH levels and normal or increased TT (Hughes et al., 2012; Corradi et al., 2016).

Since germ cells do not express androgen receptors, the impact of TT on spermatogenesis is mediated via Sertoli cells' androgen receptors (Petersen and Söder, 2006; Smith and Walker, 2014; O'Hara and Smith, 2015). We found a significant decrease in the number of Sertoli cells

expressing androgen receptors in the testis of animals treated with cART and A+cART. This implies a dysfunction of androgen receptors, which subsequently leads to spermatogenesis failure. Also, previous studies have linked depletion of androgen receptors to male infertility (O'Hara and Smith, 2015) and increased risk of germ cell malignancy (Barros et al., 2021). Although the expression of androgen receptors following alcohol or/and cART has not been widely reported, one study found a weak androgen receptors expression in the testis of animals treated with cART (Ismail et al., 2017). Other toxic chemicals such as organochlorinated pesticides, industrial chemicals, and plasticizers have been shown to diminish the number and action of androgen receptors (Luccio-Camelo and Prins, 2011). A study by Qiu et al., (2013) reported significantly decreased androgen receptor expression in the testis of rats exposed to bisphenol A. Further, in *vivo* studies in male mice have demonstrated testicular feminizing syndrome (characterized by microphallus penis, urethral hypospadias, small undescended testes, labia majora-like scrotal sac, and absence of vas deferens, epididymis, seminal vesicle, and prostate) following androgen receptor knockout (Yeh et al., 2002; Wang et al., 2009).

Conversely, a reduction in androgen receptors points to a disruption in the regulatory activity of testosterone on spermatogenesis. However, a non-significant decrease in the number of Sertoli cells expressing AR recorded in the testis of rats treated with only alcohol could be the underlying mechanism for the restoration of testicular function when alcohol abuse is discontinued. Previous human and animal studies have reported restoration of normal spermatogenesis after abstaining from alcohol (Dosumu et al., 2014; Guthauser et al., 2014). Furthermore, androgen receptor regulates the function and structure of the cells such as Leydig, Sertoli, myoid, and pericyte cells, which are involved in the regulation of spermatogenic process (Shan et al., 1997; Wang et al., 2009; Mayer et al., 2018).

Remarkably, androgen receptors expression modulates Sertoli and myoid cell secretory function (Pöllänen et al., 1985; Mayerhofer, 2013), including secretion of components of connective tissue and tubule basement membrane such as collagen and laminin (Petersen and Söder, 2006; Mayer et al., 2018). We observed a general increase in testicular capsule and seminiferous tubule basement membrane thickness of the treated groups compared to the control, but a significant increase in these parameters was only recorded in A+cART and cART treated animals respectively. Such increases may suggest structural alterations induced by treatments, which will lead to capsular and seminiferous tubule basement membrane dysfunctions (Ogedengbe et al., 2016; Olasile et al., 2018). These changes complement the

decrease in the components of connective tissue (collagen, reticulin, and elastin) recorded in testis of all treated animals. Consistent with our findings, earlier studies reported deleterious effects of alcohol (Asuquo et al., 2020) and cART (Olojede et al., 2021) on the testicular capsule. Studies by Ogedengbe et al., (2016) and Olasile et al., (2018), found distorted and thickened seminiferous tubule basement membrane in cART treated animals. Further, changes in collagen (Shayakhmetova et al., 2013) and absence of reticulin fibers (Fakoya and Ademola Caxton-Martins, 2004) have been demonstrated in rats exposed to alcohol. Testicular connective tissue, including the capsule, interstitial tissue, and seminiferous tubule basement membrane play a crucial role in maintaining testicular structural integrity and functioning and also enable spermatozoa propulsive movement to the rete testis (Aire and Ozegbe, 2007; Fleck et al., 2021). This is a crucial function in the reproductive process, and is attributed to the contractility of myoid cells (Mayerhofer, 2013; Fleck et al., 2021). Conversely, the alterations recorded in these parameters in treated groups suggest testicular toxicity and spermatogenesis failure.

Associated with the normal physiology and integrity of the testicular structure, is the constant cell division and germ cell proliferation for continuous sperm production. Thus, the germ cells at different stages of spermatogenesis express a nucleus-associated proliferation marker, the Ki-67 (Zhao et al., 2018) that regulates the cell cycle and chromosomal structure and integrity (Cuylen-Haering et al., 2020). Consistent with previous reports on testicular toxicity (Moon et al., 2014; Zhao et al., 2018), a significant decrease in the number of germ cells expressing Ki-67 was recorded in all the treated groups relative to control. This suggests impaired testicular germ cell proliferation which ultimately translate to diminished spermatozoa production.

CONCLUSIONS

This study demonstrated that exposure to alcohol, combination antiretroviral therapy (cART), or both disrupts the HPG axis function and testis structure integrity, leading to testicular dysfunction. The treated animal groups showed alteration in reproductive hormone levels, seminiferous tubule basement membrane and testicular capsule thickness, interstitial connective tissue fibers (collagen, reticulin, and elastin), and Sertoli and Leydig cell androgen receptor and germ cells Ki-67 expression. With exception of seminiferous tubule basement membrane thickness, all the observed changes were exacerbated in the animals treated with both alcohol and cART (A+cART group), implying a severe impact of alcohol and cART concurrent use on the male reproductive function. Further, our findings suggest that depletion

of androgen receptors might be an underlying mechanism for inducing testis structure and spermatogenesis impairments by chemical insults (alcohol or/and cART). Therefore, the study results may be clinically invaluable in the management of male sexual insufficiency and reproductive failure, especially in HIV/AIDS positive individuals on cART regimen and who drink alcohol regularly.

APPENDIX

Macro script for connective tissue fibers quantification

(a). run("Duplicate...", "title=[] duplicate");

(b). //run("Brightness/Contrast...");

(c). run("Enhance Contrast", "saturated=0.35");

(d). run("Apply LUT", "stack");

(e). setAutoThreshold("Default dark no-reset");

(f). //run("Threshold...");

(g). setThreshold(129, 255);

(h). setOption("BlackBackground", false);

(i). run("Convert to Mask", "method=Default background=Dark calculate");

(j). run("Invert", "stack");

(k). run("Shape Filter", "area=10-Infinity area_convex_hull=0-Infinity perimeter=0-Infinity perimeter_convex_hull=0-Infinity feret_diameter=0-Infinity min._feret_diameter=0-Infinity long_side_min._bounding_rect.=0-Infinity short_side_min._bounding_rect.=0-Infinityaspect_ratio=1-Infinity area_to_perimeter_ratio=0-Infinity circularity=0-Infinity elongation=0-1 convexity=0-1 solidity=0-1 num._of_holes=0-Infinity thinnes_ratio=0-1 contour_temperatur=0-1 fractal_box_dimension=0-2 option->box-sizes=2,3,4,6,8,12,16,32,64 draw_holes stack");

(l). run("Measure Stack...");

(m). run("Summarize").

CHAPTER 6: THIRD MANUSCRIPT

Impact of Concurrent Exposure of Diabetic male Sprague Dawley rats to Alcohol and Combination Antiretroviral Therapy (cART) on Reproductive Capacity: Evaluation of Testicular Histomorphology, Hormonal Profile, and Androgen Receptor Expression

ABSTRACT

Prevalence of diabetic patients on cART therapy and with alcohol abuse is rising in the society. Data on the impact of diabetes mellitus with concurrent exposure to alcohol and cART on testicular health and male reproductive viability is scarce and therefore was evaluated. Thirty, 10 weeks old male Sprague Dawley rats were distributed into five groups of six rats each; control, diabetic only (DM), diabetic treated with alcohol (DM+A), diabetic treated with cART (DM+cART), and diabetic treated with both alcohol and cART (DM+A+cART). After 90 days of treatment, rats were terminated, and blood and testes were harvested for immunoassay, histological, and immunohistochemistry analyses. All treated groups showed alteration in testis and seminiferous tubule morphometry, spermatogenic, Sertoli, and Leydig cells. Further, a significant decrease in Johnsen's testicular score, seminiferous tubule lesions, changes in the basement membrane and capsule thickness, and reduction of testis connective tissue fibers were demonstrated in treated groups. Also, reproductive hormone levels were altered and the number and staining intensity of Sertoli and Leydig cells expressing androgen receptor reduced significantly in all treated rats. The study results revealed that consumption of alcohol or/and cART in diabetic condition induces derangement in circulating reproductive hormone levels and in testicular structure and function which may underscore the declining male reproductive capacity.

Keywords: Testicular structure, HPG axis, Diabetes mellitus, Alcohol abuse, Antiretroviral therapy

INTRODUCTION

A decline in male fertility is increasingly becoming a global concern (Sun et al., 2019) and is associated with rising incidences of obesity, drug abuse, non-communicable diseases (NCDs), and environmental toxins (Khawcharoenporn and Sha, 2016; Mann, Shiff, et al., 2020). Diabetes mellitus (DM) is a chronic disorder of blood glucose dysregulation, marked by persistent hyperglycemia (Cho et al., 2017). DM is one of the most common NCD globally and has emerged as a public health burden in sub-Saharan Africa (Pheiffer et al., 2018). In South Africa, the prevalence of DM has almost doubled since 2017 from 5.4% to the current 11.3% (Cho et al., 2017). The fast-rising incidence of DM has been linked to the predominance of high carbohydrate staple food, obesity, and excessive alcohol consumption (Pheiffer et al., 2018). Additionally, more than 33% of the South African population consumes alcohol regularly (Vellios and van Walbeek, 2018). Unfortunately, the country is also faced with a high prevalence of human immunodeficiency virus/acquired immunodeficiency syndrome (HIV/AIDS), with almost 20% of the adult population living with HIV/AIDS, warranting an extensive use of combination antiretroviral therapy (cART) (UNAIDS, 2019).

Incidentally, an increased number of males within reproductive age are impacted with diabetes (Condorelli et al., 2018), alcohol abuse (World Health Organisation, 2011), and cART regimen (Khawcharoenporn and Sha, 2016). Moreover, an intricate connection exists among these conditions, for instance, alcohol is a recognized risk factor for diabetes (Goecke and Baumeister, 2021), and has also been implicated in the increased spread of HIV and consequently is linked to the rise in cART use (Kumar et al., 2015). Equally, an increase in alcohol use in individuals living with HIV including those on cART has also been reported (Mondal et al., 2019). Further, both HIV infection and cART have been implicated in diabetes induction (Avari and Devendra, 2017). Therefore, these three conditions can simultaneously occur in an individual and the associated testicular histopathology and reproductive health implications need to be documented.

Moreover, diabetes, alcohol consumption, and cART use have each been reported to affect the male reproductive system. Studies on diabetes have reported reproductive hormone imbalance, testicular structure derangements, seminiferous tubule lesions, reduced ejaculate volume, poor sperm quality, and sexual dysfunctions in diabetic condition (Condorelli et al., 2018; Ray and Pramanik, 2020), as well as in alcohol abuse (Dosumu et al., 2014; Oremosu and Akang, 2015; Finelli et al., 2022), and also in cART use (Kushnir and Lewis, 2011; Azu et al., 2014;

Ogedengbe et al., 2016). Unfortunately, there is no scientific literature available on the impact of the multimorbidity of these conditions (diabetes, alcohol abuse, and cART) on male fertility. Yet, such studies are particularly relevant since these conditions exist in society and are particularly rampant in the population of reproductive age. Hence, this study reports on the impact of a co-presence of alcohol and cART in a diabetic condition on testicular histomorphology and possible consequences on its reproductive function.

MATERIALS AND METHODS

Chemical and reagents

Streptozotocin (STZ) (S0130) was purchased from Sigma-Aldrich Chemical Company (St. Louis, MO, USA) and Atripla, a fixed-dose combination antiretroviral drug was purchased from Bristol-Myers Squibb and Gilead Sciences (Foster City, CA, USA). Androgen receptor rabbit monoclonal (ab105225) primary antibody was procured from Abcam (Cambridge, MA, USA) and biotinylated goat anti-rabbit (BA-1000) secondary antibody and Avidin-Biotin Complex kit (ABC) (PK-6100) were procured from Vector Laboratories (Burlingame, CA, USA). Then, ELISA kits for luteinizing hormone (LH; E-EL-R0026), follicle stimulating hormone (FSH; E-EL-R0391), testosterone (TT; E-EL-R0155), and inhibin B (INHB; E-EL-R1027) were procured from Elabscience (Houston, Texas, USA).

Ethical clearance

The Animal Research Ethics committee (AREC) University of the Witwatersrand (Wits) approved this study (approval number: 2018/011/58/C) and all experiments were carried out at the Wits Research Animal Facility (WARF) following AREC guidelines.

Animal husbandry

Thirty (30) adult (10 weeks old) male Sprague Dawley rats were utilized. Every rat was kept apart in a clean plastic cage, housed at room temperature (21-23ºC), with a 12/12-hour light/dark cycle, and fed on a standard rat chow and given drinking fluid (water and/or alcohol solution) *ad libitum* depending on treatment regimen.

Type 2 diabetes induction

A modified procedure described by Wilson and Islam, 2012 (Wilson and Islam, 2012) was used to induce type 2 diabetes mellitus. Briefly, animals were fed on a 20% fructose reconstituted

rat chow diet for two weeks, after which a single injection of 40mg/kg streptozotocin (STZ) in freshly prepared 0.05M (pH 4.5) citrate buffer was administered intraperitoneally. Then, non-fasting blood glucose levels were measured 72 hours after STZ administration and rats with glucose levels ≥ 250 mg/dl were regarded as diabetic. Once the diabetic state was confirmed in animals, they were placed on a standard rat chow diet. Further, fasting blood glucose (FBG) levels were measured following a 12 h fasting (20:00 to 08:00) biweekly through a tail prick, using the Accu-Chek meter and glucose strips.

Experimental design

The rats were divided into five groups, each consisting of six as follows. Control group, diabetic (DM) group, diabetic rats treated with 10% v/v alcohol daily (DM+A), diabetic rats treated with an extrapolated human equivalent dose of 23.22 mg/kg of cART (consisting of efavirenz 600 mg + emtricitabine 200 mg + tenofovir 245 mg) (Frampton and Croom, 2006) in gelatine cubes daily (DM+cART), and diabetic animals treated with both alcohol and cART (DM+A+cART) groups. The rats were treated for 90 days, after which they were weighed, anesthetized with 240mg/ml pentobarbitone, and terminated. Blood was drawn through a cardiac puncture and transferred into plain vacutainers, thereafter, rats were perfused with 2 mL/min of 0.1-M phosphate buffer (PB) in 0.9% saline before extracting the testes. The testes were then preserved in 10% neutral buffered formalin for subsequent processing. Collected blood samples were left to clot, then centrifuged, and the serum was transferred into a new Eppendorf tube and stored at -80℃ for immunoassays.

Testis morphometry

Testis weight and volume

The weight of the testes was recorded immediately after their extraction using an electronic scale (Kern PCB 200-2 weighing scale). Testis volume was determined using the Archimedes principle of water displacement in a measuring cylinder (Ansa et al., 2017). The initial volume (Vi) of distilled water in a graduated cylinder was recorded, and then the final volume (Vf) was determined after adding the testis to the graduated cylinder containing the known amount of distilled water. The volume of the testis (Vt) was calculated by subtracting the initial volume (Vi) from the final volume (Vf) as shown below.

$$Vt = Vf - Vi \ (\text{mm}^3)$$

Testis size

A sliding digital Vernier caliper was used to measure the width and length of the testes, as described by Parhizkar et al., (2014). Testis size was then calculated using the spheroid formula:

$$Testis\ size = width^2 \times length \times 0.523\ (mm)$$

Histology and histomorphometry (H&E)

The fixed testes were dehydrated sequentially in 70-100% alcohol grades and embedded in molten paraffin wax and sectioned at 5µm thickness. The sections were stained with H&E and examined using the Axioskop 2 plus light microscope (Nikon Eclipse Ci, 104C type). Photomicrographs of testicular tissue sections were obtained using a linked computerized Zeiss digital image system, the AxioCam 208 color (Zeiss group, Oberkochen, Germany) for morphometric assessment.

Testicular component area fractions

Testicular component (seminiferous epithelium, connective tissue, lumen, and interstitial space) area fractions were determined using the Fiji 84-intersection grid. The grid was superimposed on H&E-stained images captured at x100 magnification and the intersecting points for each component were counted. The average intersecting points for each testicular component were calculated in 24 camera fields for each animal (i.e., 144 fields per group) and each testicular component area fraction was determined using the formula below (Kangawa et al., 2019).

$$\text{Area fraction} = \frac{(area\ per\ point \times average\ number\ of\ intersecting\ points)}{total\ area\ of\ photomicrograph} \times 100\ (\%)$$

Seminiferous tubule morphometry

Seminiferous tubule area, tubule diameter, and epithelium height were measured in 50 round or nearly round seminiferous tubules for each animal (i.e., 300 tubules per group) using Fiji software. The seminiferous tubule cross-sectional area was determined by tracing around the seminiferous tubule using the Fiji freehand selection tool. The average tubule diameter and epithelial height were calculated using the minor and major axes measurements (Kumar and Nagar, 2014). To exclude longitudinal tubules, an average tubule diameter was considered only

if D1/D2 ≥ 0.85, a value of D1/D2 =1.0 representing a perfectly rounded circle (Olasile et al., 2018).

Germinal epithelium cell quantification

The number of the different germinal epithelium cells (Sertoli, spermatogonia, spermatocytes, round, and elongated spermatids) were counted in H & E-stained sections at x400. For each animal, 10 rounded VII seminiferous tubules were considered (i.e., 60 tubules per group) (Qiu et al., 2013).

Leydig cell morphometry

The diameters of 50 nuclei with distinct nucleoli were considered for each animal (i.e., 300 per group) were measured using Fiji software per group on H&E-stained images captured at x400. The nuclear volume was obtained using the formula below (Monteiro et al., 2012).

$Leydig\ cell\ nuclear\ volume\ = \frac{4}{3}\pi R^3$(µm^3). Where, Radius (R) = D/2, and π = 3.14.

Histopathological evaluation

Johnsen's testicular score

Spermatogenesis was classified in 50 seminiferous tubules (stage II-VII) per animal (i.e., 300 tubules per group) using Johnsen's testicular score. Each tubule was assigned a score from 10 to 1 according to modified Johnsen scoring criteria. Tubules with; Many spermatozoa in the tubule lumen=10, many elongated spermatids in the apical region of the epithelium=9, many elongated spermatids still embedded in the Sertoli cell membrane=8, few elongated spermatids but had many round spermatids=7, no elongated spermatids but had few round spermatids =6, no spermatids but had many spermatocytes=5, few spermatocytes=4, spermatogonia cell only=3, Sertoli cells only=2, and no seminiferous epithelial cells=1. Thereafter the number of tubules for an individual score was multiplied by the score, and then the total for all the scores was divided by 50 (the total number of tubules scored) to obtain the mean Johnsen's score per group for further analysis (Thanh et al., 2020).

Histological changes

Testicular H&E-stained sections were examined for the presence of histological changes. The observed changes were then graded in 24 microscopic fields for each animal (i.e., 144 fields per group). The changes in each field were semi-quantitatively categorized into five grades as

follows; grade 4 = very severe (change seen in >75% of the field), grade 3 = severe (change seen in >50%<75% of the field), grade 2 = moderate (change seen in >25%<50% of the field), grade 1= mild (change seen in <25% of the field), and grade 0 = none (no change in the field) (Erpek et al., 2007).

Measurement of seminiferous tubule basement membrane (STBM)

Photomicrographs of PAS-stained sections were captured at x400, and Fiji software was used to measure the thickness of the basement membrane. The thickness of STBM was measured at two points (from the minor and major axis) in 50 randomly selected tubules for each animal (i.e., 300 tubules per group) (Omar et al., 2018).

Evaluation of testicular capsule thickness

The capsule thickness was measured on Masson's Trichrome stained sections. Photomicrographs of six fields from the free surface of the capsule were captured at x400, and three points were measured on each field (i.e., 18 measurements for each animal, 108 per group) (Aire and Ozegbe, 2007).

Interstitial connective tissue quantification

Components of testicular connective tissue i.e., collagen, reticulin, and elastin fibers were quantified in the photomicrographs of sections stained with Masson's Trichrome, Gordon and Sweet's silver impregnation, and Gomori's Aldehyde Fuchsin techniques respectively. Collagen, reticulin, and elastin fibers were quantified in the 24 microscopic fields captured at x100 for each animal (i.e., 144 sections per group). Previously reported steps were followed to segment connective tissue images using ilastik (v1.3.3; https://www.ilastik.org) and subsequently quantify the segments in Fiji software (v1.52e; https://imagej.net/Fiji) (Owembabazi et al., 2023).

Immunoassay for reproductive hormones

Serum levels of reproductive hormones viz. luteinizing hormone (LH), follicle stimulating hormone (FSH), testosterone (TT), and inhibin B (INHB) were quantified using enzyme-linked immunosorbent assay (ELISA) following the manufacturer's protocols. The standards and samples were run in duplicates, and the concentration of serum TT, LH, FSH, and INHB were determined from respective standard curves plotted with the standard concentration and their optical densities.

Immunocytochemistry (IHC) technique for androgen receptor

Testicular tissue sections of 5µm thickness were mounted onto saline-coated slides and immunolabeled with AR antibody following the IHC steps we previously reported (Owembabazi et al., 2023). Briefly, sections were incubated with 1:100 anti-androgen receptor at 4°C overnight. The immunoreaction was detected using 3, 3'-diaminobenzidine tetrachloride (DAB) and counterstained in hematoxylin. The number of Sertoli cells expressing androgen receptor immunoreactivity were counted in 20 rounded seminiferous tubules (stage II-VII) (Bremner et al., 1994) for each animal (i.e., 120 tubules for each group). The number of Leydig cells expressing androgen receptor immunoreactivity were counted in 20 microscopic fields at x400 for each animal (i.e., 120 fields for each group). Further, staining intensity was quantified in 25 androgen receptor immuno-positive Sertoli and Leydig cells for each animal group (see Appendix).

Data analysis

GraphPad Prism 6 windows software was used for data analysis. Data were expressed as Mean ± SEM. Group means of parametric data were compared using a one-way analysis of variance, followed by Bonferroni's *post hoc* test. Non-parametric data (Johnsen's and histological change scores) was compared using Kruskall Wallis, followed by Dunn's *post hoc* test. Deeming a $p<0.05$ value statistically significant.

RESULTS

Blood glucose level

Fasting blood glucose (FBG) levels increased significantly in all treated groups (DM ($p=0.0325$), DM+A ($p=0.0020$), DM+cART ($p<0.0001$), and DM+A+cART ($p=0.0202$)) relative to the control. Further, the FBG level of DM+cART group was significantly increased ($p=0.0499$) relative to the DM group (Table 6.1).

Table 6.1: Mean ± SEM fasting glucose, testis and tubule morphometry, and component area fractions of animal groups

Animal groups	Control	DM	DM+A	DM+cART	DM+A+cART
Fasting glucose (mmol/L)	4.99±0.11[a]	11.35±1.70[b]	13.97±1.36[b*]	17.65±2.31[c]	12.06±0.82 [b*]
Testis morphometry					

Testis weight (g)	1.91±0.05[a]	1.69±0.07[a*]	1.31±0.27[b*]	1.72±0.05[a*]	1.72±0.09[a*]
Testis volume (mm^3)	1.88±0.09[a]	1.63±0.13[a*]	1.2±0.2[b*]	1.67±0.08[a*]	1.7±0.12[a*]
Testis size (mm)	1493±41[a]	1199±85[a*]	991±96[b*]	1271±49[a*]	1218±103[a*]
Area fractions (AF) (%)					
Epithelial (EAF)	74.25±0.5[a]	71.62±0.73[b]	69.69±0.58[b]	70.9±0.57[b]	74.08±0.42[a]
Lumen (LAF)	8.56±0.29[a]	7.02±0.23[b*]	8.68±0.34[a]	7.36±0.29[b*]	7.59±0.22[a*]
Interstitial space (ISAF)	4.93±0.12[a]	6.13±0.14[b]	6.12±0.16[b]	5.59±0.15[b]	5.76±0.16[b]
Connective tissue (CTAF)	11.97±0.31[a]	14.69±0.37[b*]	15.12±0.32[b]	15.77±0.39[b]	13.53±0.35[c*]
Tubule morphometry					
Tubule area (μm^2)	78939± 692[a]	59561± 1000[b]	49840± 1180[c]	65393± 722[d]	75870± 849[a]
Tubule diameter (µm)	310.2±1.3[a]	269.7±2.35[b]	233±3.12[c]	284.7±1.38[d]	302.8±1.55[a]
Epithelial height (µm)	97.52±0.62[a]	89.25±1[b]	64.51±1.37[c]	92.29±0.8[b]	96.31±0.78[a]
Lumen diameter (µm)	97.97±3.54[a]	79.53±2.84[b]	112.1±3.25[a]	81.79±3.16[b]	107.4±3.86[a]

For all parameters: Values in the same row with similar superscripts are not significantly different. Whilst values in the same row with different superscripts are significantly different ($p<0.05$) except when the different superscripts are both marked with an asterisk (*). DM, diabetes; DM+A, diabetes and alcohol; DM+cART, diabetes and combination antiretroviral therapy; DM+A+cART, diabetes and alcohol and combination antiretroviral therapy.

Testis morphometry

A general decrease was observed in the testicular weight, volume, and size of all treated groups relative to control, but only DM+A treated group had a significant decrease in weight ($p=0.0242$), volume ($p=0.0096$), and size ($p=0.0018$) relative to control (Table 6.1).

Testicular component area fractions

Epithelial area fraction (EAF) of treated groups, DM, DM+A, and DM+cART was significantly reduced relative to control ($p=0.0116$, $p<0.0001$, and $p=0.0004$) and DM+A+cART ($p=0.0233$, $p< 0.0001$, and $p=0.0009$) respectively (Table 6.1). However, the DM+A+cART treated group showed an insignificant reduction ($p>0.05$) in EAF relative to control. Then DM and DM+cART treated groups showed a significant decrease in the lumen area fraction (LAF) relative to control ($p=0.0011$ and $p=0.0239$) and DM+A ($p=0.0003$ and $p=0.0088$) respectively. Relative to the control group, the interstitial space area fraction (ISAF) increased significantly in DM ($p<0.0001$), DM+A ($p<0.0001$), DM+cART ($p=0.0196$), and DM+A+cART ($p=0.0009$) treated groups. A significant increase in connective tissue area

fraction (CTAF) was detected in all treated groups relative to the control group (DM ($p<0.0001$), DM+A ($p<0.0001$), DM+cART ($p<0.0001$), and DM+A+cART ($p=0.0162$)). Further, the CTAF of treated groups DM+A and DM+cART was significantly increased relative to DM+A+cART ($p=0.0129$ and $p<0.0001$ respectively) (Table 6.1).

Seminiferous tubule morphometry

Tubule area and diameter of DM, DM+A, and DM+cART treated groups reduced significantly ($p<0.0001$) relative to control and DM+A+cART (Table 6.1). Further, DM and DM+A groups showed a significant decrease ($p<0.0001$) in the tubular area and diameter compared to DM+cART group. The treated groups, DM, DM+A, and DM+cART had a significant reduction in epithelial height relative to control ($p<0.0001$, $p<0.0001$, and $p=0.0010$ respectively) as well as in comparison with DM+A+cART ($p<0.0001$, $p<0.0001$, and $p=0.0273$ respectively). However, a nonsignificant reduction ($p>0.05$) was detected in the epithelial height of DM+A+cART relative to control group. Then, epithelial height of the DM+A group was significantly reduced ($p<0.0001$) relative to DM and DM+cART treated groups. A significant decrease was found in the lumen diameter of DM and DM+cART treated groups relative to control ($p=0.0049$ and $p=0.0167$) and in comparison with DM+A ($p<0.0001$), and DM+A+cART ($p<0.0001$ and $p=0.0002$ respectively) (Table 6.1).

Germinal epithelium cells

The DM and DM+A+cART groups showed a significant increase ($p<0.0001$) of spermatogonia relative to control (Table 6.2). However, in DM+A and DM+cART treated groups, spermatogonia decreased significantly ($p<0.0001$) relative to control and the rest of the treated groups. Further, spermatogonia in the DM+A were significantly decreased ($p<0.0001$) compared to DM+cART group. Spermatocytes were significantly decreased in all treated groups relative to control group (DM, $p=0.0316$; DM+A, $p<0.0001$; DM+cART, $p<0.0001$; and DM+A+cART, $p<0.0001$). Then, treated groups DM+A and DM+cART showed a significant decrease in spermatocyte relative to DM ($p<0.0001$ for both) and DM+A+cART ($p<0.0001$ and $p=0.0068$ respectively). In addition, spermatocytes of the DM+A group were significantly decreased ($p<0.0001$) relative to DM+cART group. All treated groups showed a significant reduction in round spermatids relative to control group (DM, $p=0.0023$; DM+A, ($p<0.0001$; and DM+cART, $p<0.0001$; and DM+A+cART, $p<0.0001$), but the round spermatids of treated group DM+A reduced significantly ($p<0.0001$) relative to the other treated groups. Furthermore, a significant decrease in elongated spermatids was observed in all

treated groups relative to control group ($p<0.0001$), and elongated spermatids of DM, DM+A, and DM+cART treated groups were significantly reduced relative to DM+A+cART ($p=0.0004$, $p<0.0001$, and $p=0.0250$ respectively). Also, DM+A group had significantly decreased ($p<0.0001$) elongated spermatids relative to DM and DM+cART treated groups (Table 6.2).

Table 6.2: Mean ± SEM germinal epithelium cell count and Leydig cell morphometry of animal groups

Animal groups	Control	DM	DM+A	DM+cART	DM+A+cART
Epithelium cell count					
Spermatogonia	59.2±0.62^{a}	72.8±1.18^{b}	40.64±1.05^{c}	60.51±1.12^{a}	76.72±1.37^{b}
Spermatocytes	88.62±0.8^{a}	83.92±0.95^{b}	46.72±1.16^{c}	75.44±1.33^{d}	80.87±1.27^{b}
Round spermatids	92.3±0.95^{a}	85.7±1.66^{b}	36.33±0.55^{c}	83.48±1.49^{b}	83.57±0.86^{b}
Elongated spermatids	102.9±1.02^{a}	76.97±1.31^{b}	0.00±0.00^{c}	78.69±1.33^{b}	83.49±1.3^{d}
Sertoli	23.61±0.24^{a}	22.41±0.41^{a}	9.64±0.2^{b}	22.39±0.34^{a}	22.39±0.33^{a}
Leydig cell nuclear					
Diameter (µm)	5.85±0.04^{a}	4.82±0.06^{b}	4.24±0.07^{c}	5.16±0.06^{d}	5.52±0.05^{e}
Volume (μm^3)	110±2.46^{a}	67.67±2.63^{b}	48.43±2.07^{c}	79.8±2.65^{d}	94.09±2.46^{e}

For all parameters: Values in the same row with similar superscripts are not significantly different. Whilst values in the same row with different superscripts are significantly different ($p<0.05$). DM, diabetes; DM+A, diabetes and alcohol; DM+cART, diabetes and combination antiretroviral therapy; DM+A+cART, diabetes and alcohol and combination antiretroviral therapy.

Testicular somatic cells (Sertoli and Leydig cells)

The number of Sertoli cells reduced significantly ($p<0.0001$) in DM+A treated group relative to the control and all other treated groups (Table 6.2). A significant reduction in Leydig cell nuclear diameter (LCND) was found in all treated groups relative to control group (DM, $p<0.0001$; DM+A, $p<0.0001$; DM+cART, $p<0.0001$; and DM+A+cART, $p=0.0004$). Then, LCND of treated groups DM, DM+A, and DM+cART was significantly reduced ($p<0.0001$) relative to DM+A+cART group. Also, the LCND of DM group was significantly reduced ($p=0.0001$) relative to DM+cART, and the LCND of DM+A treated group reduced significantly ($p<0.0001$) relative to DM and DM+cART groups. Furthermore, the Leydig cell nuclear volume (LCNV) of all treated groups significantly reduced ($p<0.0001$) relative to control. In the DM, DM+A, and DM+cART treated groups, LCNV reduced significantly

relative to DM+A+cART group ($p<0.0001$, $p<0.0001$, and $p=0.0004$ respectively). The LCNV of the DM group reduced significantly ($p=0.0051$) relative to DM+cART group and DM+A group had significantly reduced ($p<0.0001$) LCNV relative to DM and DM+cART treated groups (Table 6.2).

Histopathological evaluation

Johnsen's testicular score reflects progress of spermatogenesis and the quantity of sperm cells. All treated groups showed a reduction in Johnsen's score, but only DM and DM+A treated groups significantly reduced Johnsen's score relative to the control ($p=0.0268$ and $p=0.0002$ respectively, Table 3). Further, the histology of the control group revealed a normal histoarchitecture characterized by approximately rounded tubules surrounded by a smoothly contoured basement membrane, a discretely arranged germinal epithelium with a series of spermatogenetic cells, and an interstitium consisting of blood vessels, connective tissue, Leydig cell, myoid cell, and macrophages. On the other hand, varying severity of seminiferous tubule lesions was observed in testes of the treated animals (Fig. 6.1). The comparisons for the lifting of epithelium, epithelial sloughing, and karyolysis across the animal groups (Table 6.3). An insignificant increase in the lifting of epithelium was detected in DM+cART and DM+A+cART treated groups relative to control, but lifting of epithelium in the DM+A+cART group was significantly increased ($p=0.0063$) in comparison to DM+A group. Epithelial sloughing in DM+A and DM+A+cART treated groups was significantly increased relative to control ($p=0.0100$ and $p=0.0460$) and DM+cART ($p=0.0100$ and $p=0.0460$) respectively. The DM+A and DM+cART treated groups, showed significantly increased karyolysis compared to control ($p=0.0019$ and $p=0.0003$), DM ($p=0.0026$ and $p=0.0004$), and DM+A+cART ($p=0.0026$ and $p=0.0005$) respectively. Additionally, changes such as widened intercellular space, extensive tubular atrophy, and ghost cells were predominant in the DM+A group. Then, germ cell pyknosis was mainly recorded in the DM and DM+A treated groups. Furthermore, increased germ cell size and germinal epithelium derangement were observed in DM+A and DM+A+cART treated groups (Fig. 6.1).

Table 6.3: Median Johnsen's score and histological changes observed in animal groups

Animal groups	Control	DM	DM+A	DM+cART	DM+A+cART
Johnsen's score	8.81[a]	8.44[b*]	4.04[b*]	8.61[a*]	8.62[a*]
Histological changes					
Lifting of epithelium	0.04[a*]	0.04[a*]	0.00[a]	0.13[a*]	0.58 [b*]
Epithelial sloughing	0.00[a]	0.08[a*]	0.63[b*]	0.00[a]	0.29[b*]
Karyolysis	0.00[a]	0.00[a]	0.25[b]	0.25[b]	0.00[a]

For all parameters: Values in the same row with similar superscripts are not significantly different. Whilst values in the same row with different superscripts are significantly different ($p<0.05$) except when the different superscripts are both marked with an asterisk (*). DM, diabetes; DM+A, diabetes and alcohol; DM+cART, diabetes and combination antiretroviral therapy; DM+A+cART, diabetes and alcohol and combination antiretroviral therapy.

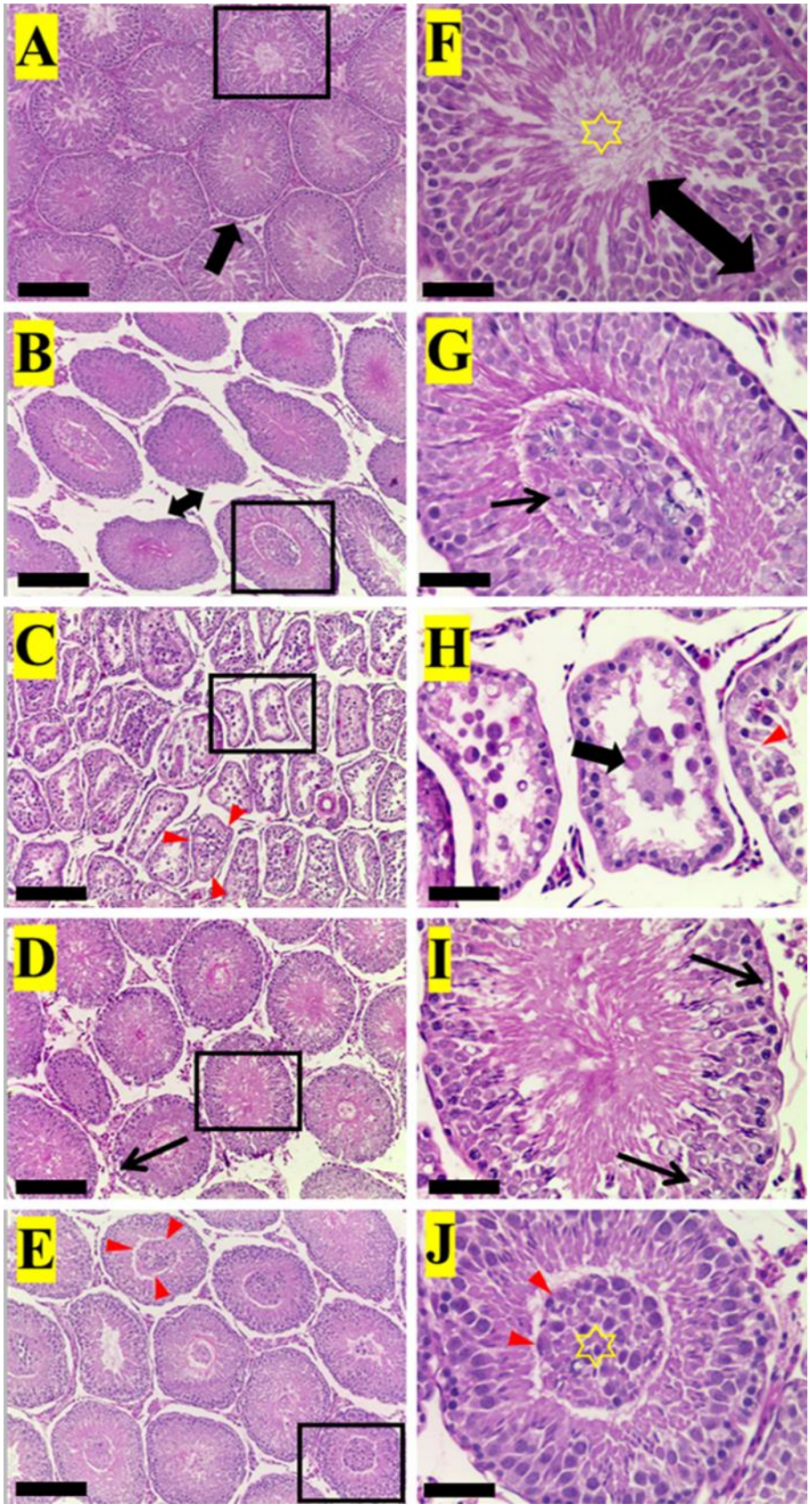


Figure 6.1: Representative photomicrographs of H&E-stained testicular section. Testis of the control group (image A) showed a normal oval-shaped seminiferous tubule (ST) separated by a layer of interstitial connective tissue (thick arrow). Changes in testicular normal morphology

were observed in animals of treated groups. Image B (DM group) shows increased interstitial space (double arrow), image C (DM+A group) shows extensive tubular atrophy and germinal epithelium derangement (arrowheads), image D (DM+cART group) shows lifting of epithelium (thin arrow), image E (DM+A+cART group) shows epithelial sloughing (arrowheads). Images F, G, H, I, and J are a magnification of the square area indicated in images A, B, C, D, and E. Demonstrated in images; F is the germinal epithelium (double arrow) consisting of a discretely arranged series of spermatogenic cells and a lumen (asterisk), G shows germ cell pyknosis (thin arrow), H is showing ghost cell (thick arrow) and widened intercellular space (arrowhead), I shows karyolysis (thin arrow), and J is showing sloughed germ cells in the lumen (asterisk) and germ cells with increased size (arrowheads). The left and right panels are ×100 and ×400 with scale bars of 200μm and 50μm respectively. DM, diabetes; DM+A, diabetes and alcohol; DM+cART, diabetes and combination antiretroviral therapy; DM+A+cART, diabetes and alcohol and combination antiretroviral therapy.

Seminiferous tubule basement membrane (STBM) thickness

The basement membrane surrounding the seminiferous tubule was identified as a thin PAS-positive staining sheet-like structure with a single layer of myoid cells (Fig. 6.2). A significant increase in the thickness of STBM was found in treated groups DM+A and DM+cART relative to control ($p<0.0001$ and $p=0.0002$ respectively), DM ($p<0.0001$ for both), and DM+A+cART ($p<0.0001$ and $p=0.0490$ respectively). Also, STBM thickness of the DM+A treated group was significantly increased ($p<0.0001$) relative to DM+cART treated group.

Testicular capsule thickness

The testicular capsule also referred to as the tunica albuginea comprised of majorly collagen fibers braced with a network of myoid cells (Fig. 6.2). The thickness of the capsule was significantly increased in treated groups DM+A and DM+A+cART in comparison to control, $p=0.0002$ and $p=0.0055$ respectively. The DM and DM+cART treated groups respectively showed an insignificant ($p>0.05$) decrease and increase in capsule thickness compared to the control, but the capsule thickness in DM+cART increased significantly ($p=0.0002$) relative to DM group.

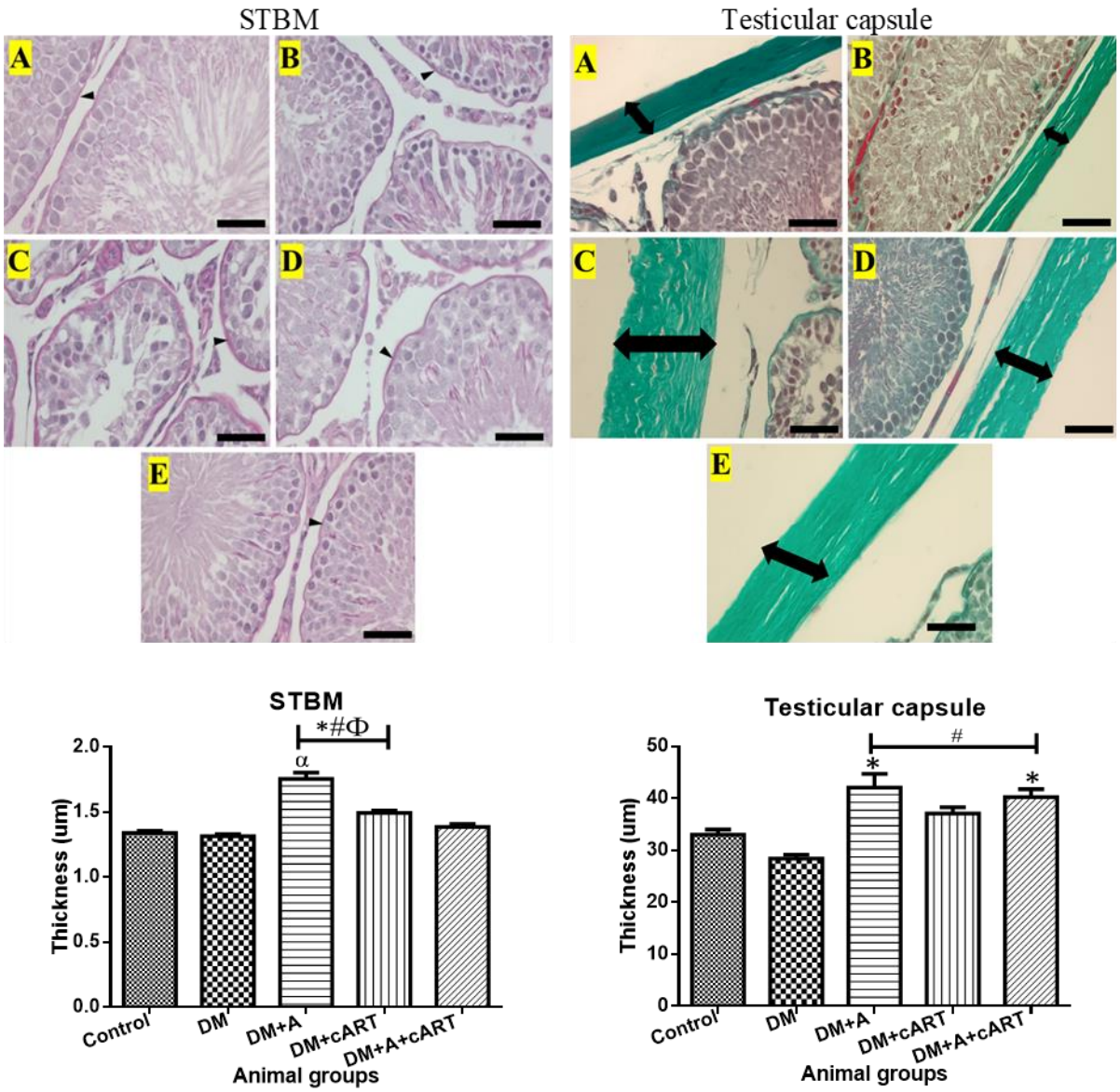
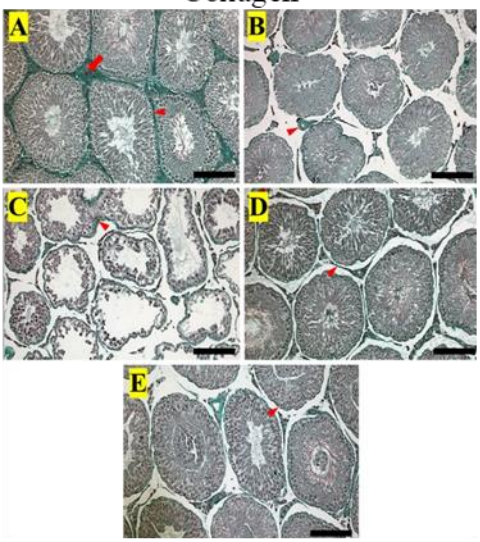


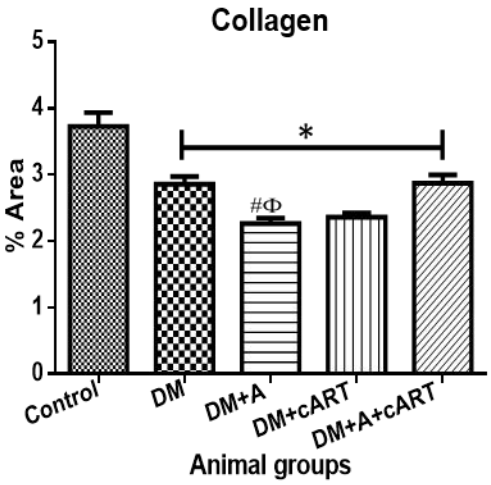
Figure 6.2: Representative seminiferous tubule basement membrane (STBM) (arrowheads) and testicular capsule (double arrows) photomicrographs, PAS and Masson's trichrome stain respectively. Graphs show respective mean ± SEM thickness. Different symbols *, #, α, and Φ represent significant differences ($p<0.05$) as analyzed by a Bonferroni's multiple comparison test; '*' significantly increased compared to control, '#' significantly increased compared to DM, 'α' significantly increased compared to DM+cART, and 'Φ' significantly increased compared to DM+A+cART. Magnification, x400; scale bar, 50µm. **Key:** Image: A; control group, B; DM group, C; DM+A group, D; DM+cART group, and E; DM+A+cART group. DM, diabetes; DM+A, diabetes and alcohol; DM+cART, diabetes and combination antiretroviral therapy; DM+A+cART, diabetes and alcohol and combination antiretroviral therapy.

Interstitial connective tissue

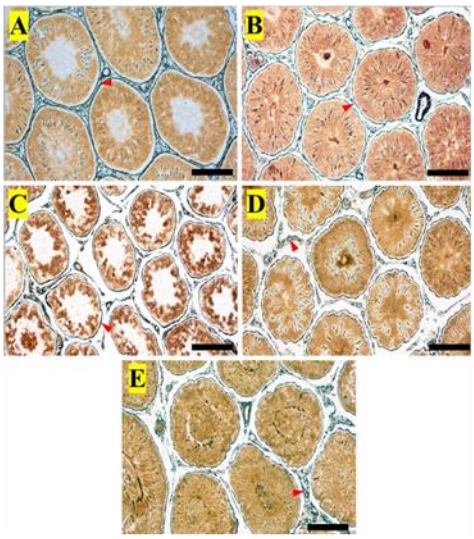
The interstitial connective tissue found between seminiferous tubules and surrounding the tubules consisted of collagen, reticulin, and elastin fibers (Fig. 6.3). All treated groups showed a significant reduction ($p<0.0001$) in collagen fibers relative to control. The DM+A treated group had significantly reduced collagen fibers compared to DM ($p=0.0141$) and DM+A+cART ($p=0.0103$). The reticulin fibers of all treated groups significantly decreased relative to control (DM, $p=0.0015$; DM+A, $p=0.0102$; DM+cART, $p=0.0035$; and DM+A+cART, $p<0.0001$). Further, relative to the control group, elastin fibers reduced significantly in all treated groups (DM, $p=0.0171$; DM+A, $p=0.0047$; DM+cART, $p<0.0001$; and DM+A+cART, $p=0.0004$).

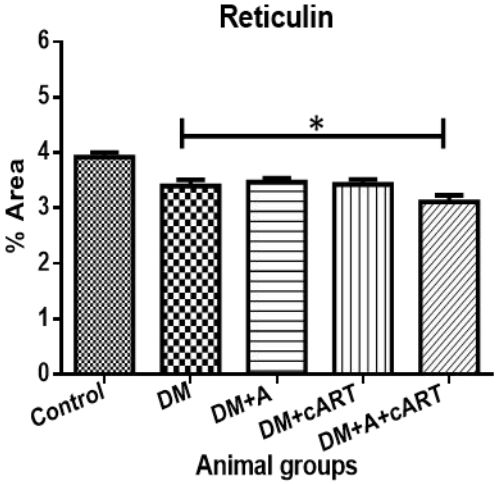
Collagen



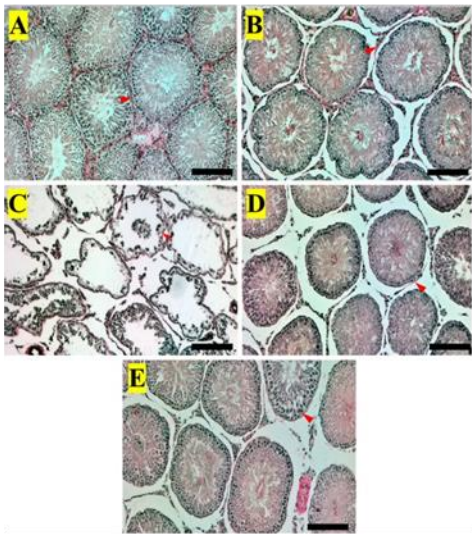


Reticulin





Elastin



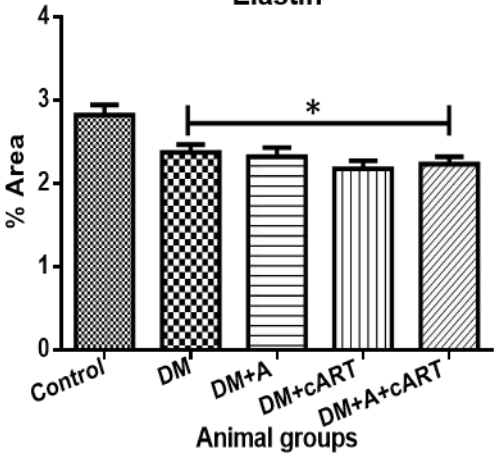


Figure 6.3: Representative collagen, reticulin, and elastin indicated with arrowheads in photomicrographs, Masson's trichrome, Gordon and Sweet's silver impregnation, and Verhoeff Van Gieson stain respectively. Graphs show respective mean ± SEM percentage area. Different symbols *, #, and Φ represent significant differences ($p<0.05$) as analyzed by a Bonferroni's multiple comparison test; '*' significantly reduced compared to control, '#' significantly reduced compared to DM, and 'Φ' significantly reduced compared to DM+A+cART. Magnification, x100; scale bar, 200μm. **Key:** Image: A; control group, B; DM group, C; DM+A group, D; DM+cART group, and E; DM+A+cART group. DM, diabetes; DM+A, diabetes and alcohol; DM+cART, diabetes and combination antiretroviral therapy; DM+A+cART, diabetes and alcohol and combination antiretroviral therapy.

Reproductive hormone profile

The serum luteinizing hormone level decreased significantly ($p=0.0142$) in the DM+A+cART group relative to the control, whereas the luteinizing hormone level of DM+A significantly increased relative to other treated groups (DM, $p=0.0035$; DM+cART, $p=0.0027$; and DM+A+cART, $p=0.0002$). A significant increase in serum follicle stimulating hormone was recorded in DM, DM+A, and DM+A+cART treated groups, relative to control ($p=0.0073$, $p=0.0004$, and $p=0.0069$ respectively). Further, the follicle stimulating hormone level of DM+A group was significantly increased ($p=0.0176$) relative to DM+cART group. Additionally, in comparison to the control group, the serum testosterone levels decreased significantly in treated groups; DM, $p=0.0102$; DM+A, $p=0.0166$; and DM+A+cART, $p=0.0016$. There was no significant difference in serum inhibin B levels between the control and treated groups, however, the inhibin B levels of DM+A+cART treated group was significantly increased ($p=0.0057$) relative to DM+cART treated group (Fig. 6.4).

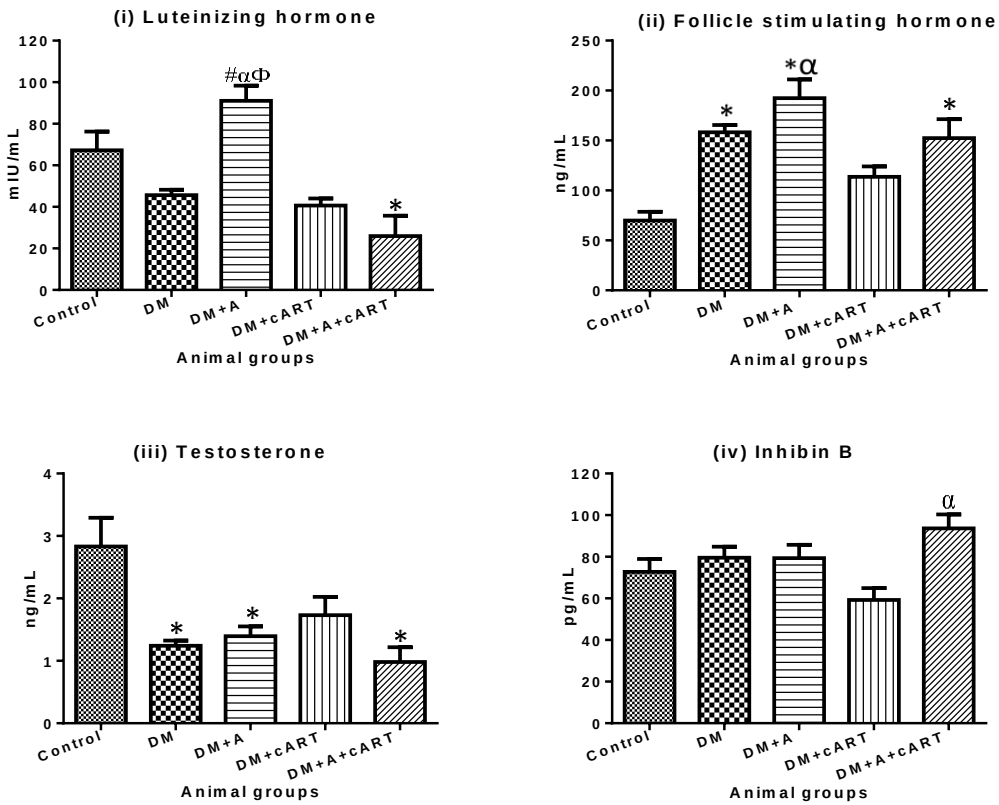


Figure 6.4: Graphs showing mean ± SEM serum levels of reproductive hormones. Different symbols *, #, α, and Φ represent significant differences ($p<0.05$) as analyzed by a Bonferroni's multiple comparison test; '*' significantly different compared to control, '#' significantly increased compared to DM, 'α' significantly increased compared to DM+cART, and 'Φ' significantly increased compared to DM+A+cART. DM, diabetes; DM+A, diabetes and alcohol; DM+cART, diabetes and combination antiretroviral therapy; DM+A+cART, diabetes and alcohol and combination antiretroviral therapy.

Androgen receptor (AR) immunoexpression and staining intensity

Testicular AR was expressed in Sertoli cells, Leydig cells, pericytes, and myoid cells of the control and all treated animals, with exception of the DM+A treated group where expression of AR was only detected in very few Sertoli cells (Fig. 6.5). In the testes of all treated groups (DM, DM+A, DM+cART, and DM+A+cART), Sertoli cell androgen receptor (SAR) expression was significantly reduced relative to the control ($p=0.0009$, $p<0.0001$, $p<0.0001$, and $p<0.0001$ respectively). But, in DM+A treated group, SAR expression reduced significantly ($p<0.0001$) relative to other treated groups. Also, expression SAR in the DM+A+cART group reduced significantly ($p=0.0049$) relative to the DM group. The result also showed that the SAR intensity was reduced significantly ($p<0.0001$) in all treated groups

relative to control, but SAR intensity in DM+A treated group reduced significantly ($p<0.0001$) compared to other treated groups. The Leydig androgen receptor (LAR) expression in all treated groups decreased significantly ($p<0.0001$) relative to the control group, However, expression of LAR in the DM+A treated group was significantly decreased ($p<0.0001$) relative to other treated groups but the LAR expression in the DM+A+cART treated group decreased significantly relative to DM ($p<0.0001$) and DM+cART ($p=0.0346$). Equally, all treated groups showed a significant reduction in the LAR intensity relative to control (DM, $p=0.0001$; DM+A, $p<0.0001$; DM+cART, $p=0.0054$; and DM+A+cART, $p= 0.0158$). Further, LAR intensity in the DM+A treated group was significantly reduced ($p<0.0001$) relative to other treated groups (Fig. 6.5).

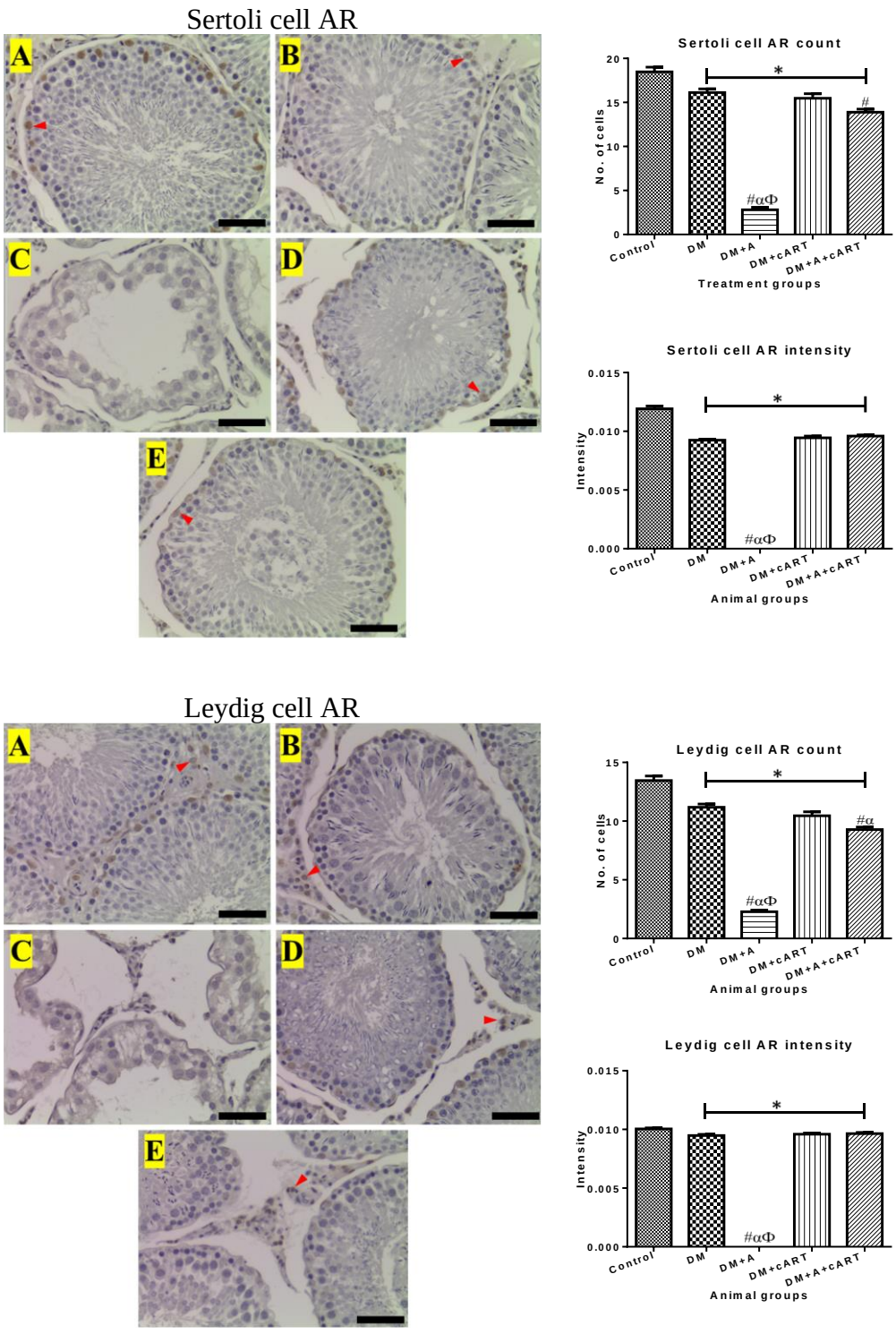


Figure 6.5: Representative photomicrographs showing Sertoli and Leydig cell androgen receptor (AR) immunoreactivity (arrowheads) and respective graphs of mean ± SEM number of immunoreactive cells and intensity. Different symbols *, #, α, and Φ represent significant differences ($p<0.05$) as analyzed by a Bonferroni's multiple comparison test; '*' significantly decreased compared to control, '#' significantly decreased compared to DM, 'α' significantly decreased compared to DM+cART, and 'Φ' significantly decreased compared to

DM+A+cART. Magnification, x400; scale bar, 50μm. **Key:** Image: A; control group, B; DM group, C; DM+A group, D; DM+cART group, and E; DM+A+cART group. DM, diabetes; DM+A, diabetes and alcohol; DM+cART, diabetes and combination antiretroviral therapy; DM+A+cART, diabetes and alcohol and combination antiretroviral therapy.

DISCUSSION

In a millennium marked by a worldwide decline in male fertility (Sun et al., 2019), the rising prevalence of; diabetes (Condorelli et al., 2018), alcohol abuse (World Health Organisation, 2011), and combination antiretroviral therapy (cART) regimen due to increasing HIV/AIDS disease (Khawcharoenporn and Sha, 2016) in males of reproductive age is of great concern. Moreover, previous studies have demonstrated the damaging effects of; diabetes (Nna et al., 2019; Ray and Pramanik, 2020), alcohol abuse (Dosumu et al., 2014; Finelli et al., 2022), and cART use (Kushnir and Lewis, 2011; Ogedengbe et al., 2016) on the male reproductive system. Additionally these conditions are intricately connected and can occur simultaneously in an individual (Kumar et al., 2015; Avari and Devendra, 2017; Mondal et al., 2019; Goecke and Baumeister, 2021), a conundrum that might elicit severe testicular dysfunctions. The present report highlights the impact of diabetes, alcohol, and cART interaction on male reproductive capacity and male fertility.

Morphometry and histopathology are widely used tools to determine perturbations of testis structure and function (Lanning et al., 2002; Azu et al., 2014) and were utilized in the present study. Although the mean morphometric and histopathological parameters of the treated groups were statistically different from the control group, we observed that certain seminiferous tubules were severely altered, some slightly altered, but others were unaltered suggesting variable tubular effects of the treatment. This implies that the degree of disruption of spermatogenesis may differ in various tubules, thus normal spermatogenesis is sustained in some tubules regardless of the treatment toxicities as previously demonstrated by Azu et al., (2014). Our findings revealed alterations in the evaluated morphometry parameters of the testis, with significant decreases in mean testicular and tubule parameters, component area fractions, and germinal epithelium cells in treated animals relative to the control group. These indicate severe testicular architecture perturbations and derangement of cellular coherency due to toxicity associated with coexistence of alcohol, cART, or both in diabetic condition. However, while the significant increases in testicular interstitium area fraction may complement the

decreases in tubule diameter, the increased lumen diameter in the alcohol and cART treated may reflect the highly significant decreases recorded in epithelial height and overall adverse effects on germinal epithelial cells. Further, the significant reduction in tubular area and diameter points to tubular shrinkage in the treated groups and suggest tubular degenerative changes following the treatments in diabetes (Ogedengbe et al., 2018; Khairuddin et al., 2020) as well as evidence of disturbed spermatogenesis. Also, the significant increment in connective tissue area fraction recorded across the treated groups may imply a build-up of fibrosis in the interstitium which corresponds to earlier report (Apa et al., 2002) in infertile men with impaired testicular integrity and cellular (Leydig, macrophage, myoid) function. Conversely, the morphometric findings conformed with the histopathological observations and the seminiferous tubule lesions across the treatment groups suggesting consistency of treatment effects on the testicular histological profile. Previous studies have documented seminiferous tubule atrophy, epithelial derangement, germ cell depletion, and distorted interstitium in animals that are diabetic (Nna et al., 2019), exposed to alcohol (Dosumu et al., 2014), and treated with cART (Ogedengbe et al., 2016). Testicular histological and morphometric alterations are morphological indicators of disruption of testicular structure integrity with its attendant dysregulation impact on spermatogenesis (Vidal and Whitney, 2014; Olojede et al., 2022). Overall, alcohol in diabetes, showed the greatest toxicosis, in all the morphometry parameters, followed by cART and then both alcohol-cART in diabetes.

The function of testicular somatic cells (Sertoli and Leydig cells) is essential for the development of the testis and regulation of spermatogenesis (Clavijo and Hsiao, 2018). Sertoli cells nurse germ cells and control the seminiferous tubules milieu (Petersen and Söder, 2006). Our results revealed a non-significant reduction in Sertoli cell number in the testis of diabetic animals and in all treated groups but a marked significant reduction in diabetic-alcohol treated group (DM+A) with extensive germ cell depletion suggesting a disruption in the critical role of Sertoli cells in spermatogenic processes. The non-significant reduction of Sertoli cell number in diabetic, diabetic plus cART, and diabetic plus alcohol plus cART groups suggests minimal perturbations of Sertoli cell function, which may be linked to its high content of anti-apoptotic makers, Bcl-w and Bcl-xL (Yuko Ito and Otsuki, 2013; Aslani et al., 2017). However, disruptions of Sertoli cell structure impair the cell's functional, which affects the blood-testis barrier and can lead to germinal epithelial detachment into the lumen (Johnson, 2014), as recorded in the present study, especially in the diabetic plus alcohol group. Previous reports show that the number of Sertoli cells determines the size of testis and the number of

spermatozoa produced (Petersen and Söder, 2006), and consequently, loss of Sertoli cells has been associated with diminished spermatozoa production (Petersen and Söder, 2006; Rebourcet et al., 2017; Oduwole et al., 2018). Furthermore, consistent with our results, diabetes has been reported to cause Sertoli cell degeneration (Meskari et al., 2018; Olojede et al., 2022) and alcohol has deleterious impacts on Sertoli and Leydig cells (Emanuele and Emanuele, 1998; Ramlau-Hansen et al., 2010) which may substantiate the observed toxicity.

Additionally, the results showed a significant decrease in the Leydig cell nuclear diameter (LCND) and volume (LCNV) in all treated groups, indicating a possible detrimental effect of treatment on the steroidogenic capacity, since studies have shown that altered nuclear volume and size are functionally associated (Wu et al., 2022). In agreement with our finding, while Giannessi et al., (2015) observed necrotic Leydig cells in testis of mice treated with alcohol, Olasile et al., (2018) reported reduced LCNV in rats treated with cART. Further, Kianifard et al., (2012) found changes in the ultrastructure of Sertoli and Leydig cells in testis of male diabetic rats. Leydig cells via the steroidogenesis process produce testosterone, a male androgen that is essential for successful spermatogenesis. The Leydig cell steroidogenic capacity is suggested to be determined by the amount of cell nuclear organelles such as mitochondria rather than the number of the cell themselves (Wang et al., 2017; Clavijo and Hsiao, 2018). Previously, researchers have shown that a reduction of Leydig cell nuclear volume is associated with decreased testosterone levels (Neves et al., 2017; Wang et al., 2017). Thus, the observed deleterious alternations of Sertoli and Leydig cells induced by the treatment may elicit dysfunction of these testicular somatic cells that will eventually lead to spermatogenesis impairments.

While the cellular components of the testis are crucial in successful reproduction, the surrounding testicular capsule and the stroma which is sandwiched between seminiferous tubules also play an essential role. These connective tissue components are essential for the maintenance of testicular structure and germinal epithelium integrity (Gao et al., 2017; Qin et al., 2017). Recently, capsular, interstitial, and peritubular connective tissue have also been recognized to play a role in transportation of spermatozoa, particularly attributed to the contractility of myoid cells that aids propulsion of spermatozoa from the tubule lumen to the rete testis (Aire and Ozegbe, 2007). Therefore, the observed significant increase in thickness of seminiferous tubule basement membrane (STBM) in the testis of DM+A and DM+cART groups and the testicular capsule in DM+A and DM+A+cART groups suggest structural distortion effects of the treatments which may adversely affect their respective functions. In

agreement with our findings, Olojede et al., (2021) found an increase in STBM and testicular capsule thickness in diabetic rats, and in the present study in the combinations of DM+cART and DM+A+cART. Further, distorted capsular collagen orientation has been reported following alcohol administration (Asuquo et al., 2020). Our results further showed that connective tissue fibers (collagen, reticulin, and elastin) were reduced in treated groups relative to control, and is consistent with previous reports that documented a reduction of collagen and reticulin fibers in rats treated with alcohol (Fakoya and Ademola Caxton-Martins, 2004; Rosa et al., 2018). Similarly, loss of elastin fibers has been reported in skin and vasculature of diabetic patients (Akhtar et al., 2010; Dremin et al., 2021). The alternations observed in testicular connective tissue show that the treatments disintegrated the testis structural integrity, which subsequently leads to testicular dysfunction.

Furthermore, the testicular structure and functions are regulated by hormones of the hypothalamic-pituitary-gonadal (HPG) axis (Corradi et al., 2016; Clavijo and Hsiao, 2018). Consequently, changes in reproductive hormone levels will lead to dysregulation of steroidogenesis and spermatogenesis. We recorded a significant decrease in luteinizing hormone (LH) (except in the DM+A group) and testosterone (TT) levels in all the treated groups, greatly in the DM+A+cART group. With significantly increased levels of follicle stimulating hormone (FSH) and insignificant increase in inhibin B (INHB) levels in all treated groups, except the DM+cART group which showed a non-significant increase in FSH and a decrease in INHB level. These perturbations of the hormonal profile reflect disturbances of endocrine homeostasis (Clavijo and Hsiao, 2018). In addition, high levels of FSH indicate an impairment in testis function, particularly the Sertoli cells that secrete INHB which regulates FSH production (Jankowska et al., 2022). Though similarities and discrepancies in hormonal profile results abound with increased levels of LH and FSH (Anderson et al., 1987) and LH and TT (Salardi et al., 2002) in diabetes, decreased level of TT in diabetes (Zha et al., 2018), alcohol consumption (Oremosu and Akang, 2015), and cART use (Akhigbe, Hamed and Odetayo, 2021) and decreased FSH in diabetes (Olojede et al., 2022). Remarkably, Rossi et al., (2020) found that Sertoli cells exposed to bisphenol A had increased INHB production. While such observed hormonal imbalances may reflect differences in research design, methods, and duration of treatment exposures, they all express adverse functional perturbations of the HPG axis. Furthermore, the balance of HPG axis hormones is regulated via a negative feedback mechanism whereby TT and INHB hormones produced by testicular cells (Leydig and Sertoli

cells respectively) modulate the pituitary secretion of LH and FSH respectively (Marques et al., 2000; Corradi et al., 2016). Conversely, decreased levels of both LH and TT and an increase in FSH levels when the level of INHB is not reduced as observed in this study might imply that the treatments disrupted the HPG axis feedback mechanism. Accordingly, the recorded hormonal imbalances conform with the observed Sertoli and Leydig cell perturbations and consequently lead to spermatogenesis and steroidogenesis impairments.

Though the impact of changes in levels of reproductive hormones has been studied extensively in male reproductive dysfunction, investigations about the changes in their receptors are scanty, notwithstanding the vital role in successful male reproduction and fertility (Petersen and Söder, 2006; Corradi et al., 2016). Androgen receptor is expressed by testicular somatic cells such as Leydig, Sertoli, myoid, and pericyte cells, and it regulates the structure and function of these cells and mediates the actions of TT on spermatogenesis (Shan et al., 1997; Wang et al., 2009). The observed significant reduction in the number and staining intensity of Sertoli and Leydig cells expressing androgen receptor in all treated groups and interestingly with severest loss recorded in the diabetes-alcohol treated group (DM+A), overall, suggests testicular toxicity and consequent dysfunctions. Our findings are consistent with previous reports on the decreased androgen receptor expression in diabetic rat testis that resulted in, weak androgen receptor signalling and led to testicular and sexual dysfunctions (Liu and Wang, 2005; Al-Shathly et al., 2020). Other studies on organochlorinated pesticides, industrial chemicals, and plasticizers have reported similar testicular toxic effects (Luccio-Camelo and Prins, 2011; Qiu et al., 2013), including several seminiferous tubule impairments in rats treated with diacerein drug (de Oliveira et al., 2021). Moreover, hypocellular testis with the arrest of spermatogenesis was reported in androgen receptor knockout animal models (Yeh et al., 2002; Wang et al., 2009). In addition, transgenic androgen receptor disruption studies have revealed the involvement of androgen receptor signalling in maintenance of spermatogonia proliferation, integrity of blood-testis barrier, spermatogenesis progression, and spermiation (O'Hara and Smith, 2015), this indicates the crucial role of androgen receptor in spermatogenesis failure, subfertility, and infertility (Yong et al., 2003; Davey and Grossmann, 2016). Therefore, the downregulation of androgen receptor in treated animals could have led to alterations in testicular morphometry, structural integrity, and spermatogenesis as observed in the current study.

It is an interesting finding that the testicular histoarchitecture was more severely affected in the diabetic-alcohol treated group (DM+A group) than in the other treated groups. This adverse effect may not be unrelated to the uncontrollable high blood glucose levels associated with alcohol abuse in diabetic condition which could have led to the exacerbated testicular damage observed (Engler et al., 2013; Pourentezari et al., 2016). However, overall, diabetes+alcohol and/or cART or both variably adversely affected the parameters evaluated. The lesser adverse effects observed in DM+A+cART treated group may be due to the shared metabolism pathway (cytochrome P450) for alcohol and cART leading to diminished impact when alcohol and cART are used concurrently in diabetes (McCance-Katz et al., 2013; Mondal et al., 2019) or due to altered bioavailability of cART (tenofovir) in diabetic-HIV patients as was previously reported (Mann et al., 2020).

CONCLUSION

This study revealed that using alcohol or/and cART in diabetic condition causes testicular morphometric and structure derangement, loss of germ and Sertoli cells, reduction of volume of Leydig cell nucleus, and seminiferous tubule lesions. These adverse effects are upon reproductive hormones dysregulation and androgen receptor reduction following the treatments, with greater toxicity demonstrated in diabetic animals treated with alcohol and points to derangements in spermatogenesis and male reproductive capacity/fertility. The results further suggest that the interaction arising from a co-presence of cART and alcohol in diabetic condition could mildly diminish their independent effects due to their common cytochrome P450 metabolic pathway. The study findings will invaluably assist clinicians in the management of male reproductive dysfunctions that could emerge in diabetic people living with HIV/AIDS on a cART regimen and who consume alcohol regularly.

APPENDIX

IHC staining intensity quantification

The Fiji software was used to measure the mean gray values (MGV) of selected stained regions of interest (ROI) as shown in figure A (Jensen, 2013; Cizkova et al., 2021). The steps below were followed.

1. Opening the image in Fiji: File > Open > Select the image > Open
2. Setting the scale: Analyze > Set scale > Ok
3. Drawing a ROI: Edit > Selection > Specify > Ok
4. Selecting the parameters: Analyze > Set measurement (check the MGV box) > Ok
5. Taking the measurement: Analyze > Measure
6. Opening the next image: File > Open next
7. Choosing the same ROI size and shape: Edit > Selection > Restore selection
8. Proceed to take the measurement: Analyze > Measure
8. Save the results as a CVS file for statistical analysis.

Worthy noting is that the darker stained areas have a low MGV and the lightly stained areas have a high MGV, thus the staining intensity is equal to the MGV reciprocal (Cizkova et al., 2021). The staining intensity of Sertoli cell AR, and Leydig cell AR was calculated as follows.

$$\text{Intensity} = \frac{1}{\text{MGV}} \quad \text{(Cizkova et al., 2021)}$$

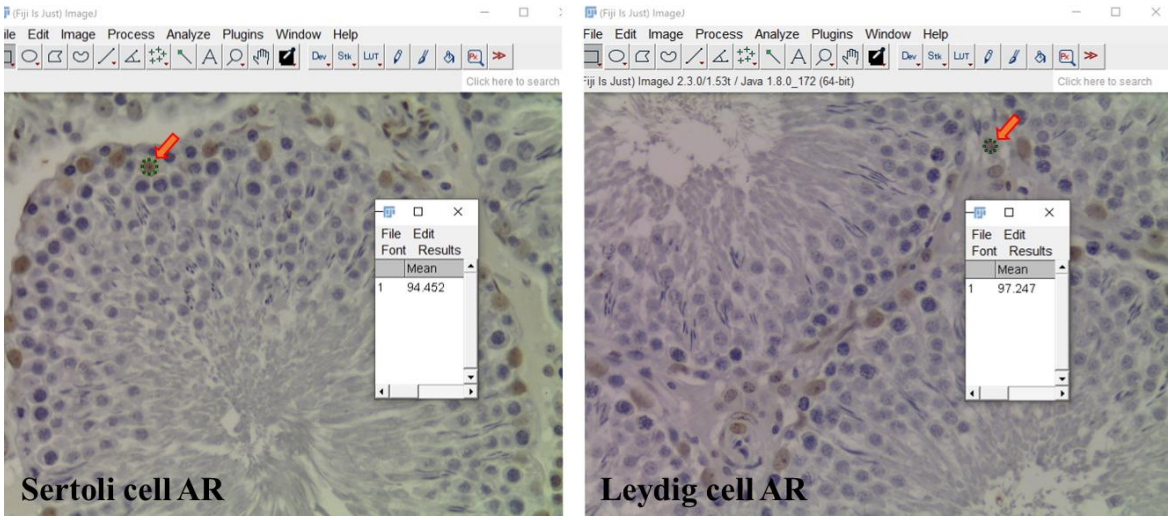


Figure A: Representative images for Sertoli cell AR and Leydig cell AR quantified in Fiji, the mean gray values of selected ROI (thick arrow) are displayed. Key; AR: androgen receptor and ROI: region of interest.

CHAPTER 7: FOURTH MANUSCRIPT

Potential Role of Inducible Nitric Oxide Synthase (iNOS) Activity in Testicular Dysfunction Following Co-administration of Alcohol and Combination Antiretroviral Therapy (cART) in Diabetic Rats

ABSTRACT

Diabetes, alcohol abuse, and combination antiretroviral therapy (cART) use have been reported to cause multi-organ complications via induction of oxidative stress and inflammation. Moreover, these are the most common factors implicated in male reproductive dysfunctions. This study evaluated testicular oxidative stress, inflammation, apoptosis, and germ cell proliferation in diabetic rats receiving alcohol and cART and their combination. Thirty adult male Sprague Dawley rats were divided into five groups, each consisting of six rats; control, diabetic only (DM), diabetic treated with alcohol (DM+A), diabetic treated with cART (DM+cART), and diabetic treated with both alcohol and cART (DM+A+cART). After 90 days of treatment administration, the rats were euthanized, and the testes were extracted and processed for immunohistochemistry analysis of oxidative stress, inflammatory, apoptosis, and proliferation markers. In comparison to the control, oxidative stress markers, inducible nitric oxide synthase (iNOS), malondialdehyde (MDA), and 8-hydroxydeoxyguanosine (8-OHDG) increased significantly in all treated groups when compared to the control. Expression of testicular proinflammatory cytokines interleukin-1β and tumor necrosis factor-α was upregulated in all treated groups, but interleukin-6 was upregulated in DM, DM+cART, and DM+A+cART treated groups and was downregulated in the DM+A treated group. All treated animal groups showed an upregulation of apoptosis marker (caspase 3) and a downregulation of proliferation marker (Ki-67), however, Ki-67 staining intensity significantly increased in treated animals compared to the control. The study findings indicate that diabetes, alcohol abuse, cART use, and their combination via iNOS upregulation can induce inflammation and oxidative stress in testicular tissue, subsequently stimulate germ cell apoptosis and proliferation inhibition that leads to spermatogenesis failure.

Keywords: Diabetes mellitus, Alcohol abuse, Antiretroviral therapy, Inflammation, Oxidative stress

INTRODUCTION

A high number of reproductive age males are diabetic (Condorelli et al., 2018), involved in lifestyle alcohol abuse (World Health Organisation, 2011), and chronic (HIV infected) or prophylaxis cART users (Khawcharoenporn and Sha, 2016). Unfortunately, diabetes (Condorelli et al., 2018; Ray and Pramanik, 2020), alcohol (Oremosu and Akang, 2015; Finelli et al., 2022), cART (Ogedengbe et al., 2016; Savasi et al., 2018) have been reported to cause alternations in reproductive hormone levels, testicular structure, and sperm parameters. Previous studies show that pathogenesis of multi-organ complications associated with diabetes (Ray and Pramanik, 2020), alcohol abuse (Rachdaoui and Sarkar, 2017), and cART use (Khan et al., 2014) is via oxidative stress and inflammation (Barcia et al., 2015; Ogedengbe, Naidu and Azu, 2018). Oxidative stress and inflammation are interlinked, and stimulate the occurrence of one another (Dutta et al., 2021) and are incidentally key characteristic features observed in reproductive dysfunctions (Tremellen, 2012; Maresch et al., 2018).

Nitric oxide synthases (NOS) are established to mediate testicular oxidative stress induction in several testis disorders including cryptorchidism, testicular torsion, varicocele, and toxicity (Köksal et al., 2003; Eid et al., 2011). The three NOS isoforms viz. endothelial (eNOS or NOS3), inducible (iNOS or NOS2), and neuronal (nNOS or NOS1) catalyze the production of nitric oxide from L-arginine (Turner and Lysiak, 2008). Nitric oxide is a free radical recognized to play a regulatory role in the process of spermatogenesis at low concentrations (O'Bryan et al., 2000; Levine et al., 2012). However, nitric oxide elevation, a consequence of NOS upregulation leads to formation of nitrogen-based reactive oxygen species (ROS), which are detrimental to the testicular tissue (Turner and Lysiak, 2008; Yu et al., 2017). Unlike eNOS and nNOS, iNOS is calcium-independent and produces NO in larger quantities, and is thus clinically important in the induction of testicular oxidative stress (Köksal et al., 2003; Kolasa et al., 2009).

Markedly, the testis is particularly vulnerable to oxidative stress because of high mitochondrial oxygen consumption to support the inherent spermatogenic cell divisions and steroidogenesis (Asadi et al., 2017). Testicular tissue is further predisposed to oxidative stress because of poor vascularization and relatively high amounts of unsaturated fatty acids (Tremellen, 2012; Guerriero et al., 2014). Therefore, based on previous reports that diabetes (Volpe et al., 2018), alcohol (Finelli et al., 2022), and cART (Ikekpeazu et al., 2019) can independently induce oxidative stress and inflammation, this study evaluated effects on testicular health of the co-

existence of cART and alcohol abuse in a diabetic condition relative to inducible nitric oxide synthase (iNOS), oxidative stress, inflammation, apoptosis, and cell proliferation.

MATERIALS AND METHODS

Chemical and reagents

Streptozotocin (STZ) (S0130) was procured from Sigma-Aldrich Chemical Company (St. Louis, MO, USA) and Atripla, a fixed-dose combination antiretroviral drug was purchased from Bristol-Myers Squibb and Gilead Sciences (Foster City, CA, USA). The primary antibodies interleukin-1beta (IL-1β) (ab2105), interleukin-6 (IL-6) (ab9324), tumor necrosis factor-alpha (TNF-α) (ab6671), inducible nitric oxide synthase (iNOS) (ab115819), malondialdehyde (MDA) (ab243066), 8-hydroxydeoxyguanosine (8-OHDG) (ab62623), caspase 3 (ab4051), and Ki-67 (ab15580) were purchased from Abcam (Cambridge, MA, USA). The biotinylated goat anti-rabbit (BA-1000) and goat anti-mouse (BA-9200) secondary antibodies, and Avidin-Biotin Complex kit (ABC) (PK-6100) were purchased from Vector Laboratories (Burlingame, CA, USA).

Ethical clearance

The Animal Research Ethics committee (AREC) of University of the Witwatersrand (Wits) approved the animal study protocol with approval number 2018/011/58/C. All experiments were carried out at Wits Animal Research Facility (WARF) per the guidelines of AREC.

Animal husbandry

For investigation, 30 adult male Sprague Dawley rats (10 weeks old; weighing 330-370 grams) were used. Every rat was housed individually in a clean plastic cage at a room temperature of 21-23ºC, with a 12/12-hour light/dark cycle, and allowed free access to rat chow and water. Throughout the 90 days treatment duration, the rats freely accessed drinking water or alcohol, and rat chow according to respective treatment groupings.

Induction of type 2 diabetes

Type 2 diabetes mellitus was induced using a modified procedure described by Wilson & Islam, 2012. Briefly, rats were fed on a 20% fructose reconstituted rat chow diet for two weeks, after which a single injection of freshly prepared 40mg/kg STZ in 0.05M (pH 4.5) citrate buffer was administered intraperitoneally. Then, non-fasting blood glucose (non-fasting) levels were measured 72 hours after STZ administration and rats with glucose levels ≥ 250 mg/dl were

regarded as diabetic. Once the diabetic state was confirmed in rats, they were placed on a standard rat chow diet.

Experimental design

The rats were divided into five groups, each with six rats as follows. Control group, Diabetic (DM) group, diabetic rats treated with 10% v/v alcohol daily (DM+A) group, diabetic rats treated with an extrapolated human equivalent dose of 23.22 mg/kg of cART (consisting of efavirenz 600 mg + emtricitabine 200 mg + tenofovir 245 mg) (Frampton and Croom, 2006) in gelatine cubes daily (DM+cART), and diabetic rats treated with both alcohol and cART (DM+A+cART) group. The rats were treated for 90 days, after which they were weighed, anesthetized with 240mg/ml pentobarbitone, and terminated. The testes were then extracted and preserved in 10% neutral buffered formalin for subsequent processing.

Food and fluid intake

The amount of food and fluid consumed by each rat was recorded daily throughout the experimental period.

Body weight and gonadosomatic index

The rats were weighed before termination (final body weight) and testis weight was recorded immediately after their extraction. Then, the final body and testis weights were used to calculate the gonadosomatic index, using the formula previously reported by Olasile et al., 2018.

$$\text{Gonadosomatic index} = \frac{Testis\ weight}{Body\ weight} \times 100\ (\%)$$

Immunohistochemistry for oxidative stress, inflammatory, apoptosis, and proliferation biomarkers

The harvested and fixed testes were dehydrated sequentially in 70-100% alcohol grades and embedded in molten paraffin wax and sectioned at 5µm thickness using a Leica RM 2125 rotatory microtome. The sections were floated in a warm water bath (45^{o}c) for 60 seconds, then mounted onto silane-coated glass slides for antibody immunolabeling. The sections were dried overnight, followed by deparaffinizing in xylene, hydrating in a series of decreasing alcohol concentrations, and rinsing in running tap water for 5 minutes. The sections were incubated in citrate buffer overnight in a water bath at 60^{o}c for antigen retrieval. Then, sections were rinsed

in phosphate-buffered saline (PBS) for 5 minutes, thereafter, immersed in 1% hydrogen peroxide in methanol for 20 minutes to inhibit endogenous peroxidase. After rinsing in phosphate-buffered saline (PBS) for three changes of five minutes each, 5% normal goat serum was added to the sections to block nonspecific antibody binding. This was tapped off after 30 minutes, and the primary antibody was added subsequently (1:100 for anti-TNF-α and anti-iNOS, 1:200 for anti-IL-1β, anti-IL-6, anti-MDA, and anti-caspase 3, and 1:1000 for anti-8-OHDG and anti-Ki-67) and left overnight (approximately 16 hours) at 4°C. Thereafter, the sections were rinsed in PBS and incubated with the secondary antibody (1:1000 biotinylated goat anti-rabbit for the IL-1β, TNF-α, iNOS, caspase 3, and Ki-67 antibodies and 1: 1000 biotinylated goat anti-mouse for IL-6, MDA, and 8-OHDG antibodies) for 30 minutes. Then, after rinsing in PBS, avidin-biotin complex (ABC) reagent was added for 30 minutes. Afterward, the sections were rinsed in PBS and incubated with 3, 3'-diaminobenzidine tetrachloride (DAB) for five minutes. DAB was then washed off under running tap water for five minutes and the slides were dipped in hematoxylin for one minute to counter-stain. Followed by rinsing in running tap water to remove excess stain, dehydration of slides in alcohol series, and coverslipped with Dibutylphthalate Polystyrene Xylene (DPX). For the antibodies with immunoreactivity localized to cell nuclei (IL-6, 8-OHDG, caspase 3, and Ki-67), the total number of cell nuclei expressing immunoreactivity were counted in 20 rounded seminiferous tubules for each animal (i.e., 120 tubules for each group) at x400. The images of antibodies with immunoreactivity localized to both cell nucleus and cytoplasm (IL-1β, TNF-α, iNOS, and MDA) were captured in 144 microscopic fields at x100 for each group and were segmented using the ilastik pixel classification workflow. Further, ilastik software (v1.3.3; https://www.ilastik.org) was used for image segmentation, then Fiji software (v1.52e; https://imagej.net/Fiji) was used to quantify immunostaining in the image segments as we previously described (Owembabazi et al., 2023). Below is the procedure for quantifying Ki-67 staining intensity.

IHC staining intensity quantification

The Fiji software (v1.52e; https://imagej.net/Fiji) was used to measure the mean gray values (MGV) of selected stained regions of interest (ROI) as shown in figure 1 (Jensen, 2013; Cizkova et al., 2021). Worth noting is that the darker stained areas have a low MGV and the lightly stained areas have a high MGV, thus the staining intensity is equal to the MGV reciprocal (Cizkova et al., 2021). The steps followed for Ki-67 staining intensity quantification were as follows; opening the image in Fiji: File > Open > Select the image > Open; setting the

scale: Analyze > Set scale > Ok; drawing an ROI: Edit > Selection > Specify > Ok; selecting the parameters: Analyze > Set measurement (check the MGV box) > Ok; taking the measurement: Analyze > Measure; opening the next image: File > Open next; choosing the same ROI size and shape: Edit > Selection > Restore selection; proceed to take the measurement: Analyze > Measure; save the results as a CVS file for statistical analysis.

Thereafter, the staining intensity of Ki-67 was calculated as follows.

$$\text{Intensity} = \frac{1}{MGV} \quad \text{(Cizkova et al., 2021)}$$

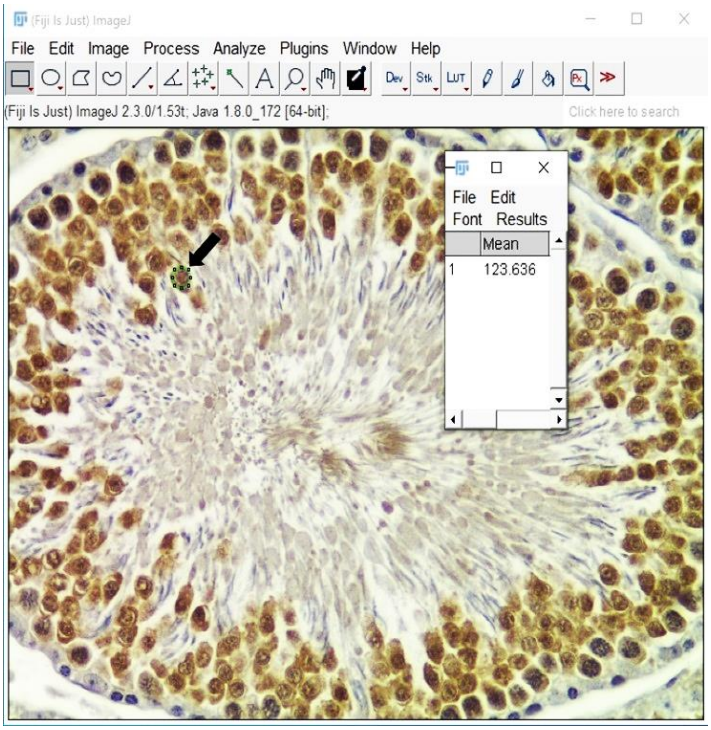


Figure 1: Representative Ki-67 image quantified in Fiji, the mean gray values of a selected region of interest (ROI) illustrated with a thick arrow.

Data analysis

The data were analyzed using the Windows version of GraphPad Prism 6 and the data was presented as Mean ± SEM. The group means were compared using one-way analysis of variance (ANOVA), and the Bonferroni *post hoc* test was performed for multiple comparisons. Deeming $P < 0.05$ value statistically significant.

RESULTS

Food and fluid intake

A general reduction in food intake was recorded in all treated groups relative to the control group but was significant in only DM+A ($p=0.0455$) and DM+A+cART ($p=0.0090$) treated rats (Fig. 2). In comparison with the control, fluid intake increased significantly ($p<0.0001$) in DM and DM+cART treated groups, however, an insignificant increase ($p>0.05$) was recorded in DM+A and DM+A+cART treated groups. Further, the fluid intake in DM and DM+cART was significantly increased ($p<0.0001$) relative to DM+A and DM+A+cART (Fig. 2).

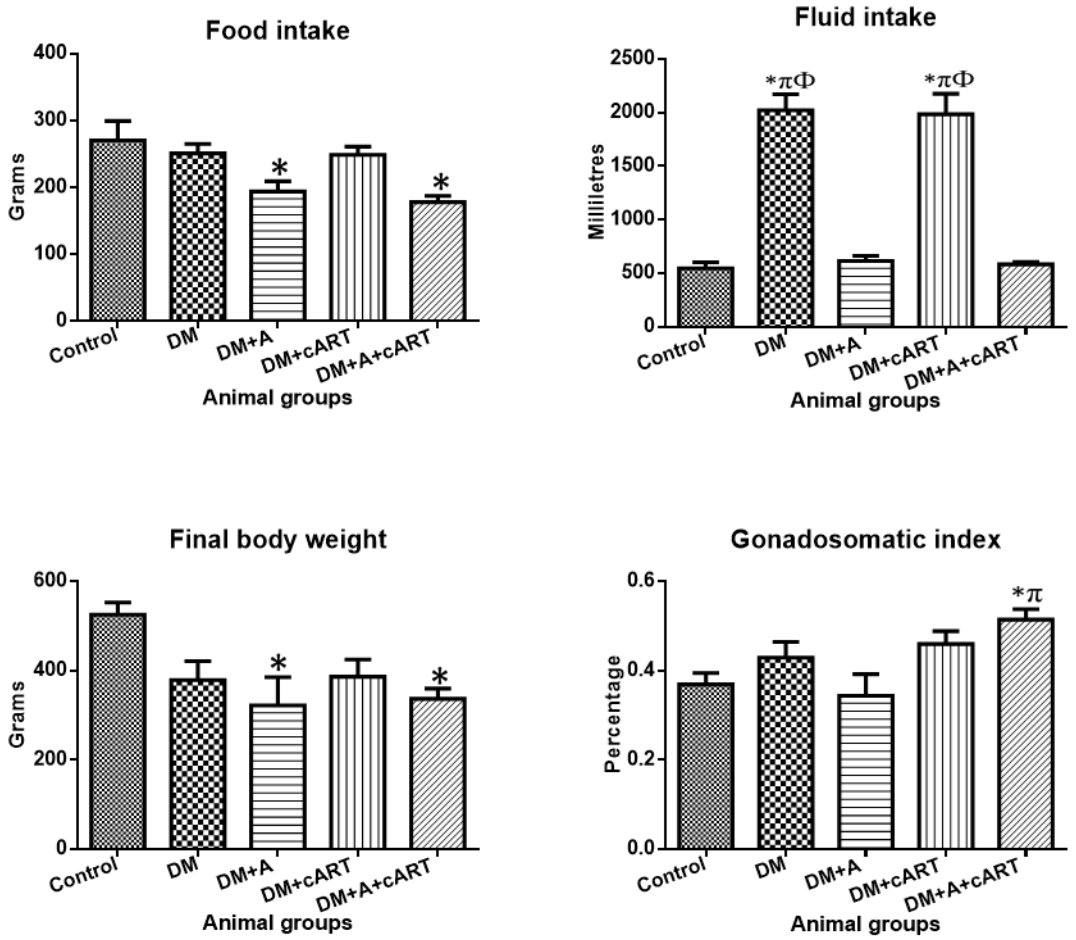


Figure 2: Graphs showing mean ± SEM food and fluid intake, final body weight, and gonadosomatic index. Different symbols *, π, and Φ represent significant differences ($p<0.05$) as analyzed by a Bonferroni's multiple comparison test; '*' significantly different compared to control, 'π' significantly increased compared to DM+A, and 'Φ' significantly increased compared to DM+A+cART. DM, diabetes; DM+A, diabetes and alcohol; DM+cART, diabetes

and combination antiretroviral therapy; DM+A+cART, diabetes and alcohol and combination antiretroviral therapy.

Body weight and gonadosomatic index

All treated groups showed a decrease in final body weight compared to the control, but a significant decrease was recorded in only DM+A ($p=0.0197$) and DM+A+cART ($p=0.0357$) treated groups (Fig. 2). Gonadosomatic index increased significantly in DM+A+cART relative to control ($p=0.0306$) and DM+A ($p=0.0190$). However, the gonadosomatic index of DM+A treated group was insignificantly deceased ($p>0.05$) compared to the control. Further, a non-significant increase ($p>0.05$) was recorded in the gonadosomatic index of DM and DM+cART treated groups relative to the control group (Fig. 2).

Oxidative stress biomarker immunoexpression

Expression of iNOS was found in the testicular interstitial cells, Leydig cells, and macrophages of the control and treated groups (Fig. 3). The DM, DM+cART, and DM+A+cART) treated groups had significantly increased iNOS expression compared to the control ($p<0.0001$ for all) and DM+A ($p=0.0005$, $p<0.0001$, and $p<0.0001$ respectively). The DM+A treated group iNOS expression increased significantly ($p=0.0041$) relative to the control group. Further, iNOS expression in DM+A+cART group was significantly increased compared to DM ($p<0.0001$) and DM+cART ($p=0.0003$). Similarly, immunostaining of MDA was detected in the Leydig cells and macrophages (Fig. 3). Compared to the control, the expression of MDA significantly increased in all treated groups (DM: $p<0.0001$, DM+A: $p<0.0001$, DM+cART: ($p=0.0041$, and DM+A+cART: $p<0.0001$). Also, the MDA expression in DM+A treated group increased significantly ($p<0.0001$) compared to the other treated groups. Furthermore, DM group MDA expression was significantly increased ($p=0.0004$) compared to DM+cART. The control and treated groups showed 8-OHDG immunostaining in the spermatogenic cells (Fig. 3). The 8-OHDG immunostaining of all treated groups increased significantly ($p<0.0001$) compared to control, whilst the expression in the DM+A treated group was respectively significantly increased ($p<0.0001$) compared to the other treated groups (DM, DM+cART, and DM+A+cART).

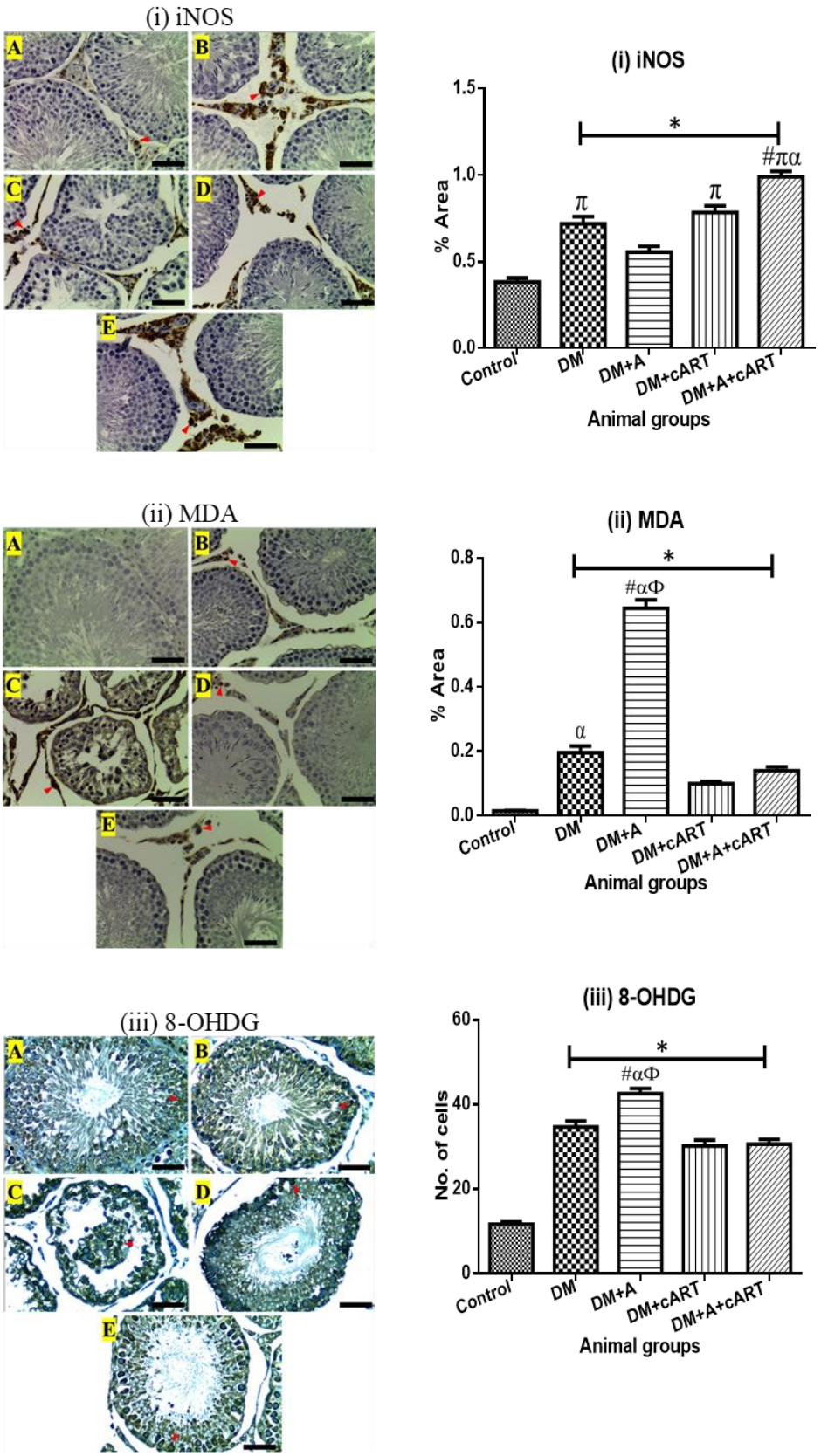


Figure 3: Photomicrographs of oxidative stress markers immunoexpression and respective mean of expression graphs. Representative immunoreactivity is indicated with arrowhead. The mean ± SEM percentage area of expression for iNOS and MDA, and the mean number of cells

expressing 8-OHDG were reported. Different symbols *, #, π, α, and Φ represent significant differences ($p<0.05$) as analyzed by a Bonferroni's multiple comparison test; '*' significantly increased compared to control, '#' significantly increased compared to DM, 'π' significantly increased compared to DM+A, 'α' significantly increased compared to DM+cART, and 'Φ' significantly increased compared to DM+A+cART. Magnification, x400; scale bar, 50μm. Key: Image: A; control group, B; DM group, C; DM+A group, D; DM+cART group, and E; DM+A+cART group DM, diabetes; DM+A, diabetes and alcohol; DM+cART, diabetes and combination antiretroviral therapy; DM+A+cART, diabetes and alcohol and combination antiretroviral therapy.

Proinflammatory cytokine immunoexpression

The interleukin-1beta (IL-1β) immunostaining was observed in the testicular interstitial cells, macrophages, and Leydig cells of the control and treated groups, except in DM+A treated group that showed IL-1β immunostaining in the germinal epithelium as well (Fig. 4). All treated groups (DM, DM+A, DM+cART, and DM+A+cART) showed significant increases in IL-1β expression in comparison with the control group ($p<0.0001$, $p<0.0001$, $p=0.0389$, and $p=0.0095$ respectively). Moreso, the expression of IL-1β in the DM group was significantly increased compared to DM+A ($p=0.0005$), DM+cART ($p<0.0001$), and DM+A+cART ($p<0.0001$) treated groups. The interleukin-6 (IL-6) immunostaining in both control and treated groups was detected in Sertoli cells, macrophages, and Leydig cells, except the DM+A group which had immunostaining in only a few Sertoli cells (Fig. 4). For this study, only immunostained Sertoli cells were quantified. The IL-6 expression in DM, DM+cART, and DM+A+cART treated groups increased significantly ($p<0.0001$) compared to control and DM+A. However, DM+A treated group had a significantly decreased ($p<0.0001$) IL-6 expression compared to control. Additionally, DM+cART group IL-6 expression was significantly increased compared to DM ($p<0.0001$) and DM+A+cART ($p=0.0001$), the IL-6 expression in DM+A+cART was increased significantly ($p<0.0001$) compared to DM group. Further, tumor necrosis factor-alpha (TNF-α) immunostaining was similar to that of IL-1β mentioned above. In comparison with control, TNF-α expression increased significantly in all treated groups (DM: $p=0.0016$, DM+A: $p<0.0001$, DM+cART: $p<0.0001$, and DM+A+cART: $p=0.0019$) (Fig. 4).

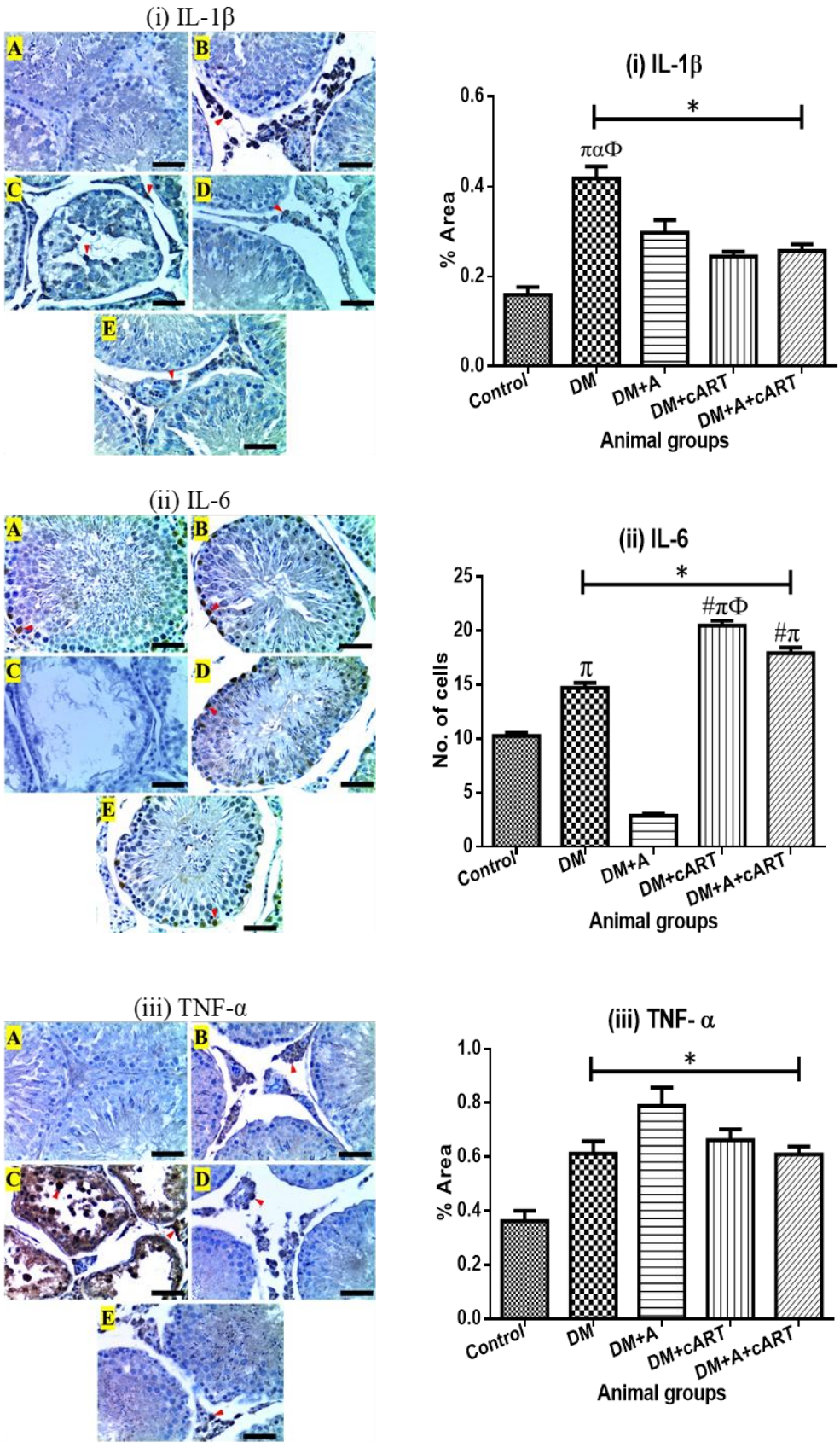


Figure 4: Photomicrographs of cytokine expression and respective mean of expression graphs. Representative immunoreactivity is indicated with arrowhead. The mean ± SEM percentage

area of expression for IL-1β and TNF-α, and the number of cells expressing IL-6 were reported. Different symbols *, #, π, α, and Φ represent significant differences ($p<0.05$) as analyzed by a Bonferroni's multiple comparison test; '*' significantly different compared to control, '#' significantly increased compared to DM, 'π' significantly increased compared to DM+A, 'α' significantly increased compared to DM+cART, and 'Φ' significantly increased compared to DM+A+cART. Magnification, x400; scale bar, 50µm. Key: Image: A; control group, B; DM group, C; DM+A group, D; DM+cART group, and E; DM+A+cART group. DM, diabetes; DM+A, diabetes and alcohol; DM+cART, diabetes and combination antiretroviral therapy; DM+A+cART, diabetes and alcohol and combination antiretroviral therapy.

Apoptosis marker, caspase 3 immunoexpression

Caspase 3 immunostaining was detected in the germinal epithelium cells of both control and treated groups (Fig. 5). Compared to the control, all treated groups showed a significant increase ($p<0.0001$) in the number of germ cells expressing caspase 3. However, the expression of caspase 3 was significantly increased in DM+A treated group in comparison with other treated groups (DM: $p=0.0385$, DM+cART: $p<0.0001$, and DM+A+cART: $p<0.0001$). and the expression in DM treated group increased significantly ($p=0.0002$) compared to DM+A+cART treated group.

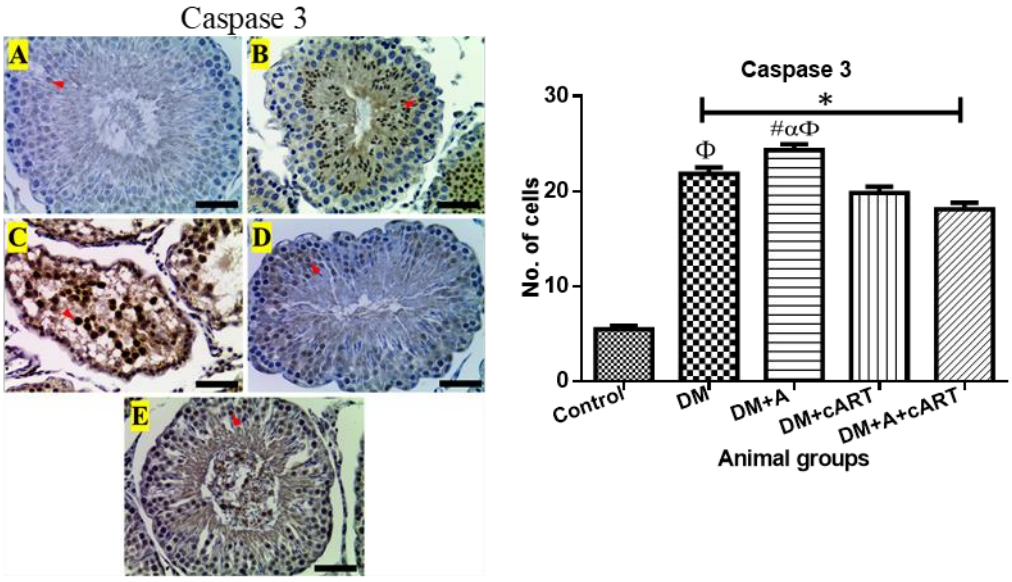


Figure 5: Representative photomicrographs showing caspase 3 expression (arrowheads) and a graph showing the mean ± SEM number of immunostained cells. Different symbols *, #, α, and Φ represent significant differences ($p<0.05$) as analyzed by a Bonferroni's multiple comparison test; '*' significantly increased compared to control, '#' significantly increased

compared to DM, 'α' significantly increased compared to DM+cART, and 'Φ' significantly increased compared to DM+A+cART. Magnification, x400; scale bar, 50µm. Key: Image: A; control group, B; DM group, C; DM+A group, D; DM+cART group, and E; DM+A+cART group. DM, diabetes; DM+A, diabetes and alcohol; DM+cART, diabetes and combination antiretroviral therapy; DM+A+cART, diabetes and alcohol and combination antiretroviral therapy.

Proliferation marker, Ki-67 immunoexpression

The Ki-67 expression was found in germ cells, majorly the spermatocytes and round spermatids of the control and treated groups (Fig. 6). A significant reduction in the number of germ cells expressing Ki-67 was detected in all treated groups ($p<0.0001$) in comparison with control. Ki-67 expression in DM+A treated group reduced significantly ($p<0.0001$) compared to the other treated groups, and the expression in DM group was also respectively significantly reduced ($p<0.0001$) when compared with treated groups DM+cART and DM+A+cART. However, Ki-67 staining intensity increased significantly ($p<0.0001$) in all treated groups compared to the control. The intensity of Ki-67 in DM+A group was significantly increased ($p<0.0001$) in comparison with the other treated groups, and the intensity in DM and DM+A+cART treated groups increased significantly ($p<0.0001$) compared with DM+cART treated group.

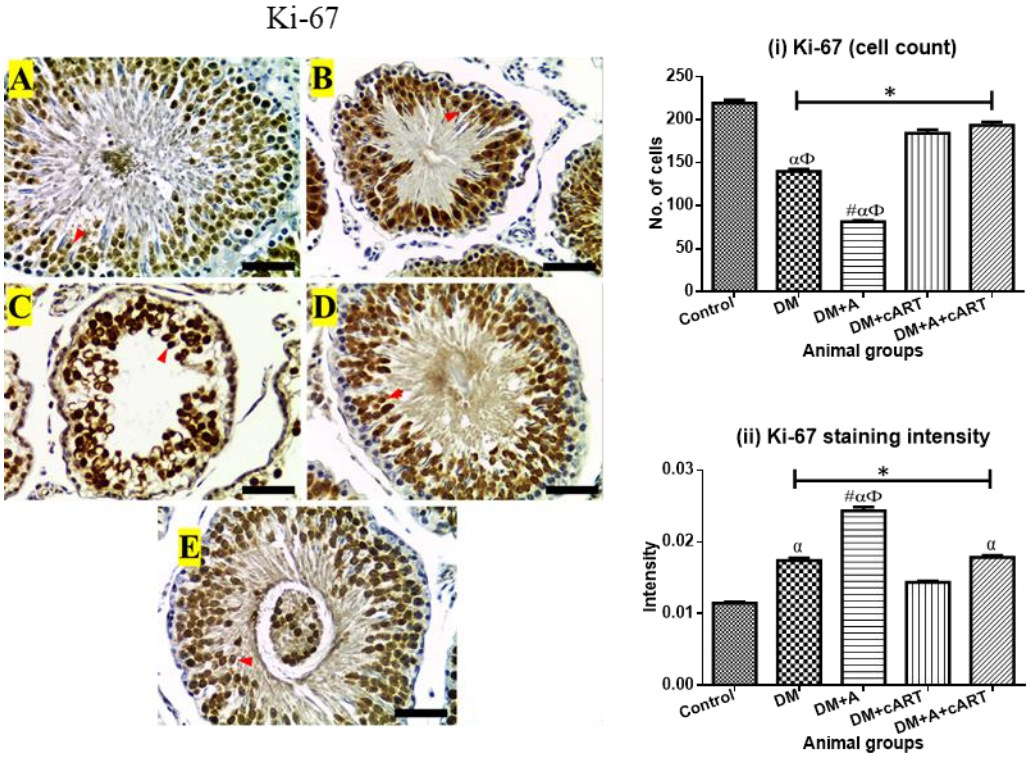


Figure 6: Representative photomicrographs showing Ki-67 expression (arrowheads) and respective graphs of the mean ± SEM number of immunostained cells and staining intensity. Different symbols *, #, α, and Φ represent significant differences ($p<0.05$) as analyzed by a Bonferroni's multiple comparison test; '*' significantly different compared to control, '#' significantly different compared to DM, 'α' significantly different compared to DM+cART, and 'Φ' significantly different compared to DM+A+cART. Magnification, x400; scale bar, 50μm. Key: Image: A; control group, B; DM group, C; DM+A group, D; DM+cART group, and E; DM+A+cART group. DM, diabetes; DM+A, diabetes and alcohol; DM+cART, diabetes and combination antiretroviral therapy; DM+A+cART, diabetes and alcohol and combination antiretroviral therapy.

DISCUSSION

Diabetes and combination antiretroviral therapy (cART) regimen due to HIV infection are a huge public health concern (Bam et al., 2020), and alcohol abuse as a lifestyle is also prevalent in society (Trangenstein et al., 2018). The prevalence of these trio (diabetes, alcohol abuse, and cART use) and their co-existence in one individual is increasing especially in sub-Saharan Africa and in males of reproductive age (Pourentezari et al., 2016; Avari and Devendra, 2017). Consistent with previous studies (Sultan et al., 2014; Olasile et al., 2018), our results showed that the treated groups had a decreased food intake but had an increased fluid intake compared to the control group. This observation could be attributed to diabetes-associated metabolism dysregulation, polydipsia, and polyuria (Olasile et al., 2018). Further, while the final body weight of all treated groups decreased, an increase was found in their gonadosomatic index (GSI) except the DM+A (diabetic animals treated with alcohol) group had a slightly decreased GSI compared to the control. GSI is an indicator of reproductive output, both increased and decreased GSI implicate impairment in testicular structure and function (Santos et al., 2020; Babaei et al., 2021). Since diabetes is known to cause body weight loss (Sultan et al., 2014) and GSI is the ratio of the gonad (testis) weight to body weight (Sultan et al., 2014; Nna et al., 2019), thus increased GSI is suggestive of an increase in testicular weight which could be due to fibrosis and/or inflammation (Santos et al., 2020). Further, a decreased GSI reflects a reduction in testis weight that could have resulted from tissue degeneration (Nna et al., 2019; Babaei et al., 2021).

In this study, highly significant upregulation of oxidative stress biomarkers evaluated, inducible nitric oxide synthase (iNOS), malondialdehyde (MDA), and 8-hydroxydeoxyguanosine (8-OHDG) in the testis of all treated groups were recorded relative to control. Oxidative stress plays a major role in the pathogenesis of testicular dysfunctions (Wu et al., 2020; Dutta et al., 2021), and incidentally, diabetes, alcohol, and cART are well-established oxidative stress inducers (Barcia et al., 2015; Ogedengbe, Naidu and Azu, 2018; Finelli et al., 2022). Corroborating with the results of this study, increased expression of iNOS has been previously reported in testis of diabetic rats (Sönmez et al., 2016), rats exposed to alcohol (Eid et al., 2011), and those treated with cART (Akhigbe, Hamed and Aremu, 2021). Moreover, a clinical study by Coştur et al., (2012) observed an intense iNOS expression in the testis of azoospermic patients. Remarkably, iNOS was greatly upregulated in diabetic animals treated with both alcohol and cART compared to other treated and control groups, suggesting a heightened oxidative stress induction due to interaction between chemicals (alcohol and cART) and disease (diabetes). In the same vein, the result further showed that cART treatment significantly upregulated iNOS more than alcohol.

Earlier studies have established that iNOS plays a key role in induction of testicular oxidative stress and its dysfunction through catalysis of nitric oxide production (Kolasa et al., 2009; Aprioku, 2013; Yu et al., 2017). Though nitric oxide level was not determined in the present study, the upregulation of iNOS would imply an increase in nitric oxide (Coştur et al., 2012; Nna et al., 2019). Nitric oxide is a free radical generated during normal mitochondrial oxidative phosphorylation and synthesized by enzymatic conversion of L-arginine to L-citrulline catalyzed by nitric oxide synthase (NOS) (Kolasa et al., 2009; Yu et al., 2017). Further, nitric oxide serves as a signaling molecule in several physiological processes (Levine et al., 2012). At low concentrations (<1µM), nitric oxide promotes homeostasis, cell proliferation, and survival, but elevated nitric oxide levels (>1µM) which may occur following induction of oxidative stress by chemical insults stimulate spermatogenic cell proliferation arrest and apoptosis (Turner and Lysiak, 2008; Aprioku, 2013; Zhu et al., 2019). This conforms with the significant germ cell loss and distortions of seminiferous tubules amongst other seminiferous lesions observed in the testis of treated animals.

Furthermore, testis tissue has relatively high amounts of unsaturated fatty acids compared to other tissues (Asadi et al., 2017; Guerriero et al., 2014) and Leydig cell also utilizes an immense amount of fatty acids during the biosynthesis of testosterone (Koganti et al., 2022) and are very

susceptible to lipid peroxidation (Wang et al., 2017). Moreover, macrophages which are a main source of iNOS/NO lie adjacent to macrophages in the testicular interstitium, making the Leydig cells immediate targets of iNOS/NO activity (Kolasa et al., 2009; Coştur et al., 2012). Consequently, high testicular iNOS/NO levels stimulate lipid peroxidation leading to production of unsaturated reactive aldehyde, malondialdehyde (MDA) (Violi et al., 1999; Zhu et al., 2019). Accordingly, elevated MDA levels were recorded in all treated groups, the diabetic animals treated with alcohol (DM+A group) had the highest MDA levels. Our findings agree with previous studies that recorded increased MDA levels in testis tissue homogenate of rats that were diabetic (Khairuddin et al., 2020), exposed to alcohol (Oremosu and Akang, 2015), and treated with cART (Ikekpeazu et al., 2019). Elevation of MDA levels is evidence of lipid peroxidation which causes testicular cell disintegration and subsequently results in steroidogenesis and spermatogenesis impairments (Violi et al., 1999; Levine et al., 2012; Su et al., 2019).

Additionally, testicular iNOS/NO upregulation stimulates an increased formation of reactive oxygen species (ROS) and lowers cellular antioxidant production (Levine et al., 2012). ROS is a potent mediator of DNA oxidation and consequently leads to DNA breakdown and generation of 8-hydroxydeoxyguanosine (8-OHDG) (Nakae et al., 2000). Conversely, increased nuclear 8-OHDG is an indicator of testicular oxidative stress (Wu et al., 2020; Dutta et al., 2021), and has been suggested to be involved in the induction of several mutations such as transitions, deletions, frameshifts, and epigenetic changes, and these could in turn lead to infertility and genetic disorders in offspring (Nakae et al., 2000; Wu et al., 2020). Therefore, the increased levels of 8-OHDG observed in the testis of treated animal groups suggests severe oxidative stress induced by the treatments, the highest upregulation recorded in diabetic-alcohol treated groups may reflect the severe adverse effects of alcohol abuse in diabetic condition. In corroboration, previous studies have reported increased testicular DNA fragmentation in rats treated with alcohol (Eid et al., 2011) and cART (Akhigbe, Hamed and Aremu, 2021), which adversely affect male reproductive capacity.

Previous studies have demonstrated that elevated iNOS/NO levels stimulate testicular inflammation via the nuclear factor- kβ (NF-kβ) pathway (Levine et al., 2012; Su et al., 2019), leading to the release of cytokines such as interleukin-1β (IL-1β), interleukin-6 (IL-6), tumor necrosis factor-α (TNF-α), and interferons (IFNs) (Aprioku, 2013; Nna et al., 2019). Although NF-kβ antibody immunostaining was nonspecific (not reported) in the present study, earlier

studies have demonstrated increased testicular NF- kβ in conditions associated with testicular oxidative stress and inflammation (Barcia et al., 2015; Dutta et al., 2021). We found significantly elevated levels of testicular pro-inflammatory cytokines such as IL-1β, IL-6, and TNF-α in the treated groups, except for the DM+A group (diabetic animals treated with alcohol) that had a significantly decreased IL-6 expression relative to the control group. This observation suggests that the treatments induced inflammation in the testis tissue, conversely, other studies have reported elevated levels of proinflammatory cytokines (IL-1β and TNF-α) in testicular tissue homogenate of diabetic rats (Khairuddin et al., 2020) and those treated with cART alone (Akhigbe, Hamed and Aremu, 2021). Further, since IL-6 is majorly expressed by Sertoli cells (Białas et al., 2009), the extensive Sertoli cell degeneration observed in the testis of DM+A group may be linked to the significant IL-6 reduction and other associated adverse effects recorded in this group.

Earlier reports have demonstrated increased levels of pro-inflammatory cytokines in testicular injury, infection, ischemia, and toxicosis (Białas et al., 2009; Pérez et al., 2013; Loveland et al., 2017). Upregulation of testicular cytokines is associated with suppressed steroidogenesis, disruption of blood-testis barrier (BTB) integrity, and diminished spermatozoa viability, subsequently leading to spermatogenesis and fertility impairments (Zhang et al., 2014; Alves-Silva et al., 2021). Furthermore, studies show that both increase and decrease in the expression of IL-1β (de Oliveira et al., 2021) and TNF-α (Suh et al., 2008) can be detrimental to Leydig cell function, through inhibition of Leydig cell cytochrome P450 steroidogenic enzymes (CYP11A1 and CYP17A1) (Suh et al., 2008; de Oliveira et al., 2021). Therefore, alternations in testicular cytokines recorded in this study corroborates earlier reports and conform with the testicular structure and cellular derangements, that eventually cause steroidogenesis and spermatogenesis failure.

Consequently, accumulation of ROS (oxidative stress) and cytokines (inflammation) are both triggers of testicular cell apoptosis (Nna et al., 2019; Asadi et al., 2021). Our results revealed that immuno-expression of caspase 3 increased significantly in testis of treated groups relative to the control. Notably, caspase 3 is a key effector protease that cleaves structural and cell cycle proteins during both extrinsic and intrinsic apoptotic pathways leading to cell death (Jana et al., 2010; Sharma and Agarwal, 2013; El-Mehi and Faried, 2019). Less testicular toxicosis has previously been reported in animals that are diabetic (Sisman et al., 2014; Nna et al., 2019), exposed to alcohol (Nishi et al., 2018; Liu et al., 2020), and treated with cART (Azu et al.,

2014; Akhigbe, Hamed and Aremu, 2021). Also, a significant decrease in the number of germ cells expressing Ki-67 but with strong staining intensity was recorded in the treated groups suggesting a disruption of germ cell proliferation and spermatogenesis dysfunction. Similar findings have been demonstrated in cryptorchidism (Moon et al., 2014) and fluoride-induced testicular toxicity (Zhao et al., 2018).

CONCLUSION

This study demonstrated that diabetes, alcohol, cART, and their concurrency trigger testicular oxidative stress, inflammation, and apoptosis and disruption of spermatogenic cell proliferation, leading to testis structural and spermatogenesis derangement. Our results suggest that the deleterious impacts of alcohol consumption or/and cART in diabetic condition on the testis may amongst others be mediated through iNOS upregulation that triggers reactive oxygen species accumulation, and in turn stimulates testicular oxidative stress and inflammation with resultant dysregulation of testis structure and function. Generally, the greatest perturbations were observed in testis of diabetic animals exposed to alcohol, cART, and both. The current study highlights the possible critical male reproductive health impact of multimorbidity of alcohol abuse and cART therapy that may arise amongst diabetic patients and further, gives clinical insight into the management of reproductive dysfunctions emerging in male diabetic patients living with HIV/AIDS who take cART and regularly consume alcohol.

CHAPTER 8: GENERAL DISCUSSION, CONCLUSION, AND RECOMMENDATIONS

8.1 Preamble

Currently, declining fertility factor is a major global health concern (Skakkebæk et al., 2022). Infertility affects 15% of couples worldwide, with more than 50% of the cases in males (Agarwal et al., 2021). An annual increase of 0·291% in male infertility was documented by the global burden of disease survey (Sun et al., 2019). Infertility is associated with socio-physiological challenges that diminish the quality of life and in males, it is considered a health-impairing condition especially when hypogonadism or/and sexual dysfunction is/are present (Ventimiglia et al., 2016; Lotti and Maggi, 2018). Myriad aetiologies have been implicated in male infertility, these include physical factors (age and weight) (Agarwal et al., 2021), lifestyle (diet, inactivity, alcohol consumption, and illicit drug use) (Sansone et al., 2018), psychological (anxiety, depression, and trauma) (Dutta et al., 2021), pathologies (non-communicable and infectious diseases) (Naz and Kamal, 2017), medication (opioids, endocrine disruptors, and long-term drugs) (Owyong and Ramasamy, 2018), and environmental (heat, radiations, chemicals, and heavy metals) (Skakkebæk et al., 2022). Conversely, the fast-rising conditions viz. diabetes, alcohol abuse, and cART use are predominant in males of reproductive age (Kalra et al., 2011; Pourentezari et al., 2016; Mann, Morrow, et al., 2020). This infers that they would experience a longer period of exposure to these conditions, which is worrisome because of the multiple long-term organ dysfunctions associated with diabetes, alcohol, and cART (Ogedengbe, Naidu and Azu, 2018; Volpe et al., 2018).

Earlier studies have reported increased production of reactive oxygen species (ROS) during diabetes (Blake and Trounce, 2014), alcohol abuse (Das and Vasudevan, 2007), and cART use (Ikekpeazu et al., 2019), which subsequently trigger oxidative stress (OS) and inflammation (Barcia et al., 2015; Ogedengbe, Naidu and Azu, 2018). These (OS and inflammation) are key factors in the pathogenesis of diabetes, alcohol, and cART induced multi-organ complications (Volpe et al., 2018; Ikekpeazu et al., 2019; Finelli et al., 2022). Incidentally, OS and inflammation are common features in conditions that damage the structure and functioning of the testis (Dutta et al., 2021). Accordingly, diabetes, alcohol, and cART have each been shown to negatively impact the male reproductive system (Azu, 2012; Condorelli et al., 2018; Finelli et al., 2022). Clinical and experimental studies have demonstrated hypothalamic-pituitary-gonadal (HPG) axis impairment, sexual dysfunctions, seminal fluid alterations, poor sperm quality, and testicular structural derangement in diabetes condition (Gandhi and Dagur, 2016;

Condorelli et al., 2018; Long et al., 2018; Ray and Pramanik, 2020), alcohol abuse (Rachdaoui and Sarkar, 2013; Dosumu et al., 2014; Oremosu and Akang, 2015; Finelli et al., 2022), and cART use (Kushnir and Lewis, 2011; Azu et al., 2014; Ogedengbe et al., 2016; Savasi et al., 2018).

Moreover, diabetes, alcohol, and cART have an intricate connection. While alcohol is a potent risk factor for diabetes (Rehm, 2011; Goecke and Baumeister, 2021) and the spread of HIV, which leads to cART use (Watson et al., 2014; Kumar et al., 2015; Schneider et al., 2016; Scott-Sheldon et al., 2016). A high incidence of alcohol consumption, majorly for euphoric purposes has been reported amongst people living with HIV including those on cART (McCance-Katz et al., 2013; Mondal et al., 2019). Unfortunately, both HIV infection and cART are associated with increased diabetes onset (Avari and Devendra, 2017; Bam et al., 2020), suggesting their possible simultaneous co-existence of in the body or in an individual. Therefore, impact of using alcohol and cART concurrently during a diabetic health condition was evaluated to determine the effect on the functioning of HPG axis and testis, and testicular structure integrity based on morphometry changes, alterations in reproductive hormone levels, oxidative stress, inflammation, apoptosis, germ cell proliferation, and androgen receptor expression in diabetic rats exposed to alcohol and/or cART regimen of extrapolated daily recommended cART dose in animals.

8.1.1 The effect of diabetes, alcohol, cART, and their combinations on testicular morphometry

The application of morphometry techniques in testicular toxicology and/or histomorphology studies is scientifically accepted and adopted (Lanning et al., 2002; Azu et al., 2014). Using this technique, the study findings revealed a general alteration (increase or decrease) in all treated groups (A, cART, A+cART, DM, DM+A, DM+cART, and DM+A+cART) relative to control group, in all the parameters evaluated which included testis weight, volume, and size, the epithelial area fraction, epithelial height, tubule area and diameter, luminal area fraction and luminal diameter. Additionally, connective tissue and interstitial area fraction values were similarly significantly increased in all treated groups. These changes were consistent previous report on adverse impact of diabetes (Trindade et al., 2013), alcohol consumption (Dosumu et al., 2014), and cART use (Ogedengbe et al., 2016) on testicular morphometry parameters. Morphometric parameters reflect the state of testis tissue (Monteiro, Luis, and Predes, 2012; Soliman et al., 2014), consequently, the observed changes indicate structural derangement and dysfunction of the testis (Liu et al., 2009; Vidal and Whitney, 2014). The organ morpho-

functional relationship is scientifically established and underline the functional or pathology organ output.

8.1.2 The effect of diabetes, alcohol, cART, and their combinations on spermatogenic germ cells

The assessment of the number of different testicular spermatogenic epithelial cells viz. spermatogonia, spermatocytes, round spermatids, and elongated spermatids also showed alterations (increase and decreases) in the treated groups (A, cART, DM, and DM+A+cART) compared to the control group, suggesting testicular toxicosis due to the treatments. These changes agree with alterations reported in previous reports which found increased spermatogonia in non-obstructive azoospermia patients (Fietz et al., 2020), and possibly suggests an attempt to increase in the germ cell pool in response to a decline in spermatogenesis (Griswold, 2016; Pohl et al., 2019). However, with exception of spermatocytes number in alcohol group. Similar other in vivo studies have reported germ cell depletion, decreased sperm quality, and increased immotile sperms (Ogedengbe et al., 2018; Olasile et al., 2018; Olojede et al., 2022). This indicates that the treatments are deleterious to germ cells, and consequently will lead to dysfunctions of the process of spermatogenesis and possible associated fertility problems.

8.1.3 The effect of diabetes, alcohol, cART, and their combinations on testicular somatic cells

The decrease in the number of Sertoli cells and in the Leydig cell diameter and volume in all the treated groups (A, cART, A+cART, DM, DM+A, DM+cART, and DM+A+cART) compared to the control group, suggest reduction and disturbance of their crucial critical role in the maintenance of spermatogenesis, through their physiological control of male reproductive hormone regulation. Additionally, the reduction of Sertoli cell number may adversely affect male reproductive function since in adult testis, Sertoli cells play a role in the retention of normal adult Leydig cell population and also support the function of normal peritubular myoid cell. Consequently, the process of spermatogenesis and reproductive processes will be adversely impacted and may result in fertility problems (Rebourcet et al., 2017). Additionally, consistent with our results, previous studies have demonstrated deleterious effects of diabetes (Kianifard et al., 2012; Meskari et al., 2018), alcohol (Emanuele and Emanuele, 1998; Giannessi et al., 2015), and cART (Olasile et al., 2018; Olojede et al., 2022) on Sertoli and Leydig cells and in the present study the adverse effects of the combined alcohol and/or cART in diabetes..

8.1.4 The effect of diabetes, alcohol, cART, and their combinations on testis histology

The significant reduction in Johnsen's testicular score in all the treated groups (A, A+cART, DM, and DM+A) relative to the control group points to adverse implications of the treatments on the testicular histomorphology architecture. The testicular histology alterations indicate deleterious impacts of the treatments on the testis structure and function (Lanning et al., 2002; Vidal and Whitney, 2014). Johnsen's score is a widely used histological evaluation tool for profiling the progress of spermatogenesis in animal and human testis (Mushtaq et al., 2013; Ito et al., 2020; Thanh et al., 2020). Similar findings were previously reported in STZ-induced diabetes (Long et al., 2018) and in mice treated with alcohol (Liu et al., 2020). Numerous studies have shown that a reduction in Johnsen's score is linked to incomplete/unsuccessful spermatogenesis and inadequate spermatozoa production (Teixeira et al., 2019; Ito et al., 2020). Additionally, varying severity of seminiferous tubules (ST) lesions such as atrophied ST, lifting of epithelium, widened intercellular space, karyolysis, epithelial sloughing, multinucleated giant cells, and germinal epithelium derangement were observed across the treated animal group, this was parallel with previous studies (Ogedengbe et al., 2018; Olasile et al., 2018; Olojede et al., 2022).

8.1.5 The effect of diabetes, alcohol, cART, and their combinations on testicular connective tissue

The significant increase in the ST basement membrane and testicular capsule thicknesses in the treatment groups (A+cART, DM+A, and DM+A+cART) compared to the control group and suggests alteration on the structural integrity of these structures which will ultimately adversely affect their function in the productive processes. The increased thickness may be due to decrease in the compactness of the ST basement membrane and testicular capsule. The observed general increase in testicular capsule and seminiferous tubule basement membrane thickness of the treated groups compared to the control, but with significant increase recorded in A+cART and cART treated animals, may suggest structural alterations induced by treatments, which will lead to capsular and seminiferous tubule basement membrane dysfunctions (Ogedengbe et al., 2016; Olasile et al., 2018). These changes complement the decrease in the components of connective tissue (collagen, reticulin, and elastin) recorded in testis of all treated animals. Conversely, earlier studies demonstrated elevated collagenase enzyme activity in diabetes (Huang and Kyriakides, 2020), alcohol abuse (Kanbak et al., 2012) and cART use (Hansen et al., 2013), which causes fibroblast dysfunction and increased

connective tissue fibre degradation, and consequently lead to a reduction in connective tissue deposit (Kanbak et al., 2012; Hansen et al., 2013). In addition, Ranzer et al., (2011) found that decreased fibroblast proliferative activity and its type 1 collagen synthesis capacity led to a reduction of collagen content following alcohol exposure. However, due to a shared cytochrome P450 metabolic pathway, the interaction between the treatment chemicals (alcohol and cART) could mildly diminish some of their independent impacts as reflected by the lesser decrease in collagen content in testis of animals treated with both alcohol and cART (A+cART group).

8.1.6 The effect of diabetes, alcohol, cART, and their combinations on reproductive hormones

The treatments generally and variably affected the hormonal levels indicating possible disturbances of the steroidogenic processes involved in spermatogenesis. In this study, LH was significantly elevated in A and A+cART groups but significantly reduced in the DM+A+cART group. However, FSH increased significantly in all treated, with exception of the DM+cART group. The level of testosterone was significantly reduced in DM, DM+A, and DM+A+cART groups, but no significant difference ($p>0.05$) was found in the inhibin B level of all treated groups compared to the control. Previous studies have shown that changes in reproductive hormone levels implicate a disruption in HPG axis function, which adversely affects testicular functions (Corradi et al., 2016; Olojede et al., 2022). Our findings suggest that the treatments interfered with Leydig cell steroidogenic activity, leading to low levels of TT, and in response, the pituitary increases the secretion of gonadotropin (LH and FSH) (La Vignera et al., 2012). However, the low LH levels in the DM+A+cART group when TT is significantly reduced could imply that this treatment impaired the TT-LH feedback mechanism. Dysfunctions of the HPG axis and the hormone feedback loop are associated with impaired steroidogenesis and spermatogenesis (Clavijo and Hsiao, 2018; Sengupta et al., 2022).

8.1.7 The effect of diabetes, alcohol, cART, and their combinations on the expression of testicular androgen receptor

Study findings revealed a significant reduction in the intensity and number of Sertoli and Leydig cells expressing androgen receptors (AR) in all treated groups (A, cART, A+cART, DM, DM+A, DM+cART, and DM+A+cART), except for the number of Sertoli cells expressing AR in the alcohol (A) group. The insignificant reduction of Sertoli cells expressing AR recorded in the testis of animals treated with only alcohol is suggested to contribute to

restoration of testicular function following abstinence from alcohol as previously reported (Vicari et al., 2002; Dosumu, Osinubi, and Duru, 2014; Guthauser et al, 2014). Conversely, loss of AR and suppression of its action has been observed following exposure to some medical drugs and chemicals such as organochlorinated pesticides, industrial chemicals, and plasticizers (Luccio-Camelo and Prins, 2011; de Oliveira et al., 2021). A study by Qiu et al., (2013) demonstrated a downregulation of AR expression in the testis of rats administered with bisphenol A (BPA), leading to spermatogenesis dysfunction (Qiu et al., 2013). Furthermore, studies using AR knockout (ARKO) and transgenic AR disruption animal models have demonstrated that AR is required for development and maintenance of male reproductive organs, and the initiation and regulation of spermatogenesis (Yeh et al., 2002; Wang et al., 2009). Consequently, the downregulation of AR expression has been previously reported to be linked to testicular dysfunctions (Luccio-Camelo and Prins, 2011; O'Hara and Smith, 2015) and the reduced AR expression may imply disruption of receptor structural integrity with its resultant adverse impact on spermatogenesis via depletion of AR, which is consistent with previous study reports (Qiu et al., 2013; de Oliveira et al., 2021). In addition to the testis, AR is expressed in other reproductive organs including the epididymis and prostate, and non-reproductive organs including the liver, brain, and muscle. Thus, the AR-testosterone signalling is involved in regulation of several physiological processes such as reproductive, musculoskeletal, metabolic, cardiovascular, nervous, immune, and hemopoiesis is thus essential for the maintenance of male fecundity and well-being (Davey and Grossmann, 2016; Martin, 2016; Lotti et al., 2021).

8.1.8 The effect of diabetes, alcohol, cART, and their combinations on the expression of oxidative stress markers in the testis

Oxidative stress (OS), a state of elevated reactive oxygen species (ROS), is a common factor in testicular dysfunctions and mediates cellular damages through lipids, proteins and DNA damages. Oxidative stress has been associated with numerous pathologies (Turner and Lysiak, 2008; Tremellen, 2012; Sakr and Nooh, 2013; Asadi et al., 2017; Wu et al., 2020; Dutta et al., 2021). The significant increase in testicular expression of oxidative stress biomarkers viz. inducible nitric oxide synthase (iNOS), malondialdehyde (MDA), and 8-hydroxydeoxyguanosine (8-OHDG) in all treated groups, with exception of MDA in the alcohol treated group showed that oxidative stress system was impacted and may be involved in the histopathological derangements recorded in this study. Incidentally, OS plays a key role

in the pathogenesis of complications associated with diabetes (Barcia et al., 2015), alcohol abuse (Finelli et al., 2022), and cART treatment (Ogedengbe, Naidu and Azu, 2018). In agreement with this study's findings, increased iNOS expression was observed in testis of rats treated with alcohol (Eid et al., 2011). Further, increased levels of MDA have been detected in testis tissue homogenate of diabetic rats (Olojede et al., 2022), exposed to alcohol (Oremosu and Akang, 2015), and treated with cART (Ogedengbe et al., 2018). Though, the present study did not investigate the treatment effect on DNA of spermatozoa, previous reports identified testicular OS as the main cause of spermatozoa DNA fragmentation (SDF), a well-known contributing factor to male infertility (Robinson et al., 2012; Cho and Agarwal, 2018).

8.1.9 The effect of diabetes, alcohol, cART, and their combinations on testicular cytokines

The proinflammatory cytokine interleukin-1β (IL-1β), interleukin-6 (IL-6), and tumor necrosis factor-α (TNF-α)) levels significantly increased in the testis of all treated groups, with exception of IL-1β in A+cART group and TNF-α in cART and A+cART groups. Inflammation is a predominant factor in male infertility and common testicular disorders that cause inflammation such as testicular torsion, varicocele, and orchitis are associated with deterioration of spermatogenesis (Dutta et al., 2021). Cytokines, IL-1β, IL-6, and TNF-α are major mediators of testicular inflammation and their increased production has been reported in testis injury, infection, and ischemia (Hedger and Meinhardt, 2003; Lampiao and du Plessis, 2008; Loveland et al., 2017). Corroborating with our results, Nna et al., (2019) showed testicular upregulation of IL-1β and TNF-α expression in experimental diabetes. A study by Akhigbe et al., (2021) reported inflammation in testis of rats treated with cART, demonstrated by elevated myeloperoxidase activity. Testicular cytokines upregulation has been reported to impair the steroidogenesis process, Sertoli cell function, and blood-testis barrier (BTB) dynamics, consequently leading to derangement of testicular structure and spermatogenesis failure (Lampiao and du Plessis, 2008; Zhang et al., 2014; Alves-Silva et al., 2021).

8.1.10 The effect of diabetes, alcohol, cART, and their combinations on germ cell apoptosis

The upregulation of caspase 3 (apoptosis marker) in all treated groups (A, cART, A+cART, DM, DM+A, DM+cART, and DM+A+cART) is indicative of testicular perturbations of apoptotic pathway and the normal apoptotic processes due to the treatments. Apoptosis, as a process of regulated/programmed cell death, serves numerous vital roles in the testis, some of which include preserving proper germ cell to Sertoli cells ratio, removal of defective/imperfect germ cells and preserving overall quality control in sperm production (Hai et al., 2014; Asadi

et al., 2021). However, the increased apoptotic activity is evidence of treatment effect, is detrimental to germ cells, and consequently will lead to reduced sperm production, which will reflect on inadequate spermatogenesis or its dysfunction (Sisman et al., 2014). It has been previously reported that removal of follicles stimulating hormone (FSH) and luteinizing hormone (LH) induces germ cell apoptosis through indirect effects (Shukla et al., 2012), which complements perturbations of the anterior pituitary hormonal system recorded in the present study. Other studies have also reported increased germ cell apoptosis in the testis of diabetic rats (Nna et al., 2019), alcohol-treated mice (Liu et al., 2020), and cART treated rats (Akhigbe, Hamed and Aremu, 2021). The present study reports elevated apoptosis in combinations of alcohol and cART in diabetic condition. Generally, in the testis, apoptosis, is essential in regulation of the spermatogenesis process (Shaha et al., 2010; Asadi et al., 2021).

8.1.11 The effect of diabetes, alcohol, cART, and their combinations on the testicular expression of proliferation marker, Ki-67

The significant reduction found in the number of germ cells expressing proliferation marker Ki-67 in all treated groups (A, cART, A+cART, DM, DM+A, DM+cART, and DM+A+cART) with significantly increased staining intensity points to reduced germ proliferation and consequently will result in reduced spermatogenic cells. An earlier study reported reduction in proliferating cell nuclear antigen (PCNA) immunoreactive spermatogenic cells in testis of diabetic rats (Nna et al., 2019). Additionally, strong staining intensity of Ki-67 and PCNA expression was detected in fluoride-induced testicular toxicity (Zhao et al., 2018). Both Ki-67 and PCNA reflect the state of germ cell proliferation and also play a regulatory role in the spermatogenesis process (He et al., 2016; Zhao et al., 2018). Although PCNA immunostaining was not part of this study, the decreased germ cell expression of Ki-67 detected suggests that the treatments impaired germ cell proliferation.

8.2 Conclusion

The overall result suggests a variation in the effects of the different treatments on the studied parameters in diabetic condition. This study has demonstrated that diabetes, alcohol, and cART, either separately or in their combinations are detrimental to HPG axis function, testis structure, and spermatogenesis evidenced by alternations in reproductive hormone levels, testicular histomorphology architecture, interstitial connective tissue, expression of androgen receptor, and Ki-67 expression. Furthermore, the results show that the treatments perturbed multiple molecular pathways evidenced by the alterations of biomarkers for oxidative stress

(iNOS, MDA, and 8-OHDG), inflammation (IL-1β, IL-6, and TNF-α), and apoptosis (caspase 3) in all treated animal groups. Leading to increased ROS formation that subsequently induces oxidative stress and inflammation in the testis. Additionally, testicular and spermatogenesis perturbations observed in treated groups might have been mediated via the recorded androgen receptor depletion and HPG axis dysregulation. Conversely, exacerbated alternations were observed in the combined alcohol and/or cART in diabetes, and were most severe in the diabetic animals treated with alcohol (DM+A group). This could be due to aggravated ROS production, resulting from uncontrollable high blood glucose levels associated with consumption of alcohol in diabetes. The results also suggest that cART and alcohol, acting through the same enzyme system, P450, mildly reduced the activity of each other when present concomitantly in the body and also, Our study findings are a vital contribution to science on the impact of diabetes, alcohol abuse, and cART multimorbidity on the male reproductive system which has not been previously reported and will invaluably assist in the clinical management of male reproductive dysfunctions that could emerge in diabetic people living with HIV/AIDS (PLWHA) on cART and who consume alcohol regularly.

8.3 Recommendations and further studies

Recommendations

Analysis of our results suggests that alcohol consumption should be minimized in diabetic patients and amongst PLWHA who are diabetic, especially amongst those with a desire to reproduce. Supplementation of antioxidants to ameliorate oxidative stress in the categories of patients suffering from reproductive dysfunctions should be considered by fertility clinicians. In addition, it might be necessary to review and adjust the antiretroviral drug type and dosage of cART for PLWHA who are diabetic.

Further studies

Since the present study did not involve HIV virus, further studies should utilize HIV model and consider incorporating anti-diabetic agents in the study to delineate the reproductive perturbations which mimics a complete clinical situation of diabetic PLWHA receiving anti-diabetic drugs and cART and help to unveil the mechanisms reproductive toxicity by the treatments. This will be instrumental in the development of suitable treatment drug delivery strategies that will be effective in management of testicular perturbations arising in diabetes and/or alcohol abuse and/or cART use. Additionally, further investigations using transmission electron microscopy to obtain detailed pathological changes in the testis that include studies on Sertoli cell mitochondria and genetic analysis will be considered.

REFERENCE LIST

Acharyya, S. (2021), "Immune and endocrine aspects of the testis and its relation to male infertility", *Chemical Biology Letters*.

Adaramoye, O.A., Akanni, O.O., Adewumi, O.M. and Owumi, S.E. (2015), "Lopinavir/ Ritonavir, an antiretroviral drug, lowers sperm quality and induces testicular oxidative damage in rats", *Tokai Journal of Experimental and Clinical Medicine*, Vol. 40 No. 2, pp. 51–57.

Adaramoye, O.A., Akanni, O.O. and Farombi, E.O. (2013), "Nevirapine induces testicular toxicity in wistar rats: Reversal effect of kolaviron (biflavonoid from garcinia kola seeds)", *Journal of Basic and Clinical Physiology and Pharmacology*, Vol. 24 No. 4, pp. 313–320, doi: 10.1515/jbcpp-2012-0078.

Agarwal, A., Baskaran, S., Parekh, N., Cho, C.L., Henkel, R., Vij, S., Arafa, M., et al. (2021), "Male infertility", *The Lancet*, Elsevier Ltd, Vol. 397 No. 10271, pp. 319–333, doi: 10.1016/S0140-6736(20)32667-2.

Agarwal, A., Mulgund, A., Hamada, A. and Chyatte, M.R. (2015), "A unique view on male infertility around the globe", *Reproductive Biology and Endocrinology*, Statistics South Africa, Vol. 13 No. 1, p. 37, doi: 10.1186/s12958-015-0032-1.

Agarwal, A., Rana, M., Qiu, E., AlBunni, H., Bui, A.D. and Henkel, R. (2018), "Role of oxidative stress, infection and inflammation in male infertility", *Andrologia*, Vol. 50 No. 11, p. e13126, doi: 10.1111/and.13126.

Agbaje, I.M., Rogers, D.A., McVicar, C.M., McClure, N., Atkinson, A.B., Mallidis, C. and Lewis, S.E.M. (2007), "Insulin dependant diabetes mellitus: Implications for male reproductive function", *Human Reproduction*, Vol. 22 No. 7, pp. 1871–1877, doi: 10.1093/humrep/dem077.

Aghazadeh, Y., Zirkin, B.R. and Papadopoulos, V. (2015), "Pharmacological Regulation of the Cholesterol Transport Machinery in Steroidogenic Cells of the Testis", *Vitamins and Hormones*, Vol. 98, pp. 189–227, doi: 10.1016/bs.vh.2014.12.006.

Aire, T.A. and Ozegbe, P.C. (2007), "The testicular capsule and peritubular tissue of birds: Morphometry, histology, ultrastructure and immunohistochemistry", *Journal of Anatomy*, Vol. 210 No. 6, pp. 731–740, doi: 10.1111/j.1469-7580.2007.00726.x.

Aitken, R.J., Findlay, J.K., Hutt, K.J. and Kerr, J.B. (2011), "Apoptosis in the germ line", *Reproduction*, doi: 10.1530/REP-10-0232.

Aitken, R.J. and Roman, S.D. (2008), "Antioxidant systems and oxidative stress in the testes.", *Oxidative Medicine and Cellular Longevity*, Vol. 1 No. 1, pp. 15–24, doi: 10.4161/oxim.1.1.6843.

Ajayi, A.F. and Akhigbe, R.E. (2020), "The physiology of male reproduction: Impact of drugs and their abuse on male fertility", *Andrologia*, Vol. 52 No. 9, p. e13672, doi: 10.1111/and.13672.

Akang, E.N., Adana, M.Y., Peter, A.I., Naidu, E.C.S., Mackraj, I. and Azu, O.O. (2019), "Testicular 3beta hydroxysteroid dehydrogenase in naringenin adjuvant under highly active antiretroviral therapy (HAART); preliminary data using Sprague-Dawley rats", *European Journal of Anatomy*, Vol. 23 No. 1, pp. 1–7.

Akang, E.N., Dosumu, O.O., Okoko, I.I.E., Faniyan, O., Oremosu, A.A. and Akanmu, A.S. (2020), "Microscopic and biochemical changes on liver and kidney of Wistar rats on combination antiretroviral therapy: The impact of naringenin and quercetin", *Toxicology Research*, Vol. 9 No. 5, pp. 601–608, doi: 10.1093/TOXRES/TFAA060.

Akerman, J.P., Hayon, S. and Coward, R.M. (2020), "Sperm Extraction in Obstructive Azoospermia: What's Next?", *Urologic Clinics of North America*, doi: 10.1016/j.ucl.2019.12.003.

Akhigbe, R.E., Hamed, M.A. and Aremu, A.O. (2021), "HAART exacerbates testicular damage and impaired spermatogenesis in anti-Koch-treated rats via dysregulation of lactate transport and glutathione content", *Reproductive Toxicology*, Vol. 103, pp. 96–107, doi: 10.1016/j.reprotox.2021.06.007.

Akhigbe, R.E., Hamed, M.A. and Odetayo, A.F. (2021), "HAART and anti-Koch's impair sexual competence, sperm quality and offspring quality when used singly and in combination in male Wistar rats", *Andrologia*, Vol. 53 No. 2, doi: 10.1111/and.13951.

Akhtar, R., Cruickshank, J.K., Gardiner, N.J., Derby, B. and Sherratt, M.J. (2010), "The effect of type 1 diabetes on the structure and function of fibrillin microfibrils", *Materials Research Society Symposium Proceedings*, Vol. 1274, pp. 57–61, doi: 10.1557/proc-1274-qq05-17.

Al-Shathly, M.R., Ali, S.S. and Ayuob, N.N. (2020), "Zingiber officinale preserves testicular structure and the expression of androgen receptors and proliferating cell nuclear antigen in diabetic rats", *Andrologia*, Vol. 52 No. 3, p. e13528, doi: 10.1111/and.13528.

Aladamat, N. and Tadi, P. (2022), *Histology, Leydig Cells*, *StatPearls*.

Alves-Silva, T., Freitas, G.A., Húngaro, T.G.R., Arruda, A.C., Oyama, L.M., Avellar, M.C.W. and Araujo, R.C. (2021), "Interleukin-6 deficiency modulates testicular function by increasing the expression of suppressor of cytokine signaling 3 (SOCS3) in mice", *Scientific Reports*, Vol. 11 No. 1, p. 11456, doi: 10.1038/s41598-021-90872-6.

Alves, M.G., Martins, A.D., Cavaco, J.E., Socorro, S. and Oliveira, P.F. (2013), "Diabetes, insulin-mediated glucose metabolism and Sertoli/blood-testis barrier function", *Tissue Barriers*, Vol. 1 No. 2, p. e23992, doi: 10.4161/tisb.23992.

Alves, M.G., Martins, A.D., Rato, L., Moreira, P.I., Socorro, S. and Oliveira, P.F. (2013), *Molecular Mechanisms beyond Glucose Transport in Diabetes-Related Male Infertility*, *Biochimica et Biophysica Acta - Molecular Basis of Disease*, Vol. 1832, pp. 626–635, doi: 10.1016/j.bbadis.2013.01.011.

Anderson, J.E., Jones, D., Penner, S.B. and Thliveris, J.A. (1987), "Primary hypoandrogenism in experimental diabetes in the Long-Evans rat", *Diabetes*, Vol. 36 No. 10, pp. 1104–1110, doi: 10.2337/diab.36.10.1104.

Andric, S.A. and Kostic, T.S. (2019), "Regulation of Leydig cell steroidogenesis: intriguing network of signaling pathways and mitochondrial signalosome", *Current Opinion in Endocrine and Metabolic Research*, doi: 10.1016/j.coemr.2019.03.001.

Ansa, A.A., Akpere, O. and Imasuen, J.A. (2017), "<b>Semen traits, testicular morphometry and histopathology of cadmium-exposed rabbit bucks administered methanolic extract of *Phoenix dactylifera* fruit", *Acta Scientiarum. Animal Sciences*, Vol. 39 No. 2, p. 207, doi: 10.4025/actascianimsci.v39i2.32858.

Apa, D.D., Çayan, S., Polat, A. and Akbay, E. (2002), "Mast cells and fibrosis on testicular biopsies in male infertility", *Archives of Andrology*, Vol. 48 No. 5, pp. 337–344, doi: 10.1080/01485010290099183.

Apolikhin, O.I. and Krasnyak, S.S. (2021), "The impact of alcohol on the male reproductive system", *Public Health*, Vol. 1 No. 2, pp. 62–69, doi: 10.21045/2782-1676-2021-1-2-62-69.

Aprioku, J.S. (2013), "Pharmacology of free radicals and the impact of reactive oxygen species on the testis", *Journal of Reproduction and Infertility*, Vol. 14 No. 4, pp. 158–172.

Arendt, L.H., Lindhard, M.S., Henriksen, T.B., Olsen, J., Cnattingius, S., Petersson, G., Parner, E.T., et al. (2018), "Maternal Diabetes Mellitus and Genital Anomalies in Male Offspring: A Nationwide Cohort Study in 2 Nordic Countries", *Epidemiology*, Vol. 29 No. 2, pp. 280–289, doi: 10.1097/EDE.0000000000000781.

Asadi, A., Ghahremani, R., Abdolmaleki, A. and Rajaei, F. (2021), "Role of sperm apoptosis and oxidative stress in male infertility: A narrative review", *International Journal of Reproductive BioMedicine*, Vol. 19 No. 6, pp. 493–504, doi: 10.18502/ijrm.v19i6.9371.

Asadi, N., Bahmani, M., Kheradmand, A. and Rafieian-Kopaei, M. (2017), "The impact of oxidative stress on testicular function and the role of antioxidants in improving it: A review", *Journal of Clinical and Diagnostic Research*, Vol. 11 No. 5, pp. IE01–IE05, doi: 10.7860/JCDR/2017/23927.9886.

Aslani, F., Sebastian, T., Keidel, M., Fröhlich, S., Elsässer, H.P., Schuppe, H.C., Klug, J., et al. (2017), "Resistance to apoptosis and autophagy leads to enhanced survival in sertoli cells", *Molecular Human Reproduction*, Vol. 23 No. 6, pp. 370–380, doi: 10.1093/molehr/gax022.

Asmat, U., Abad, K. and Ismail, K. (2016), "Diabetes mellitus and oxidative stress—A concise review", *Saudi Pharmaceutical Journal*, King Saud University, Vol. 24 No. 5, pp. 547–553, doi: 10.1016/j.jsps.2015.03.013.

Asuquo, I.E., Edagha, I.A., Ekandem, G.J. and Peter, A.I. (2020), "Carica papaya attenuates testicular histomorphological and hormonal alterations following alcohol-induced gonado toxicity in male rats", *Toxicological Research*, Vol. 36 No. 2, pp. 149–157, doi: 10.1007/s43188-019-00017-1.

Atwood, C.S., Meethal, S.V., Liu, T., Wilson, A.C., Gallego, M., Smith, M.A. and Bowen, R.L. (2005), "Dysregulation of the hypothalamic-pituitary-gonadal axis with menopause and andropause promotes neurodegenerative senescence", *Journal of Neuropathology and Experimental Neurology*, Vol. 64 No. 2, pp. 93–103, doi: 10.1093/jnen/64.2.93.

Auten, R.L. and Davis, J.M. (2009), "Oxygen toxicity and reactive oxygen species: The devil is in the details", *Pediatric Research*, Vol. 66 No. 2, pp. 121–127, doi: 10.1203/PDR.0b013e3181a9eafb.

Avallet, O., Vigier, M., Leduque, P., Dubois, P.M. and Saez, J.M. (1994), "Expression and regulation of transforming growth factor-β 1 messenger ribonucleic acid and protein in cultured porcine leydig and sertoli cells", *Endocrinology*, Vol. 134 No. 5, pp. 2079–2087, doi: 10.1210/endo.134.5.8156908.

Avari, P. and Devendra, S. (2017), "Human immunodeficiency virus and type 2 diabetes",

London Journal of Primary Care, Taylor & Francis, Vol. 9 No. 3, pp. 38–42, doi: 10.1080/17571472.2017.1302872.

Awodele, O., Popoola, T.D., Idowu, O., Bashua, B.M., Awolola, N.A. and Okunowo, W.O. (2018), "Investigations into the risk of reproductive toxicity following exposure to highly active anti-retroviral drugs in rodents", *Tokai Journal of Experimental and Clinical Medicine*, Vol. 43 No. 2, pp. 54–63.

Azenabor, A., Ekun, A.O. and Akinloye, O. (2015), "Impact of inflammation on male reproductive tract", *Journal of Reproduction and Infertility*.

Azu, O.O. (2012), "Highly active antiretroviral therapy (HAART) and testicular morphology: Current status and a case for a stereologic approach", *Journal of Andrology*, Vol. 33 No. 6, pp. 1130–1142, doi: 10.2164/jandrol.112.016758.

Azu, O.O., Naidu, E.C.S., Naidu, J.S., Masia, T., Nzemande, N.F., Chuturgoon, A. and Singh, S. (2014), "Testicular histomorphologic and stereological alterations following short-term treatment with highly active antiretroviral drugs (HAART) in an experimental animal model", *Andrology*, Vol. 2 No. 5, pp. 772–779, doi: 10.1111/j.2047-2927.2014.00233.x.

Babaei, M., Alizadeh-Fanalou, S., Nourian, A., Yarahmadi, S., Farahmandian, N., Nabi-Afjadi, M., Alipourfard, I., et al. (2021), "Evaluation of testicular glycogen storage, FGF21 and LDH expression and physiological parameters of sperm in hyperglycemic rats treated with hydroalcoholic extract of Securigera Securidaca seeds, and Glibenclamide", *Reproductive Biology and Endocrinology*, Vol. 19 No. 1, p. 104, doi: 10.1186/s12958-021-00794-1.

Bam, N.E., Mabunda, S.A., Ntsaba, J., Apalata, T., Nomatshila, S.C. and Chitha, W. (2020), "The association between HIV tri-therapy with the development of Type-2 Diabetes Mellitus in a rural South African District: A case-control study", *PLoS ONE*, Vol. 15 No. 12 December, p. e0244067, doi: 10.1371/journal.pone.0244067.

Barber, T.M., Kyrou, I., Kaltsas, G., Grossman, A.B., Randeva, H.S. and Weickert, M.O. (2021), "Mechanisms of central hypogonadism", *International Journal of Molecular Sciences*, doi: 10.3390/ijms22158217.

Barbotin, A.-L., Peigné, M., Malone, S.A. and Giacobini, P. (2019), "Emerging Roles of Anti-Müllerian Hormone in Hypothalamic-Pituitary Function", *Neuroendocrinology*, Vol. 109 No. 3, pp. 218–229, doi: 10.1159/000500689.

Barboza, J.M., Medina, H., Doria, M., Rivero, L., Hernandez, L. and Joshi, N. V. (2004), "Use of atomic force microscopy to reveal sperm ultrastructure in HIV-patients on highly active antiretroviral therapy", *Archives of Andrology*, Vol. 50 No. 2, pp. 121–129, doi: 10.1080/01485010490269524.

Barcia, J.M., Flores-Bellver, M., Muriach, M., Sancho-Pelluz, J., Lopez-Malo, D., Urdaneta, A.C., Martinez-Gil, N., et al. (2015), "Matching Diabetes and Alcoholism: Oxidative Stress, Inflammation, and Neurogenesis Are Commonly Involved", *Mediators of Inflammation*, Hindawi Publishing Corporation, Vol. 2015, p. 624287, doi: 10.1155/2015/624287.

Bardach, A.E., Alcaraz, A.O., Ciapponi, A., Garay, O.U., Riviere, A.P., Palacios, A., Cremonte, M., et al. (2019), "Alcohol consumption's attributable disease burden and cost-effectiveness of targeted public health interventions: A systematic review of

mathematical models", *BMC Public Health*, doi: 10.1186/s12889-019-7771-4.

Barros, B.A., De Oliveira, L.R., Surur, C.R.C., Barros-Filho, A.D.A., Maciel-Guerra, A.T. and Guerra-Junior, G. (2021), "Complete androgen insensitivity syndrome and risk of gonadal malignancy: Systematic review", *Annals of Pediatric Endocrinology and Metabolism*, doi: 10.6065/apem.2040170.085.

Basiri, M., Asadi-Shekaari, M., Ezzatabdipour, M., Sarv Azad, A. and Nematollahimahani, S.N. (2016), "Immunohistochemistry Study on Androgen and Estrogen Receptors of Rat Seminal Vesicle Submitted to Simultaneous Alcohol-Nicotine Treatment.", *Cell Journal*, Vol. 18 No. 3, pp. 458–63, doi: 10.22074/cellj.2016.4574.

Bassil, N., Alkaade, S. and Morley, J.E. (2009), "The benefits and risks of testosterone replacement therapy: A review", *Therapeutics and Clinical Risk Management*, Vol. 5 No. 1, pp. 427–448, doi: 10.2147/tcrm.s3025.

Basu, S. (2011), "Male Reproductive Anatomy and Physiology", *Male Reproductive Dysfunction*, Jaypee Brothers Medical Publishers (P) Ltd., pp. 15–15, doi: 10.5005/jp/books/11208_2.

baydilli, numan. (2020), "Protective role of poplar propolis against alcohol-induced biochemical and histological changes in liver and testes tissues of rats", *Erciyes Medical Journal*, Vol. 42 No. 2, pp. 132–138, doi: 10.14744/etd.2020.83097.

Beattie, M.C., Adekola, L., Papadopoulos, V., Chen, H. and Zirkin, B.R. (2015), "Leydig cell aging and hypogonadism", *Experimental Gerontology*, Vol. 68, pp. 87–91, doi: 10.1016/j.exger.2015.02.014.

Beigbeder, Y. (2018), "The Global HIV/AIDS Epidemic", *International Public Health*, Routledge, pp. 73–83, doi: 10.4324/9781351155441-6.

Bennett, N.E. (2010), "Functional anatomy of the hypothalamic–Pituitary–gonadal axis and themale reproductive tract", *Fertility Preservation in Male Cancer Patients*, Cambridge University Press, pp. 1–10, doi: 10.1017/CBO9780511997761.001.

Berg, S., Kutra, D., Kroeger, T., Straehle, C.N., Kausler, B.X., Haubold, C., Schiegg, M., et al. (2019), "Ilastik: Interactive Machine Learning for (Bio)Image Analysis", *Nature Methods*, Springer US, Vol. 16 No. 12, pp. 1226–1232, doi: 10.1038/s41592-019-0582-9.

Bernie, A.M., Ramasamy, R. and Schlegel, P.N. (2013), "Predictive factors of successful microdissection testicular sperm extraction", *Basic and Clinical Andrology*, doi: 10.1186/2051-4190-23-5.

Bhatia, R., Murphy, A.B., Raper, J.L., Chamie, G., Kitahata, M.M., Drozd, D.R., Mayer, K., et al. (2015), "Testosterone replacement therapy among HIV-infected men in the CFAR network of integrated clinical systems", *Aids*, Vol. 29 No. 1, pp. 77–81, doi: 10.1097/QAD.0000000000000521.

Białas, M., Fiszer, D., Rozwadowska, N., Kosicki, W., Jedrzejczak, P. and Kurpisz, M. (2009), "The role of IL-6, IL-10, TNF-alpha and its receptors TNFR1 and TNFR2 in the local regulatory system of normal and impaired human spermatogenesis.", *American Journal of Reproductive Immunology (New York, N.Y. : 1989)*, Vol. 62 No. 1, pp. 51–9, doi: 10.1111/j.1600-0897.2009.00711.x.

Bianco, S.D.C. and Kaiser, U.B. (2009), "The genetic and molecular basis of idiopathic

hypogonadotropic hypogonadism", *Nature Reviews Endocrinology*, Vol. 5 No. 10, pp. 569–576, doi: 10.1038/nrendo.2009.177.

Blair, J.A., McGee, H., Bhatta, S., Palm, R. and Casadesus, G. (2015), "Hypothalamic-pituitary-gonadal axis involvement in learning and memory and Alzheimer's disease: More than 'just' estrogen", *Frontiers in Endocrinology*, Vol. 6 No. MAR, doi: 10.3389/fendo.2015.00045.

Blair, M. (2016), "Diabetes Mellitus Review", *Urologic Nursing*, Vol. 36 No. 1, pp. 27–36, doi: 10.7257/1053-816x.2016.36.1.27.

Blake, R. and Trounce, I.A. (2014), "Mitochondrial dysfunction and complications associated with diabetes", *Biochimica et Biophysica Acta - General Subjects*, Vol. 1840 No. 4, pp. 1404–1412, doi: 10.1016/j.bbagen.2013.11.007.

Borg, H., Kabel, A., Estfanous, R. and Abd Elmaaboud, M. (2020), "Effect of the combination between empagliflozin and calcipotriol on cadmium-induced testicular toxicity in rats", *Bulletin of Egyptian Society for Physiological Sciences*, Vol. 40 No. 1, pp. 15–31, doi: 10.21608/besps.2019.14918.1029.

Braithwaite, R.S. and Bryant, K.J. (2010), "Influence of alcohol consumption on adherence to and toxicity of antiretroviral therapy and survival", *Alcohol Research and Health*, Vol. 33 No. 3, pp. 280–287.

Braithwaite, R.S., Conigliaro, J., Roberts, M.S., Shechter, S., Schaefer, A., McGinnis, K., Rodriguez, M.C., et al. (2007), "Estimating the impact of alcohol consumption on survival for HIV+ individuals", *AIDS Care - Psychological and Socio-Medical Aspects of AIDS/HIV*, Vol. 19 No. 4, pp. 459–466, doi: 10.1080/09540120601095734.

Bremner, W.J., Millar, M.R., Sharpe, R.M. and Saunders, P.T.K. (1994), "Immunohistochemical localization of androgen receptors in the rat testis: Evidence for stage-dependent expression and regulation by androgens", *Endocrinology*, Vol. 135 No. 3, pp. 1227–1234, doi: 10.1210/endo.135.3.8070367.

Brown, T.T., Cole, S.R., Li, X., Kingsley, L.A., Palella, F.J., Riddler, S.A., Visscher, B.R., et al. (2005), "Antiretroviral therapy and the prevalence and incidence of diabetes mellitus in the multicenter AIDS cohort study", *Archives of Internal Medicine*, Vol. 165 No. 10, pp. 1179–1184, doi: 10.1001/archinte.165.10.1179.

Bulstra, C.A., Hontelez, J.A.C., Giardina, F., Steen, R., Nagelkerke, N.J.D., Bärnighausen, T. and de Vlas, S.J. (2020), "Mapping and characterising areas with high levels of HIV transmission in sub-Saharan Africa: A geospatial analysis of national survey data", edited by Barnabas, R. V.*PLoS Medicine*, Vol. 17 No. 3, p. e1003042, doi: 10.1371/journal.pmed.1003042.

Calogero, A.E., Duca, Y., Condorelli, R.A. and La Vignera, S. (2017), "Male accessory gland inflammation, infertility, and sexual dysfunctions: a practical approach to diagnosis and therapy", *Andrology*, doi: 10.1111/andr.12427.

CDC. (2015), "Fact Sheets - Binge Drinking", *Alcohol and Public Health*.

Centers for Disease Control and Prevention. (2019), "HIV Risk and Prevention Estimates", *HIV Risk and Prevention*.

Chander, G., Lau, B. and Moore, R.D. (2006), "Hazardous alcohol use: A risk factor for non-adherence and lack of suppression in HIV infection", *Journal of Acquired Immune*

Deficiency Syndromes, Vol. 43 No. 4, pp. 411–417, doi: 10.1097/01.qai.0000243121.44659.a4.

Chen, H., Lui, W. yee, Mruk, D.D., Xiao, X., Ge, R., Lian, Q., Lee, W.M., et al. (2018), "Monitoring the integrity of the blood-testis barrier (BTB): An in vivo assay", *Methods in Molecular Biology*, Vol. 1748, pp. 245–252, doi: 10.1007/978-1-4939-7698-0_17.

Chen, L.Y., Brown, P.R., Willis, W.B. and Eddy, E.M. (2014), "Peritubular myoid cells participate in male mouse spermatogonial stem cell maintenance", *Endocrinology*, Vol. 155 No. 12, pp. 4964–4974, doi: 10.1210/en.2014-1406.

Cheng, C.Y. and Mruk, D.D. (2009), "An intracellular trafficking pathway in the seminiferous epithelium regulating spermatogenesis: A biochemical and molecular perspective", *Critical Reviews in Biochemistry and Molecular Biology*, Vol. 44 No. 5, pp. 245–263, doi: 10.1080/10409230903061207.

Cheng, C.Y., Wong, E.W.P., Lie, P.P.Y., Li, M.W.M., Mruk, D.D., Yan, H.H.N., Mok, K.-W., et al. (2011), "Regulation of blood-testis barrier dynamics by desmosome, gap junction, hemidesmosome and polarity proteins", *Spermatogenesis*, Taylor & Francis, Vol. 1 No. 2, pp. 105–115, doi: 10.4161/spmg.1.2.15745.

Chim, Y.H., Davies, H.A., Mason, D., Nawaytou, O., Field, M., Madine, J. and Akhtar, R. (2020), "Bicuspid valve aortopathy is associated with distinct patterns of matrix degradation", *Journal of Thoracic and Cardiovascular Surgery*, Elsevier Inc., Vol. 160 No. 6, pp. e239–e257, doi: 10.1016/j.jtcvs.2019.08.094.

Cho, C.L. and Agarwal, A. (2018), "Role of sperm DNA fragmentation in male factor infertility: A systematic review", *Arab Journal of Urology*, Vol. 16 No. 1, pp. 21–34, doi: 10.1016/j.aju.2017.11.002.

Cho, N., Kirigia, J., Ogurstova, K. and Reja, A. (2017), "IDF Diabetes Atlas, tenth edition", *International Diabetes Federation*, available at: www.diabetesatlas.org.

Cicero, T.J., Bell, R.D., Meyer, E.R. and Badger, T.M. (1980), "Ethanol and acetaldehyde directly inhibit testicular steroidogenesis", *Journal of Pharmacology and Experimental Therapeutics*, Vol. 213 No. 2, pp. 228–233.

Cizkova, K., Foltynkova, T., Gachechiladze, M. and Tauber, Z. (2021), "Comparative analysis of immunohistochemical staining intensity determined by light microscopy, imagej and qupath in placental hofbauer cells", *Acta Histochemica et Cytochemica*, Vol. 54 No. 1, pp. 21–29, doi: 10.1267/ahc.20-00032.

Clavijo, R.I. and Hsiao, W. (2018), "Update on male reproductive endocrinology", *Translational Andrology and Urology*, Vol. 7 No. S3, pp. S367–S372, doi: 10.21037/tau.2018.03.25.

Coetzee, A., Beukes, A., Dreyer, R., Solomon, S., van Wyk, L., Mistry, R., Conradie, M., et al. (2019), "The prevalence and risk factors for diabetes mellitus in healthcare workers at Tygerberg hospital, Cape Town, South Africa: a retrospective study", *Journal of Endocrinology, Metabolism and Diabetes of South Africa*, Taylor & Francis, Vol. 24 No. 3, pp. 77–82, doi: 10.1080/16089677.2019.1620009.

Collazos, J., Martínez, E., Mayo, J. and Ibarra, S. (2002), "Sexual dysfunction in HIV-infected patients treated with highly active antiretroviral therapy", *Journal of Acquired Immune Deficiency Syndromes*, Vol. 31 No. 3, pp. 322–326, doi: 10.1097/00126334-

200211010-00008.

Condorelli, R.A., Calogero, A.E., Vicari, E. and La Vignera, S. (2015), "Chronic consumption of alcohol and sperm parameters: Our experience and the main evidences", *Andrologia*, Vol. 47 No. 4, pp. 368–379, doi: 10.1111/and.12284.

Condorelli, R.A., Vicari, E., Calogero, A.E. and La Vignera, S. (2014), "Male accessory gland inflammation prevalence in type 2 diabetic patients with symptoms possibly reflecting autonomic neuropathy", *Asian Journal of Andrology*, Vol. 16 No. 5, pp. 761–766, doi: 10.4103/1008-682X.125911.

Condorelli, R.A., Vignera, S. La, Mongioì, L.M., Alamo, A. and Calogero, A.E. (2018), "Diabetes mellitus and infertility: Different pathophysiological effects in type 1 and type 2 on sperm function", *Frontiers in Endocrinology*, Vol. 9 No. MAY, doi: 10.3389/fendo.2018.00268.

Coppack, S.W. (2001), "Pro-inflammatory cytokines and adipose tissue", *Proceedings of the Nutrition Society*, Vol. 60 No. 3, pp. 349–356, doi: 10.1079/pns2001110.

Cordatos, K. (2002), "Theory and Practice of Histological Techniques: Fifth Edition", *Pathology*, Vol. 34 No. 4, p. 384, doi: 10.1016/s0031-3025(16)34462-2.

Cornell, M., Johnson, L.F., Wood, R., Tanser, F., Fox, M.P., Prozesky, H., Schomaker, M., et al. (2017), "Twelve-year mortality in adults initiating antiretroviral therapy in South Africa", *Journal of the International AIDS Society*, Vol. 20 No. 1, p. 21902, doi: 10.7448/IAS.20.1.21902.

Corradi, P.F., Corradi, R.B. and Greene, L.W. (2016), "Physiology of the Hypothalamic Pituitary Gonadal Axis in the Male", *Urologic Clinics of North America*, Vol. 43 No. 2, pp. 151–162, doi: 10.1016/j.ucl.2016.01.001.

Coss, D. (2018), "Regulation of reproduction via tight control of gonadotropin hormone levels", *Molecular and Cellular Endocrinology*, Vol. 463, pp. 116–130, doi: 10.1016/j.mce.2017.03.022.

Coştur, P., Filiz, S., Gonca, S., Çulha, M., Gülecen, T., Solakoğlu, S., Canberk, Y., et al. (2012), "Êxpression of inducible nitric oxide synthase (iNOS) in the azoospermic human testis", *Andrologia*, Vol. 44 No. SUPPL.1, pp. 654–660, doi: 10.1111/j.1439-0272.2011.01245.x.

Crane, H.M., McCaul, M.E., Chander, G., Hutton, H., Nance, R.M., Delaney, J.A.C., Merrill, J.O., et al. (2017), "Prevalence and Factors Associated with Hazardous Alcohol Use Among Persons Living with HIV Across the US in the Current Era of Antiretroviral Treatment", *AIDS and Behavior*, Vol. 21 No. 7, pp. 1914–1925, doi: 10.1007/s10461-017-1740-7.

Cudicini, C., Lejeune, H., Gomez, E., Bosmans, E., Ballet, F., Saez, J. and Jégou, B. (1997), "Human leydig cells and sertoli cells are producers of interleukins-1 and-6", *Journal of Clinical Endocrinology and Metabolism*, Vol. 82 No. 5, pp. 1426–1433, doi: 10.1210/jcem.82.5.3938.

Cupp, A.S. and Skinner, M.K. (2001), "Expression, action, and regulation of transforming growth factor alpha and epidermal growth factor receptor during embryonic and perinatal rat testis development", *Journal of Andrology*, Vol. 22 No. 6, pp. 1019–1029, doi: 10.1002/j.1939-4640.2001.tb03443.x.

Cuylen-Haering, S., Petrovic, M., Hernandez-Armendariz, A., Schneider, M.W.G., Samwer, M., Blaukopf, C., Holt, L.J., et al. (2020), "Chromosome clustering by Ki-67 excludes cytoplasm during nuclear assembly", *Nature*, Vol. 587 No. 7833, pp. 285–290, doi: 10.1038/s41586-020-2672-3.

D'Autréaux, B. and Toledano, M.B. (2007), "ROS as signalling molecules: Mechanisms that generate specificity in ROS homeostasis", *Nature Reviews Molecular Cell Biology*, Vol. 8 No. 10, pp. 813–824, doi: 10.1038/nrm2256.

Dandona, P. and Rosenberg, M.T. (2010), "A practical guide to male hypogonadism in the primary care setting", *International Journal of Clinical Practice*, Vol. 64 No. 6, pp. 682–696, doi: 10.1111/j.1742-1241.2010.02355.x.

Das, S.K. and Vasudevan, D.M. (2007), "Alcohol-induced oxidative stress", *Life Sciences*, Vol. 81 No. 3, pp. 177–187, doi: 10.1016/j.lfs.2007.05.005.

Davey, R.A. and Grossmann, M. (2016), "Androgen Receptor Structure, Function and Biology: From Bench to Bedside.", *The Clinical Biochemist. Reviews*, Vol. 37 No. 1, pp. 3–15.

Davies, K.J.A. (2003), "Free Radical Biology & Medicine", *Free Radical Biology and Medicine*, Vol. 35 No. 12, p. ii, doi: 10.1016/s0891-5849(03)00778-0.

Deshmukh, S.K., Gupta, S.K., Ingole, S.P., Chaurasia, D. and Gupta, M. (2013), "Histological Study on Testis of Grower and Adult Wistar Rat", Vol. 25 No. June, pp. 43–44.

"Diagnosis and classification of diabetes mellitus". (2014), *Diabetes Care*, Vol. 37 No. SUPPL.1, pp. 81–90, doi: 10.2337/dc14-S081.

Dieckmann, K.P. and Pichlmeier, U. (2004), "Clinical epidemiology of testicular germ cell tumors", *World Journal of Urology*, doi: 10.1007/s00345-004-0398-8.

Dimakopoulou, A., Jayasena, C.N., Radia, U.K., Algefari, M., Minhas, S., Oliver, N. and Dhillo, W.S. (2019), "Animal Models of Diabetes-Related Male Hypogonadism", *Frontiers in Endocrinology*, Vol. 10 No. September, pp. 18–21, doi: 10.3389/fendo.2019.00628.

Dimitriadis, F., Adonakis, G., Kaponis, A., Mamoulakis, C., Takenaka, A. and Sofikitis, N. (2017), "Pre-Testicular, Testicular, and Post-Testicular Causes of Male Infertility", pp. 981–1027, doi: 10.1007/978-3-319-44441-3_33.

Ding, D., Lawson, K.D., Kolbe-Alexander, T.L., Finkelstein, E.A., Katzmarzyk, P.T., van Mechelen, W. and Pratt, M. (2016), "The economic burden of physical inactivity: a global analysis of major non-communicable diseases", *The Lancet*, Vol. 388 No. 10051, pp. 1311–1324, doi: 10.1016/S0140-6736(16)30383-X.

Ding, G.L., Liu, Y., Liu, M.E., Pan, J.X., Guo, M.X., Sheng, J.Z. and Huang, H.F. (2015), "The effects of diabetes on male fertility and epigenetic regulation during spermatogenesis", *Asian Journal of Andrology*, Vol. 17 No. 6, pp. 948–953, doi: 10.4103/1008-682X.150844.

Diouf, A., Cournil, A., Ba-Fall, K., Ngom-Guèye, N.F., Eymard-Duvernay, S., Ndiaye, I., Batista, G., et al. (2012), "Diabetes and Hypertension among Patients Receiving Antiretroviral Treatment Since 1998 in Senegal: Prevalence and Associated Factors", *Isrn Aids*, Vol. 2012, pp. 1–8, doi: 10.5402/2012/621565.

Dissanayake, D.M.I.H., Keerthirathna, W.L.R. and Peiris, L.D.C. (2019), “Male Infertility Problem: A Contemporary Review on Present Status and Future Perspective”, *Gender and the Genome*, Vol. 3, p. 247028971986824, doi: 10.1177/2470289719868240.

Divi, R.L., Leonard, S.L., Kuo, M.M., Nagashima, K., Thamire, C., St. Claire, M.C., Wade, N.A., et al. (2007), “Transplacentally exposed human and monkey newborn infants show similar evidence of nucleoside reverse transcriptase inhibitor-induced mitochondrial toxicity”, *Environmental and Molecular Mutagenesis*, Vol. 48 No. 3–4, pp. 201–209, doi: 10.1002/em.20201.

Domke, L.M., Rickelt, S., Dörflinger, Y., Kuhn, C., Winter-Simanowski, S., Zimbelmann, R., Rosin-Arbesfeld, R., et al. (2014), “The cell-cell junctions of mammalian testes: I. The adhering junctions of the seminiferous epithelium represent special differentiation structures”, *Cell and Tissue Research*, Vol. 357 No. 3, pp. 645–665, doi: 10.1007/s00441-014-1906-9.

Donkin, I. and Barrès, R. (2018), “Sperm epigenetics and influence of environmental factors”, *Molecular Metabolism*, doi: 10.1016/j.molmet.2018.02.006.

Dosumu, O.O., Osinubi, A.A.A. and Duru, F.I.O. (2014), “Alcohol induced testicular damage: Can abstinence equal recovery?”, *Middle East Fertility Society Journal*, Vol. 19 No. 3, pp. 221–228, doi: 10.1016/j.mefs.2014.01.003.

Doɬan, B.A., Karakilic ̧, E., Tuna, M.M., Arduc ̧, A., Berker, D. and Güler, S. (2015), “Effect of androgen replacement therapy on atherosclerotic risk markers in young-to-middle-aged men with idiopathic hypogonadotropic hypogonadism”, *Clinical Endocrinology*, Vol. 82 No. 3, pp. 422–428, doi: 10.1111/cen.12617.

Dremin, V., Marcinkevics, Z., Zherebtsov, E., Popov, A., Grabovskis, A., Kronberga, H., Geldnere, K., et al. (2021), “Skin Complications of Diabetes Mellitus Revealed by Polarized Hyperspectral Imaging and Machine Learning.”, *IEEE Transactions on Medical Imaging*, Vol. 40 No. 4, pp. 1207–1216, doi: 10.1109/TMI.2021.3049591.

Duca, Y., Aversa, A., Condorelli, R.A., Calogero, A.E. and La Vignera, S. (2019), “Substance abuse and male hypogonadism”, *Journal of Clinical Medicine*, Vol. 8 No. 5, p. 732, doi: 10.3390/jcm8050732.

Dufour, J.M., Gores, P., Hemendinger, R., Emerich, D.F. and Halberstadt, C.R. (2004), “Transgenic Sertoli Cells as a Vehicle for Gene Therapy”, *Cell Transplantation*, doi: 10.3727/000000004772664833.

Duluc, L., Andriantsitohaina, R. and Simard, G. (2014), “Mitochondrial and free radical metabolism - Biological and pathological implications”, *Systems Biology of Free Radicals and Antioxidants*, Vol. 9783642300, Springer Berlin Heidelberg, Berlin, Heidelberg, pp. 279–293, doi: 10.1007/978-3-642-30018-9_7.

Dutra Gonçalves, G., Antunes Vieira, N., Rodrigues Vieira, H., Dias Valério, A., Elóisa Munhoz de Lion Siervo, G., Fernanda Felipe Pinheiro, P., Eduardo Martinez, F., et al. (2017), “Role of resistance physical exercise in preventing testicular damage caused by chronic ethanol consumption in UChB rats”, *Microscopy Research and Technique*, Vol. 80 No. 4, pp. 378–386, doi: 10.1002/jemt.22806.

Dutta, S. and Sengupta, P. (2021), “SARS-CoV-2 and Male Infertility: Possible Multifaceted Pathology”, *Reproductive Sciences*, Vol. 28 No. 1, pp. 23–26, doi: 10.1007/s43032-020-00261-z.

Dutta, S., Sengupta, P., Slama, P. and Roychoudhury, S. (2021), "Oxidative stress, testicular inflammatory pathways, and male reproduction", *International Journal of Molecular Sciences*, Vol. 22 No. 18, p. 10043, doi: 10.3390/ijms221810043.

Eid, N., Ito, Y. and Otsuki, Y. (2011), "Involvement of inducible nitric oxide synthase in DNA fragmentation in various testicular germ cells of ethanol-treated rats", *Journal of Men's Health*, Vol. 8 No. SUPPL. 1, pp. S36–S40, doi: 10.1016/S1875-6867(11)60018-3.

Eisenberg, M.L., Betts, P., Herder, D., Lamb, D.J. and Lipshultz, L.I. (2013), "Increased risk of cancer among azoospermic men", *Fertility and Sterility*, Vol. 100 No. 3, pp. 681-685.e1, doi: 10.1016/j.fertnstert.2013.05.022.

El-Mehi, A.E. and Faried, M.A. (2019), "Effect of high-fructose diet-induced metabolic syndrome on the pituitary-gonadal axis from adolescence through adulthood in male albino rats and the possible protective role of ginger extract. A biochemical, histological and immunohistochemical study", *Folia Morphologica (Poland)*, Vol. 74 No. 9, pp. 690–708, doi: 10.5603/FM.A2019.0139.

Emanuele, M.A. and Emanuele, N. V. (1998), "Alcohols effects on male reproduction", *Alcohol Research and Health*, Vol. 22 No. 3, pp. 195–201.

Engler, P.A., Ramsey, S.E. and Smith, R.J. (2013), "Alcohol use of diabetes patients: The need for assessment and intervention", *Acta Diabetologica*, Vol. 50 No. 2, pp. 93–99, doi: 10.1007/s00592-010-0200-x.

Erpek, S., Bilgin, M.D., Dikicioglu, E. and Karul, A. (2007), "The effects of low frequency electric field in rat testis", *Revue de Medecine Veterinaire*, Vol. 158 No. 4, pp. 206–212.

Evenson, D.P. (2013), "Sperm Chromatin Structure Assay (SCSA®): 30 Years of Experience with the SCSA®", *Sperm Chromatin for the Researcher*, pp. 221–255, doi: 10.1007/978-1-4614-8459-2_12.

Fakoya, F.A. and Ademola Caxton-Martins, E. (2004), "Morphological alterations in the seminiferous tubules of adult Wistar rats: The effects of prenatal ethanol exposure", *Folia Morphologica*, Vol. 63 No. 2, pp. 195–202.

Falade, T.E., Olude, M.A., Mustapha, O.A., Mbajiorgu, E.F., Ihunwo, A.O., Olopade, J.O. and Oke, B.O. (2017), "Connective tissue, glial and neuronal expressions in testis of the African giant rat (Cricetomys gambianus)", *Journal of Morphological Sciences*, Vol. 34 No. 3, pp. 186–193, doi: 10.4322/jms.109117.

Fietz, D., Pilatz, A., Diemer, T., Wagenlehner, F., Bergmann, M. and Schuppe, H.C. (2020), "Excessive unilateral proliferation of spermatogonia in a patient with non-obstructive azoospermia - Adverse effect of clomiphene citrate pre-treatment?", *Basic and Clinical Andrology*, Vol. 30 No. 1, p. 13, doi: 10.1186/s12610-020-00111-7.

Fijak, M. and Meinhardt, A. (2006), "The testis in immune privilege", *Immunological Reviews*, doi: 10.1111/j.1600-065X.2006.00438.x.

Finelli, R., Mottola, F. and Agarwal, A. (2022), "Impact of alcohol consumption on male fertility potential: A narrative review", *International Journal of Environmental Research and Public Health*, Vol. 19 No. 1, p. 328, doi: 10.3390/ijerph19010328.

Fleck, D., Kenzler, L., Mundt, N., Strauch, M., Uesaka, N., Moosmann, R., Bruentgens, F., et al. (2021), "Atp activation of peritubular cells drives testicular sperm transport", *ELife*,

Vol. 10, pp. 1–30, doi: 10.7554/eLife.62885.

Fontes Marx, M., London, L., Harker, N. and Ataguba, J.E. (2021), "Assessing Intertemporal Socioeconomic Inequalities in Alcohol Consumption in South Africa", *Frontiers in Public Health*, Vol. 9, p. 606050, doi: 10.3389/fpubh.2021.606050.

Forouhi, N.G. and Wareham, N.J. (2019), "Epidemiology of diabetes", *Medicine (United Kingdom)*, Vol. 47 No. 1, pp. 22–27, doi: 10.1016/j.mpmed.2018.10.004.

Forouzanfar, M.H., Afshin, A., Alexander, L.T., Biryukov, S., Brauer, M., Cercy, K., Charlson, F.J., et al. (2016), "Global, regional, and national comparative risk assessment of 79 behavioural, environmental and occupational, and metabolic risks or clusters of risks, 1990–2015: a systematic analysis for the Global Burden of Disease Study 2015", *The Lancet*, Vol. 388 No. 10053, pp. 1659–1724, doi: 10.1016/S0140-6736(16)31679-8.

Foyouzi, N. (2019), "Fertility in Disorders of Sex Development: Evidence and Uncertainties", *Reproductive Medicine, Gynecology & Obstetrics*, Vol. 4 No. 1, pp. 1–14, doi: 10.24966/rmgo-2574/100015.

Fraietta, R., Zylberstejn, D.S. and Esteves, S.C. (2013), "Hypogonadotropic hypogonadism revisited", *Clinics*, Vol. 68 No. SUPPL. 1, pp. 81–88, doi: 10.6061/clinics/2013(Sup01)09.

Frampton, J.E. and Croom, K.F. (2006), "Efavirenz/emtricitabine/tenofovir disoproxil fumarate: Triple combination tablet", *Drugs*, Vol. 66 No. 11, pp. 1501–1512, doi: 10.2165/00003495-200666110-00012.

França, L.R., Hess, R.A., Dufour, J.M., Hofmann, M.C. and Griswold, M.D. (2016), "The Sertoli cell: One hundred fifty years of beauty and plasticity", *Andrology*, Vol. 4 No. 2, pp. 189–212, doi: 10.1111/andr.12165.

Francavilla, S., D'Abrizio, P., Rucci, N., Silvano, G., Properzi, G., Straface, E., Cordeschi, G., et al. (2000), "Fas and Fas ligand expression in fetal and adult human testis with normal or deranged spermatogenesis", *Journal of Clinical Endocrinology and Metabolism*, Vol. 85 No. 8, pp. 2692–2700, doi: 10.1210/jcem.85.8.6723.

French, L.E., Hahne, M., Viard, I., Radlgruber, G., Zanone, R., Becker, K., Müller, C., et al. (1996), "Fas and Fas ligand in embryos and adult mice: Ligand expression in several immune-privileged tissues and coexpression in adult tissues characterized by apoptotic cell turnover", *Journal of Cell Biology*, Vol. 133 No. 2, pp. 335–343, doi: 10.1083/jcb.133.2.335.

Frias, J., Torres, J.M., Miranda, M.T., Ruiz, E. and Ortega, E. (2002), "Effects of acute alcohol intoxication on pituitary-gonadal axis hormones, pituitary-adrenal axis hormones, β-endorphin and prolactin in human adults of both sexes", *Alcohol and Alcoholism*, Vol. 37 No. 2, pp. 169–173, doi: 10.1093/alcalc/37.2.169.

Gandhi, J. and Dagur, G. (2016), "Effect of Diabetes Mellitus on Sexual Arousal and Intercourse", *Translational Biomedicine*, Vol. 7 No. 2, doi: 10.21767/2172-0479.100057.

Gao, Y., Chen, H., Lui, W.Y., Lee, W.M. and Cheng, C.Y. (2017), "Basement membrane laminin α2 regulation of BTB dynamics via its effects on F-Actin and microtubule cytoskeletons is mediated through mTORC1 signaling", *Endocrinology*, The Endocrine Society, Vol. 158 No. 4, pp. 963–978, doi: 10.1210/en.2016-1630.

Gardner, K., Hall, P.A., Chinnery, P.F. and Payne, B.A.I. (2014), "HIV Treatment and Associated Mitochondrial Pathology:Review of 25 Years of in Vitro, Animal, and Human Studies", *Toxicologic Pathology*, Vol. 42 No. 5, pp. 811–822, doi: 10.1177/0192623313503519.

Ge, R.S., Dong, Q., Sottas, C.M., Papadopoulos, V., Zirkin, B.R. and Hardy, M.P. (2006), "In search of rat stem Leydig cells: Identification, isolation, and lineage-specific development", *Proceedings of the National Academy of Sciences of the United States of America*, Vol. 103 No. 8, pp. 2719–2724, doi: 10.1073/pnas.0507692103.

Giannessi, F., Scavuzzo, M.C., Giambelluca, M.A., Fornai, F., Morelli, G. and Ruffoli, R. (2015), "Chronic alcohol administration causes expression of calprotectin and RAGE altering the distribution of zinc ions in mouse testis", *Systems Biology in Reproductive Medicine*, Vol. 61 No. 1, pp. 18–25, doi: 10.3109/19396368.2014.949905.

Gianoulakis, C. (1990), "Characterization of the effects of acute ethanol administration on the release of β-endorphin peptides by the rat hypothalamus", *European Journal of Pharmacology*, Vol. 180 No. 1, pp. 21–29, doi: 10.1016/0014-2999(90)90588-W.

Gilbert, S.F. and Barresi, M.J.F. (2017), "Developmental Biology, 11Th Edition 2016", *American Journal of Medical Genetics Part A*, Vol. 173 No. 5, pp. 1430–1430, doi: 10.1002/ajmg.a.38166.

Gnanasekaran, N. (2020), "The missing link between HAART, mitochondrial damage and insulin resistance", *Biomedical and Pharmacology Journal*, Vol. 13 No. 2, pp. 965–972, doi: 10.13005/BPJ/1965.

Gnessi, L., Scarselli, F., Minasi, M.G., Mariani, S., Lubrano, C., Basciani, S., Greco, P.F., et al. (2018), "Testicular histopathology, semen analysis and FSH, predictive value of sperm retrieval: Supportive counseling in case of reoperation after testicular sperm extraction (TESE)", *BMC Urology*, BMC Urology, Vol. 18 No. 1, p. 63, doi: 10.1186/s12894-018-0379-7.

Goecke, M. and Baumeister, K. (2021), "Smoking and alcohol consumption as risk factors for type 2 diabetes-implications for prevention", *Public Health Forum*, Vol. 29 No. 4, pp. 335–338, doi: 10.1515/pubhef-2021-0095.

Gofur, M., Khan, M., Karim, M. and Islam, M. (1970), "Histomorphology and histochemistry of testis of indigenous bull (*Bos indicus*) of Bangladesh", *Bangladesh Journal of Veterinary Medicine*, Vol. 6 No. 1, pp. 67–74, doi: 10.3329/bjvm.v6i1.1341.

Goluža, T., Boscanin, A., Cvetko, J., Kozina, V., Kosović, M., Bernat, M.M., Kasum, M., et al. (2014), "Macrophages and leydig cells in testicular biopsies of azoospermic men", *BioMed Research International*, Vol. 2014, doi: 10.1155/2014/828697.

Gong, M. and Han, D. (2021), "Immunologic Environment of the Testis", *Advances in Experimental Medicine and Biology*, Vol. 1288, pp. 49–67, doi: 10.1007/978-3-030-77779-1_3.

Gordon, G.G., Southren, A.L., Vittek, J. and Lieber, C.S. (1979), "The effect of alcohol ingestion on hepatic aromatase activity and plasma steroid hormones in the rat", *Metabolism*, Vol. 28 No. 1, pp. 20–24, doi: 10.1016/0026-0495(79)90163-X.

Gow, R.M., O'Bryan, M.K., Canny, B.J., Ooi, G.T. and Hedger, M.P. (2001), "Differential effects of dexamethasone treatment on lipopolysaccharide-induced testicular

inflammation and reproductive hormone inhibition in adult rats", *Journal of Endocrinology*, Vol. 168 No. 1, pp. 193–201, doi: 10.1677/joe.0.1680193.

Griswold, M.D. (1995), "Interactions between germ cells and Sertoli cells in the testis", *Biology of Reproduction*, Vol. 52 No. 2, pp. 211–216, doi: 10.1095/biolreprod52.2.211.

Griswold, M.D. (1998), "The central role of Sertoli cells in spermatogenesis", *Seminars in Cell and Developmental Biology*, Vol. 9 No. 4, pp. 411–416, doi: 10.1006/scdb.1998.0203.

Griswold, M.D. (2016), "Spermatogenesis: The commitment to Meiosis", *Physiological Reviews*, Vol. 96 No. 1, pp. 1–17, doi: 10.1152/physrev.00013.2015.

Griswold, S.L. and Behringer, R.R. (2009), "Fetal leydig cell origin and development", *Sexual Development*, doi: 10.1159/000200077.

Guerriero, G., Trocchia, S., Abdel-Gawad, F.K. and Ciarcia, G. (2014), "Roles of reactive oxygen species in the spermatogenesis regulation", *Frontiers in Endocrinology*, Vol. 5 No. APR, doi: 10.3389/fendo.2014.00056.

Gurung, P. and Jialal, I. (2019), *Physiology, Male Reproductive System*, *StatPearls*.

Guthauser, B., Boitrelle, F., Plat, A., Thiercelin, N. and Vialard, F. (2014), "Chronic excessive alcohol consumption and male fertility: A case report on reversible azoospermia and a literature review", *Alcohol and Alcoholism*, Vol. 49 No. 1, pp. 42–44, doi: 10.1093/alcalc/agt133.

Hadley, G. (2007), "Basic Histology", *Journal of Anatomy*, Vol. 211 No. 3, pp. 412–412, doi: 10.1111/j.1469-7580.2007.771_1.x.

Hai, Y., Hou, J., Liu, Y., Liu, Y., Yang, H., Li, Z. and He, Z. (2014), "The roles and regulation of Sertoli cells in fate determinations of spermatogonial stem cells and spermatogenesis", *Seminars in Cell and Developmental Biology*, Vol. 29, pp. 66–75, doi: 10.1016/j.semcdb.2014.04.007.

Haider, S.G. (2007), "Leydig cell steroidogenesis: Unmasking the functional importance of mitochondria", *Endocrinology*, doi: 10.1210/en.2007-0330.

Hales, D.B. (2002), "Testicular macrophage modulation of Leydig cell steroidogenesis", *Journal of Reproductive Immunology*, Vol. 57 No. 1–2, pp. 3–18, doi: 10.1016/S0165-0378(02)00020-7.

Halsted, C.H. and Medici, V. (2012), "Alcohol: Effects of Consumption on Diet and Nutritional Status", *Encyclopedia of Human Nutrition*, Vol. 1–4, pp. 50–56, doi: 10.1016/B978-0-12-375083-9.00007-6.

Hamad Zubi, Z.B. and Hamad Alfarisi, H.A. (2021), "Hyperlipidemia and male infertility", *Egyptian Journal of Basic and Applied Sciences*, Vol. 8 No. 1, pp. 385–396, doi: 10.1080/2314808X.2021.1977080.

Hamada, A.J., Esteves, S.C. and Agarwal, A. (2013), "A comprehensive review of genetics and genetic testing in azoospermia", *Clinics*, doi: 10.6061/clinics/2013(Sup01)06.

Hamilton, T.R.D.S., Mendes, C.M., Castro, L.S. De, Assis, P.M. De, Siqueira, A.F.P., Delgado, J.D.C., Goissis, M.D., et al. (2016), "Evaluation of lasting effects of heat stress on sperm profile and oxidative status of ram semen and epididymal sperm", *Oxidative*

Medicine and Cellular Longevity, Vol. 2016, doi: 10.1155/2016/1687657.

Hammer, J.H., Parent, M.C., Spiker, D.A. and World Health Organization. (2018), "Global status report on alcohol and health 2018", *Global Status Report on Alcohol*, Vol. 65 No. 1, pp. 74–85, doi: 10.1037/cou0000248.

Hansen, L., Parker, I., Monet Roberts, L.D., Sutliff, R.L., Platt, M.O. and Gleason, R.L. (2013), "Azidothymidine (AZT) leads to arterial stiffening and intima-media thickening in mice", *Journal of Biomechanics*, Vol. 46 No. 9, pp. 1540–1547, doi: 10.1016/j.jbiomech.2013.03.021.

Hardy, H., Esch, L.D. and Morse, G.D. (2001), "Glucose disorders associated with HIV and its drug therapy", *Annals of Pharmacotherapy*, doi: 10.1345/aph.10044.

Harman, S.M., Metter, E.J., Tobin, J.D., Pearson, J. and Blackman, M.R. (2001), "Longitudinal effects of aging on serum total and free testosterone levels in healthy men", *Journal of Clinical Endocrinology and Metabolism*, Vol. 86 No. 2, pp. 724–731, doi: 10.1210/jcem.86.2.7219.

Harnaen, E.J., Na, A.F., Shenker, N.S., Sourial, M., Farmer, P.J., Southwell, B.R. and Hutson, J.M. (2007), "The anatomy of the cremaster muscle during inguinoscrotal testicular descent in the rat", *Journal of Pediatric Surgery*, doi: 10.1016/j.jpedsurg.2007.08.012.

Haugen, T.B., Landmark, B.F., Josefsen, G.M., Hansson, V. and Högset, A. (1994), "The mature form of interleukin-1α is constitutively expressed in immature male germ cells from rat", *Molecular and Cellular Endocrinology*, Vol. 105 No. 2, doi: 10.1016/0303-7207(94)90177-5.

He, M., Wang, L., Chen, Y., Zhang, T. and Guo, J. (2016), "Effect of Wuziyanzong pill on levels of sex hormones, and expressions of nuclear- associated antigen Ki-67 and androgen receptor in testes of young rats", *Journal of Traditional Chinese Medicine = Chung i Tsa Chih Ying Wen Pan*, Vol. 36 No. 6, pp. 743–748, doi: 10.1016/s0254-6272(17)30009-2.

HE, Z., YIN, G., LI, Q.Q., ZENG, Q. and DUAN, J. (2021), "Diabetes mellitus causes male reproductive dysfunction: A review of the evidence and mechanisms", *In Vivo*, doi: 10.21873/INVIVO.12531.

Hedger, M.P. and Meinhardt, A. (2003), "Cytokines and the immune-testicular axis", *Journal of Reproductive Immunology*, Vol. 58 No. 1, pp. 1–26, doi: 10.1016/S0165-0378(02)00060-8.

Van Heertum, K. and Rossi, B. (2017), "Alcohol and fertility: how much is too much?", *Fertility Research and Practice*, Fertility Research and Practice, Vol. 3 No. 1, p. 10, doi: 10.1186/s40738-017-0037-x.

Heinrich, A. and DeFalco, T. (2020), "Essential roles of interstitial cells in testicular development and function", *Andrology*, Vol. 8 No. 4, pp. 903–914, doi: 10.1111/andr.12703.

Heske, E.J. and Ostfeld, R.S. (1990), "Sexual dimorphism in size, relative size of testes, and mating systems in North American voles", *Journal of Mammalogy*, Vol. 71 No. 4, pp. 510–519, doi: 10.2307/1381789.

Hess, R.A. and França, L.R. (2004), "Structure of the Sertoli Cell", *Sertoli Cell Biology*, pp.

19–40, doi: 10.1016/B978-012647751-1/50004-0.

Hess, R.A. and De Franca, L.R. (2008), "Spermatogenesis and cycle of the seminiferous epithelium", *Advances in Experimental Medicine and Biology*, Vol. 636, pp. 1–15, doi: 10.1007/978-0-387-09597-4_1.

Hess, R.A. and Vogl, A.W. (2015), "Sertoli cell anatomy and cytoskeleton", *Sertoli Cell Biology*, pp. 1–55, doi: 10.1016/b978-0-12-417047-6.00001-6.

Ho, H.-J., Shirakawa, H. and Komai, M. (2017), "Menaquinone-4 Enhances Steroidogenesis in Testis Derived Tumor Cells Via the Elevation of cAMP Level", *Vitamin K2 - Vital for Health and Wellbeing*, InTech, doi: 10.5772/63982.

Hogarth, C.A. and Griswold, M.D. (2010), "The key role of vitamin A in spermatogenesis", *Journal of Clinical Investigation*, doi: 10.1172/JCI41303.

Hooker, C.W. (1970), "The Intertubular Tissue of the Testis", *Development, Anatomy, and Physiology*, pp. 483–550, doi: 10.1016/b978-0-12-386601-1.50014-7.

Howard, A.A., Arnsten, J.H. and Gourevitch, M.N. (2004), "Effect of alcohol consumption on diabetes mellitus: a systematic review.", *Annals of Internal Medicine*, Vol. 140 No. 3, pp. 211–9, doi: 10.7326/0003-4819-140-6-200403160-00011.

Huang, Y. and Kyriakides, T.R. (2020), "The role of extracellular matrix in the pathophysiology of diabetic wounds", *Matrix Biology Plus*, Vol. 6–7, p. 100037, doi: 10.1016/j.mbplus.2020.100037.

Hughes, I.A., Davies, J.D., Bunch, T.I., Pasterski, V., Mastroyannopoulou, K. and Macdougall, J. (2012), "Androgen insensitivity syndrome", *The Lancet*, doi: 10.1016/S0140-6736(12)60071-3.

Hussain, A.N., Hussain, F. and Hashmi, S.K. (2020), "Role of testosterone in COVID-19 patients – A double-edged sword?", *Medical Hypotheses*, Vol. 144, doi: 10.1016/j.mehy.2020.110287.

Hutson, J.M., Southwell, B.R., Li, R., Lie, G., Ismail, K., Harisis, G. and Chen, N. (2013), "The regulation of testicular descent and the effects of cryptorchidism", *Endocrine Reviews*, Vol. 34 No. 5, pp. 725–752, doi: 10.1210/er.2012-1089.

Ikekpeazu, J.E., Orji, O.C., Uchendu, I.K. and Ezeanyika, L.U.S. (2019), "Mitochondrial and Oxidative Impacts of Short and Long-term Administration of HAART on HIV Patients", *Current Clinical Pharmacology*, Vol. 15 No. 2, pp. 110–124, doi: 10.2174/1574884714666190905162237.

İlhan, M.N. and Yapar, D. (2020), "Alcohol consumption and alcohol policy", *Turkish Journal of Medical Sciences*, Vol. 50 No. 5, pp. 1197–1202, doi: 10.3906/sag-2002-237.

Inhorn, M.C. and Patrizio, P. (2014), "Infertility around the globe: New thinking on gender, reproductive technologies and global movements in the 21st century", *Human Reproduction Update*, Vol. 21 No. 4, pp. 411–426, doi: 10.1093/humupd/dmv016.

Ishikawa, T., Kondo, Y., Goda, K. and Fujisawa, M. (2005), "Overexpression of endothelial nitric oxide synthase in transgenic mice accelerates testicular germ cell apoptosis induced by experimental cryptorchidism", *Journal of Andrology*, Vol. 26 No. 2, pp. 281–288, doi: 10.1002/j.1939-4640.2005.tb01096.x.

Islam, R., Yoon, H., Kim, B.S., Bae, H.S., Shin, H.R., Kim, W.J., Yoon, W.J., et al. (2017), "Blood-testis barrier integrity depends on Pin1 expression in Sertoli cells", *Scientific Reports*, Nature Publishing Group, Vol. 7 No. 1, p. 6977, doi: 10.1038/s41598-017-07229-1.

Ismail, O.O., Isaac, J.A., Ugochukwu, O., Oluwatosin, O.O., Aniekan, P.I., Edwin, N.C.S. and Onyemaechi, A.O. (2017), "Impaired expression of testicular androgen receptor and collagen fibers in the testis of diabetic rats under HAART: The role of hypoxis hemerocallidea", *Folia Histochemica et Cytobiologica*, Vol. 55 No. 3, pp. 149–158, doi: 10.5603/FHC.a2017.0016.

Ito, Y., Unagami, M., Yamabe, F., Mistui, Y., Nakajima, K., Nagao, K. and Kobayashi, H. (2020), "New Criteria for Histopathological Classification of Testis Based on Johnsen Score for Male Infertility Using Automated Deep Learning Software", *SSRN Electronic Journal*, No. 11, p. 9962, doi: 10.2139/ssrn.3723666.

Ivell, R., Heng, K. and Anand-Ivell, R. (2014), "Insulin-like factor 3 and the HPG axis in the male", *Frontiers in Endocrinology*, Vol. 5 No. JAN, doi: 10.3389/fendo.2014.00006.

Jamison, D.T. and Mosley, W.H. (1991), "Disease control priorities in developing countries: Health policy responses to epidemiological change", *American Journal of Public Health*, Vol. 81 No. 1, pp. 15–22, doi: 10.2105/AJPH.81.1.15.

Jana, K., Jana, N., De, D.K. and Guha, S.K. (2010), "Ethanol induces mouse spermatogenic cell apoptosis in vivo through over-expression of Fas/Fas-L, p53, and caspase-3 along with cytochrome c translocation and glutathione depletion", *Molecular Reproduction and Development*, Vol. 77 No. 9, pp. 820–833, doi: 10.1002/mrd.21227.

Jankowska, K., Suszczewicz, N., Rabijewski, M., Dudek, P., Zgliczyński, W. and Maksym, R.B. (2022), "Inhibin-B and FSH Are Good Indicators of Spermatogenesis but Not the Best Indicators of Fertility", *Life*, Vol. 12 No. 4, p. 511, doi: 10.3390/life12040511.

Jelodar, G., Khaksar, Z. and Pourahmadi, M. (2009), "Endocrine profile and testicular histomorphometry in adult rat offspring of diabetic mothers", *Journal of Physiological Sciences*, Vol. 59 No. 5, pp. 377–382, doi: 10.1007/s12576-009-0045-7.

Jensen, E.C. (2013), "Quantitative Analysis of Histological Staining and Fluorescence Using ImageJ", *Anatomical Record*, Vol. 296 No. 3, pp. 378–381, doi: 10.1002/ar.22641.

Johnson, K.J. (2014), "Testicular histopathology associated with disruption of the Sertoli cell cytoskeleton", *Spermatogenesis*, Vol. 4 No. 2, p. e979106, doi: 10.4161/21565562.2014.979106.

Jungmann, N.A., Lang, D., Saleh, S., Van Der Mey, D. and Gerisch, M. (2019), "In vitro–in vivo correlation of the drug–drug interaction potential of antiretroviral HIV treatment regimens on CYP1A1 substrate riociguat", *Expert Opinion on Drug Metabolism and Toxicology*, Vol. 15 No. 11, pp. 975–984, doi: 10.1080/17425255.2019.1681968.

Jungwirth, A., Giwercman, A., Tournaye, H., Diemer, T., Kopa, Z., Dohle, G. and Krausz, C. (2012), "European association of urology guidelines on male infertility: The 2012 update", *European Urology*, Vol. 62 No. 2, pp. 324–332, doi: 10.1016/j.eururo.2012.04.048.

Kalinowski, A. and Humphreys, K. (2016), "Governmental standard drink definitions and low-risk alcohol consumption guidelines in 37 countries", *Addiction*, Vol. 111 No. 7, pp.

1293–1298, doi: 10.1111/add.13341.

Kalra, S., Kalra, B., Agrawal, N. and Unnikrishnan, A. (2011), "Understanding diabetes in patients with HIV/AIDS", *Diabetology and Metabolic Syndrome*, Vol. 3 No. 1, p. 2, doi: 10.1186/1758-5996-3-2.

Kanbak, G., Canbek, M., Oğlakçı, A., Kartkaya, K., Sentürk, H., Bayramoğlu, G., Bal, C., et al. (2012), "Preventive role of gallic acid on alcohol dependent and cysteine protease-mediated pancreas injury.", *Molecular Biology Reports*, Vol. 39 No. 12, pp. 10249–55, doi: 10.1007/s11033-012-1901-8.

Kangawa, A., Otake, M., Enya, S., Yoshida, T. and Shibata, M. (2019), "Histological Changes of the Testicular Interstitium during Postnatal Development in Microminipigs", *Toxicologic Pathology*, Vol. 47 No. 4, pp. 469–482, doi: 10.1177/0192623319827477.

Kanmaz, T.J. and Lee, N.J. (2000), "Significant toxicities associated with antiretroviral therapy", *Journal of Pharmacy Practice*, Vol. 13 No. 6, pp. 457–474, doi: 10.1106/2UU8-8JJD-UHRU-C14R.

Kann, L., Kinchen, S., Shanklin, S.L., Flint, K.H., Hawkins, J., Harris, W.A., Lowry, R., et al. (2014), "Youth risk behavior surveillance - United States, 2013", *MMWR Surveillance Summaries*, Vol. 63 No. 1, pp. 1–168.

Kaser, S., Winhofer-Stöckl, Y., Kazemi-Shirazi, L., Hofer, S.E., Brath, H., Sourij, H., Vila, G., et al. (2019), "Other specific types of diabetes and exocrine pancreatic insufficiency (Update 2019)", *Wiener Klinische Wochenschrift*, Vol. 131 No. Suppl 1, pp. 16–26, doi: 10.1007/s00508-019-1454-0.

Kaur, G., Thompson, L.A. and Dufour, J.M. (2014), "Sertoli cells - Immunological sentinels of spermatogenesis", *Seminars in Cell and Developmental Biology*, Vol. 30, pp. 36–44, doi: 10.1016/j.semcdb.2014.02.011.

Kaur, G., Wright, K., Verma, S., Haynes, A. and Dufour, J.M. (2021), "The Good, the Bad and the Ugly of Testicular Immune Regulation: A Delicate Balance Between Immune Function and Immune Privilege", *Advances in Experimental Medicine and Biology*, Vol. 1288, pp. 21–47, doi: 10.1007/978-3-030-77779-1_2.

Kehl, S., Weigel, M., Müller, D., Gentili, M., Hornemann, A. and Sütterlin, M. (2011), "HIV-infection and modern antiretroviral therapy impair sperm quality", *Archives of Gynecology and Obstetrics*, Vol. 284 No. 1, pp. 229–233, doi: 10.1007/s00404-011-1898-6.

Kelly, P., Saloojee, H., Chen, J.Y. and Chung, R.T. (2014), "Noncommunicable diseases in HIV infection in low-and middle-income countries: Gastrointestinal, hepatic, and nutritional aspects", *Journal of Acquired Immune Deficiency Syndromes*, Vol. 67 No. SUPPL.1, pp. S79-86, doi: 10.1097/QAI.0000000000000260.

Kemnic, T.R. and Gulick, P.G. (2019), *HIV Antiretroviral Therapy*, *StatPearls*.

Khairuddin, K., Sudirman, S., Huang, L. and Kong, Z.-L. (2020), "Caulerpa lentillifera Polysaccharides-Rich Extract Reduces Oxidative Stress and Proinflammatory Cytokines Levels Associated with Male Reproductive Functions in Diabetic Mice", *Applied Sciences*, Vol. 10 No. 24, p. 8768, doi: 10.3390/app10248768.

Khan, K., Khan, A.H., Sulaiman, S.A., Soo, C.T. and Aftab, R.A. (2014), "Adverse Effect of Highly Active Anti-Retroviral Therapy (HAART) In HIV/AIDS Patients", *Indian*

Journal of Pharmacy Practice, Vol. 7 No. 3, pp. 29–35, doi: 10.5530/ijopp.7.3.7.

Khawcharoenporn, T. and Sha, B.E. (2016), "HIV Infection and Infertility", *Genital Infections and Infertility*, InTech, pp. 178–199, doi: 10.5772/62390.

Kianifard, D., Sadrkhanlou, R.A. and Hasanzadeh, S. (2012), "The ultrastructural changes of the sertoli and leydig cells following streptozotocin induced diabetes", *Iranian Journal of Basic Medical Sciences*, Vol. 15 No. 1, pp. 623–635.

Kim, S.H. (2015), "Congenital hypogonadotropic hypogonadism and Kallmann syndrome: Past, present, and future", *Endocrinology and Metabolism*, Vol. 30 No. 4, pp. 456–466, doi: 10.3803/EnM.2015.30.4.456.

Kim, S.J. and Kim, D.J. (2012), "Alcoholism and diabetes mellitus", *Diabetes and Metabolism Journal*, Vol. 36 No. 2, pp. 108–115, doi: 10.4093/dmj.2012.36.2.108.

Kocyigit, E. (2015), "WHO | Infertility definitions and terminology. World Health Organization";, *Ekp*.

Koganti, P.P., Tu, L.N. and Selvaraj, V. (2022), "Functional metabolite reserves and lipid homeostasis revealed by the MA-10 Leydig cell metabolome", edited by Field, M.*PNAS Nexus*, Vol. 1 No. 4, pp. 1–14, doi: 10.1093/pnasnexus/pgac215.

Kohen, R. and Nyska, A. (2002), "Oxidation of biological systems: Oxidative stress phenomena, antioxidants, redox reactions, and methods for their quantification", *Toxicologic Pathology*, Vol. 30 No. 6, pp. 620–650, doi: 10.1080/01926230290166724.

Köksal, I.T., Erdoğru, T., Gülkesen, H., Sezer, C., Usta, M., Çiftçioğlu, A. and Baykara, M. (2003), "The potential role of inducible nitric oxide synthase (iNOS) activity in the testicular dysfunction associated with varicocele: An experimental study", *International Urology and Nephrology*, Vol. 36 No. 1, pp. 67–72, doi: 10.1023/B:UROL.0000032687.58462.4f.

Kolasa, A., Marchlewicz, M., Kurzawa, R., Głąbowski, W., Trybek, G., Wenda-Różewicka, L. and Wiszniewska, B. (2009), "The expression of inducible Nitric Oxide Synthase (iNOS) in the testis and epididymis of rats with a dihydrotestosterone (DHT) deficiency", *Cellular and Molecular Biology Letters*, Vol. 14 No. 3, pp. 511–527, doi: 10.2478/s11658-009-0019-z.

Kolesnikova, L.I., Kolesnikov, S.I., Kurashova, N.A. and Bairova, T.A. (2015), "Causes and factors of male infertility", *Vestnik Rossiiskoi Akademii Meditsinskikh Nauk*, Vol. 70 No. 5, pp. 579–584, doi: 10.15690/vramn.v70.i5.1445.

Korivi, B.R. and Pagliaro, L.C. (2022), "Testicular Germ Cell Tumors", *Oncologic Imaging: A Multidisciplinary Approach*, doi: 10.1016/B978-0-323-69538-1.00021-5.

Krausz, C. (2011), "Male infertility: Pathogenesis and clinical diagnosis", *Best Practice and Research: Clinical Endocrinology and Metabolism*, Vol. 25 No. 2, pp. 271–285, doi: 10.1016/j.beem.2010.08.006.

Kumar, A. and Nagar, M. (2014), "Histomorphometric study of testis in deltamethrin treated albino rats", *Toxicology Reports*, The Authors, Vol. 1, pp. 401–410, doi: 10.1016/j.toxrep.2014.07.005.

Kumar, S., Jin, M., Ande, A., Sinha, N., Silverstein, P.S. and Kumar, A. (2012), "Alcohol consumption effect on antiretroviral therapy and HIV-1 pathogenesis: Role of

cytochrome P450 isozymes", *Expert Opinion on Drug Metabolism and Toxicology*, Vol. 8 No. 11, pp. 1363–1375, doi: 10.1517/17425255.2012.714366.

Kumar, S., Rao, P.S.S., Earla, R. and Kumar, A. (2015), "Drug-drug interactions between anti-retroviral therapies and drugs of abuse in HIV systems", *Expert Opinion on Drug Metabolism and Toxicology*, Vol. 11 No. 3, pp. 343–355, doi: 10.1517/17425255.2015.996546.

Kumari, D., Nair, N. and Bedwal, R.S. (2011), "Effect of dietary zinc deficiency on testes of Wistar rats: Morphometric and cell quantification studies", *Journal of Trace Elements in Medicine and Biology*, Elsevier GmbH., Vol. 25 No. 1, pp. 47–53, doi: 10.1016/j.jtemb.2010.11.002.

Kurutas, E.B. (2016), "The importance of antioxidants which play the role in cellular response against oxidative/nitrosative stress: Current state", *Nutrition Journal*, Vol. 15 No. 1, p. 71, doi: 10.1186/s12937-016-0186-5.

Kushnir, V.A. and Lewis, W. (2011), "Human immunodeficiency virus/acquired immunodeficiency syndrome and infertility: Emerging problems in the era of highly active antiretrovirals", *Fertility and Sterility*, Vol. 96 No. 3, pp. 546–553, doi: 10.1016/j.fertnstert.2011.05.094.

Lampiao, F. and du Plessis, S.S. (2008), "TNF-α and IL-6 affect human sperm function by elevating nitric oxide production", *Reproductive BioMedicine Online*, Vol. 17 No. 5, pp. 628–631, doi: 10.1016/S1472-6483(10)60309-4.

Lanning, L.L., Creasy, D.M., Chapin, R.E., Mann, P.C., Barlow, N.J., Regan, K.S. and Goodman, D.G. (2002), "Recommended approaches for the evaluation of testicular and epididymal toxicity", *Toxicologic Pathology*, Vol. 30 No. 4, pp. 507–520, doi: 10.1080/01926230290105695.

Lara, N.L.M., Costa, G.M.J., Avelar, G.F., Lacerda, S.M.S.N., Hess, R.A. and França, L.R. (2018), "Testis physiology-overview and histology", *Encyclopedia of Reproduction*, Elsevier, pp. 105–116, doi: 10.1016/B978-0-12-801238-3.64567-1.

LaRocca, T.J., Sosunov, S.A., Shakerley, N.L., Ten, V.S. and Ratner, A.J. (2016), "Hyperglycemic conditions prime cells for RIP1-dependent necroptosis", *Journal of Biological Chemistry*, Vol. 291 No. 26, pp. 13753–13761, doi: 10.1074/jbc.M116.716027.

Larson, R., Capili, B., Eckert-Norton, M., Colagreco, J.P. and Anastasi, J.K. (2006), "Disorders of glucose metabolism in the context of human immunodeficiency virus infection", *Journal of the American Academy of Nurse Practitioners*, Vol. 18 No. 3, pp. 92–103, doi: 10.1111/j.1745-7599.2006.00109.x.

Lascar, N., Brown, J., Pattison, H., Barnett, A.H., Bailey, C.J. and Bellary, S. (2018), "Type 2 diabetes in adolescents and young adults", *The Lancet Diabetes and Endocrinology*, Vol. 6 No. 1, pp. 69–80, doi: 10.1016/S2213-8587(17)30186-9.

LEBLOND, C.P. and CLERMONT, Y. (1952), "Definition of the stages of the cycle of the seminiferous epithelium in the rat.", *Annals of the New York Academy of Sciences*, Vol. 55 No. 4, pp. 548–573, doi: 10.1111/j.1749-6632.1952.tb26576.x.

Van Leeuwen, E., Wit, F.W., Repping, S., Eeftinck Schattenkerk, J.K.M., Reiss, P., Van Der Veen, F. and Prins, J.M. (2008), "Effects of antiretroviral therapy on semen quality",

Aids, Vol. 22 No. 5, pp. 637–642, doi: 10.1097/QAD.0b013e3282f4de10.

Leisegang, K. and Henkel, R. (2018), "The in vitro modulation of steroidogenesis by inflammatory cytokines and insulin in TM3 Leydig cells", *Reproductive Biology and Endocrinology*, Vol. 16 No. 1, p. 26, doi: 10.1186/s12958-018-0341-2.

Leung, A., Mira, J. and Hsiao, W. (2014), "Updates on sperm retrieval techniques", *Translational Andrology and Urology*, doi: 10.3978/j.issn.2223-4683.2014.02.03.

Levine, A.B., Punihaole, D. and Levine, T.B. (2012), "Characterization of the role of nitric oxide and its clinical applications", *Cardiology (Switzerland)*, Vol. 122 No. 1, pp. 55–68, doi: 10.1159/000338150.

Lewko, W.M. and Oldham, R.K. (2009), "Cytokines", *Principles of Cancer Biotherapy: 5th Edition*, pp. 155–276, doi: 10.1007/978-90-481-2289-9_8.

Li, N., Wang, T. and Han, D. (2012), "Structural, cellular and molecular aspects of immune privilege in the testis", *Frontiers in Immunology*, Vol. 3 No. JUN, pp. 1–12, doi: 10.3389/fimmu.2012.00152.

Lie, P.P.Y., Mruk, D.D., Lee, W.M. and Cheng, C.Y. (2010), "Cytoskeletal dynamics and spermatogenesis", *Philosophical Transactions of the Royal Society B: Biological Sciences*, Vol. 365 No. 1546, pp. 1581–1592, doi: 10.1098/rstb.2009.0261.

Lin, S.P., Wu, C.Y., Wang, C.B., Li, T.C., Ko, N.Y. and Shi, Z.Y. (2018), "Risk of diabetes mellitus in HIV-infected patients receiving highly active antiretroviral therapy: A nationwide population-based study", *Medicine (United States)*, Vol. 97 No. 36, p. e12268, doi: 10.1097/MD.0000000000012268.

Lippman, S.A., El Ayadi, A.M., Grignon, J.S., Puren, A., Liegler, T., Venter, W.D.F., Ratlhagana, M.J., et al. (2019), "Improvements in the South African HIV care cascade: findings on 90-90-90 targets from successive population-representative surveys in North West Province", *Journal of the International AIDS Society*, Vol. 22 No. 6, p. e25295, doi: 10.1002/jia2.25295.

Liu, C., Gu, J., Ma, W., Zhang, Q., Song, M., Ha, L., Xu, X., et al. (2020), "Lycium barbarum polysaccharide protects against ethanol-induced spermiotoxicity and testicular degeneration in Immp2l+/− mice", *Andrologia*, Vol. 52 No. 4, doi: 10.1111/and.13554.

Liu, S. huan and Wang, Z. shan. (2005), "Study on the expression of androgen receptor in testis, epididymis and prostate of adult rats with diabetes", *Zhonghua Nan Ke Xue = National Journal of Andrology*, Vol. 11 No. 12, pp. 891–894.

Liu, Z., Chang, Q., Xu, Z.L. and Zhang, Z.G. (2009), "Stereological measurement of rat's seminiferous tubule", *Chinese Medical Journal*, Vol. 122 No. 21, pp. 2643–2646, doi: 10.3760/cma.j.issn.0366-6999.2009.21.022.

Long, L., Qiu, H., Cai, B., Chen, N., Lu, X., Zheng, S., Ye, X., et al. (2018), "Hyperglycemia induced testicular damage in type 2 diabetes mellitus rats exhibiting microcirculation impairments associated with vascular endothelial growth factor decreased via PI3K/Akt pathway", *Oncotarget*, Vol. 9 No. 4, pp. 5321–5336, doi: 10.18632/oncotarget.23915.

Losinno, A.D., Morales, A., Fernández, D. and Lopez, L.A. (2012), "Peritubular myoid cells from rat seminiferous tubules contain actin and myosin filaments distributed in two independent layers", *Biology of Reproduction*, Oxford Academic, Vol. 86 No. 5, pp. 150, 1–8, doi: 10.1095/biolreprod.111.095158.

Lossi, L. (2022), “The concept of intrinsic versus extrinsic apoptosis”, *Biochemical Journal*, doi: 10.1042/BCJ20210854.

Lotti, F. and Maggi, M. (2018), “Sexual dysfunction and male infertility”, *Nature Reviews Urology*, doi: 10.1038/nrurol.2018.20.

Lotti, F., Marchiani, S., Corona, G. and Maggi, M. (2021), “Metabolic syndrome and reproduction”, *International Journal of Molecular Sciences*, doi: 10.3390/ijms22041988.

Loveland, K.L., Klein, B., Pueschl, D., Indumathy, S., Bergmann, M., Loveland, B.E., Hedger, M.P., et al. (2017), “Cytokines in male fertility and reproductive pathologies: Immunoregulation and beyond”, *Frontiers in Endocrinology*, Vol. 8 No. NOV, doi: 10.3389/fendo.2017.00307.

Luccio-Camelo, D.C. and Prins, G.S. (2011), “Disruption of androgen receptor signaling in males by environmental chemicals”, *Journal of Steroid Biochemistry and Molecular Biology*, Vol. 127 No. 1–2, pp. 74–82, doi: 10.1016/j.jsbmb.2011.04.004.

Lucero, H.A., Patterson, S., Matsuura, S. and Ravid, K. (2016), “Quantitative histological image analyses of reticulin fibers in a myelofibrotic mouse”, *Journal of Biological Methods*, Vol. 3 No. 4, p. e60, doi: 10.14440/jbm.2016.152.

Lui, W.Y. and Cheng, C.Y. (2007), “Regulation of cell junction dynamics by cytokines in the testis-A molecular and biochemical perspective”, *Cytokine and Growth Factor Reviews*, doi: 10.1016/j.cytogfr.2007.04.009.

Mabwe, P., Kessy, A.T. and Semali, I. (2017), “Understanding the magnitude of occupational exposure to human immunodeficiency virus (HIV) and uptake of HIV post-exposure prophylaxis among healthcare workers in a rural district in Tanzania”, *Journal of Hospital Infection*, Vol. 96 No. 3, pp. 276–280, doi: 10.1016/j.jhin.2015.04.024.

Mallidis, C., Agbaje, I., McClure, N. and Kliesch, S. (2011), “Einfluss des diabetes mellitus auf die fertilität des mannes. Ein wenig untersuchter faktor der männlichen infertilität”, *Urologe - Ausgabe A*, Vol. 50 No. 1, pp. 33–37, doi: 10.1007/s00120-010-2440-3.

Mann, S.C., Morrow, M., Coyle, R.P., Coleman, S.S., Saderup, A., Zheng, J.H., Ellison, L., et al. (2020), “Lower Cumulative Antiretroviral Exposure in People Living with HIV and Diabetes Mellitus”, *Journal of Acquired Immune Deficiency Syndromes*, Vol. 85 No. 4, pp. 483–488, doi: 10.1097/QAI.0000000000002460.

Mann, U., Shiff, B. and Patel, P. (2020), “Reasons for worldwide decline in male fertility”, *Current Opinion in Urology*, Vol. 30 No. 3, pp. 296–301, doi: 10.1097/MOU.0000000000000745.

Maresch, C.C., Stute, D.C., Alves, M.G., Oliveira, P.F., de Kretser, D.M. and Linn, T. (2018), “Diabetes-induced hyperglycemia impairs male reproductive function: A systematic review”, *Human Reproduction Update*, Vol. 24 No. 1, pp. 86–105, doi: 10.1093/humupd/dmx033.

Marques, P., Skorupskaite, K., George, J.T. and Anderson, R.A. (2000), *Physiology of GNRH and Gonadotropin Secretion*, *Endotext*.

Martin, L.J. (2016), “Cell interactions and genetic regulation that contribute to testicular Leydig cell development and differentiation.”, *Molecular Reproduction and Development*, Vol. 83 No. 6, pp. 470–87, doi: 10.1002/mrd.22648.

Martins, A.D., Majzoub, A. and Agawal, A. (2019), “Metabolic syndrome and male fertility”, *World Journal of Men?S Health*, Vol. 37 No. 2, pp. 113–127, doi: 10.5534/wjmh.180055.

Mastan, S.K., Chaitanya, G., Raghunandan Reddy, K. and Eswar Kumar, K. (2009), “Glucose disorders associated with antiretroviral therapy: An overview”, *Biomedical and Pharmacology Journal*.

Mateus, I., Feijó, M., Espínola, L.M., Vaz, C. V., Correia, S. and Socorro, S. (2018), “Glucose and glutamine handling in the Sertoli cells of transgenic rats overexpressing regucalcin: Plasticity towards lactate production”, *Scientific Reports*, Vol. 8 No. 1, doi: 10.1038/s41598-018-28668-4.

Mattli, R., Wieser, S., Probst-Hensch, N., Schmidt-Trucksäss, A. and Schwenkglenks, M. (2019), “Physical inactivity caused economic burden depends on regional cultural differences”, *Scandinavian Journal of Medicine and Science in Sports*, Vol. 29 No. 1, pp. 95–104, doi: 10.1111/sms.13311.

Mauduit, C., Hamamah, S. and Benahmed, M. (1999), “Stem cell factor/c-kit system in spermatogenesis”, *Human Reproduction Update*, doi: 10.1093/humupd/5.5.535.

Mayer, C., Adam, M., Walenta, L., Schmid, N., Heikelä, H., Schubert, K., Flenkenthaler, F., et al. (2018), “Insights into the role of androgen receptor in human testicular peritubular cells”, *Andrology*, Vol. 6 No. 5, pp. 756–765, doi: 10.1111/andr.12509.

Mayerhofer, A. (2013), “Human testicular peritubular cells: More than meets the eye”, *Reproduction*, Vol. 145 No. 5, pp. R107-16, doi: 10.1530/REP-12-0497.

McCance-Katz, E.F., Gruber, V.A., Beatty, G., Lum, P.J. and Rainey, P.M. (2013), “Interactions between alcohol and the antiretroviral medications ritonavir or efavirenz”, *Journal of Addiction Medicine*, Vol. 7 No. 4, pp. 264–270, doi: 10.1097/ADM.0b013e318293655a.

McLachlan, R.I., Rajpert-De Meyts, E., Hoei-Hansen, C.E., de Kretser, D.M. and Skakkebaek, N.E. (2007), “Histological evaluation of the human testis - Approaches to optimizing the clinical value of the assessment: Mini Review”, *Human Reproduction*, Vol. 22 No. 1, pp. 2–16, doi: 10.1093/humrep/del279.

Meethal, S.V. and Atwood, C.S. (2005), “The role of hypothalamic-pituitary-gonadal hormones in the normal structure and functioning of the brain”, *Cellular and Molecular Life Sciences*, Vol. 62 No. 3, pp. 257–270, doi: 10.1007/s00018-004-4381-3.

Meinhardt, A., Bacher, M., McFarlane, J.R., Metz, C.N., Seitz, J., Hedger, M.P., De Kretser, D.M., et al. (1996), “Macrophage migration inhibitory factor production by Leydig cells: Evidence for a role in the regulation of testicular function”, *Endocrinology*, Vol. 137 No. 11, pp. 5090–5095, doi: 10.1210/endo.137.11.8895383.

Meistrich, M.L. and Hess, R.A. (2013), “Assessment of spermatogenesis through staging of seminiferous tubules”, *Methods in Molecular Biology*, Vol. 927, pp. 299–307, doi: 10.1007/978-1-62703-38-0_27.

Meskari, T., Ghafari, S., Khouri, V., Azarhoush, R. and Golalipour, M.J. (2018), “Gestational diabetes reduced sertoli cells in 12 weeks age rat offsprings testis”, *Journal of the Anatomical Society of India*, Vol. 67 No. 1, pp. 35–39, doi: 10.1016/j.jasi.2018.05.002.

Michel, L., Carrieri, M.P., Fugon, L., Roux, P., Aubin, H.J., Lert, F., Obadia, Y., et al.

(2010), “Harmful alcohol consumption and patterns of substance use in HIV-infected patients receiving antiretrovirals (ANRS-EN12-VESPA Study): Relevance for clinical management and intervention”, *AIDS Care - Psychological and Socio-Medical Aspects of AIDS/HIV*, Vol. 22 No. 9, pp. 1136–1145, doi: 10.1080/09540121003605039.

Miller, S.R. and Cherrington, N.J. (2018), “Transepithelial transport across the blood–testis barrier”, *Reproduction*, Vol. 156 No. 6, pp. R187–R194, doi: 10.1530/REP-18-0338.

Miller, W.L. and Auchus, R.J. (2011), “The molecular biology, biochemistry, and physiology of human steroidogenesis and its disorders”, *Endocrine Reviews*, doi: 10.1210/er.2010-0013.

Mocroft, A., Reiss, P., Rakhmanova, A., Banhegyi, D., Phillips, A.N., De Wit, S., Ristola, M., et al. (2014), “A survey of ATRIPLA use in clinical practice as first-line therapy in HIV-positive persons in Europe”, *Infection*, Vol. 42 No. 4, pp. 757–762, doi: 10.1007/s15010-014-0630-4.

Modelska-Ziolkiewicz, A. (2009), “Male aging & its management”, *Turkiye Klinikleri Journal of Medical Sciences*, Vol. 29 No. SUPPL.

Moffit, J.S., Bryant, B.H., Hall, S.J. and Boekelheide, K. (2007), “Dose-dependent effects of sertoli cell toxicants 2,5-hexanedione, carbendazim,and mono-(2-ethylhexyl) phthalate in adult rat testis”, *Toxicologic Pathology*, Vol. 35 No. 5, pp. 719–727, doi: 10.1080/01926230701481931.

Mondal, S., Ghosh, P., Biswas, D. and Roy, P.K. (2019), “Effect of alcohol consumption during antiretroviral therapy on HIV-1 replication: Role of Cytochrome P3A4 enzyme”, *International Journal of Mathematical, Engineering and Management Sciences*, Vol. 4 No. 4, pp. 922–935, doi: 10.33889/IJMEMS.2019.4.4-073.

Monteiro, J.C., da Matta, S.L.P., Predes, F.S. and de Paula, T.A.R. (2012), “Testicular morphology of adult wistar rats treated with Rudgea viburnoides (Cham.) Benth. Leaf infusion”, *Brazilian Archives of Biology and Technology*, Vol. 55 No. 1, pp. 101–105, doi: 10.1590/S1516-89132012000100013.

Moon, J.H., Yoo, D.Y., Jo, Y.K., Kim, G.A., Jung, H.Y., Choi, J.H., Hwang, I.K., et al. (2014), “Unilateral chryptochidism induces morphological changes of testes and hyperplasia of Sertoli cells in a dog”, *Laboratory Animal Research*, Vol. 30 No. 4, p. 185, doi: 10.5625/lar.2014.30.4.185.

Moore, C. and Hutson, J.C. (1994), “Physiological relevance of tumor necrosis factor in mediating macrophage-leydig cell interactions”, *Endocrinology*, Vol. 134 No. 1, pp. 63–69, doi: 10.1210/endo.134.1.8275970.

Morales-Montor, J., Baig, S., Mitchell, R., Deway, K., Hallal-Calleros, C. and Damian, R.T. (2001), “Immunoendocrine interactions during chronic cysticercosis determine male mouse feminization: role of IL-6.”, *Journal of Immunology (Baltimore, Md. : 1950)*, Vol. 167 No. 8, pp. 4527–33, doi: 10.4049/jimmunol.167.8.4527.

Mruk, D.D. and Cheng, C.Y. (2004), “Sertoli-sertoli and sertoli-germ cell interactions and their significance in germ cell movement in the seminiferous epithelium during spermatogenesis”, *Endocrine Reviews*, Vol. 25 No. 5, pp. 747–806, doi: 10.1210/er.2003-0022.

Mruk, D.D. and Cheng, C.Y. (2015), “The mammalian blood-testis barrier: Its biology and

regulation", *Endocrine Reviews*, Vol. 36 No. 5, pp. 564–591, doi: 10.1210/er.2014-1101.

Mulholland, J., Mallidis, C., Agbaje, I. and McClure, N. (2011), "Male diabetes mellitus and assisted reproduction treatment outcome", *Reproductive BioMedicine Online*, Reproductive Healthcare Ltd., Vol. 22 No. 2, pp. 215–219, doi: 10.1016/j.rbmo.2010.10.005.

Murphy, C.J. and Richburg, J.H. (2014), "Implications of Sertoli cell induced germ cell apoptosis to testicular pathology", *Spermatogenesis*, Vol. 4 No. 2, p. e979110, doi: 10.4161/21565562.2014.979110.

Mushtaq, H., Alam, S. and Khan, M.A. (2013), "Histopathological Patterns of Testicular Biopsies in Male Infertility Introduction: Male infertility contributes to about 20%", *Journal of Islamabad Medical & Dental College (JIMDC)*, Vol. 2 No. 4, pp. 81–86.

Muthusami, K.R. and Chinnaswamy, P. (2005), "Effect of chronic alcoholism on male fertility hormones and semen quality", *Fertility and Sterility*, Vol. 84 No. 4, pp. 919–924, doi: 10.1016/j.fertnstert.2005.04.025.

Nakae, D., Akai, H., Kishida, H., Kusuoka, O., Tsutsumi, M. and Konishi, Y. (2000), "Age and organ dependent spontaneous generation of nuclear 8- hydroxydeoxyguanosine in male Fischer 344 rats", *Laboratory Investigation*, Vol. 80 No. 2, pp. 249–261, doi: 10.1038/labinvest.3780028.

Nakai, M. and Hess, R.A. (1994), "Morphological changes in the rat sertoli cell induced by the microtubule poison carbendazim", *Tissue and Cell*, Vol. 26 No. 6, pp. 917–927, doi: 10.1016/0040-8166(94)90041-8.

Nakata, H., Sonomura, T. and Iseki, S. (2017), "Three-dimensional analysis of seminiferous tubules and spermatogenic waves in mice", *Reproduction*, Vol. 154 No. 5, pp. 569–579, doi: 10.1530/REP-17-0391.

National Institute on Alcohol Abuse and Alcoholism. (2004), "NIAAA Newsletter", *U.S. Department of Health and Human Services*, Vol. 3.

Navarro-Casado, L., Juncos-Tobarra, M.A., Cháfer-Rudilla, M., Íñiguez De Onzoño, L., Blázquez-Cabrera, J.A. and Miralles-García, J.M. (2010), "Effect of experimental diabetes and STZ on male fertility capacity. Study in rats", *Journal of Andrology*, Vol. 31 No. 6, pp. 584–592, doi: 10.2164/jandrol.108.007260.

Naz, M. and Kamal, M. (2017), "Classification, causes, diagnosis and treatment of male infertility: a review", *Oriental Pharmacy and Experimental Medicine*, Vol. 17 No. 2, pp. 89–109, doi: 10.1007/s13596-017-0269-7.

Necho, M., Belete, A. and Getachew, Y. (2020), "The prevalence and factors associated with alcohol use disorder among people living with HIV/AIDS in Africa: A systematic review and meta-analysis", *Substance Abuse: Treatment, Prevention, and Policy*, Vol. 15 No. 1, p. 63, doi: 10.1186/s13011-020-00301-6.

Neves, B.V.D., Lorenzini, F., Veronez, D., de Miranda, E.P., Neves, G.D. and De Fraga, R. (2017), "Numeric and volumetric changes in leydig cells during aging of rats", *Acta Cirurgica Brasileira*, Vol. 32 No. 10, pp. 807–815, doi: 10.1590/s0102-865020170100000002.

Newton, A.S., Dong, K., Mabood, N., Ata, N., Ali, S., Gokiert, R., Vandermeer, B., et al. (2013), "Brief emergency department interventions for youth who use alcohol and other

drugs: A systematic review", *Pediatric Emergency Care*, Vol. 29 No. 5, pp. 673–684, doi: 10.1097/PEC.0b013e31828ed325.

Nishi, K., Ramakrishnan, S., Gunasekaran, V.P., Parkash, K., Ramakrishnan, A., Vijayakumar, N. and Ganeshan, M. (2018), "Protective effects of p-coumaric acid on ethanol induced male reproductive toxicity", *Life Sciences*, Vol. 209, pp. 1–8, doi: 10.1016/j.lfs.2018.07.045.

Nna, V.U., Bakar, A.B.A., Ahmad, A., Eleazu, C.O. and Mohamed, M. (2019), "Oxidative stress, NF-κB-mediated inflammation and apoptosis in the testes of streptozotocin–induced diabetic rats: Combined protective effects of malaysian propolis and metformin", *Antioxidants*, Vol. 8 No. 10, p. 465, doi: 10.3390/antiox8100465.

Nojilana, B., Bradshaw, D., Pillay-van Wyk, V., Msemburi, W., Laubscher, R., Somdyala, N.I.M., Joubert, J.D., et al. (2016), "Emerging trends in non-communicable disease mortality in South Africa, 1997 – 2010", *South African Medical Journal*, Vol. 106 No. 5, pp. 477–484, doi: 10.7196/SAMJ.2016.v106i5.10674.

O'Bryan, M.K., Schlatt, S., Gerdprasert, O., Phillips, D.J., De Kretser, D.M. and Hedger, M.P. (2000), "Inducible nitric oxide synthase in the rat tesis: Evidence for potential roles in both normal function and inflammation-mediated infertility", *Biology of Reproduction*, Vol. 63 No. 5, pp. 1285–1293, doi: 10.1095/biolreprod63.5.1285.

O'Donnell, L., Narula, A., Balourdos, G., Gu, Y.-Q., Wreford, N.G., Robertson, D.M., Bremner, W.J., et al. (2001), " Impairment of Spermatogonial Development and Spermiation after Testosterone-Induced Gonadotropin Suppression in Adult Monkeys (Macaca fascicularis) 1 ", *The Journal of Clinical Endocrinology & Metabolism*, Vol. 86 No. 4, pp. 1814–1822, doi: 10.1210/jcem.86.4.7400.

O'Donnell, L., Smith, L.B. and Rebourcet, D. (2022), "Sertoli cells as key drivers of testis function", *Seminars in Cell and Developmental Biology*, doi: 10.1016/j.semcdb.2021.06.016.

O'Hara, L. and Smith, L.B. (2015), "Androgen receptor roles in spermatogenesis and infertility", *Best Practice and Research: Clinical Endocrinology and Metabolism*, Vol. 29 No. 4, pp. 595–605, doi: 10.1016/j.beem.2015.04.006.

Oduwole, O.O., Peltoketo, H. and Huhtaniemi, I.T. (2018), "Role of follicle-stimulating hormone in spermatogenesis", *Frontiers in Endocrinology*, Vol. 9, doi: 10.3389/fendo.2018.00763.

Ogedengbe, O.O., Jegede, A.I., Onanuga, I.O., Offor, U., Naidu, E.C.S., Peter, A.I. and Azu, O.O. (2016), "Coconut oil extract mitigates testicular injury following adjuvant treatment with antiretroviral drugs", *Toxicological Research*, Vol. 32 No. 4, pp. 317–325, doi: 10.5487/TR.2016.32.4.317.

Ogedengbe, O.O., Jegede, A.I., Onanuga, I.O., Offor, U., Peter, A.I., Akang, E.N., Naidu, E.C.S., et al. (2018), "Adjuvant potential of virgin coconut oil extract on antiretroviral therapy-induced testicular toxicity: An ultrastructural study", *Andrologia*, Vol. 50 No. 3, p. e12930, doi: 10.1111/and.12930.

Ogedengbe, O.O., Naidu, E.C.S., Akang, E.N., Offor, U., Onanuga, I.O., Peter, A.I., Jegede, A.I., et al. (2018), "Virgin coconut oil extract mitigates testicular-induced toxicity of alcohol use in antiretroviral therapy", *Andrology*, Vol. 6 No. 4, pp. 616–626, doi: 10.1111/andr.12490.

Ogedengbe, O.O., Naidu, E.C.S. and Azu, O.O. (2018), "Antiretroviral Therapy and Alcohol Interactions: X-raying Testicular and Seminal Parameters Under the HAART Era", *European Journal of Drug Metabolism and Pharmacokinetics*, Springer International Publishing, Vol. 43 No. 2, pp. 121–135, doi: 10.1007/s13318-017-0438-6.

Olasile, I.O., Ayoola Jegede, I., Ugochukwu, O., Oluwatosin Ogedengbe, O., Edwin Naidu, C.S., Aniekan Peter, I. and Onyemaechi Azu, O. (2018), "Histo-morphological and seminal evaluation of testicular parameters in diabetic rats under antiretroviral therapy: Interactions with hypoxis hemerocallidea", *Iranian Journal of Basic Medical Sciences*, Vol. 21 No. 12, pp. 1316–1324, doi: 10.22038/ijbms.2018.25046.6213.

de Oliveira, S.A., Cerri, P.S. and Sasso-Cerri, E. (2021), "Impaired macrophages and failure of steroidogenesis and spermatogenesis in rat testes with cytokines deficiency induced by diacerein", *Histochemistry and Cell Biology*, Vol. 156 No. 6, pp. 561–581, doi: 10.1007/s00418-021-02023-7.

Olojede, S.O., Lawal, S.K., Dare, A., Moodley, R., Rennie, C.O., Naidu, E.C.S. and Azu, O.O. (2021), "Highly active antiretroviral therapy conjugated silver nanoparticle ameliorates testicular injury in type-2 diabetic rats", *Heliyon*, Vol. 7 No. 12, doi: 10.1016/j.heliyon.2021.e08580.

Olojede, S.O., Lawal, S.K., Dare, A., Naidu, E.C.S., Rennie, C.O. and Azu, O.O. (2022), "Evaluation of tenofovir disoproxil fumarate loaded silver nanoparticle on testicular morphology in experimental type-2 diabetic rats", *Artificial Cells, Nanomedicine and Biotechnology*, Taylor & Francis, Vol. 50 No. 1, pp. 71–80, doi: 10.1080/21691401.2022.2042009.

Olojede, S.O., Lawal, S.K., Faborode, O.S., Dare, A., Aladeyelu, O.S., Moodley, R., Rennie, C.O., et al. (2022), "Testicular ultrastructure and hormonal changes following administration of tenofovir disoproxil fumarate-loaded silver nanoparticle in type-2 diabetic rats.", *Scientific Reports*, Nature Publishing Group UK, Vol. 12 No. 1, p. 9633, doi: 10.1038/s41598-022-13321-y.

Omar, S.S., Aly, R.G. and Badae, N.M. (2018), "Vitamin E improves testicular damage in streptozocin-induced diabetic rats, via increasing vascular endothelial growth factor and poly(ADP-ribose) polymerase-1", *Andrologia*, Vol. 50 No. 3, p. e12925, doi: 10.1111/and.12925.

Omolaoye Temidayo, S. and Du Plessis Stefan, S. (2018), "Diabetes mellitus and male infertility", *Asian Pacific Journal of Reproduction*, Vol. 7 No. 1, pp. 6–14, doi: 10.4103/2305-0500.220978.

ONUSIDA. (2017), "Data 2017", *Programme on HIV/AIDS*, pp. 1–248.

Oremosu, A.A. and Akang, E.N. (2015), "Impact of alcohol on male reproductive hormones, oxidative stress and semen parameters in Sprague-Dawley rats", *Middle East Fertility Society Journal*, Middle East Fertility Society, Vol. 20 No. 2, pp. 114–118, doi: 10.1016/j.mefs.2014.07.001.

Owembabazi, E., Nkomozepi, P., Calvey, T. and Mbajiorgu, E.F. (2023), "Co-administration of alcohol and combination antiretroviral therapy (cART) in male Sprague Dawley rats: A study on testicular morphology, oxidative and cytokines perturbations", *Anatomy & Cell Biology*, doi: 10.5115/acb.22.229.

Owyong, M. and Ramasamy, R. (2018), "Epidemiology of oxidative stress in male fertility",

Oxidants, Antioxidants, and Impact of the Oxidative Status in Male Reproduction, Elsevier, pp. 81–90, doi: 10.1016/B978-0-12-812501-4.00009-2.

Oyeyipo, I.P., Skosana, B.T., Everson, F.P., Strijdom, H. and du Plessis, S.S. (2018), "Highly active antiretroviral therapy alters sperm parameters and testicular antioxidant status in diet-induced obese rats", *Toxicological Research*, Vol. 34 No. 1, pp. 41–48, doi: 10.5487/TR.2018.34.1.041.

Pajarinen, J.T. and Karhunen, P.J. (1994), "Spermatogenic arrest and 'Sertoli cell-only' syndrome—common alcohol-induced disorders of the human testis", *International Journal of Andrology*, Vol. 17 No. 6, pp. 292–299, doi: 10.1111/j.1365-2605.1994.tb01259.x.

Palleti, H.J. (2008), "Comments on 'The process of spermatogenesis liberates significant heat and the scrotum has a role in body thermoregulation'", *Medical Hypotheses*, doi: 10.1016/j.mehy.2007.07.013.

Papadopoulos, V. and Miller, W.L. (2012), "Role of mitochondria in steroidogenesis", *Best Practice and Research: Clinical Endocrinology and Metabolism*, doi: 10.1016/j.beem.2012.05.002.

Parhizkar, S., Zulkifli, S.B. and Dollah, M.A. (2014), "Testicular morphology of male rats exposed to Phaleria macrocarpa (Mahkota dewa) aqueous extract", *Iranian Journal of Basic Medical Sciences*, Vol. 17 No. 5, pp. 389–395, doi: 10.22038/ijbms.2014.2791.

Patel, V., Chisholm, D., Parikh, R., Charlson, F.J., Degenhardt, L., Dua, T., Ferrari, A.J., et al. (2016), "Global Priorities for Addressing the Burden of Mental, Neurological, and Substance Use Disorders", *Disease Control Priorities, Third Edition (Volume 4): Mental, Neurological, and Substance Use Disorders*, pp. 1–27, doi: 10.1596/978-1-4648-0426-7_ch1.

Patrick, M.E., Cronce, J.M., Fairlie, A.M., Atkins, D.C. and Lee, C.M. (2016), "Day-to-day variations in high-intensity drinking, expectancies, and positive and negative alcohol-related consequences", *Addictive Behaviors*, Vol. 58, pp. 110–116, doi: 10.1016/j.addbeh.2016.02.025.

Pavili, L., Daudin, M., Moinard, N., Walschaerts, M., Cuzin, L., Massip, P., Pasquier, C., et al. (2010), "Decrease of mitochondrial DNA level in sperm from patients infected with human immunodeficiency virus-1 linked to nucleoside analogue reverse transcriptase inhibitors", *Fertility and Sterility*, Vol. 94 No. 6, pp. 2151–2156, doi: 10.1016/j.fertnstert.2009.12.080.

Perey, B., Clermont, Y. and Leblond, C.P. (1961), "The wave of the seminiferous epithelium in the rat", *American Journal of Anatomy*, Vol. 108 No. 1, pp. 47–77, doi: 10.1002/aja.1001080105.

Pérez, C. V., Theas, M.S., Jacobo, P. V., Jarazo-Dietrich, S., Guazzone, V.A. and Lustig, L. (2013), "Dual role of immune cells in the testis", *Spermatogenesis*, Vol. 3 No. 1, p. e23870, doi: 10.4161/spmg.23870.

Pérez, C.V., Sobarzo, C.M., Jacobo, P.V., Pellizzari, E.H., Cigorraga, S.B., Denduchis, B. and Lustig, L. (2012), "Loss of occludin expression and impairment of blood-testis barrier permeability in rats with autoimmune orchitis: effect of interleukin 6 on Sertoli cell tight junctions.", *Biology of Reproduction*, Vol. 87 No. 5, p. 122, doi: 10.1095/biolreprod.112.101709.

Petersen, C. and Söder, O. (2006), "The Sertoli cell - A hormonal target and 'super' nurse for germ cells that determines testicular size", *Hormone Research*, Vol. 66 No. 4, pp. 153–161, doi: 10.1159/000094142.

Pheiffer, C., Pillay-Van Wyk, V., Joubert, J.D., Levitt, N., Nglazi, M.D. and Bradshaw, D. (2018), "The prevalence of type 2 diabetes in South Africa: A systematic review protocol", *BMJ Open*, Vol. 8 No. 7, p. e021029, doi: 10.1136/bmjopen-2017-021029.

Pienkowski, C., Cartault, A., Caula-Legriel, S., Ajaltouni, Z., Daudin, M. and Tauber, M. (2011), "Syndrome de Klinefelter et syndrome de Turner : pour une meilleure prise en charge", *Gynecologie Obstetrique et Fertilite*, Vol. 39, pp. 521–524, doi: 10.1016/j.gyobfe.2011.07.009.

Pike, C.J., Rosario, E.R. and Nguyen, T.V. V. (2006), "Androgens, aging, and Alzheimer's disease", *Endocrine*, Vol. 29 No. 2, pp. 233–241, doi: 10.1385/ENDO:29:2:233.

Pillai, R.N. and McEleny, K. (2021), "Management of male infertility", *Obstetrics, Gynaecology and Reproductive Medicine*, doi: 10.1016/j.ogrm.2021.05.003.

Pinney, S.E. and Simmons, R.A. (2012), "Metabolic programming, Epigenetics, and gestational diabetes mellitus", *Current Diabetes Reports*, Vol. 12 No. 1, pp. 67–74, doi: 10.1007/s11892-011-0248-1.

Piquet-Pellorce, C., Dorval-Coiffec, I., Pham, M.D. and Jégou, B. (2000), "Leukemia inhibitory factor expression and regulation within the testis", *Endocrinology*, Vol. 141 No. 3, pp. 1136–1141, doi: 10.1210/endo.141.3.7399.

Pitteloud, N., Hardin, M., Dwyer, A.A., Valassi, E., Yialamas, M., Elahi, D. and Hayes, F.J. (2005), "Increasing insulin resistance is associated with a decrease in Leydig cell testosterone secretion in men", *Journal of Clinical Endocrinology and Metabolism*, Vol. 90 No. 5, pp. 2636–2641, doi: 10.1210/jc.2004-2190.

Plant, T.M. (2015), "The hypothalamo-pituitary-gonadal axis", *Journal of Endocrinology*, Vol. 226 No. 2, pp. T41–T54, doi: 10.1530/JOE-15-0113.

Pohl, E., Höffken, V., Schlatt, S., Kliesch, S., Gromoll, J. and Wistuba, J. (2019), "Ageing in men with normal spermatogenesis alters spermatogonial dynamics and nuclear morphology in Sertoli cells", *Andrology*, Vol. 7 No. 6, pp. 827–839, doi: 10.1111/andr.12665.

Pöllänen, P.P., Kallajoki, M., Risteli, L., Risteli, J. and Suominen, J.J.O. (1985), "Laminin and type IV collagen in the human testis", *International Journal of Andrology*, Vol. 8 No. 5, pp. 337–347, doi: 10.1111/j.1365-2605.1985.tb00846.x.

Pourentezari, M., Talebi, A.R., Mangoli, E., Anvari, M. and Rahimipour, M. (2016), "Additional deleterious effects of alcohol consumption on sperm parameters and DNA integrity in diabetic mice", *Andrologia*, Vol. 48 No. 5, pp. 564–569, doi: 10.1111/and.12481.

Print, C.G. and Loveland, K.L. (2000), "Germ cell suicide: New insights into apoptosis during spermatogenesis", *BioEssays*, doi: 10.1002/(SICI)1521-1878(200005)22:5<423::AID-BIES4>3.0.CO;2-0.

Pryor, W.A., Houk, K.N., Foote, C.S., Fukuto, J.M., Ignarro, L.J., Squadrito, G.L. and Davies, K.J.A. (2006), "Free radical biology and medicine: it's a gas, man!", *American Journal of Physiology. Regulatory, Integrative and Comparative Physiology*, Vol. 291

No. 3, pp. R491-511, doi: 10.1152/ajpregu.00614.2005.

Purohit, V. (2000), "Can alcohol promote aromatization of androgens to estrogens? A review", *Alcohol*, Vol. 22 No. 3, pp. 123–127, doi: 10.1016/S0741-8329(00)00124-5.

Qin, Q., Liu, J., Ma, Y., Wang, Y., Zhang, F., Gao, S. and Dong, L. (2017), "Aberrant expressions of stem cell factor/c-KIT in rat testis with varicocele", *Journal of the Formosan Medical Association*, Vol. 116 No. 7, pp. 542–548, doi: 10.1016/j.jfma.2016.09.001.

Qiu, L.L., Wang, X., Zhang, X. hui, Zhang, Z., Gu, J., Liu, L., Wang, Y., et al. (2013), "Decreased androgen receptor expression may contribute to spermatogenesis failure in rats exposed to low concentration of bisphenol A", *Toxicology Letters*, Vol. 219 No. 2, pp. 116–124, doi: 10.1016/j.toxlet.2013.03.011.

Rachdaoui, N. and Sarkar, D.K. (2013), "Effects of Alcohol on the Endocrine System", *Endocrinology and Metabolism Clinics of North America*, Vol. 42 No. 3, pp. 593–615, doi: 10.1016/j.ecl.2013.05.008.

Rachdaoui, N. and Sarkar, D.K. (2017), "Pathophysiology of the Effects of Alcohol Abuse on the Endocrine System", *Alcohol Research : Current Reviews*, Vol. 38 No. 2, pp. 255–276.

Raheem, A.A. and Ralph, D. (2011), "Male infertility: causes and investigations", *Trends in Urology & Men's Health*, Vol. 2 No. 5, pp. 8–11, doi: 10.1002/tre.216.

Raheem, A.A., Rees, R. and Ralph, D. (2019), "Male infertility", *Blandy's Urology*, Wiley, Treasure Island (FL), Vol. 22 No. 1, pp. 803–815, doi: 10.1002/9781118863343.ch40.

Ramaswamy, S. and Weinbauer, G.F. (2014), "Endocrine control of spermatogenesis: Role of FSH and LH/ testosterone", *Spermatogenesis*, Vol. 4 No. 2, p. e996025, doi: 10.1080/21565562.2014.996025.

Ramlau-Hansen, C.H., Toft, G., Jensen, M.S., Strandberg-Larsen, K., Hansen, M.L. and Olsen, J. (2010), "Maternal alcohol consumption during pregnancy and semen quality in the male offspring: Two decades of follow-up", *Human Reproduction*, Vol. 25 No. 9, pp. 2340–2345, doi: 10.1093/humrep/deq140.

Ranzer, M.J., Chen, L. and DiPietro, L.A. (2011), "Fibroblast Function and Wound Breaking Strength Is Impaired by Acute Ethanol Intoxication", *Alcoholism: Clinical and Experimental Research*, Vol. 35 No. 1, pp. 83–90, doi: 10.1111/j.1530-0277.2010.01324.x.

Ravindranath, N., Dettin, L. and Dym, M. (2003), "Mammalian Testes: Structure and Function", *Introduction to Mammalian Reproduction*, Springer US, Boston, MA, pp. 1–19, doi: 10.1007/978-1-4615-0273-9_1.

Ray, S. and Pramanik, S. (2020), "Reproductive Dysfunctions in Males with Type 2 Diabetes Mellitus: An Updated Review", *EMJ Diabetes*, pp. 79–89, doi: 10.33590/emjdiabet/20-00171.

Rebourcet, D., Darbey, A., Monteiro, A., Soffientini, U., Tsai, Y.T., Handel, I., Pitetti, J.L., et al. (2017), "Sertoli cell number defines and predicts germ and leydig cell population sizes in the adult mouse testis", *Endocrinology*, Oxford Academic, Vol. 158 No. 9, pp. 2955–2969, doi: 10.1210/en.2017-00196.

Rehm, J. (2011), “The risks associated with alcohol use and alcoholism”, *Alcohol Research and Health*, Vol. 34 No. 2, pp. 135–143.

Rehm, J., Mathers, C., Popova, S., Thavorncharoensap, M., Teerawattananon, Y. and Patra, J. (2009), “Global burden of disease and injury and economic cost attributable to alcohol use and alcohol-use disorders”, *The Lancet*, doi: 10.1016/S0140-6736(09)60746-7.

Rey, R.A., Grinspon, R.P., Gottlieb, S., Pasqualini, T., Knoblovits, P., Aszpis, S., Pacenza, N., et al. (2013), “Male hypogonadism: an extended classification based on a developmental, endocrine physiology-based approach.”, *Andrology*, doi: 10.1111/j.2047-2927.2012.00008.x.

Riera, M.F., Galardo, M.N., Pellizzari, E.H., Meroni, S.B. and Cigorraga, S.B. (2009), “Molecular mechanisms involved in Sertoli cell adaptation to glucose deprivation”, *American Journal of Physiology - Endocrinology and Metabolism*, Vol. 297 No. 4, pp. E907–E914, doi: 10.1152/ajpendo.00235.2009.

Rk, S., Ra, B., Ak, G., Jk, B. and Sharma, R.K. (2015), “Germ Cells Apoptosis during Spermatogenesis in Mammals”, *Journal of Entomology and Zoology Studies JEZS*, Vol. 3 No. 33, pp. 506–515.

Roan, F., Obata-Ninomiya, K. and Ziegler, S.F. (2019), “Epithelial cell–derived cytokines: More than just signaling the alarm”, *Journal of Clinical Investigation*, Vol. 129 No. 4, pp. 1441–1451, doi: 10.1172/JCI124606.

Robinson, L., Gallos, I.D., Conner, S.J., Rajkhowa, M., Miller, D., Lewis, S., Kirkman-Brown, J., et al. (2012), “The effect of sperm DNA fragmentation on miscarriage rates: A systematic review and meta-analysis”, *Human Reproduction*, doi: 10.1093/humrep/des261.

Rochira, V., Zirilli, L., Orlando, G., Santi, D., Brigante, G., Diazzi, C., Carli, F., et al. (2011), “Premature decline of serum total testosterone in HIV-infected men in the HAART-Era”, *PLoS ONE*, Vol. 6 No. 12, doi: 10.1371/journal.pone.0028512.

Rosa, D.F., Sarandy, M.M., Novaes, R.D., Freitas, M.B., do Carmo Gouveia Pelúzio, M. and Gonçalves, R.V. (2018), “High-fat diet and alcohol intake promotes inflammation and impairs skin wound healing in Wistar rats”, *Mediators of Inflammation*, Vol. 2018, p. 4658583, doi: 10.1155/2018/4658583.

Rossi, G., Dufrusine, B., Lizzi, A.R., Luzi, C., Piccoli, A., Fezza, F., Iorio, R., et al. (2020), “Bisphenol a deranges the endocannabinoid system of primary sertoli cells with an impact on inhibin b production”, *International Journal of Molecular Sciences*, Vol. 21 No. 23, pp. 1–15, doi: 10.3390/ijms21238986.

Sadler, T.. (2012), “Langman’s Medical Embryology Twelth Edition”, *The Human Skeleton*, pp. 225–227.

Saeedi, P., Petersohn, I., Salpea, P., Malanda, B., Karuranga, S., Unwin, N., Colagiuri, S., et al. (2019), “Global and regional diabetes prevalence estimates for 2019 and projections for 2030 and 2045: Results from the International Diabetes Federation Diabetes Atlas, 9th edition”, *Diabetes Research and Clinical Practice*, Elsevier Ireland Ltd, Vol. 157, p. 107843, doi: 10.1016/j.diabres.2019.107843.

SAEZ, J.M., AVALLET, O., NAVILLE, D., PERRARD-SAPORI, M.H. and CHATELAIN, P.G. (1989), “Sertoli-Leydig Cell Communications”, *Annals of the New York Academy*

of Sciences, Vol. 564 No. 1, pp. 210–231, doi: 10.1111/j.1749-6632.1989.tb25899.x.

Sakr, S.A. and Nooh, H.Z. (2013), " Effect of Ocimum basilicum extract on cadmium-induced testicular histomorphometric and immunohistochemical alterations in albino rats ", *Anatomy & Cell Biology*, Vol. 46 No. 2, p. 122, doi: 10.5115/acb.2013.46.2.122.

Salardi, S., Zucchini, S., Cicognani, A., Gualandi, S., Barbieri, E. and Cacciari, E. (2002), "Inhibin B levels in adolescents and young adults with type 1 diabetes", *Hormone Research*, Vol. 57 No. 5–6, pp. 205–208, doi: 10.1159/000058384.

Salman, I., Munazza, A., Hina, M.A., Tahir, S., Yasir, A. and Gul-E-, N. (2014), "Evaluation of spermatogenesis in prepubertal albino rats with date palm pollen supplement", *African Journal of Pharmacy and Pharmacology*, Vol. 8 No. 2, pp. 59–65, doi: 10.5897/ajpp2013.3662.

Salonia, A., Rastrelli, G., Hackett, G., Seminara, S.B., Huhtaniemi, I.T., Rey, R.A., Hellstrom, W.J.G., et al. (2019), "Paediatric and adult-onset male hypogonadism.", *Nature Reviews. Disease Primers*, Vol. 5 No. 1, p. 38, doi: 10.1038/s41572-019-0087-y.

Sansone, A., Di Dato, C., de Angelis, C., Menafra, D., Pozza, C., Pivonello, R., Isidori, A., et al. (2018), "Smoke, alcohol and drug addiction and male fertility", *Reproductive Biology and Endocrinology*, Reproductive Biology and Endocrinology, Vol. 16 No. 1, p. 3, doi: 10.1186/s12958-018-0320-7.

Santos, C.R., Benjamin, A.C.A., Chies, A.B., Domeniconi, R.F., Zochio, G.P. and Spadella, M.A. (2020), "Adjuvant-induced arthritis affects testes and ventral prostate of Wistar rats", *Andrology*, Vol. 8 No. 2, pp. 473–485, doi: 10.1111/andr.12693.

Savasi, V., Oneta, M., Laoreti, A., Parisi, F., Parrilla, B., Duca, P. and Cetin, I. (2018), "Effects of Antiretroviral Therapy on Sperm DNA Integrity of HIV-1-Infected Men", *American Journal of Men's Health*, Vol. 12 No. 6, pp. 1835–1842, doi: 10.1177/1557988318794282.

Savasi, V., Parisi, F., Oneta, M., Laoreti, A., Parrilla, B., Duca, P. and Cetin, I. (2019), "Effects of highly active antiretroviral therapy on semen parameters of a cohort of 770 HIV-1 infected men", *PLoS ONE*, Public Library of Science, Vol. 14 No. 2, p. e0212194, doi: 10.1371/journal.pone.0212194.

Schneider, M., Chersich, M., Temmerman, M. and Parry, C.D. (2016), "Addressing the intersection between alcohol consumption and antiretroviral treatment: Needs assessment and design of interventions for primary healthcare workers, the Western Cape, South Africa", *Globalization and Health*, Globalization and Health, Vol. 12 No. 1, p. 65, doi: 10.1186/s12992-016-0201-9.

Schneider, M., Neuman, M., Chersich, M. and Parry, C. (2012), "Alcohol and antiretroviral therapy - A lethal cocktail", *Journal of AIDS and Clinical Research*, Vol. 3 No. SPL ISS1A, pp. 1–8, doi: 10.4172/2155-6113.S1-005.

Schoeller, E.L., Schon, S. and Moley, K.H. (2012), "The effects of type 1 diabetes on the hypothalamic, pituitary and testes axis", *Cell and Tissue Research*, Vol. 349 No. 3, pp. 839–847, doi: 10.1007/s00441-012-1387-7.

Scott-Sheldon, L.A.J., Carey, K.B., Cunningham, K., Johnson, B.T. and Carey, M.P. (2016), "Alcohol Use Predicts Sexual Decision-Making: A Systematic Review and Meta-Analysis of the Experimental Literature", *AIDS and Behavior*, Vol. 20 No. S1, pp. 19–

39, doi: 10.1007/s10461-015-1108-9.

Seevagan, T., Hulligan, S., Phull, J. and Aboumarzouk, O.M. (2019), "Testes structure and function", *Blandy's Urology*, Wiley, pp. 731–739, doi: 10.1002/9781118863343.ch35.

Semião-Francisco, L., De Almeida Ferreira Braga, D.P., De Cássia Savio Figueira, R., Madaschi, C., Pasqualotto, F.F., Iaconelli, A. and Borges, E. (2010), "Assisted reproductive technology outcomes in azoospermic men: 10 years of experience with surgical sperm retrieval", *Aging Male*, Vol. 13 No. 1, pp. 44–50, doi: 10.3109/13685530903342203.

Sengupta, P., Dutta, S., Karkada, I.R. and Chinni, S. V. (2022), "Endocrinopathies and male infertility", *Life*, doi: 10.3390/life12010010.

Shah, W., Khan, R., Shah, B., Khan, A., Dil, S., Liu, W., Wen, J., et al. (2021), "The Molecular Mechanism of Sex Hormones on Sertoli Cell Development and Proliferation", *Frontiers in Endocrinology*, Vol. 12, doi: 10.3389/fendo.2021.648141.

Shaha, C., Tripathi, R. and Prasad Mishra, D. (2010), "Male germ cell apoptosis: Regulation and biology", *Philosophical Transactions of the Royal Society B: Biological Sciences*, doi: 10.1098/rstb.2009.0124.

Shaikh, H., Shrivastava, V.K. and Amir, M. (2016), "Diabetes Mellitus and Impairment of Male Reproductive Function: Role of Hypothalamus Pituitary Testicular Axis and Reactive Oxygen Species", *Iranian Journal of Diabetes and Obesity*, Vol. 8 No. 1, p. 41.

Shan, L.X., Bardin, C.W. and Hardy, M.P. (1997), "Immunohistochemical analysis of androgen effects on androgen receptor expression in developing leydig and Sertoli cells", *Endocrinology*, Vol. 138 No. 3, pp. 1259–1266, doi: 10.1210/endo.138.3.4973.

Sharma, R. and Agarwal, A. (2011), "Spermatogenesis: An Overview", *Sperm Chromatin*, Springer New York, New York, NY, pp. 19–44, doi: 10.1007/978-1-4419-6857-9_2.

Sharma, R. and Agarwal, A. (2013), "Spermatogenesis: An Overview", *Sperm Chromatin for the Researcher*, Springer New York, New York, NY, pp. 127–160, doi: 10.1007/978-1-4614-8459-2_8.

Sharpe, R.M., Fraser, H.M., Cooper, I. and Rommerts, F.F.G. (1981), "Sertoli-Leydig cell communication via an LHRH-like factor", *Nature*, Vol. 290 No. 5809, pp. 785–787, doi: 10.1038/290785a0.

Sharpe, R.M., McKinnell, C., Kivlin, C. and Fisher, J.S. (2003), "Proliferation and functional maturation of Sertoli cells, and their relevance to disorders of testis function in adulthood", *Reproduction*, doi: 10.1530/rep.0.1250769.

Shayakhmetova, G.M., Bondarenko, L.B., Kovalenko, V.M. and Ruschak, V. V. (2013), "CYP2E1 testis expression and alcohol-mediated changes of rat spermatogenesis indices and type I collagen", *Arhiv Za Higijenu Rada i Toksikologiju*, Vol. 64 No. 2, pp. 237–246, doi: 10.2478/10004-1254-64-2013-2313.

Shima, Y. and Morohashi, K. ichirou. (2017), "Leydig progenitor cells in fetal testis", *Molecular and Cellular Endocrinology*, Vol. 445, pp. 55–64, doi: 10.1016/j.mce.2016.12.006.

Shirasaka, T. (2010), "Adverse effects of antiretroviral agents, and their treatment", *Nippon*

Rinsho. Japanese Journal of Clinical Medicine, Vol. 68 No. 3, pp. 480–485.

Shokoohi, M., Madarek, E.O.S., Khaki, A., Shoorei, H., Khaki, A.A., Soltani, M. and Ainehchi, N. (2018), "Investigating the effects of onion juice on male fertility factors and pregnancy rate after testicular torsion/detorsion by intrauterine insemination method", *International Journal of Women's Health and Reproduction Sciences*, Vol. 6 No. 4, pp. 499–505, doi: 10.15296/ijwhr.2018.82.

Shubber, Z., Mills, E.J., Nachega, J.B., Vreeman, R., Freitas, M., Bock, P., Nsanzimana, S., et al. (2016), "Patient-Reported Barriers to Adherence to Antiretroviral Therapy: A Systematic Review and Meta-Analysis", edited by Weiser, S.D.*PLoS Medicine*, Vol. 13 No. 11, p. e1002183, doi: 10.1371/journal.pmed.1002183.

Shukla, K.K., Mahdi, A.A. and Rajender, S. (2012), "Apoptosis, spermatogenesis and male infertility.", *Frontiers in Bioscience (Elite Edition)*, Vol. 4 No. 2, pp. 746–54, doi: 10.2741/415.

Da Silva, M., Shevchuk, M.M., Cronin, W.J., Armenakas, N.A., Tannenbaum, M., Fracchia, J.A. and Ioachim, H.L. (1990), "Detection of HIV-related protein in testes and prostates of patients with AIDS", *American Journal of Clinical Pathology*, Vol. 93 No. 2, pp. 196–201, doi: 10.1093/ajcp/93.2.196.

Simões, D., Meireles, P., Rocha, M., Freitas, R., Aguiar, A. and Barros, H. (2021), "Knowledge and Use of PEP and PrEP Among Key Populations Tested in Community Centers in Portugal", *Frontiers in Public Health*, Vol. 9, doi: 10.3389/fpubh.2021.673959.

Simpson, E. (2006), "A historical perspective on immunological privilege", *Immunological Reviews*, doi: 10.1111/j.1600-065X.2006.00434.x.

Singh, V. (2014), "Textbook of Clinical Embryology", *The Obstetrician & Gynaecologist*, Elsevier, Vol. 16 No. 4, pp. 294–295, doi: 10.1111/tog.12137.

Singh, V.P., Bali, A., Singh, N. and Jaggi, A.S. (2014), "Advanced glycation end products and diabetic complications", *Korean Journal of Physiology and Pharmacology*, Vol. 18 No. 1, pp. 1–14, doi: 10.4196/kjpp.2014.18.1.1.

Sisman, A.R., Kiray, M., Camsari, U.M., Evren, M., Ates, M., Baykara, B., Aksu, I., et al. (2014), "Potential novel biomarkers for diabetic testicular damage in streptozotocin-induced diabetic rats: Nerve growth factor beta and vascular endothelial growth factor", *Disease Markers*, Hindawi Publishing Corporation, Vol. 2014, p. 108106, doi: 10.1155/2014/108106.

Siu, M.K.Y. and Cheng, C.Y. (2004), "Extracellular matrix: Recent advances on its role in junction dynamics in the seminiferous epithelium during spermatogenesis", *Biology of Reproduction*, Vol. 71 No. 2, pp. 375–391, doi: 10.1095/biolreprod.104.028225.

Sivangala, R. and Sumanlatha, G. (2015), "Cytokines that mediate and regulate immune responses", *Innovative Immunology*, pp. 1–26.

Skakkebæk, N.E., Lindahl-Jacobsen, R., Levine, H., Andersson, A.M., Jørgensen, N., Main, K.M., Lidegaard, Ø., et al. (2022), "Environmental factors in declining human fertility", *Nature Reviews Endocrinology*, Vol. 18 No. 3, pp. 139–157, doi: 10.1038/s41574-021-00598-8.

Skandhan, K.P. and Rajahariprasad, A. (2007), "The process of spermatogenesis liberates

significant heat and the scrotum has a role in body thermoregulation", *Medical Hypotheses*, Vol. 68 No. 2, pp. 303–307, doi: 10.1016/j.mehy.2006.06.058.

Smith, L.B. and Walker, W.H. (2014), "The regulation of spermatogenesis by androgens", *Seminars in Cell and Developmental Biology*, Vol. 30, pp. 2–13, doi: 10.1016/j.semcdb.2014.02.012.

SÖDER, O., SYED, V., CALLARD, G. V., TOPPARI, J., PÖLLÄNEN, P., PARVINEN, M., FRÖYSA, B., et al. (1991), "Production and secretion of an interleukin-l-like factor is stage-dependent and correlates with spermatogonial DNA synthesis in the rat seminiferous epithelium", *International Journal of Andrology*, Vol. 14 No. 3, pp. 223–231, doi: 10.1111/j.1365-2605.1991.tb01084.x.

Somade, O.T., Ajayi, B.O., Safiriyu, O.A., Oyabunmi, O.S. and Akamo, A.J. (2019), "Renal and testicular up-regulation of pro-inflammatory chemokines (RANTES and CCL2) and cytokines (TNF-α, IL-1β, IL-6) following acute edible camphor administration is through activation of NF-kB in rats", *Toxicology Reports*, Vol. 6, pp. 759–767, doi: 10.1016/j.toxrep.2019.07.010.

Sönmez, M.F., Kiliç, E., Karabulut, D., Çilenk, K.T., Deligönül, E. and Dündar, M. (2016), "Nitric oxide synthase in diabetic rat testicular tissue and the effects of pentoxifylline therapy", *Systems Biology in Reproductive Medicine*, Vol. 62 No. 1, pp. 22–30, doi: 10.3109/19396368.2015.1085605.

Srinivasa, S. and Grinspoon, S.K. (2014), "Metabolic and body composition effects of newer antiretrovirals in HIV-infected patients", *European Journal of Endocrinology*, Vol. 170 No. 5, pp. R185-202, doi: 10.1530/EJE-13-0967.

Steyn, N.P., Parker, W., Nel, J.H., Ayah, R. and Mbithe, D. (2012), "Urbanisation and the nutrition transition: A comparison of diet and weight status of South African and Kenyan women", *Scandinavian Journal of Public Health*, Vol. 40 No. 3, pp. 229–238, doi: 10.1177/1403494812443605.

Su, L., Mruk, D.D. and Cheng, C.Y. (2011), "Drug transporters, the blood-testis barrier, and spermatogenesis", *Journal of Endocrinology*, Vol. 208 No. 3, pp. 207–223, doi: 10.1677/JOE-10-0363.

Su, L.J., Zhang, J.H., Gomez, H., Murugan, R., Hong, X., Xu, D., Jiang, F., et al. (2019), "Reactive Oxygen Species-Induced Lipid Peroxidation in Apoptosis, Autophagy, and Ferroptosis", *Oxidative Medicine and Cellular Longevity*, Vol. 2019, p. 5080843, doi: 10.1155/2019/5080843.

Suarez-Pinzon, W., Korbutt, G.S., Power, R., Hooton, J., Rajotte, R. V. and Rabinovitch, A. (2000), "Testicular Sertoli cells protect islet β-cells from autoimmune destruction in NOD mice by a transforming growth factor-β1-dependent mechanism", *Diabetes*, Vol. 49 No. 11, pp. 1810–1818, doi: 10.2337/diabetes.49.11.1810.

Suh, J.H., Gong, E.Y., Hong, C.Y., Park, E., Ahn, R.S., Park, K.S. and Lee, K. (2008), "Reduced testicular steroidogenesis in tumor necrosis factor-α knockout mice", *Journal of Steroid Biochemistry and Molecular Biology*, Vol. 112 No. 1–3, pp. 117–121, doi: 10.1016/j.jsbmb.2008.09.003.

Sultan, M.T., Butt, M.S., Karim, R., Zia-Ul-Haq, M., Batool, R., Ahmad, S., Aliberti, L., et al. (2014), "Nigella sativa fixed and essential oil supplementation modulates hyperglycemia and allied complications in streptozotocin-induced diabetes mellitus",

Evidence-Based Complementary and Alternative Medicine, Vol. 2014, pp. 1–8, doi: 10.1155/2014/826380.

Sun, H., Gong, T.T., Jiang, Y.T., Zhang, S., Zhao, Y.H. and Wu, Q.J. (2019), "Global, Regional, and National Prevalence and Disability-Adjusted Life-Years for Infertility in 195 Countries and Territories, 1990-2017: Results from a Global Burden of Disease Study, 2017", *Aging*, Vol. 11 No. 23, pp. 10952–10991, doi: 10.18632/aging.102497.

Surampudi, P.N., Wang, C. and Swerdloff, R. (2012), "Hypogonadism in the Aging Male Diagnosis, Potential Benefits, and Risks of Testosterone Replacement Therapy", *International Journal of Endocrinology*, Vol. 2012, pp. 1–20, doi: 10.1155/2012/625434.

Syriou, V., Papanikolaou, D., Kozyraki, A. and Goulis, D.G. (2018), "Cytokines and male infertility", *European Cytokine Network*, Vol. 29 No. 3, pp. 73–82, doi: 10.1684/ecn.2018.0412.

Tarulli, G.A., Stanton, P.G., Lerchl, A. and Meachem, S.J. (2006), "Adult sertoli cells are not terminally differentiated in the Djungarian hamster: Effect of FSH on proliferation and junction protein organization", *Biology of Reproduction*, Vol. 74 No. 5, pp. 798–806, doi: 10.1095/biolreprod.105.050450.

Tarulli, G.A., Stanton, P.G. and Meachem, S.J. (2012), "Is the adult sertoli cell terminally differentiated?", *Biology of Reproduction*, doi: 10.1095/biolreprod.111.095091.

Teixeira, T.A., Pariz, J.R., Dutra, R.T., Saldiva, P.H., Costa, E. and Hallak, J. (2019), "Cut-off values of the Johnsen score and Copenhagen index as histopathological prognostic factors for postoperative semen quality in selected infertile patients undergoing microsurgical correction of bilateral subclinical varicocele", *Translational Andrology and Urology*, Vol. 8 No. 4, pp. 346–355, doi: 10.21037/tau.2019.06.23.

Thanh, T.N., Van, P.D., Cong, T.D., Le Minh, T. and Vu, Q.H.N. (2020), "Assessment of testis histopathological changes and spermatogenesis in male mice exposed to chronic scrotal heat stress", *Journal of Animal Behaviour and Biometeorology*, Vol. 8 No. 3, pp. 174–180, doi: 10.31893/JABB.20023.

Titi-Lartey, O.A. and Khan, Y.S. (2020), *Embryology, Testicle*, *StatPearls*.

Tournaye, H. (2000), "Management of male infertility by assisted reproductive technologies", *Best Practice and Research: Clinical Endocrinology and Metabolism*, Vol. 14 No. 3, pp. 423–435, doi: 10.1053/beem.2000.0089.

Trangenstein, P.J., Morojele, N.K., Lombard, C., Jernigan, D.H. and Parry, C.D.H. (2018), "Heavy drinking and contextual risk factors among adults in South Africa: Findings from the International Alcohol Control study", *Substance Abuse: Treatment, Prevention, and Policy*, Substance Abuse Treatment, Prevention, and Policy, Vol. 13 No. 1, p. 43, doi: 10.1186/s13011-018-0182-1.

Tremellen, K. (2012), "Oxidative stress and male infertility: A clinical perspective", *Studies on Men's Health and Fertility*, Vol. 14, Humana Press, Totowa, NJ, pp. 325–353, doi: 10.1007/978-1-61779-776-7_16.

Trindade, A.A.T., Simões, A.C.P., Silva, R.J., Macedo, C.S. and Spadella, C.T. (2013), "Long term evaluation of morphometric and ultrastructural changes of testes of alloxan-induced diabetic rats", *Acta Cirurgica Brasileira*, Vol. 28 No. 4, pp. 256–265, doi:

10.1590/S0102-86502013000400005.

Tripathi, A., Thangaraj, A., Chivero, E.T., Periyasamy, P., Burkovetskaya, M.E., Niu, F., Guo, M.L., et al. (2020), "N-Acetylcysteine Reverses Antiretroviral-Mediated Microglial Activation by Attenuating Autophagy-Lysosomal Dysfunction", *Frontiers in Neurology*, Vol. 11, doi: 10.3389/fneur.2020.00840.

Türk, G., Rişvanlı, A., Çeribaşı, A.O., Sönmez, M., Yüce, A., Güvenç, M., Arslan Özkan, H., et al. (2018), "Effect of gestational diabetes mellitus on testis and pancreatic tissues of male offspring", *Andrologia*, Vol. 50 No. 4, doi: 10.1111/and.12976.

Turner, T.T. and Lysiak, J.J. (2008), "Oxidative stress: A common factor in testicular dysfunction", *Journal of Andrology*, Vol. 29 No. 5, pp. 488–498, doi: 10.2164/jandrol.108.005132.

Tywanek, E., Trojanowska, P., Wronecki, J., Wiśniewska-Ślepaczuk, K. and Łuczyk, R.J. (2021), "Male hypogonadism – brief review of symptoms, types and ways of treatment", *Journal of Education, Health and Sport*, Vol. 11 No. 9, pp. 538–543, doi: 10.12775/jehs.2021.11.09.070.

UNAIDS. (2016), "HIV/AIDS Fact sheet n°360", *United Nations Programme on HIV/AIDS*.

UNAIDS. (2019), "UNAIDS Fact sheet Report", *Global HIV Statistics*, pp. 1–476.

UNAIDS. (2022), "Global HIV Statistics Fact Sheet", *Fact Sheet 2021*.

Vellios, N.G. and van Walbeek, C.P. (2018), "Self-reported alcohol use and binge drinking in South Africa: Evidence from the national income dynamics study, 2014 - 2015", *South African Medical Journal*, Vol. 108 No. 1, pp. 33–39, doi: 10.7196/SAMJ.2018.v108i1.12615.

Ventimiglia, E., Capogrosso, P., Boeri, L., Ippolito, S., Scano, R., Moschini, M., Gandaglia, G., et al. (2016), "Validation of the American Society for Reproductive Medicine guidelines/recommendations in white European men presenting for couple's infertility", *Fertility and Sterility*, Vol. 106 No. 5, pp. 1076-1082.e1, doi: 10.1016/j.fertnstert.2016.06.044.

Verma, A.S., Singh, I.G., Bansal, R. and Singh, A. (2013), "HIV and Antiretroviral Drugs", *Animal Biotechnology: Models in Discovery and Translation*, pp. 155–176, doi: 10.1016/B978-0-12-416002-6.00009-2.

Vicari, E., Arancio, A., Giuffrida, V., D'Agata, R. and Calogero, A.E. (2002), "A case of reversible azoospermia following withdrawal from alcohol consumption", *Journal of Endocrinological Investigation*, Vol. 25 No. 5, pp. 473–476, doi: 10.1007/BF03344041.

Victor, E., Osarugue, I., Mega Obukohwo, O., Eze Kingsley, N. and Alexander Obidike, N. (2022), "Endocrine Functions of the Testes", *Male Reproductive Anatomy*, doi: 10.5772/intechopen.101170.

Vidal, J.D. and Whitney, K.M. (2014), "Morphologic manifestations of testicular and epididymal toxicity", *Spermatogenesis*, Vol. 4 No. 2, p. e979099, doi: 10.4161/21565562.2014.979099.

La Vignera, S., Condorelli, R., Vicari, E., D'Agata, R. and Calogero, A.E. (2012), "Diabetes mellitus and minireview sperm parameters", *Journal of Andrology*, Vol. 33 No. 2, pp. 145–153, doi: 10.2164/jandrol.111.013193.

La Vignera, S., Condorelli, R.A., Balercia, G., Vicari, E. and Calogero, A.E. (2013), "Does alcohol have any effect on male reproductive function? A review of literature", *Asian Journal of Andrology*, Vol. 15 No. 2, pp. 221–225, doi: 10.1038/aja.2012.118.

Violi, F., Marino, R., Milite, M.T. and Loffredo, L. (1999), "Nitric oxide and its role in lipid peroxidation", *Diabetes/Metabolism Research and Reviews*, Vol. 15 No. 4, pp. 283–288, doi: 10.1002/(SICI)1520-7560(199907/08)15:4<283::AID-DMRR42>3.0.CO;2-U.

Volpe, C.M.O., Villar-Delfino, P.H., Dos Anjos, P.M.F. and Nogueira-Machado, J.A. (2018), "Cellular death, reactive oxygen species (ROS) and diabetic complications review-Article", *Cell Death and Disease*, Vol. 9 No. 2, p. 119, doi: 10.1038/s41419-017-0135-z.

Wake, A.D. (2021), "Alcohol consumption and the incidence of type 2 diabetic mellitus: 'issue that requires more attention'", *Endocrinology&Metabolism International Journal*, Vol. 8 No. 6, pp. 143–147, doi: 10.15406/emij.2021.08.00298.

Walsh, T.J., Croughan, M.S., Schembri, M., Chan, J.M. and Turek, P.J. (2009), "Increased risk of testicular germ cell cancer among infertile men", *Archives of Internal Medicine*, Vol. 169 No. 4, pp. 351–356, doi: 10.1001/archinternmed.2008.562.

Wang, R.S., Yeh, S., Tzeng, C.R. and Chang, C. (2009), "Androgen receptor roles in spermatogenesis and fertility: Lessons from testicular cell-specific androgen receptor knockout mice", *Endocrine Reviews*, Vol. 30 No. 2, pp. 119–132, doi: 10.1210/er.2008-0025.

Wang, Y., Chen, F., Ye, L., Zirkin, B. and Chen, H. (2017), "Steroidogenesis in leydig cells: Effects of aging and environmental factors", *Reproduction*, Vol. 154 No. 4, pp. R111–R122, doi: 10.1530/REP-17-0064.

Wangikar, P., Ahmed, T. and Vangala, S. (2011), "Toxicologic Pathology of the Reproductive System", *Reproductive and Developmental Toxicology*, Elsevier, pp. 1003–1026, doi: 10.1016/B978-0-12-382032-7.10076-1.

Watson, C.A., Weng, C.X., French, T., Anderson, B.J., Nemeth, C., McNutt, L.A. and Smith, L.C. (2014), "Substance abuse treatment utilization, HIV risk behaviors, and recruitment among suburban injection drug users in Long Island, New York", *AIDS and Behavior*, Vol. 18 No. SUPPL. 3, doi: 10.1007/s10461-013-0512-2.

Wen, Q., Tang, E.I., Li, N., Mruk, D.D., Lee, W.M., Silvestrini, B. and Cheng, C.Y. (2018), "Regulation of blood-testis barrier (BTB) dynamics, role of actin-, and microtubule-based cytoskeletons", *Methods in Molecular Biology*, Vol. 1748, pp. 229–243, doi: 10.1007/978-1-4939-7698-0_16.

WHO,. (2019), "WHO Implementation tool for pre-exposure prophylaxis (PrEP) of HIV infection. Module 1: Clinical. Geneva: World Health Organization; 2017 (WHO/HIV/2017.17). Licence: CC BY-NC-SA 3.0 IGO.", *Definisi HIV*, No. July.

WHO/IDF Consultation. (2006), *Definition and Diagnosis of Diabetes Mellitus and Intermediate Hyperglycemia: Report of AWHO, IDF Consultation*.

WHO. (2013), "Summary of New Recommedations", *WHO Guidelines*, pp. 1–9.

WHO. (2021), "HIV and AIDS Key Facts", *World Health Organization*, No. july, pp. 1–7.

Wilson, R.D. and Islam, M.S. (2012), "Fructose-fed streptozotocin-injected rat: An

alternative model for type 2 diabetes", *Pharmacological Reports*, Vol. 64 No. 1, pp. 129–139, doi: 10.1016/S1734-1140(12)70739-9.

Wong, C.H. and Cheng, C.Y. (2005), "The Blood-Testis Barrier: Its Biology, Regulation, and Physiological Role in Spermatogenesis", *Current Topics in Developmental Biology*, doi: 10.1016/S0070-2153(05)71008-5.

Wong, N., Levy, M. and Stephenson, I. (2017), "Hypogonadism in the HIV-Infected Man", *Current Treatment Options in Infectious Diseases*, Vol. 9 No. 1, pp. 104–116, doi: 10.1007/s40506-017-0110-3.

World Health Organisation. (2011), "Global status report on alcohol and health", *World Health Organization*, Vol. 122 No. December 1994, pp. 1–85.

World Health Organization. (2021), "World AIDS Day 2021", *World Health Organization*.

Wu, P.Y., Scarlata, E. and O'flaherty, C. (2020), "Long-term adverse effects of oxidative stress on rat epididymis and spermatozoa", *Antioxidants*, Vol. 9 No. 2, p. 170, doi: 10.3390/antiox9020170.

Wu, Y., Pegoraro, A.F., Weitz, D.A., Janmey, P. and Sun, S.X. (2022), "The correlation between cell and nucleus size is explained by an eukaryotic cell growth model", edited by Igoshin, O.A.*PLoS Computational Biology*, Vol. 18 No. 2, p. e1009400, doi: 10.1371/journal.pcbi.1009400.

Yagan, N. (2000), "Testicular US findings after biopsy", *Radiology*, Vol. 215 No. 3, pp. 768–773, doi: 10.1148/radiology.215.3.r00jn17768.

Yan Cheng, C. and Mruk, D.D. (2012), "The blood-testis barrier and its implications for male contraception", edited by Sibley, D.R.*Pharmacological Reviews*, Vol. 64 No. 1, pp. 16–64, doi: 10.1124/pr.110.002790.

Yan, W., Suominen, J., Samson, M., Jégou, B. and Toppari, J. (2000), "Involvement of Bcl-2 family proteins in germ cell apoptosis during testicular development in the rat and pro-survival effect of stem cell factor on germ cells in vitro", *Molecular and Cellular Endocrinology*, Vol. 165 No. 1–2, pp. 115–129, doi: 10.1016/S0303-7207(00)00257-4.

Yeap, B.B. (2014), "Hormonal changes and their impact on cognition and mental health of ageing men", *Maturitas*, doi: 10.1016/j.maturitas.2014.05.015.

Yee, J.B. and Hutson, J.C. (1985), "Effects of testicular macrophage-conditioned medium on leydig cells in culture", *Endocrinology*, Vol. 116 No. 6, pp. 2682–2684, doi: 10.1210/endo-116-6-2682.

Yeh, S., Tsai, M.Y., Xu, Q., Mu, X.M., Lardy, H., Huang, K.E., Lin, H., et al. (2002), "Generation and characterization of androgen receptor knockout (ARKO) mice: An in vivo model for the study of androgen functions in selective tissues", *Proceedings of the National Academy of Sciences of the United States of America*, Vol. 99 No. 21, pp. 13498–13503, doi: 10.1073/pnas.212474399.

Yong, E.L., Loy, C.J. and Sim, K.S. (2003), "Androgen receptor gene and male infertility", *Human Reproduction Update*, Vol. 9 No. 1, pp. 1–7, doi: 10.1093/humupd/dmg003.

Young, B., James, L., Alan, S. and John, H. (2013), "Wheater's Functional Histology. A text and colour atlas.", doi: 0702047473.

Young, R.C., De Ferrero, E., Carr, C., Montgomery, W.P., Hackney, R.L. and Harden, K.A. (1967), "Pneumoconio-tuberculosis in soft coal miners: comparison of course, prognosis and physiologic impairment in non-miners with tuberculosis.", *Journal of the National Medical Association*, Vol. 59 No. 2, pp. 81-89 passim.

Yu, Q., Li, T., Li, J., Zhong, L. and Mao, X. (2017), "Nitric Oxide Synthase in Male Urological and Andrologic Functions", *Nitric Oxide Synthase - Simple Enzyme-Complex Roles*, InTech, doi: 10.5772/67562.

Yuko Ito, N.E. and Otsuki, Y. (2013), "Anti-Apoptotic Mechanisms of Sertoli Cells against Ethanol Toxicity", *Journal of Alcoholism & Drug Dependence*, Vol. 01 No. 01, pp. 1–2, doi: 10.4172/2329-6488.1000105.

Zaccardi, F., Webb, D.R., Yates, T. and Davies, M.J. (2016), "Pathophysiology of type 1 and type 2 diabetes mellitus: A 90-year perspective", *Postgraduate Medical Journal*, doi: 10.1136/postgradmedj-2015-133281.

Zamora, R., Vodovotz, Y. and Billiar, T.R. (2000), "Inducible nitric oxide synthase and inflammatory diseases.", *Molecular Medicine (Cambridge, Mass.)*, Vol. 6 No. 5, pp. 347–373, doi: 10.1007/bf03401781.

Zha, W., Bai, Y., Xu, L., Liu, Y., Yang, Z., Gao, H. and Li, J. (2018), "Curcumin Attenuates Testicular Injury in Rats with Streptozotocin-Induced Diabetes", *BioMed Research International*, Vol. 2018, p. 7468019, doi: 10.1155/2018/7468019.

Zhang, H., Yin, Y., Wang, G., Liu, Z., Liu, L. and Sun, F. (2014), "Interleukin-6 disrupts blood-testis barrier through inhibiting protein degradation or activating phosphorylated ERK in Sertoli cells", *Scientific Reports*, Vol. 4 No. 1, p. 4260, doi: 10.1038/srep04260.

Zhang, L. and Zhang, L. (2011), "Voluntary oral administration of drugs in mice", *Protocol Exchange*, doi: 10.1038/protex.2011.236.

Zhao, K., Huang, Z., Lu, H., Zhou, J. and Wei, T. (2010), "Induction of inducible nitric oxide synthase increases the production of reactive oxygen species in RAW264.7 macrophages.", *Bioscience Reports*, Vol. 30 No. 4, pp. 233–241, doi: 10.1042/BSR20090048.

Zhao, S., Zhu, W., Xue, S. and Han, D. (2014), "Testicular defense systems: Immune privilege and innate immunity", *Cellular and Molecular Immunology*, Vol. 11 No. 5, pp. 428–437, doi: 10.1038/cmi.2014.38.

Zhao, W., Jing, J., Shao, Y., Zeng, R., Wang, C., Yao, B. and Hang, D. (2020), "Circulating sex hormone levels in relation to male sperm quality", *BMC Urology*, Vol. 20 No. 1, p. 101, doi: 10.1186/s12894-020-00674-7.

Zhao, W.P., Wang, H.W., Liu, J., Tan, P.P., Luo, X.L., Zhu, S.Q., Chen, X.L., et al. (2018), "Positive PCNA and Ki-67 expression in the testis correlates with spermatogenesis dysfunction in fluoride-treated rats", *Biological Trace Element Research*, Vol. 186 No. 2, pp. 489–497, doi: 10.1007/s12011-018-1338-6.

Zhu, Q., Meisinger, J., Emanuele, N. V., Emanuele, M.A., LaPaglia, N. and Van Thiel, D.H. (2000), "Ethanol exposure enhances apoptosis within the testes", *Alcoholism: Clinical and Experimental Research*, Vol. 24 No. 10, pp. 1550–1556, doi: 10.1097/00000374-200010000-00013.

Zhu, X., Guo, F., Tang, H., Huang, C., Xie, G., Huang, T., Li, Y., et al. (2019), "Islet

Transplantation Attenuating Testicular Injury in Type 1 Diabetic Rats Is Associated with Suppression of Oxidative Stress and Inflammation via Nrf-2/HO-1 and NF-κ B Pathways", *Journal of Diabetes Research,* Vol. 2019, p. 8712492, doi: 10.1155/2019/8712492.

Zhu, Y., Yin, Q., Wei, D., Yang, Z., Du, Y. and Ma, Y. (2019), "Autophagy in male reproduction", *Systems Biology in Reproductive Medicine,* doi: 10.1080/19396368.2019.1606361.

Zirkin, B.R. and Papadopoulos, V. (2018), "Leydig cells: Formation, function, and regulation", *Biology of Reproduction,* Vol. 99 No. 1, pp. 101–111, doi: 10.1093/biolre/ioy059.

Zubkova, E. V. and Robaire, B. (2006), "Effects of ageing on spermatozoal chromatin and its sensitivity to in vivo and in vitro oxidative challenge in the Brown Norway rat", *Human Reproduction,* Vol. 21 No. 11, pp. 2901–2910, doi: 10.1093/humrep/del193.

APPENDIX

Ethics clearance certificate

STRICTLY CONFIDENTIAL

ANIMAL RESEARCH ETHICS COMMITTEE (AREC)

CLEARANCE CERTIFICATE NO. 2018/011/58/C

APPLICANT: Dr I Eguavoen

SCHOOL: Anatomical Sciences
DEPARTMENT:
LOCATION:

PROJECT TITLE: Characterization of Streptozontocin induced diabetic male Sprague-Dawley rats with chronic alcohol intake and antiretroviral therapy

Number and Species

120X 10 weeks/270-320g male Sprague-Dawley rats

Approval was given for the use of animals for the project described above at an AREC meeting held on 2018/11/27. This approval remains valid until 2021/02/13.
Unreported changes to the application may invalidate the clearance given by the AREC
An annual progress report must be provided

The use of these animals is subject to AREC guidelines for the use and care of animals, is limited to the procedures described in the application form and is subject to any additional conditions listed below:

Signed: _____ (Chairperson, AREC) Date: 23rd April 2019

I am satisfied that the persons listed in this application are competent to perform the procedures therein, in terms of Section 23 (1) (c) of the Veterinary and Para-Veterinary Professions Act (19 of 1982)

Signed: _____ (Registered Veterinarian) Date: 23 April 2019

cc: Supervisor: Prof E Mbajirogu and Dr R Ndou
Director: CAS

Works 2000/lain0015/AESCCert.wps

Sample size calculation

Two samples sizes of 8 and 10 with 9 groups (7 experimental and 2 controls) were used based on the null analysis (the mean of 2 groups do not differ).

A power of 0.8 (80%) for sample size of 8 rats and a power of 0.9 (90%) for sample size of 10 rats was obtained.

The following values were used in other to arrive at the power size of 80% or 90%.

Effect size (medium value) of clinical or scientific importance since we have more than one experimental/treatment groups which interacts with each other,

Therefore, we chose a medium effect size of 1.

Effect size = 1 (Mean 1- mean 2/SD)

Number of groups = 9

Sample size of 8 rats/group for power analysis of 80% and 10 rats/group for power analysis of 90%

Significance level of 0.05 (5%)

Finally, we have chosen the total sample of 90 animals which will be divided into 9 groups (7 treatment/ experimental group and 2 controls) having the sample size (the number of 10 rats in each group).

The power level of 0.9 (90%) was achieved using the STATA statistical software.

The larger the sample size, the higher the power size.

Treatment preparation and dosage calculation

High (20%) fructose diet preparation

To prepare 1kg of high fructose diet, 800 grams of ground normal rodent chow was mixed with 200 grams of fructose (granulated fruit sugar, Nature's choice). Water was then added to form a uniform mixture, which was poured into the pellet food mold and dehydrated in a low-temperature oven to obtain the high (20%) fructose reconstituted rodent chow.

Streptozotocin (STZ) 40mg/kg in 0.05M (pH 4.5) citrate buffer

The 0.05M citrate buffer was prepared by adding 3 parts of 0.05M citrate acid to 2 parts of 0.05m sodium citrate and stirring, followed by adjusting the pH to 4.5.

For an STZ 40mg/Kg body weight (BW) dose in 0.05M (pH 4.5), citrate buffer the calculation was as follows.

40mg STZ in 10ml citrate buffer = 1 Kg BW, then 10ml STZ in citrate buffer =1000g BW, and 1 ml STZ in citrate buffer = 100g BW. Therefore, X ml STZ in citrate buffer = X g BW x 0.01 X ml STZ in citrate buffer was administered to each animal according to its body weight.

Atripla® drug dose calculations

An average adolescent of 45kg body weight (BW) receives 1 tablet of Atripla (efavirenz 600mg+ emtricitabine 200mg+ tenofovir 245mg) per day.

Since 1 tablet =1045mg active ingredients (AI), therefore, 1kg BW = 1045/45 (23.22) mg AI per day, and 1g BW= 0.0232mg AI per day. Moreso, one Atripla® tablet with 1045mg AI weighs 1612mg, thus, 1mg tablet = 1X1045/1612 (0.648) AI/mg tablet.

If 1g BW requires 0.0232mg AI per day, Then Xg BW requires Xg x0.0232 mg AI per day/ 0.648mg AI/mg tablet.

Gelatine Cubes preparations

The mixture for each gelatine consisted of 5ml distilled water, 0.25g sugar, 2g gelatine, and 0.1g beefy Bovril. The required amount of water was heated to boiling in a sterile beaker, all other ingredients were added to the beaker while stirring. When the mixture had cooled the required crushed Atripla tablet amount per cube was added and then the mixture was stirred for 5 minutes. Thereafter, the mixture was aliquoted using a syringe into gelatine molds (5ml each) and placed in the fridge to set. The cART treated groups received one gelatine cube daily.

Published article

Original Article
https://doi.org/10.5115/acb.22.229
pISSN 2093-3665 eISSN 2093-3673
Anatomy & Cell Biology acb

Co-administration of alcohol and combination antiretroviral therapy (cART) in male Sprague Dawley rats: A study on testicular morphology, oxidative and cytokines perturbations

Elna Owembabazi[1,4], Pilani Nkomozepi[2], Tanya Calvey[3], Ejikeme Felix Mbajiorgu[1]
[1]School of Anatomical Sciences, University of the Witwatersrand, Johannesburg, [2]Department of Human Anatomy and Physiology, University of Johannesburg, Johannesburg, [3]Division of Clinical Anatomy and Biological Anthropology, University of the Cape Town, Cape Town, South Africa, [4]Department of Human Anatomy, Kampala International University, Western Campus, Uganda

Abstract: Alcohol consumption alongside combination antiretroviral therapy (cART) has attracted research interest, especially because of increasing male infertility. This study investigated the combined effects of alcohol and cART on testicular morphology, biomarkers of oxidative stress, inflammation, and apoptosis. Rats, weighing 330–370 g, were divided into four groups of six animals each; control, alcohol treated (A), cART, and alcohol plus cART treated (A+cART). Following 90 days treatment period, animals were euthanized, testis extracted, and routinely processed for histology and immunohistochemical analysis. Significantly decreased epithelial area fraction, increased luminal and connective tissue area fractions, and reduction of epithelial height and spermatocyte number, were recorded in the treated groups compared to control. Extensive seminiferous epithelial lesions including widened intercellular space, karyolysis, and sloughing of germinal epithelium were recorded in all the treated groups. Furthermore, upregulation of inducible nitric oxide synthase and 8-hydroxydeoxyguanosine, interleukin-6, and caspase 3 recorded in treated animals, was more significant in A+cART group. Also, the levels of interleukin-1β and tumor necrosis factor-α were more elevated in A and cART treated groups than in A+cART, while MDA was significantly elevated in cART and A+cART treated groups compared to control group. Altogether, the results indicate testicular toxicity of the treatments. It is concluded that consuming alcohol or cART induces oxidative stress, inflammation, and apoptosis in testis of rats, which lead to testicular structural and functional derangements, which are exacerbated when alcohol and cART are consumed concurrently. The result will invaluably assist clinicians in management of reproductive dysfunctions in male HIV/AIDS-alcoholic patients on cART.

Key words: Alcohol abuse, Antiretroviral therapy, Testicular dysfunction, Oxidative stress, Inflammatory cytokines

Received November 14, 2022; 1st Revised December 22, 2022; 2nd Revised January 3, 2023; Accepted January 3, 2023

Introduction

Male infertility incidence is rising steadily worldwide and accounts for more than 50% of infertility cases [1, 2]. Equally, there is a worldwide increase in human immunodeficiency virus (HIV) infection [3] and alcohol abuse [4]. For instance, about 33% of South African (SA) population consumes alcohol regularly and the SA's average consumed

Corresponding author:
Elna Owembabazi
School of Anatomical Sciences, University of the Witwatersrand, Johannesburg 2193, South Africa
E-mail: 2278202@students.wits.ac.za

Copyright © 2023. Anatomy & Cell Biology

This is an Open Access article distributed under the terms of the Creative Commons Attribution Non-Commercial License (http://creativecommons.org/licenses/by-nc/4.0/) which permits unrestricted non-commercial use, distribution, and reproduction in any medium, provided the original work is properly cited.

alcohol per capita (APC) almost doubles the global average APC [5, 6]. Equally, the country is burdened with high HIV prevalence and has the biggest combination antiretroviral therapy (cART) program globally [7, 8]. Currently, cART prophylaxis is encouraged among healthcare workers following accidental needle prick, and amongst prostitutes and individuals after unsafe and casual sex with unknown persons or HIV infected individuals [3, 9]. While the influence of alcohol on risky sexual activity is associated with an increase in the spread of HIV infection [10-12] and the consequent use of cART, many HIV patients on cART therapy continue to consume alcohol regularly for euphoric purposes [13, 14]. Furthermore, alcohol has been associated with reduced viral suppression dose-dependently [15, 16]; aggravated HIV progression, and reduced cART efficacy [14].

Alcohol and cART have each been shown to have negative long-term consequences on both male and female reproductive organs and other body systems [17-20]. Excessive alcohol consumption is reckoned as a leading cause of male impotence and infertility [21]. Several testicular and sexual dysfunctions have been reported in habitual/chronic alcohol consumers [22-24]. Also, cART has been shown to alter reproductive hormones and sperm parameters [25, 26]. A reduction in testosterone levels, sperm concentration, and DNA integrity have been implicated in long-term use of cART [27, 28]. Only two reports in literature have shown adverse effects of alcohol and cART interaction on testicular histology [29, 30]. The present study evaluated specifically the impact of this interaction on Sertoli and Leydig cells and immunohistochemical localization of the oxidative stress, inflammatory, and apoptotic markers to further delineate possible physio-biochemical impact of alcohol plus cART treatment on the testis. Currently, increasing HIV infection and male infertility are reported among reproductive age individuals, with high desire for procreation, and might also be regular alcohol consumers [30]. This implies increased alcohol and cART interaction amongst the age group, making their reproductive health a huge health concern. Against this backdrop, this study evaluated testicular toxicity associated with concurrence of alcohol and cART in the body using HIV-naïve male rat model to mimic conditions of cART regimen.

Materials and Methods

Chemical and reagents

These were procured from different reliable sources. A combination antiretroviral drug (Atripla) consisting of 600 mg of Efavirenz, 300 mg Tenofovir disproxil Fumurate, and 245 mg Emtricitabine was procured from Bristol-Myers Squibb and Gilead Sciences. Rabbit polyclonal for primary antibodies interleukin-1beta (IL-1β) (ab2105), tumor necrosis factor-alpha (TNF-α) (ab6671), and caspase 3 (ab4051), rabbit monoclonal for primary antibody inducible nitric oxide synthase (iNOS) (ab115819), and mouse monoclonal for primary antibodies interleukin-6 (IL-6) (ab9324), malondialdehyde (MDA) (ab243066), and 8-hydroxydeoxyguanosine (8-OHDG) (ab62623) were procured from Abcam . Whilst biotinylated goat anti-rabbit (BA-1000) and goat anti-mouse (BA-9200) secondary antibodies, and Avidin-Biotin Complex kit (ABC) (PK-6100) were procured from Vector Laboratories.

Ethical clearance

This study was approved by the Animal Research Ethics committee (AREC) (approval number: 2018/011/58/C) of University of the Witwatersrand (Wits) and all experiments were conducted at the Wits Research Animal Facility in compliance with the guidelines set forth by AREC.

Animals

Twenty-four adult male Sprague Dawley rats (10 weeks old), weighing between 330–370 g were used in the study. Each rat was separately housed under sterile conditions in a plastic cage. Animals were fed on normal rat chow and water *ad libitum* and were maintained at 21°C–23°C room temperature, with lighting conditions of 12/12-hour light/dark cycle.

Experimental design

Animals were divided into four groups of six rats each as follows; control group, received no treatment; alcohol group (A), which received 10% v/v alcohol in drinking water daily [31]; the cART group, received extrapolated human equivalent dose of 23 mg/kg of cART (consisting of efavirenz 600 mg+emtricitabine 200 mg+tenofovir 245 mg) in gelatine cubes daily [32]; and alcohol plus cART group (A+cART), received both alcohol and cART daily at same doses indicated above. After 90 days of treatment, the animals were weighed,

anesthetized with 240 mg/ml pentobarbitone dose, and sacrificed. The animals were perfused with 2 ml/min of 0.1 M phosphate buffer (PB) in 0.9% saline and the testes were harvested, weighed, and the wet weight recorded and thereafter fixed in 10% neutral buffered formalin for histology and further analysis.

Testicular morphometry

Testis weight and volume

The weight of the testes was recorded immediately after their extraction using an electronic scale (Kern PCB 200-2 weighing scale). Testis volume was determined using the Archimedes principle of water displacement in a measuring cylinder [33]. The initial volume (Vi) of distilled water in a graduated cylinder was recorded, and then the final volume (Vf) was determined after adding the testis to the graduated cylinder containing the known amount of distilled water. The volume of the testis (Vt) was calculated by subtracting the initial volume from the final volume as shown below.

$$Vt=Vf–Vi\ (mm^3)$$

Testis size

A sliding digital Vernier caliper was used to measure the width and length of the testes, as described by Parhizkar et al. [34]. Testis size was then calculated using the formula below [34].

$$\text{Testis size}=\text{width}^2\times\text{length}\times 0.523\ (\text{mm})$$

Histology and histomorphometry (H&E)

The fixed testes were dehydrated sequentially in 70%–100% alcohol grades and embedded in molten paraffin wax and serially sectioned at 5 μm thickness. The sections were stained with H&E and examined using the Axioskop 2 plus light microscope (Nikon Eclipse Ci, 104C type). Photomicrographs of testicular tissue sections were obtained using a linked computerized Zeiss digital image system, the AxioCam 208 color (Zeiss group) for morphometric assessment. Six camera fields from 4 sections per animal, from six animals per group (*i.e.*, 144 images per group) were captured and used for morphometry and analysis.

Testicular component area fractions

Testicular component (epithelial, luminal, connective tissue, and interstitial space) area fractions were determined using Fiji 84-intersection grid. The grid was superimposed on H&E-stained images captured at ×100 and the intersecting points for each component were counted. The average intersecting points for each testicular component were calculated in 144 microscopic field images per group and each testicular component area fraction was determined using the formula below [35].

$$\text{Area fraction}=\frac{(\text{Area per point}\times\text{average number of intersecting points})}{\text{Total area of photomicrograph}}\times 100\ (\%)$$

Seminiferous tubule morphometry

Seminiferous tubule area (TA), tubule diameter (TD), epithelium height (EH), and luminal diameter (LD) were measured in 50 round or nearly round seminiferous tubules for each animal (*i.e.*, 300 tubules per group) using Fiji software. The seminiferous TA was determined by tracing around the seminiferous tubule using the Fiji freehand selection tool. The average TD and epithelial height were calculated using the minor and major axes measurements [36]. To exclude longitudinal tubules, an average TD was considered only if D1/D2 ≥0.85, a value of D1/D2=1.0 representing a perfectly rounded circle [37].

Germinal epithelium cell quantification

The number of the different germinal epithelium cells (Sertoli, spermatogonia, spermatocytes, round, and elongated spermatids) were counted in H&E-stained sections at ×400. Ten rounded seminiferous tubules (stage VII) [38] for each animal were considered (*i.e.*, 60 tubules per group).

Leydig cell morphometry

Using Fiji software, diameters (D) of fifty Leydig nuclei with distinct nucleoli were measured for each animal on H&E-stained images captured at ×400. The nuclear volume (an important parameter in a variety of cell functions) was determined in accordance with previously reported methods [39], with the formula below.

$$\text{Leydig cell nuclear volume}=\frac{4}{3}\pi R^3(\mu m^3).$$

Where, Radius (R)=D/2, and π=3.14.

https://doi.org/10.5115/acb.22.229

Histopathological evaluation

Johnsen's testicular score

Spermatogenesis was classified in 50 stage II-VII seminiferous tubules per animal (*i.e.*, 300 tubules per group) using Johnsen's testicular score. Each tubule was assigned a score from 10 to 1, accordingly, thereafter the number of tubules for an individual score was multiplied by the score, and then the total for all the scores was divided by 50 (the total number of tubules scored) to obtain the mean Johnsen's score per group for further analysis [40].

The modified Johnsen scoring criteria used is shown in Table 1.

Histological changes

Testicular H&E-stained sections were examined for the presence of histological changes. Observed changes were graded in 24 microscopic fields (six fields from each of the four sections) for each animal (*i.e.*, 144 fields per group). The changes in each field were semi-quantitatively categorized into five grades as follows; grade 4=very severe (change seen in >75% of the field), grade 3=severe (change seen in >50% <75% of the field), grade 2=moderate (change seen in >25% <50% of the field), grade 1=mild (change seen in <25% of the field), and grade 0=none (no change in the field) as previously reported by Erpek et al. [41].

Immunohistochemistry for oxidative stress, inflammation, and apoptosis

Testicular tissue sections were mounted on silane-coated slides for antibody immunolabeling. Assessment of oxidative stress using iNOS, MDA, and 8-OHDG, inflammation (IL-1β), TNF-α, and IL-6, and caspase 3 for apoptosis were carried out. The sections were incubated in citrate buffer overnight in a water bath at 60°C for antigen retrieval. Then, the endogenous peroxidase was inhibited using 1% hydrogen peroxide in methanol for 20 minutes. After rinsing in phosphate buffered saline (PBS) for three changes of five minutes each, 5% normal goat serum was added to the sections to block nonspecific antibody binding. This was tapped off after 30 minutes, and the primary antibody was added subsequently (1:100 for anti-TNF-α and anti-iNOS, 1:200 for anti-IL-1β, anti-IL-6, anti-MDA, and anti-caspase 3, and 1:1,000 for anti-8-OHDG) and left overnight (approximately 16 hours) at 4°C. Thereafter, the sections were rinsed in PBS and incubated with the secondary antibody (1:1,000 biotinylated goat anti-rabbit for the IL-1β, TNF-α, iNOS, and caspase 3 antibodies and 1:1,000 biotinylated goat anti-mouse for IL-6, MDA, and 8-OHDG antibodies) for 30 minutes. Then, after rinsing in PBS, ABC reagent was added for 30 minutes. Afterward, the sections were rinsed in PBS and incubated with 3, 3'-diaminobenzidine tetrachloride (DAB) for five minutes. DAB was then washed off under running tap water for five minutes and the slides were dipped in hematoxylin for one minute to counter stain. Followed by rinsing in running tap water to remove excess stain, dehydration of slides in alcohol series, and coverslipped with Dibutylphthalate Polystyrene Xylene. The images of antibodies with immunoreactivity localized to both cell nucleus and cytoplasm (IL-1β, TNF-α, iNOS, and MDA) were captured in 24 microscopic fields at ×100 for each animal (*i.e.*, 144 sections per group) and were segmented using the ilastik pixel classification workflow. Fiji was used for quantification of the ilastik exported image segments to extract numerical data for statistical analysis. Details of image segmentation and quantification are shown in Appendix 1–2. The percentage area of expression for antibodies was calculated using the formula below.

$$\% \text{ Area of expression} = \frac{\text{Immunoreactive area}}{\text{Total area of photomicrograph}} \times 100$$

For the antibodies with immunoreactivity localized to cell nuclei (IL-6, 8-OHDG, and caspase 3), the total number of cell nuclei expressing immunoreactivity were counted in 20 rounded stage VII seminiferous tubules for each animal (*i.e.*, 120 tubules for each group).

Data analysis

GraphPad Prism 6 windows software was used for data analysis. Data were expressed as Mean±SEM. Group means

Table 1. Modified Johnsen scoring criteria

Spermatogenesis level	Johnsen's score
Many spermatozoa in the tubule lumen	10
Many elongated spermatids in the apical region of the epithelium	9
Many elongated spermatids still embedded in the Sertoli cell membrane	8
Few elongated spermatids, many round spermatids	7
No elongated spermatids, few round spermatids	6
No spermatids, many spermatocytes	5
Few spermatocytes	4
Spermatogonia cell only	3
Sertoli cells only	2
No seminiferous epithelial cells	1

of parametric data were compared using a one-way ANOVA, followed by Bonferroni's *post hoc* test. Non-parametric data (Johnsen's and histological change scores) were compared using Kruskall Wallis, followed by Dunn's *post hoc* test. Deeming a *P*-value of <0.05 statistically significant.

Results

Testicular morphometry

All treated groups (A, cART, and A+cART) showed a non-significant decrease in testis weights, testis volume, and testis size in comparison with the control (Table 2).

Testicular area fractions

The epithelial area fraction (EAF) of treated groups significantly reduced compared to the control, (A, *P*=0.0012; cART, *P*=0.0078; and A+cART, *P*<0.0001) (Table 2). The luminal area fraction (LAF) of cART group decreased significantly compared to control (*P*=0.0123), A (*P*=0.0059) and A+cART (*P*<0.0001), but was significantly increased in A+cART compared to control (*P*=0.0141). The connective tissue and interstitial space area fractions (CTAF and ISAF respectively) of all the treated groups (A, cART, and A+cART) were increased compared to the control. The increase was significant in CTAF of all treated groups (A: *P*=0.0017, cART: *P*<0.0001, and A+cART: *P*<0.0001) and in ISAF of A (*P*=0.0008) and cART (*P*=0.0003) groups. Furthermore, CTAF of cART and A+cART treated groups was significantly higher when compared with group A (*P*=0.0110 and *P*=0.0038 respectively), while ISAF of A+cART group was significantly reduced compared to A (*P*=0.0025) and cART (*P*=0.0010) groups (Table 2).

Seminiferous tubule morphometry

All seminiferous tubule measured parameters (area, diameter, epithelium, and lumen) were decreased in all treated groups compared to control, except for lumen of A+cART treated that increased non-significantly (*P*>0.05) (Table 3). TA and diameter significantly decreased (*P*<0.0001) in A, cART, and A+cART treated groups relative to control. The TA of cART treated group significantly decreased compared to A treated group (*P*=0.0413). In addition, TA and diameter were significantly higher in A+cART than in A (*P*=0.0155 and 0.0089 respectively) and cART (*P*<0.0001) groups. In comparison with the control group, the epithelial height of groups A, cART, and A+cART decreased significantly (*P*=0.0002, 0.0001, and 0.0001 respectively) while the LD of A+cART group increased significantly (*P*=0.0013). However, the LD of cART group was significantly decreased compared to control (*P*=0.0340), A (*P*=0.0004), and A+cART (*P*<0.0001) treated groups.

Germinal epithelium cell count

The results are as shown in Table 3. The mean number of spermatogonia increased significantly in A and cART-treated groups (*P*<0.0001and *P*<0.0002 respectively) relative to con-

Table 2. Mean testicular morphometry and component area fractions of testes from rats treated with A, cART, and both

Animal groups	Control	A	cART	A+cART
Testis morphometry				
Testis weight (g)	1.91±0.05^{a}	1.78±0.04^{a}	1.85±0.03^{a}	1.78±0.09^{a}
Testis volume (mm^{3})	1.88±0.09^{a}	1.83±0.08^{a}	1.83±0.08^{a}	1.67±0.11^{a}
Testis size (mm)	1,493±40.52^{a}	1,491±24.19^{a}	1,378±46.83^{a}	1,409±43.89^{a}
AF (%)				
EAF	74.25±0.50^{a}	71.43±0.60^{b}	71.82±0.53^{b}	70.59±0.47^{b}
LAF	8.56±0.29^{a}	8.64±0.27^{a}	7.38±0.24^{b}	9.80±0.30^{c}
CTAF	11.97±0.31^{a}	13.66±0.35^{b}	15.11±0.32^{c}	15.26±0.33^{c}
ISAF	4.93±0.12^{a*}	5.73±0.17^{b}	5.77±0.16^{b}	4.99±0.12^{c*}

For all parameters: Values in the same row with similar superscripts are not significantly different. Whilst values in the same row with different superscripts are significantly different except when the different superscripts are both marked with an asterisk (*). A, alcohol; cART, combination antiretroviral therapy; AF, area fractions; EAF, epithelial; LAF, luminal; CTAF, connective tissue; ISAF, interstitial space. EAF of A, cART, and A+cART groups significantly decreased relative to control (^{b}P=0.0012, ^{b}P=0.0078 and ^{b}P<0.0001). LAF of cART group significantly decreased relative to control and A (^{b}P=0.0123 and ^{b}P=0.0059) and A+cART significantly increased relative to control, A, and cART (^{c}P=0.0141, ^{c}P=0.0271, and ^{c}P<0.0001). CTAF of A, cART, and A+cART groups significantly increased relative to control (^{b}P=0.0017, ^{c}P<0.0001, and ^{c}P<0.0001) and cART and A+cART significantly increased compared to A (^{c}P=0.0110 and ^{c}P=0.0038). ISAF of A and cART groups significantly increased compared to control (^{b}P=0.0008 and ^{b}P=0.0003), but A+cART significantly decreased compared to A and cART (^{c}P=0.0025 and ^{c}P=0.0010).

https://doi.org/10.5115/acb.22.229

Table 3. Mean for seminiferous tubule, germinal epithelium cell count, and Leydig cell morphometry of testes from rats treated with A, cART, and both

Animal groups	Control	A	cART	A+cART
Tubule measurements				
TA (μm^2)	78,939±692^a	68,854±773^b	65,972±739^c	72,069±803^d
TD (μm)	310.2±1.30^a	286.5±1.54^b	283.0±1.52^b	293.2±1.56^c
EH (μm)	97.51±0.62^a	93.34±0.71^b	92.52±0.72^b	89.46±0.78^c
LD (μm)	97.97±3.54^a	105.90±2.67^{a*}	84.95±2.06^b	116.9±3.38^{c*}
Epithelium cell count				
Spermatogonia	59.20±0.62^a	67.93±1.50^b	66.43±1.18^{b*}	61.97±1.33^{a*}
Spermatocytes	88.62±0.80^a	86.00±1.00^{a*}	84.33±0.71^{b*}	83.72±0.95^{b*}
Round spermatids	92.30±0.95^a	80.41±1.47^b	84.25±1.43^b	83.79±1.18^b
Elongated spermatids	102.9±1.02^a	83.20±1.13^b	85.93±1.48^b	85.75±0.80^b
Sertoli	23.61±0.24^a	22.56±0.38^a	22.75±0.28^a	22.54±0.31^a
Leydig cell nuclear				
Diameter (μm)	5.85±0.04^a	5.37±0.04^b	5.48±0.05^b	5.42±0.04^b
Volume (μm^3)	110.00±2.46^a	85.95±2.18^b	91.73±2.28^b	88.03±2.13^b

For all parameters: Values in the same row with similar superscripts are not significantly different. Whilst values in the same row with different superscripts are significantly different except when the different superscripts are both marked with an asterisk (*). A, alcohol; cART, combination antiretroviral therapy; TA, tubule area; TD, tubule diameter; EH, epithelium height; LD, luminal diameter. TA of A, cART, and A+cART groups significantly decreased compared to control ($^{b,c,d}P<0.0001$), cART significantly decreased compared to A ($^cP=0.0413$), and A+cART significantly increased compared to A and cART ($^dP=0.0155$ and $^dP<0.0001$). TD of A, cART, and A+cART groups significantly decreased compared to control ($^{b,c}P<0.0001$) and A+cART significantly increased compared to A and cART ($^cP=0.0089$ and $^cP<0.0001$). EH of A, cART, and A+cART groups significantly decreased compared to control ($^bP=0.0002$, $^bP<0.0001$, and $^cP<0.0001$) and A+cART significantly decreased compared to A and cART ($^cP=0.0007$ and $^cP=0.0143$). LD of cART group significantly decreased compared to control ($^bP=0.0340$), A ($^bP=0.0004$), and A+cART ($^bP<0.0001$), whilst A+cART increased significantly ($^cP=0.0013$) compared to control. Spermatogonia count of A and cART groups significantly increased compared to control ($^bP<0.0001$ and $^bP=0.0002$ respectively), and A+cART significantly decreased compared to A ($^aP=0.0032$). Spermatocytes count of cART and A+cART groups significantly decreased compared to control ($^bP=0.0043$ and $^bP=0.0007$). Round and elongated spermatids significantly decreased ($^bP<0.0001$) in treated groups A, cART, and A+cART compared to control. Leydig cell diameter and volume significantly decreased in A, cART, and A+cART groups compared to control ($^bP<0.0001$).

Table 4. Median Johnsen's score and histological changes observed and their score range in testes of rats treated with A, cART, and both

Animal groups	Control	A	cART	A+cART
Johnsen's score	8.81^a	8.29^{b*}	8.50^{a*}	8.38^{b*}
Histological changes				
Lifting of epithelium	0.06±0.01^a	0.18±0.04^a	0.09±0.02^a	0.15±0.02^a
	(0–1)	(0–2)	(0–1)	(0–2)
Widened intercellular space	0.06±0.02^a	0.37±0.14^{a*}	0.29±0.09^{a*}	0.82±0.17^{b*}
	(0–1)	(0–2)	(0–2)	(0–4)
Karyolysis	0.00±0.00^a	0.11±0.02^a	0.17±0.04^b	0.13±0.03^b
	(0–0)	(0–1)	(0–1)	(0–1)

For all parameters: Values in the same row with similar superscripts are not significantly different. Whilst values in the same row with different superscripts are significantly different except when the different superscripts are both marked with asterisk (*). A, alcohol; cART, combination antiretroviral therapy. Johnsen's score of A and A+cART treated groups significantly decreased compared to control ($^bP=0.0115$ and $^bP=0.0256$). Widened intercellular space of A+cART group significantly increased compared to control ($^bP=0.0029$). Karyolysis of cART and A+cART groups significantly increased compared to control ($^bP=0.0081$ and $^bP=0.0346$ respectively).

trol but was significantly decreased in A+cART ($P=0.0032$) relative to A group. However, spermatocytes were significantly reduced in cART and A+cART groups compared to control, ($P=0.0043$ and $P=0.0007$ respectively). Both round and elongated spermatids decreased significantly ($P<0.0001$) in all treated groups compared to the control. Furthermore, a non-significant decrease ($P>0.05$) in the number of Sertoli cells was found in all the treated groups (A, cART, and A+cART) compared to control.

Leydig cell

Leydig cell nuclear diameter and volume decreased significantly ($P<0.0001$) in all the treated groups (A, cART, and A+cART) compared to control (Table 3).

Histopathological evaluation

Johnsen's testicular score

Johnsen's score was used to profile the progress/status of spermatogenesis in the seminiferous tubules. Compared to the control, a significant reduction in Johnsen's score was recorded in A ($P=0.0115$) and A+cART groups ($P=0.0256$) (Table 4).

Histological changes

The most common histological changes observed were lifting of germinal epithelium, widened intercellular space, and karyolysis (Fig. 1) and were different across the groups (Table 4). However, the difference in epithelial lifting was not significant across the groups but widened intercellular space was significantly higher in A+cART ($P=0.0029$) compared to control group. Additionally, karyolysis in cART and A+cART groups was significantly high when compared to the control group ($P=0.0081$ and 0.0346 respectively). Furthermore, seminiferous tubule shrinkage was observed in all treated groups, with sloughing of germinal epithelium into the lumen recorded in A+cART treated animals.

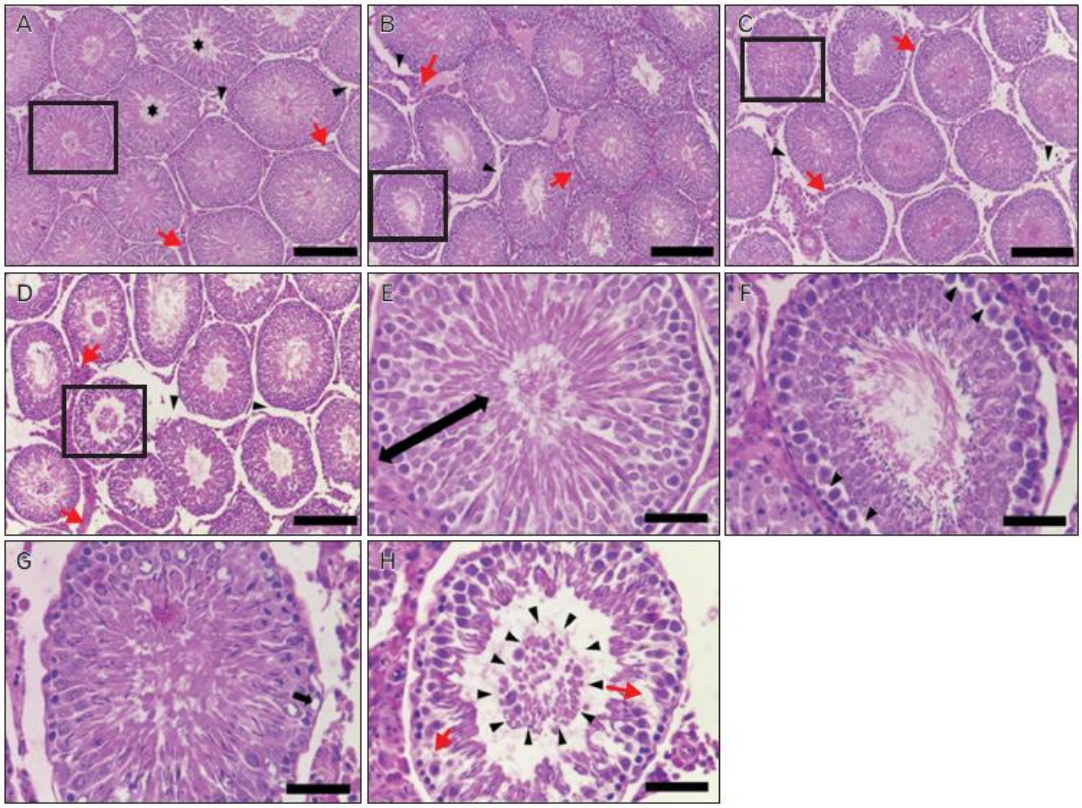


Fig. 1. Representative photomicrographs of H&E-stained testicular section. Control (A) shows normal oval-shaped seminiferous tubule with a lumen (asterisks), lying between adjacent tubules is a layer of interstitial (thin arrows) populated with Leydig cells interspersed within the connective tissue, and a thin interstitial space (arrowheads) between the tubules. Treated groups; A (B), cART (C), and A+cART (D) showed shrinkage of seminiferous tubules and increased interstitial space (arrowheads). (E–H) are a magnification of the square area indicated in (A–D). (E) shows the germinal epithelium (double arrow) consisting of discretely arranged series of spermatogenic cells, (F) shows lifting of epithelium (arrowheads) from the basal cells, (G) shows karyolysis (thick arrow) of spermatogonia and spermatocytes, and (H) shows sloughing of epithelium (arrowheads) into the lumen and widened intercellular germ space (thin arrows). A, alcohol; cART, combination antiretroviral therapy. The left and right panels are ×100 and ×400 with scale bars of 200 μm and 50 μm respectively.

https://doi.org/10.5115/acb.22.229

Immunohistochemistry: oxidative stress, inflammation, and apoptosis

Oxidative stress markers

Oxidative stress markers immunoreactivity (Fig. 2) was localized in the cytoplasm and nucleus of macrophages and Leydig cells for both iNOS and MDA. While 8-OHDG immunoreactivity was localized in the spermatogenic cell nuclei and residual bodies. All treated groups (A, cART, and A+cART) demonstrated a significant increase (P<0.0001) in expression of iNOS and 8-OHDG relative to the control group (Fig. 2). A significant increase of MDA expression was detected in cART and A+cART groups relative to the control group (P<0.0001) and in cART and A+cART groups relative to group A (P<0.0001 and P=0.0302 respectively) (Fig. 2).

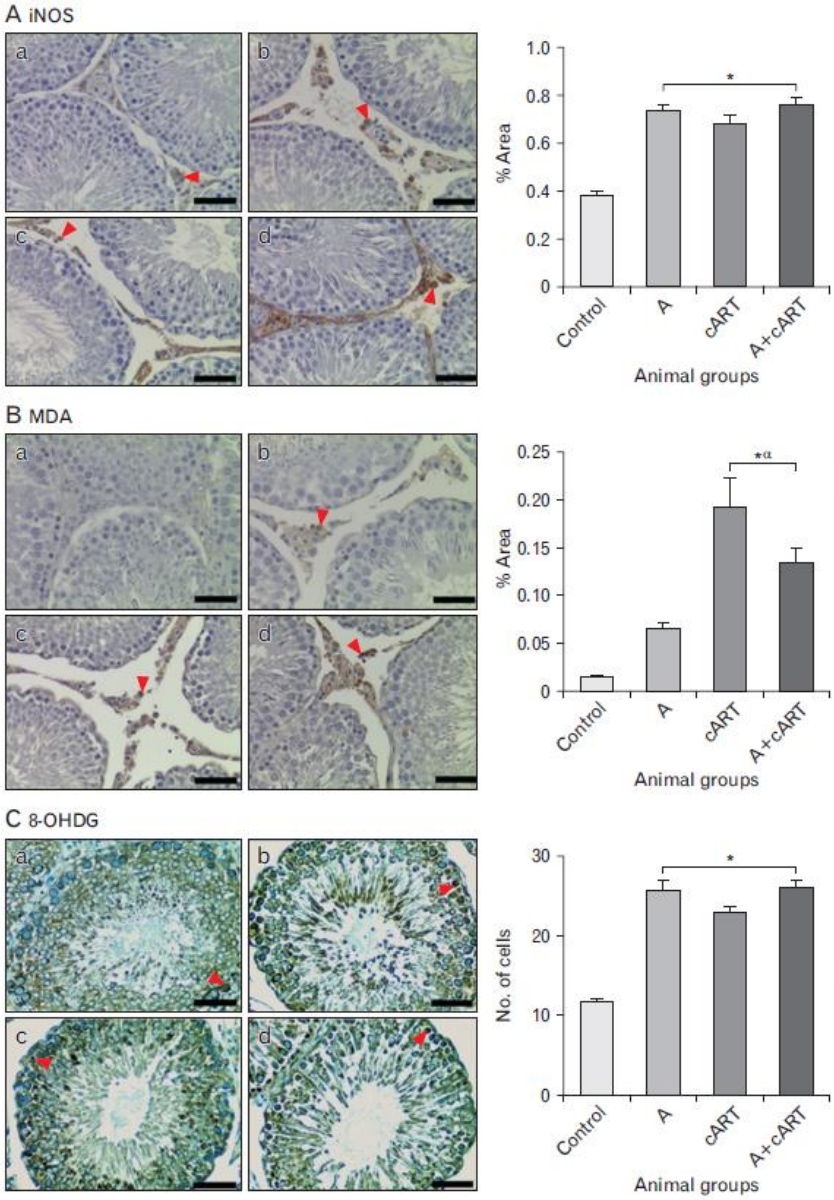


Fig. 2. Photomicrographs of oxidative stress expression and respective mean of expression graphs. Representative immunoreactivity is indicated with arrowhead. The mean percentage area of expression for iNOS and MDA, and mean number of cells expressing 8-OHDG were reported. Different symbols *, α, and ǂ represent comparison with groups control, A, and cART respectively. (A) iNOS of A, cART, and A+cART groups significantly increased compared to control (*P<0.0001). (B) MDA of cART and A+cART groups significantly increased compared to control (*P<0.0001) and A ($^{\alpha}P$<0.0001 and $^{\alpha}P$=0.0302 respectively). (C) 8-OHDG of A, cART, and A+cART groups significantly increased compared to control (*P<0.0001). iNOS, inducible nitric oxide synthase; MDA, malondialdehyde; 8-OHDG, 8-hydroxydeoxyguanosine; A, alcohol; cART, combination antiretroviral therapy. Magnification, ×400; scale bar, 50 μm. (a) Control, (b) A, (c) cART, (d) A+cART. Key: Image: (a) control group, (b) A-treated group, (c) cART-treated group, and (d) A+cART-treated group.

https://doi.org/10.5115/acb.22.229

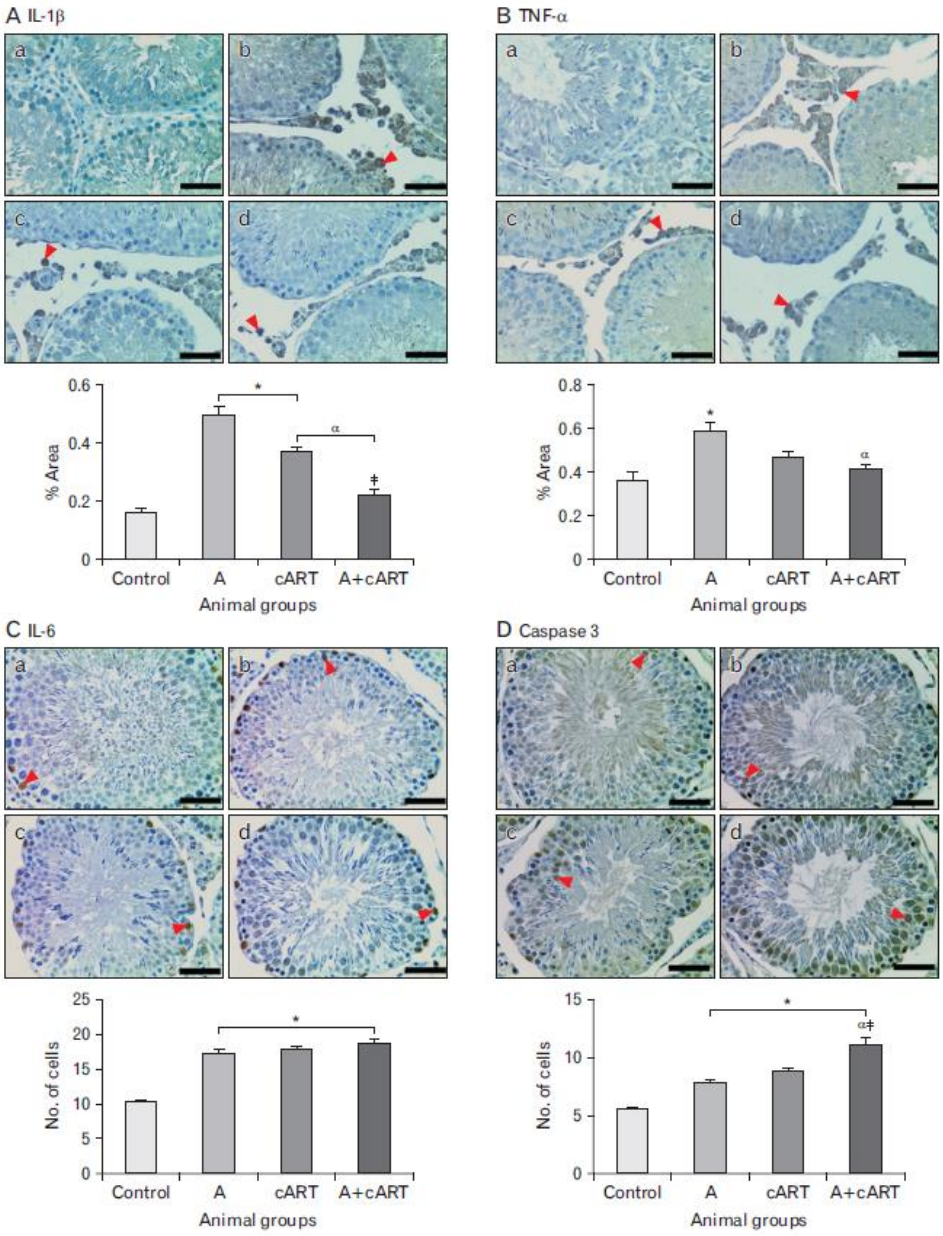


Fig. 3. Photomicrographs of inflammatory and apoptosis expression and respective mean of expression graphs. Representative immunoreactivity is indicated with arrowhead. The mean percentage area of expression for IL-1β and TNF-α, and the number of cells expressing IL-6 and caspase 3 were reported. Different symbols *, α, and ‡ represent comparison with groups, control, A (a), and cART (c) respectively. (A) IL-1β of A and cART groups significantly increased compared to control (*P<0.0001), cART and A+cART significantly decreased compared to A ($^{\alpha}P$=0.0006 and $^{\alpha}P$<0.0001), and A+cART significantly decreased compared to cART ($^{\ddagger}P$<0.0001). (B) TNF-α of group A significantly increased compared to control (*P<0.0001); and A+cART significantly decreased compared to A ($^{\alpha}P$=0.0011). (C) IL-6 of A, cART, and A+cART groups significantly increased compared to control (*P<0.0001). (D) Caspase 3 of A, cART, and A+cART groups significantly increased compared to control (*P=0.0023 and *P<0.0001) and A+cART significantly increased compared to A and cART ($^{\alpha}P$<0.0001 and $^{\ddagger}P$=0.0013).
IL-1β, interleukin-1beta; TNF-α, tumor necrosis factor-alpha; IL-6, interleukin-6; A, alcohol; cART, combination antiretroviral therapy. Magnification, ×400; scale bar, 50 μm. Key: Image: (a) control group, (b) A-treated group, (c) cART-treated group, and (d) A+cART-treated group.

https://doi.org/10.5115/acb.22.229

Inflammatory and apoptosis markers

Expressions of IL-1β, TNF-α, IL-6, and caspase 3 were as presented in Fig. 3. IL-1β expression was significantly elevated ($P<0.0001$) in A and cART treated groups compared to the control. But the expression of IL-1β in cART and A+cART treated groups was significantly decreased relative to A treated group ($P=0.0006$ and $P<0.0001$ respectively) and significantly decreased ($P<0.0001$) in A+cART compared to cART. Although, the expression of TNF-α was increased in all the treated groups against the control, the increase was only significant in A treated animals ($P=0.0001$). Further, the expression TNF-α in A group increased significantly ($P=0.0011$) compared to A+cART treated group. IL-6 was significantly upregulated ($P<0.0001$) in all treated groups (A, cART, and A+cART) compared to the control. Whilst caspase 3 expression significantly increased in A ($P=0.0023$), cART ($P<0.0001$), and A+cART ($P<0.0001$) groups relative to control. Further, caspase 3 expression in A+cART group was significantly higher in comparison to A ($P<0.0001$) and cART ($P=0.0013$) treated groups (Fig. 3).

Discussion

Infertility is a worrisome reproductive health problem in families globally [2] with a soaring prevalence of male infertility [1]. The chronic use of combined antiretroviral (cART) blended with alcohol abuse has introduced new variables in male reproductive dysfunctions. Moreover, a high incidence of alcohol use among people living with HIV/AIDS (PLWHA) and on cART has also been reported [13, 14]. Markedly, cART and alcohol have individually been reported to negatively impact the male reproductive system [17, 19] and thus their concomitant use may pose major reproductive dysfunctional challenges, particularly amongst PLWHA that desire to have biological children [26], which is a critical societal necessity.

The result from this study showed non-significant decrease in testicular weight, volume, and size across the treatment groups compared to the control group which is consistent with previous reports [29, 37, 39, 42] and may suggest minimal perturbations of testicular architecture. However, the significantly decreased EAF, and the significantly increased LAF in A+cART treated group point to perturbations of testicular structure and cellular coherency. Furthermore, the significant increases in ISAF in A and cART treated groups and non-significant in the A+cART treated group may suggest specific treatment effects and the impact of the A+cART interaction on this parameter. Overall, these changes in the histological component of the testis reflect an alteration of the integrity of testicular morphology, pointing to disruption of the normal testicular paracrine/autocrine factors (such as cytokines) involved in regulation of spermatogenesis and consequently will lead to a decline in spermatogenesis [27, 35].

Furthermore, the increased number of spermatogonia (proliferation of spermatogenesis) observed in testis of the alcohol and cART treated groups, could be an attempt to increase the germ cell pool so as to counteract the diminishing spermatogenesis processes which is in line with a previous clinical study that reported a massive increase in the number of normally differentiated spermatogonia and elevated spermatogonia proliferative activity in a biopsy of patient with non-obstructive azoospermia [43]. Additionally, the (LAF and diameter (LD) were both slightly increased in the A group but significantly increased in the A+cART group, suggesting varying degrees of germ cell layer reduction due to different treatments as well as seminiferous tubule shrinkage.

Notably, tubular shrinkage was depicted by the significant reduction in TA and TD in testis of treated groups (A, cART, and A+cART), and was consistent with previous findings [27, 29, 44]. However, LAF and LD were also significantly decreased in the treated groups except in cART group regardless of the diminished EAF, EH, and germinal epithelium cell layers. This could have been due to the prominent seminiferous tubule shrinkage observed in cART treated group which also recorded the greatest reductions in TA and TD. Further, shrunken seminiferous tubules are suggestive of tubule degenerative changes induced by the treatments and subsequently result in germ cell death [45]. Accordingly, shrinkage of the seminiferous tubules resulted in an increase in ISAF in the treated groups compared to the control animals.

Equally, a significant increment in CTAF was recorded in the testis of treated animals, suggesting formation of fibrosis in the testis interstitium. Our findings go in line with that of a previous study that reported fibrosis led to increase in thickness of the testicular interstitium in the infertile males [46]. Testicular fibrosis usually occurs following testis trauma and inflammation amongst others [47]. Fibrosis impairs the integrity of the testicular interstitium and alters the structure and function of the interstitial cells (Leydig,

macrophages, and myoid cells), and consequently adversely affects testicular structure and function [47, 48].

Furthermore, the number of Sertoli cells was not significantly reduced in the treated animals compared to control animals, suggesting that Sertoli cells were less adversely affected. Previous report indicated that Sertoli cells are resistant to apoptosis compared to germ cells [49], because they contain high levels of anti-apoptotic markers, Bcl-w and Bcl-xL [50]. It has been reported that while the number of Sertoli cells is not usually affected [50, 51], disruptions in its structure are relatively common and can alter the cell's functions, the integrity of the blood-testis barrier [52] and consequently lead to dysregulation of spermatogenesis. Though, the present study did not include effects on the Sertoli cell cytoskeleton, previous studies show that its alteration and/or damage leads to sloughing of germ cells into the lumen and separation of germinal epithelium from the basement membrane [53-55], which were both observed in treated animals in the current study.

However, Leydig cell nuclear diameter and volume in testis of treated animals were significantly reduced relative to the control animals and may imply disturbances of Leydig cell function [37, 52, 56]. The nucleus is the lifeline of the cell, and a previous study showed that quantitative measurements of the nucleus is important in understanding the cell's response to injury and further reported that nuclear volume correlates strongly with cell volume and function [57]. Leydig cells are present in the testis interstitium, and synthesize androgens via steroidogenesis [58]. Therefore, shrinkage of the nucleus will ultimately affect the Leydig cell's steroidogenic capacity and subsequently lead to disruption of spermatogenesis [58-60].

Additionally, in parallel with previous findings [61, 62], Johnsen's score of the treated groups was reduced compared with the control animal group. Reduction in Johnsen's score is linked to interruption of normal germ cell maturation, germ cell layer loss, and tubule lesions [63, 64]. Also, seminiferous tubule germinal epithelium lesions such as lifting of epithelium, widened interstitial space, karyolysis, and sloughed germ cells were more evident in the treated groups compared to control animal group, which supports the reduction in Johnson's score recorded in treated groups. This result confirm testicular toxicity of the treatments (alcohol or/and cART) [20, 53].

Oxidative stress is a common feature in most male reproductive system dysfunctions [65-67], occurring as a result of an imbalance between rate of production and clearance of reactive oxygen species (ROS) [68, 69]. High ROS levels have been reported in 30%–80% of infertile males [65, 69]. Our findings showed upregulation of oxidative stress markers *i.e.*, iNOS, MDA, and 8-OHDG in the testis of treated animals. This indicates that alcohol, cART, and their combination induced oxidative stress in the testis. Reports show that iNOS upregulation leads to increased ROS formation [70], ROS have been shown to induce lipid peroxidation and DNA fragmentation in the testis [71-73]. These are the most common consequences of testicular oxidative stress resulting into increased MDA and 8-OHDG formation respectively [66, 74, 75]. Previous studies have reported that ROS-induced lipid peroxidation is implicated in male reproductive dysfunction [65-67], due to substantial amounts of unsaturated fatty acids in the testis tissue [71, 76].

Reportedly, elevation of ROS stimulates release of several inflammatory cytokines such as IL-1, TNF-α, and IL-6 mostly via the nuclear factor-kappa beta pathway [74, 75, 77]. In the testis, cytokines are majorly derived from interstitial macrophages, but Leydig and Sertoli cells also secrete cytokines [78-80]. Studies show that during testicular injury, activated macrophages, Leydig, and Sertoli cells produce a high concentration of cytokines and iNOS [75, 78, 79]. In consonance with the above, the elevated levels of pro-inflammatory cytokines observed in the present study may adversely affect the process of spermatogenesis, as reported by previous studies [80, 81]. Somade et al. [82] found that elevated cytokine levels in testis and kidney of Wistar albino rats, was associated with testiculo-renal toxicosis following acute administration of edible camphor. Additionally, testicular cytokines have been shown to affect germ cell proliferation, as well as Leydig and Sertoli cells functions and secretions [80]. This study findings show that oxidative stress and inflammation are interlinked mechanisms associated with germ cell apoptosis, which might underlie the multidimensional changes observed in testis of animals treated with alcohol or/and cART.

Overall, the study has revealed some important findings in testicular toxicity of the treatments relative to the parameters studied. Interestingly, though the levels of IL-1β and TNF-α, and MDA were elevated in A+cART treated group compared to control animals but comparatively were not as elevated as that of IL-6, iNOS, 8-OHDG, and caspase 3 expression in A+cART treated group. These results suggest possible effect of cytochrome P450 enzyme pathway involved

in the metabolism of alcohol and cART [14, 30, 83], resulting in reduction of the level of these parameters (IL-1β, TNF-α, and MDA) in A+cART treated group. Additionally, it may suggest a variation in the effects of different treatment on the studied parameters.

In conclusion, our results show that consumption of alcohol or cART can cause perturbations in the testis morphometric parameters and seminiferous tubule lesions via upregulation of oxidative stress and pro-inflammatory cytokines. In addition, consumption of alcohol and cART concurrently can exacerbate testicular damage. The findings from this study are invaluable for the clinical management of male fertility challenges that could emerge in PLWHA on cART therapy who consume alcohol regularly.

ORCID

Elna Owembabazi:
https://orcid.org/0000-0003-3000-8057
Pilani Nkomozepi:
https://orcid.org/0000-0001-6656-6590
Tanya Calvey: https://orcid.org/0000-0002-7540-2130
Ejikeme Felix Mbajiorgu:
https://orcid.org/0000-0001-7462-2433

Author Contributions

Conceptualization: EO, EFM. Data acquisition: EO, PN, EFM. Data analysis or interpretation: EO, PN, TC. Drafting of the manuscript: EO, EFM. Critical revision of the manuscript: EO, PN, TC, EFM. Approval of the final version of the manuscript: all authors.

Conflicts of Interest

No potential conflict of interest relevant to this article was reported.

Funding

This research was funded partly by Professor Mbajiorgu's Wits Faculty of Health Sciences Research Publication Incentive (grant no. 001.167.8421101.5122201/4228) and supplemented by Dr Calvey's Medical Research Council of South Africa Self-Initiated Research grant (grant no. 001.407.8421101.5122201CALV018).

Acknowledgments

We appreciate the collaborative efforts of our colleagues Jaclyn Asouzu Johnson, Idemudia Eguavoen, and Vaughan Perry and extend special appreciation to Hasiena Ali for her laboratory assistance.

References

1. Sun H, Gong TT, Jiang YT, Zhang S, Zhao YH, Wu QJ. Global, regional, and national prevalence and disability-adjusted life-years for infertility in 195 countries and territories, 1990-2017: results from a global burden of disease study, 2017. Aging (Albany NY) 2019;11:10952-91.
2. Agarwal A, Baskaran S, Parekh N, Cho CL, Henkel R, Vij S, Arafa M, Panner Selvam MK, Shah R. Male infertility. Lancet 2021;397:319-33.
3. Simões D, Meireles P, Rocha M, Freitas R, Aguiar A, Barros H. Knowledge and use of PEP and PrEP among key populations tested in community centers in Portugal. Front Public Health 2021;9:673959.
4. Ilhan MN, Yapar D. Alcohol consumption and alcohol policy. Turk J Med Sci 2020;50:1197-202.
5. Vellios NG, Van Walbeek CP. Self-reported alcohol use and binge drinking in South Africa: evidence from the national income dynamics study, 2014-2015. S Afr Med J 2017;108:33-9.
6. Trangenstein PJ, Morojele NK, Lombard C, Jernigan DH, Parry CDH. Heavy drinking and contextual risk factors among adults in South Africa: findings from the International Alcohol Control study. Subst Abuse Treat Prev Policy 2018;13:43.
7. Cornell M, Johnson LF, Wood R, Tanser F, Fox MP, Prozesky H, Schomaker M, Egger M, Davies MA, Boulle A. Twelve-year mortality in adults initiating antiretroviral therapy in South Africa. J Int AIDS Soc 2017;20:21902.
8. Lippman SA, El Ayadi AM, Grignon JS, Puren A, Liegler T, Venter WDF, Ratlhagana MJ, Morris JL, Naidoo E, Agnew E, Barnhart S, Shade SB. Improvements in the South African HIV care cascade: findings on 90-90-90 targets from successive population-representative surveys in North West Province. J Int AIDS Soc 2019;22:e25295.
9. Mabwe P, Kessy AT, Semali I. Understanding the magnitude of occupational exposure to human immunodeficiency virus (HIV) and uptake of HIV post-exposure prophylaxis among healthcare workers in a rural district in Tanzania. J Hosp Infect 2017;96:276-80.
10. Scott-Sheldon LA, Carey KB, Cunningham K, Johnson BT, Carey MP. Alcohol use predicts sexual decision-making: a systematic review and meta-analysis of the experimental literature. AIDS Behav 2016;20(Suppl 1):S19-39.
11. Kumar S, Rao PS, Earla R, Kumar A. Drug-drug interactions between anti-retroviral therapies and drugs of abuse in HIV systems. Expert Opin Drug Metab Toxicol 2015;11:343-55.

12. Schneider M, Chersich M, Temmerman M, Parry CD. Addressing the intersection between alcohol consumption and antiretroviral treatment: needs assessment and design of interventions for primary healthcare workers, the Western Cape, South Africa. Global Health 2016;12:65.
13. McCance-Katz EF, Gruber VA, Beatty G, Lum PJ, Rainey PM. Interactions between alcohol and the antiretroviral medications ritonavir or efavirenz. J Addict Med 2013;7:264-70.
14. Mondal S, Ghosh P, Biswas D, Roy PK. Effect of alcohol consumption during antiretroviral therapy on HIV-1 replication: role of Cytochrome P3A4 enzyme. Int J Math Eng Manag Sci 2019;4:922-35.
15. Chander G, Lau B, Moore RD. Hazardous alcohol use: a risk factor for non-adherence and lack of suppression in HIV infection. J Acquir Immune Defic Syndr 2006;43:411-7.
16. Braithwaite RS, Conigliaro J, Roberts MS, Shechter S, Schaefer A, McGinnis K, Rodriguez MC, Rabeneck L, Bryant K, Justice AC. Estimating the impact of alcohol consumption on survival for HIV+ individuals. AIDS Care 2007;19:459-66.
17. Kushnir VA, Lewis W. Human immunodeficiency virus/acquired immunodeficiency syndrome and infertility: emerging problems in the era of highly active antiretrovirals. Fertil Steril 2011;96:546-53.
18. Ogedengbe OO, Jegede AI, Onanuga IO, Offor U, Peter AI, Akang EN, Naidu ECS, Azu OO. Adjuvant potential of virgin coconut oil extract on antiretroviral therapy-induced testicular toxicity: an ultrastructural study. Andrologia 2018;50:e12930.
19. Apolikhin OI, Krasnyak SS. The impact of alcohol on the male reproductive system. Public Health 2021;1:62-9.
20. Duca Y, Aversa A, Condorelli RA, Calogero AE, La Vignera S. Substance abuse and male hypogonadism. J Clin Med 2019;8:732.
21. La Vignera S, Condorelli RA, Balercia G, Vicari E, Calogero AE. Does alcohol have any effect on male reproductive function? A review of literature. Asian J Androl 2013;15:221-5.
22. Condorelli RA, Calogero AE, Vicari E, La Vignera S. Chronic consumption of alcohol and sperm parameters: our experience and the main evidences. Andrologia 2015;47:368-79.
23. Oremosu AA, Akang EN. Impact of alcohol on male reproductive hormones, oxidative stress and semen parameters in Sprague-Dawley rats. Middle East Fertil Soc J 2015;20:114-8.
24. Van Heertum K, Rossi B. Alcohol and fertility: how much is too much? Fertil Res Pract 2017;3:10.
25. Oyeyipo IP, Skosana BT, Everson FP, Strijdom H, du Plessis SS. Highly active antiretroviral therapy alters sperm parameters and testicular antioxidant status in diet-induced obese rats. Toxicol Res 2018;34:41-8.
26. Savasi V, Parisi F, Oneta M, Laoreti A, Parrilla B, Duca P, Cetin I. Effects of highly active antiretroviral therapy on semen parameters of a cohort of 770 HIV-1 infected men. PLoS One 2019;14:e0212194.
27. Azu OO. Highly active antiretroviral therapy (HAART) and testicular morphology: current status and a case for a stereologic approach. J Androl 2012;33:1130-42.
28. Savasi V, Oneta M, Laoreti A, Parisi F, Parrilla B, Duca P, Cetin I. Effects of antiretroviral therapy on sperm DNA integrity of HIV-1-infected men. Am J Mens Health 2018;12:1835-42.
29. Ogedengbe OO, Naidu ECS, Akang EN, Offor U, Onanuga IO, Peter AI, Jegede AI, Azu OO. Virgin coconut oil extract mitigates testicular-induced toxicity of alcohol use in antiretroviral therapy. Andrology 2018;6:616-26.
30. Ogedengbe OO, Naidu ECS, Azu OO. Antiretroviral therapy and alcohol interactions: X-raying testicular and seminal parameters under the HAART era. Eur J Drug Metab Pharmacokinet 2018;43:121-35.
31. Dutra Gonçalves G, Antunes Vieira N, Rodrigues Vieira H, Dias Valério A, Elóisa Munhoz de Lion Siervo G, Fernanda Felipe Pinheiro P, Eduardo Martinez F, Alessandra Guarnier F, Rampazzo Teixeira G, Scantamburlo Alves Fernandes G. Role of resistance physical exercise in preventing testicular damage caused by chronic ethanol consumption in UChB rats. Microsc Res Tech 2017;80:378-86.
32. Frampton JE, Croom KF. Efavirenz/emtricitabine/tenofovir disoproxil fumarate: triple combination tablet. Drugs 2006;66:1501-12; discussion 1513-4.
33. Ansa AA, Akpere O, Imasuen JA. Semen traits, testicular morphometry and histopathology of cadmium-exposed rabbit bucks administered methanolic extract of Phoenix dactylifera fruit. Acta Sci Anim Sci 2017;39:207-15.
34. Parhizkar S, Zulkifli SB, Dollah MA. Testicular morphology of male rats exposed to Phaleria macrocarpa (Mahkota dewa) aqueous extract. Iran J Basic Med Sci 2014;17:384-90.
35. Kangawa A, Otake M, Enya S, Yoshida T, Shibata M. Histological changes of the testicular interstitium during postnatal development in microminipigs. Toxicol Pathol 2019;47:469-82.
36. Kumar A, Nagar M. Histomorphometric study of testis in deltamethrin treated albino rats. Toxicol Rep 2014;1:401-10.
37. Olasile IO, Jegede IA, Ugochukwu O, Ogedengbe OO, Naidu EC, Peter IA, Azu OO. Histo-morphological and seminal evaluation of testicular parameters in diabetic rats under antiretroviral therapy: interactions with *Hypoxis hemerocallidea*. Iran J Basic Med Sci 2018;21:1322-30.
38. Qiu LL, Wang X, Zhang XH, Zhang Z, Gu J, Liu L, Wang Y, Wang X, Wang SL. Decreased androgen receptor expression may contribute to spermatogenesis failure in rats exposed to low concentration of bisphenol A. Toxicol Lett 2013;219:116-24.
39. Monteiro JC, da Matta SLP, Predes FS, de Paula TAR. Testicular morphology of adult Wistar rats treated with Rudgea viburnoides (Cham.) Benth. Leaf infusion. Braz Arch Biol Technol 2012;55:101-5.
40. Thanh TN, Van PD, Cong TD, Le Minh T, Vu QHN. Assessment of testis histopathological changes and spermatogenesis in male mice exposed to chronic scrotal heat stress. J Anim Behav Biometeorol 2020;8:174-80.
41. Erpek S, Bilgin MD, Dikicioglu E, Karul A. The effects of low frequency electric field in rat testis. Rev Med Vet 2007;158:206-12.
42. Adaramoye OA, Akanni OO, Adewumi OM, Owumi SE. Lopinavir/Ritonavir, an antiretroviral drug, lowers sperm quality

and induces testicular oxidative damage in rats. Tokai J Exp Clin Med 2015;40:51-7.
43. Fietz D, Pilatz A, Diemer T, Wagenlehner F, Bergmann M, Schuppe HC. Excessive unilateral proliferation of spermatogonia in a patient with non-obstructive azoospermia - adverse effect of clomiphene citrate pre-treatment? Basic Clin Androl 2020;30:13.
44. Dosumu OO, Osinubi AAA, Duru FIO. Alcohol induced testicular damage: can abstinence equal recovery? Middle East Fertil Soc J 2014;19:221-8.
45. Azu OO, Naidu EC, Naidu JS, Masia T, Nzemande NF, Chuturgoon A, Singh S. Testicular histomorphologic and stereological alterations following short-term treatment with highly active antiretroviral drugs (HAART) in an experimental animal model. Andrology 2014;2:772-9.
46. Apa DD, Cayan S, Polat A, Akbay E. Mast cells and fibrosis on testicular biopsies in male infertility. Arch Androl 2002;48:337-44.
47. Yagan N. Testicular US findings after biopsy. Radiology 2000;215:768-73.
48. Mayerhofer A. Human testicular peritubular cells: more than meets the eye. Reproduction 2013;145:R107-16.
49. Wangikar P, Ahmed T, Vangala S. Toxicologic pathology of the reproductive system. In: Gupta RC, editor. Reproductive and Developmental Toxicology. London: Elsevier; 2011. p.1003-26.
50. Eid N, Ito Y, Otsuki Y. Anti-apoptotic mechanisms of Sertoli cells against ethanol toxicity. J Alcohol Drug Depend 2013;1:1000105.
51. Pajarinen JT, Karhunen PJ. Spermatogenic arrest and 'Sertoli cell-only' syndrome--common alcohol-induced disorders of the human testis. Int J Androl 1994;17:292-9.
52. Trindade AA, Simões AC, Silva RJ, Macedo CS, Spadella CT. Long term evaluation of morphometric and ultrastructural changes of testes of alloxan-induced diabetic rats. Acta Cir Bras 2013;28:256-65.
53. Moffit JS, Bryant BH, Hall SJ, Boekelheide K. Dose-dependent effects of sertoli cell toxicants 2,5-hexanedione, carbendazim, and mono-(2-ethylhexyl) phthalate in adult rat testis. Toxicol Pathol 2007;35:719-27.
54. Lie PP, Mruk DD, Lee WM, Cheng CY. Cytoskeletal dynamics and spermatogenesis. Philos Trans R Soc Lond B Biol Sci 2010;365:1581-92.
55. Johnson KJ. Testicular histopathology associated with disruption of the Sertoli cell cytoskeleton. Spermatogenesis 2015;4:e979106.
56. Jelodar G, Khaksar Z, Pourahmadi M. Endocrine profile and testicular histomorphometry in adult rat offspring of diabetic mothers. J Physiol Sci 2009;59:377-82.
57. Wu Y, Pegoraro AF, Weitz DA, Janmey P, Sun SX. The correlation between cell and nucleus size is explained by an eukaryotic cell growth model. PLoS Comput Biol 2022;18:e1009400.
58. Zirkin BR, Papadopoulos V. Leydig cells: formation, function, and regulation. Biol Reprod 2018;99:101-11.
59. Kumari D, Nair N, Bedwal RS. Effect of dietary zinc deficiency on testes of Wistar rats: morphometric and cell quantification studies. J Trace Elem Med Biol 2011;25:47-53.
60. Neves BVD, Lorenzini F, Veronez D, Miranda EP, Neves GD, Fraga R. Numeric and volumetric changes in Leydig cells during aging of rats. Acta Cir Bras 2017;32:807-15.
61. Akhigbe RE, Hamed MA, Aremu AO. HAART exacerbates testicular damage and impaired spermatogenesis in anti-Koch-treated rats via dysregulation of lactate transport and glutathione content. Reprod Toxicol 2021;103:96-107.
62. Baydilli N, Akınsal EC, Doğanyiğit Z, Ekmekçioğlu O, Silici S. The protective role of poplar propolis against alcohol-induced biochemical and histological changes in liver and testes tissues of rats. Erciyes Med J 2020;42:132-8.
63. Iftikhar S, Ahmad M, Aslam HM, Saeed T, Yasir A, Nazish GE. Evaluation of spermatogenesis in prepubertal albino rats with date palm pollen supplement. Afr J Pharm Pharmacol 2014;8:59-65.
64. Shokoohi M, Madarek EOS, Khaki A, Shoorei H, Khaki AA, Soltani M, Ainehchi N. Investigating the effects of onion juice on male fertility factors and pregnancy rate after testicular torsion/detorsion by intrauterine insemination method. Int J Women's Health Reprod Sci 2018;6:499-505.
65. Tremellen K. Oxidative stress and male infertility: a clinical perspective. In: Agarwal A, Aitken R, Alvarez J, editors. Studies on Men's Health and Fertility. Totowa: Humana Press; 2012. p.325-53.
66. Asadi N, Bahmani M, Kheradmand A, Rafieian-Kopaei M. The impact of oxidative stress on testicular function and the role of antioxidants in improving it: a review. J Clin Diagn Res 2017;11:IE01-5.
67. Sakr SA, Nooh HZ. Effect of Ocimum basilicum extract on cadmium-induced testicular histomorphometric and immunohistochemical alterations in albino rats. Anat Cell Biol 2013;46:122-30.
68. Turner TT, Lysiak JJ. Oxidative stress: a common factor in testicular dysfunction. J Androl 2008;29:488-98.
69. Wu PY, Scarlata E, O'Flaherty C. Long-term adverse effects of oxidative stress on rat epididymis and spermatozoa. Antioxidants (Basel) 2020;9:170.
70. Zhao K, Huang Z, Lu H, Zhou J, Wei T. Induction of inducible nitric oxide synthase increases the production of reactive oxygen species in RAW264.7 macrophages. Biosci Rep 2010;30:233-41.
71. Aitken RJ, Roman SD. Antioxidant systems and oxidative stress in the testes. Oxid Med Cell Longev 2008;1:15-24.
72. Sharma R, Agarwal A. Spermatogenesis: an overview. In: Zini A, Agarwal A, editors. Sperm Chromatin. New York: Springer; 2011. p.19-44.
73. Ikekpeazu JE, Orji OC, Uchendu IK, Ezeanyika LUS. Mitochondrial and oxidative impacts of short and long-term administration of HAART on HIV patients. Curr Clin Pharmacol 2020;15:110-24.
74. Aprioku JS. Pharmacology of free radicals and the impact of reactive oxygen species on the testis. J Reprod Infertil 2013;14:

158-72.
75. Dutta S, Sengupta P, Slama P, Roychoudhury S. Oxidative stress, testicular inflammatory pathways, and male reproduction. Int J Mol Sci 2021;22:10043.
76. Guerriero G, Trocchia S, Abdel-Gawad FK, Ciarcia G. Roles of reactive oxygen species in the spermatogenesis regulation. Front Endocrinol (Lausanne) 2014;5:56.
77. Nna VU, Abu Bakar AB, Ahmad A, Eleazu CO, Mohamed M. Oxidative stress, NF-κB-mediated inflammation and apoptosis in the testes of streptozotocin-induced diabetic rats: combined protective effects of Malaysian propolis and metformin. Antioxidants (Basel) 2019;8:465.
78. Kolasa A, Marchlewicz M, Kurzawa R, Głabowski W, Trybek G, Wenda-Rózewicka L, Wiszniewska B. The expression of inducible nitric oxide synthase (iNOS) in the testis and epididymis of rats with a dihydrotestosterone (DHT) deficiency. Cell Mol Biol Lett 2009;14:511-27.
79. Coştur P, Filiz S, Gonca S, Çulha M, Gülecen T, Solakoğlu S, Canberk Y, Çalışkan E. Êxpression of inducible nitric oxide synthase (iNOS) in the azoospermic human testis. Andrologia 2012;44(Suppl 1):654-60.
80. Loveland KL, Klein B, Pueschl D, Indumathy S, Bergmann M, Loveland BE, Hedger MP, Schuppe HC. Cytokines in male fertility and reproductive pathologies: immunoregulation and beyond. Front Endocrinol (Lausanne) 2017;8:307.
81. Hedger MP, Meinhardt A. Cytokines and the immune-testicular axis. J Reprod Immunol 2003;58:1-26.
82. Somade OT, Ajayi BO, Safiriyu OA, Oyabunmi OS, Akamo AJ. Renal and testicular up-regulation of pro-inflammatory chemokines (RANTES and CCL2) and cytokines (TNF-α, IL-1β, IL-6) following acute edible camphor administration is through activation of NF-kB in rats. Toxicol Rep 2019;6:759-67.
83. Kumar S, Jin M, Ande A, Sinha N, Silverstein PS, Kumar A. Alcohol consumption effect on antiretroviral therapy and HIV-1 pathogenesis: role of cytochrome P450 isozymes. Expert Opin Drug Metab Toxicol 2012;8:1363-75.
84. Berg S, Kutra D, Kroeger T, Straehle CN, Kausler BX, Haubold C, Schiegg M, Ales J, Beier T, Rudy M, Eren K, Cervantes JI, Xu B, Beuttenmueller F, Wolny A, Zhang C, Koethe U, Hamprecht FA, Kreshuk A. ilastik: interactive machine learning for (bio) image analysis. Nat Methods 2019;16:1226-32.
85. Chim YH, Davies HA, Mason D, Nawaytou O, Field M, Madine J, Akhtar R. Bicuspid valve aortopathy is associated with distinct patterns of matrix degradation. J Thorac Cardiovasc Surg 2020;160:e239-57.

https://doi.org/10.5115/acb.22.229

Appendix

Image segmentation

Ilastik software (v1.3.3; https://www.ilastik.org) was used for image segmentation. Images were segmented into 3, 3'-diaminobenzidine tetrachloride (DAB) positive area and background [84, 85]. A pixel classifier was trained with eight sample images selected from all animal groups (two images per group). The available features *i.e.*, intensity/color, texture, and edge at a sigma of 0.3–10 pixels were included in the classification algorithms. To train the classifier an appropriate brush was used to annotate a few DAB-positive areas (yellow color), and representative areas not stained with DAB were annotated as the background (blue color). To place the annotations precisely, the images were zoomed out. The prediction was inspected after adding each annotation. Then more annotations were added to all training images to refine the classifier and increase its applicability to large training naïve image sets. Once the prediction was of a good standard across the sample images, the trained classifier was applied to image sets, and their simple segmentations were exported for quantification (Fig. 1).

Image quantification

Segmented images were quantified using Fiji software (v1.52e; https://imagej.net/Fiji) into numerical values for statistical analysis [85]. The ilastik exported image segments were imported into Fiji through the ilastik plugin. Then, the Fiji scale was adjusted according to the magnification of the image. The parameters to measure (area and area fraction) were selected and limited to the threshold. The segments were analyzed using a newly generated macro shown in Fig. 2. The percentage area of expression for antibodies was calculated using the formula below.

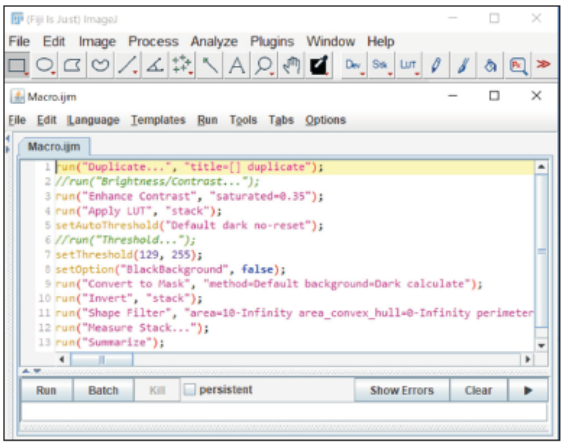


Fig. 2. Generated macro showing the steps for quantifying image segments in Fiji.

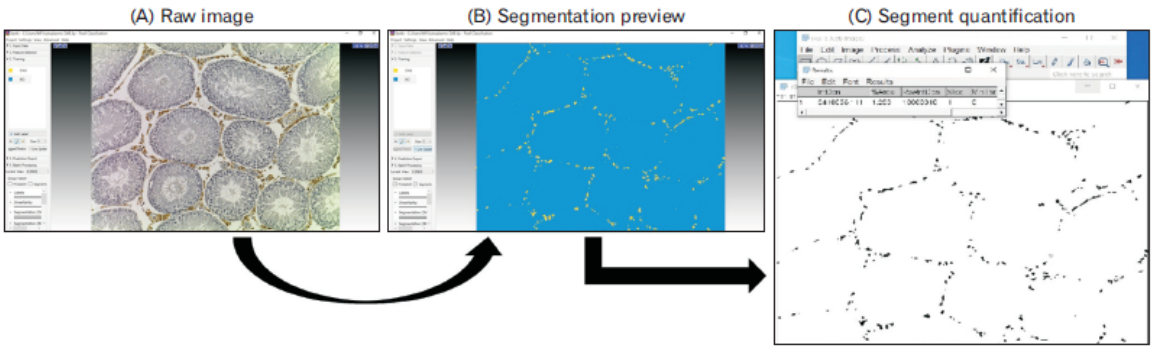


Fig. 1. Representative image segmentation and quantification in ilastik and Fiji respectively for antibodies showing positive DAB staining in both cell nucleus and cytoplasm. (A) shows an immunohistochemically DAB labeled image opened in ilastik, (B) illustrates a preview of the segmentation after adding annotations, and (C) show an ilastik exported image segment opened in Fiji displaying quantified DAB positive area.

Manuscript submission confirmation

Second manuscript



Dear Dr. Owembabazi,

Congratulations, the manuscript titled "Androgen Receptor (AR) Depletion Underlies the Reproductive Dysfunctions in Male Rats Exposed to Alcohol and Combination Antiretroviral Therapy (cART) " has been successfully submitted to Andrologia.

We will confirm this submission with all authors of the manuscript, but you will be the primary recipient of communications from the journal. As submitting author, you will be responsible for responding to editorial queries and making updates to the manuscript.

In order to view the status of the manuscript, please visit the manuscript details page.

Thank you for submitting your work to Andrologia.

MANUSCRIPT DETAILS

Kind regards,
Gowtham Chandran
Andrologia

Third manuscript

[Applied Sciences] Manuscript ID: applsci-2295390

External Inbox ×

Editorial Office <applsci@mdpi.com>
to me, Pilani, Ejikeme

Dear Ms. Owembabazi,

Thank you very much for uploading the following manuscript to the MDPI submission system. One of our editors will be in touch with you soon.

Journal name: Applied Sciences
Manuscript ID: applsci-2295390
Type of manuscript: Article
Title: Impact of Concurrent Exposure of Diabetic male Sprague Dawley rats to Alcohol and Combination Antiretroviral Therapy (cART) on reproductive capacity: Evaluation of testicular histomorphology, hormonal profile, and androgen receptor expression
Authors: Elna Owembabazi *, Pilani Nkomozepi, Ejikeme F. Mbajiorgu

Fourth manuscript

Toxicological Research (TXRS) <em@editorialmanager.com> Thu, 23 Mar, 22:50 (6 days ago)
to me

Dear Ms Owembabazi,

Thank you for submitting your manuscript,
"Potential Role of Inducible nitric oxide Synthase (iNOS) Activity in Testicular Dysfunction Following Co-administration of Alcohol and Combination Antiretroviral Therapy (cART) in Diabetic Rats: An Immunohistochemistry Study", to Toxicological Research

The submission id is: TXRS-D-23-00070
Please refer to this number in any future correspondence.

During the review process, you can keep track of the status of your manuscript by accessing the journal's web site.

Your username is: Elna
If you forgot your password, you can click the 'Send Login Details' link on the EM Login page at https://www.editorialmanager.com/txrs/.

With kind regards,

Journals Editorial Office TXRS
Springer

Turnitin report

Elna-2278202 PhD Thesis for Examination-2.docx

ORIGINALITY REPORT

20%	14%	16%	5%
SIMILARITY INDEX	INTERNET SOURCES	PUBLICATIONS	STUDENT PAPERS

PRIMARY SOURCES

1	www.science.gov Internet Source	1%
2	Submitted to University of Witwatersrand Student Paper	1%
3	www.mdpi.com Internet Source	1%
4	journals.plos.org Internet Source	1%
5	"Endocrinology of the Testis and Male Reproduction", Springer Science and Business Media LLC, 2017 Publication	<1%
6	worldwidescience.org Internet Source	<1%
7	www.researchsquare.com Internet Source	<1%
8	Submitted to Universiti Sains Malaysia Student Paper	<1%